UFL/COEL 92/001

SHORT COURSE ON PRINCIPLES AND APPLICATIONS OF BEACH NOURISHMENT

FEBRUARY 11 - 12, 1992

INSTRUCTORS

THOMAS CAMPBELL
ROBERT G. DEAN
HSIANG WANG

ORGANIZED BY

FLORIDA SHORE AND BEACH PRESERVATION ASSOCIATION
AND
COASTAL AND OCEANOGRAPHIC ENGINEERING DEPARTMENT
UNIVERSITY OF FLORIDA

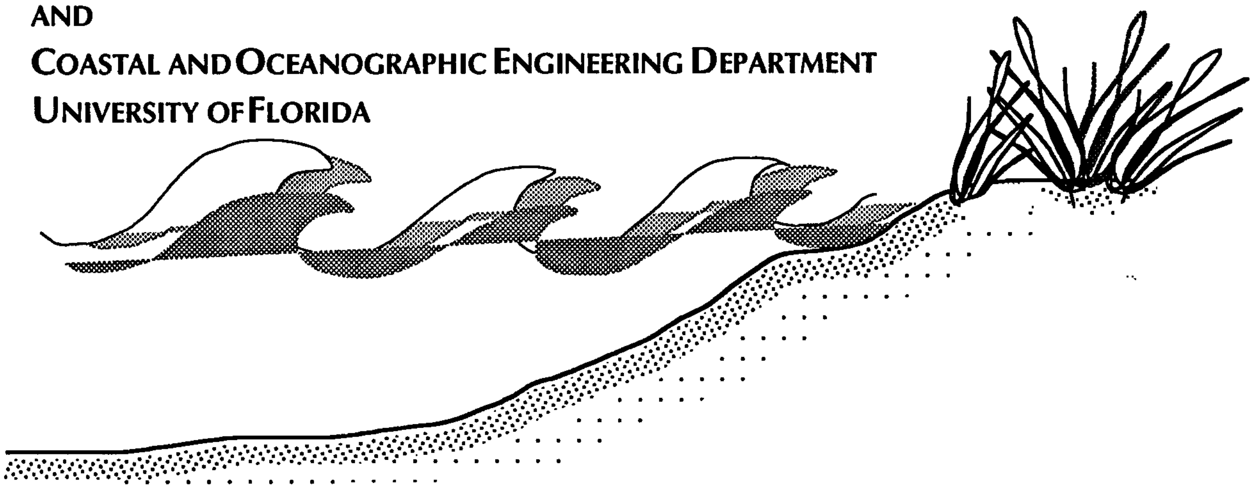

SHORT COURSE
ON
PRINCIPLES AND APPLICATIONS
OF
BEACH NOURISHMENT

··· Instructors ···

Thomas Campbell
Robert G. Dean
Hsiang Wang

··· Organized by ···

Coastal and Oceanographic Engineering Department
University of Florida
Gainesville, Florida 32611

TABLE OF CONTENTS

Chapter 1

OVERVIEW

Hsiang Wang
Coastal & Oceanographic Engineering Department
University of Florida, Gainesville

AIM OF BEACH NOURISHMENT

At present, there are only three alternatives to shoreline recession; retreat as shoreline regresses, harden the shoreline with protective structures and replenish the beach. One should not, however, confuse them as three coastal protective alternatives as the primary goal served by each alternative is different. Retreat from shoreline achieves the main purpose of seeking harmony with nature, it offers little or no help to coastal protection in the usual sense. Harden the shoreline with protective structures, on the other hand, is meant to protect upland; seeking harmony with nature, at best, is a constraint but not the goal. The primary aim of beach nourishment is to maintain a beach, although its benefit is often measured in terms of recreation, coastal protection or other social and economic factors.

Once communities have settled on the coast, coast and beaches become part of the utility system much the same as highways and power supplies that the community relies upon. If society wants to use them, it must be prepared to pay to maintain and preserve them. Therefore, beach nourishment is a means to maintain the community utility at a cost.

Case review reveals that the decision to select beach nourishment over other alternatives is often based upon one or more of the following reasons:

1. Maintain a beach at a designated location.

2. Soften the impact on adjacent coast.

3. Offer a certain degree of upland protection.

4. Spread the cost.

5. Can be reversed to natural state with minimal effort.

Many people perceive beach nourishment as a simple task of dumping sand on the beach. This simplistic view is similar to claiming that a highway is simply the pouring of asphalt over cowpath. In reality, beach nourishment, like any engineering work, in a harsh environment, it is a complicated task. Our present technology, however, is at its infancy. The intent of the short course is to review the state of art and to present the essential elements of beach nourishment design.

HISTORY AND OUTLOOK

Americans were the pioneers in beach nourishment practice. The earliest documented beach nourishment work can be traced back to 1922, at Coney Island, New York. It was actually a fairly large scale operation at the time. Approximately 1.7 million cubic yards of material from New York Harbor was transferred to the 0.7 miles beach at Coney Island through hydraulic dredging, at a cost of about 21 cents per cubic yard. Numerous projects were carried out afterwards.

Hall (1951) complied a list of 72 beach nourishment projects in the United States during the period of 1922 to 1950 (a number of them were actually one project of different segments). The majority of these projects were for the purpose of beach restoration and shore nourishment; 12 of these 72 projects were actually carried out for the primary purpose of dredge disposal. During this period, most of the nourishment projects were along the southern California coast and mid-Atlantic coast of New York and New Jersey. Only a handful of projects were along the southeast Atlantic coast and Gulf coast.

In this early stage, there was really no basic criterion pertaining to artificial beach nourishment. Hall did propose a set of design criteria suggesting some simple rules on nourishment configuration and required quantity of material. Since there was no follow-up study on any of these projects, little knowledge was gained.

In the last three decades, the number of beach nourishment projects increased considerably, particularly along the east coast and the coast of Florida. Tonya and Pilkey (1988), for instance, identified more than 90 documented cases of replenishment in over 200 separate pumping operations along the U.S. Atlantic barrier shore (Long Island, New York to Key Biscayne, Florida) alone. Table 1.1 shows the number of locations in each state along the barrier shore than beach nourishment projects have been identified. Of the 75 locations, 31 were in Florida, or more than 40%.

Table 1.1: Locations in Each State Along the East Coast Barrier Shore with Nourishment Projects

State	NY	NJ	DE	MD	VA	NC	SC	GA	FL	Total
Number of Locations	5	17	1	1	2	13	4	2	31	75

In terms of expenditure, Florida was also the highest. Under the Florida Beach Erosion Control Program, a total of 67.3 miles of beach has been restored or renourished during the period from 1965 to 1984 with a total cost of some 115.6 million (Florida DNR report, 1984). Figure 1.1 shows funds spent for restoration/renourishment projects during 1965-1984 in 5 year intervals. The trend of increased spending was clear. According to the data compiled by the Florida Department of Natural Resources 92.7 million were spent to restore 51.12 miles of shoreline and 22.9 million have been used to renourish (maintenance) 16.18 miles of beaches. Table 1.2 shows the actual expenditures of each individual beach nourishment

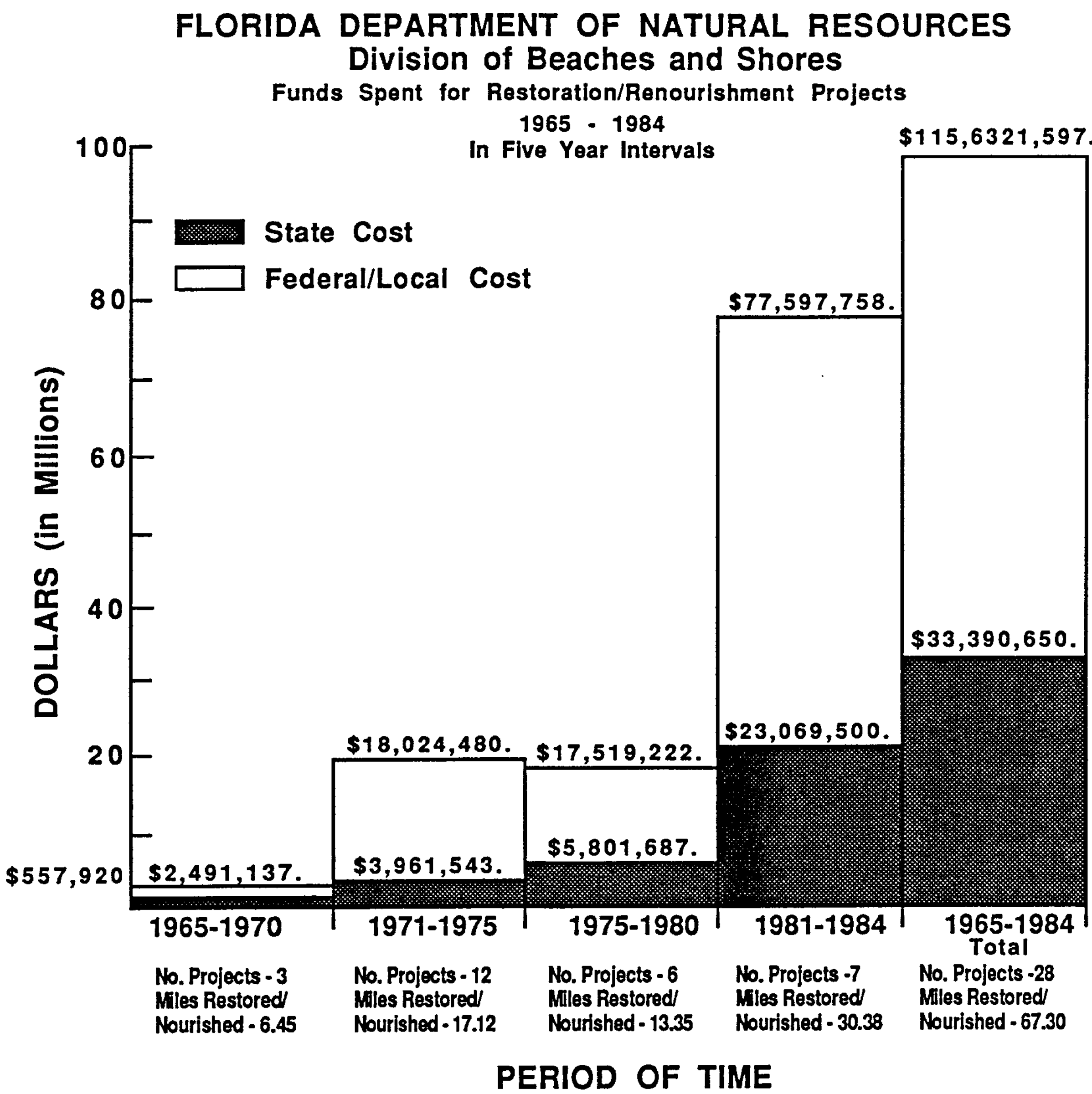

Figure 1.1 Funds Spent for Restoration/Renourishment Projects in Florida from 1965 - 1986 (DNR, 1984).

Name of Project	Total Cost Of Project	State Share Of Cost	Project Length (miles)	Total Cost Of Project	State Share Of Cost	Project Length (miles)
Mexico Beach Restoration	$ 40,625	$ 20,312	.65			
Mexico Bch Renourishment	---	---	---	$ 41,155	20,000	.55
Pompano/Lauderdale By-The-Sea Restoration	1,873,437	468,359	3.30	---	---	---
Pompano Beach Renourishment	---	---	---	10,273,340	3,549,453	5.20
Virgina Key/Key Biscayne Rest.	577,075	69,249	2.50	---	---	---
Virginia Key Renourishment	---	---	---	2,381,742	262,516	1.30
Cape Canaveral Beach Restoration	1,050,000	241,055	2.80	---	---	---
Hallandale Beach Restoration	779,977	292,491	.78	---	---	---
Delray Beach Restoration	3,015,383	976,044	2.67	---	---	---
Delray Beach Nourishment	---	---	---	1,660,584	564,423	2.70
Delray Beach Renourishment	---	---	---	3,949,117	1,408,713	2.63
St. Petersburg Beach Restoration	682,716	305,109	.50	---	---	---
Venice Beach Restoration	49,700	36,668	.17	---	---	---
Ft. Pierce Beach Restoration	621,288	150,041	1.30	---	---	---
Ft. Pierce Renourishment	---	---	---	1,559,431	493,259	1.30
Bal Harbour Restoration	4,962,420	819,154	.85	---	---	---
Indialantic/Melbourne Restoration	3,582,000	1,162,911	2.10	---	---	---
John U. Lloyd Restoration	2,945,262	784,340	1.50	---	---	---
Hollywood/Hallandale Restoration	7,743,376	2,825,513	4.73	---	---	---
Lido Key Restoration	360,000	150,000	.62	---	---	---
Miami Beach Restoration	49,892,000	14,530,114	9.65	---	---	---
North Redington Beach Restoration	369,000	247,125	.30	---	---	---
Jacksonville Beach Restoration	9,757,900	2,267,086	10.50	---	---	---
Mullet Key Restoration	649,878	97,483	1.20	---	---	---
Jupiter Island Restoration	3,574,221	716,332	4.60	---	---	---
Treasure Island Restoration	216,000	44,650	.40	---	---	---
Treasure Island Renourishment	---	---	---	1,228,000	314,500	1.70
Treasure Island Renourishment	---	---	---	1,796,970	573,750	.80
Total Restoration Projects	$ 92,742,258	$26,204,036	51.12	---	---	---
Total Renourishment Projects	---	---	---	$22,890,339	$7,186,614	16.18

Note: Total Restoration
Renourishment $115,632,597 $33,390,650 67.12
Cost per mile = 1,718,166 Renourishment
1,944,214 Restoration
Total Number of Projects 28 Restoration

Table 1.2. Expenditure on Individual Beach Restoration/Renourishment Projects, 1965-1984 (DNR, 1984).

project during this period. As you can see, Miami Beach restoration project was far the largest, with a listed cost of $49,892,000. The actual cost up to date probably exceeded 54 million. 14.4 million cubic yards of sand were placed on a stretch of beach about 10 miles long. More detailed information on beach restoration projects in the State of Florida can be found in literature compiled by Walton (1977) and Wang (1988).

During this period, technology of beach nourishment began to develop. The concept of overfill ratio was first proposed by Krumbein (1957) and Krumbein and James (1965) which allows rational estimation of the required volume of borrow material to retain a unit volume of beach material after nourishment and sorting by natural forces. The method of computation was further refined by Dean (1974), James (1975) and Hobson (1977). The ideal of equilibrium beach profile (Bruun, 1954; Dean, 1977; Moore, 1982) was applied to beach nourishment to determine the shape of original and nourished beaches. Since the 1970's computer modelings on shoreline changes were developed and were being applied to beach nourishment design. These models include one-line models, two-line models, N-line models, the GENESIS (Generalized Shoreline Change Numerical Model for Engineering Use, Hanson, 1987), dune erosion models, etc. Methods of beach nourishment have also expanded. In addition to the conventional approach of placing sand on the beach face through hydraulic dredging, feeder beach, inlet sand by- passing, perched beach, sub-aqueous nourishment, beach scraping, stock piling, and other means were all experimented. There was also a growing awareness of environmental concern. Environmental impact assessment now becomes an integral part of beach nourishment design. We also begin to see some effort in performance monitoring.

Outside the United States, the Netherlands and Germany are among the more active ones in beach nourishment engineering. Australia, Belgium and Singapore have also seen some limited activities.

In the Netherlands, beach nourishment was experimented as early as 1953 when 70,000 m^3 of sand was placed on the beach at Scheveningen (Edelman, 1960). Since then nourishment projects were carried out at numerous locations covering the entire coast of the country. Roelse (1986) compiled a list of 32 projects completed between 1952-1985. Figure 1.2 shows the locations of artificial beach nourishment along the Dutch Coast. Of these projects, the Hoek Van Holland project was the largest. During the years of 1971- 72, 18.94 million m^3 (24.92 million yd^3) were dredged from the entrance channel of Europort via hopper dredgers to create a beach 3300 m long and 900 m wide. This project serves the dual purposes of dredge spoil disposal and land reclamation. The cost of the project was at an amazingly low figure of 7.4 million DFL (approximately 3.9 million U.S. dollars). Even when converted to 1987 cost, it came to approximately 11 million dollars, or, $0.46/$yd^3$. This was an exceptional case. In general, the cost of dredging and placement in the Netherlands is about half that of a comparable job in the United States.

Since land reclamation and shore protection is a national priority in the Netherlands, considerable advances have been made there in beach nourishment technology even though they are a late comer on the scene. In fact, the first and, at present, the only artificial beach nourishment design manual was published by the Dutches (Manual, 1986).

In Germany, the major beach nourishment effort is along the 40 km shoreline of Island of Sylt. Sylt is the popular resort island in northern Germany. It is under heavy erosional stress with dune recession in excess of 1 m per year along the entire coast. Various nourishment projects were carried out since 1972 (Kramer, 1972; Fuhrboter, 1974; Gartner and Dette, 1987). On a per unit length basis, the stretch of beach is probably the most frequently nourished coast in the world. It is also the location where various nourishment schemes were tested on a prototype scale including various planforms - a unique sand groyne configuration, multiple sand groynes, rectangular shapes of different length to width ratios as well as various profile geometries - different proportions and slopes at different elevations. A performance monitoring program has been instituted since 1972. Therefore, it is one of the few nourishment projects, systematic monitoring and documentation were carried out on a long term basis.

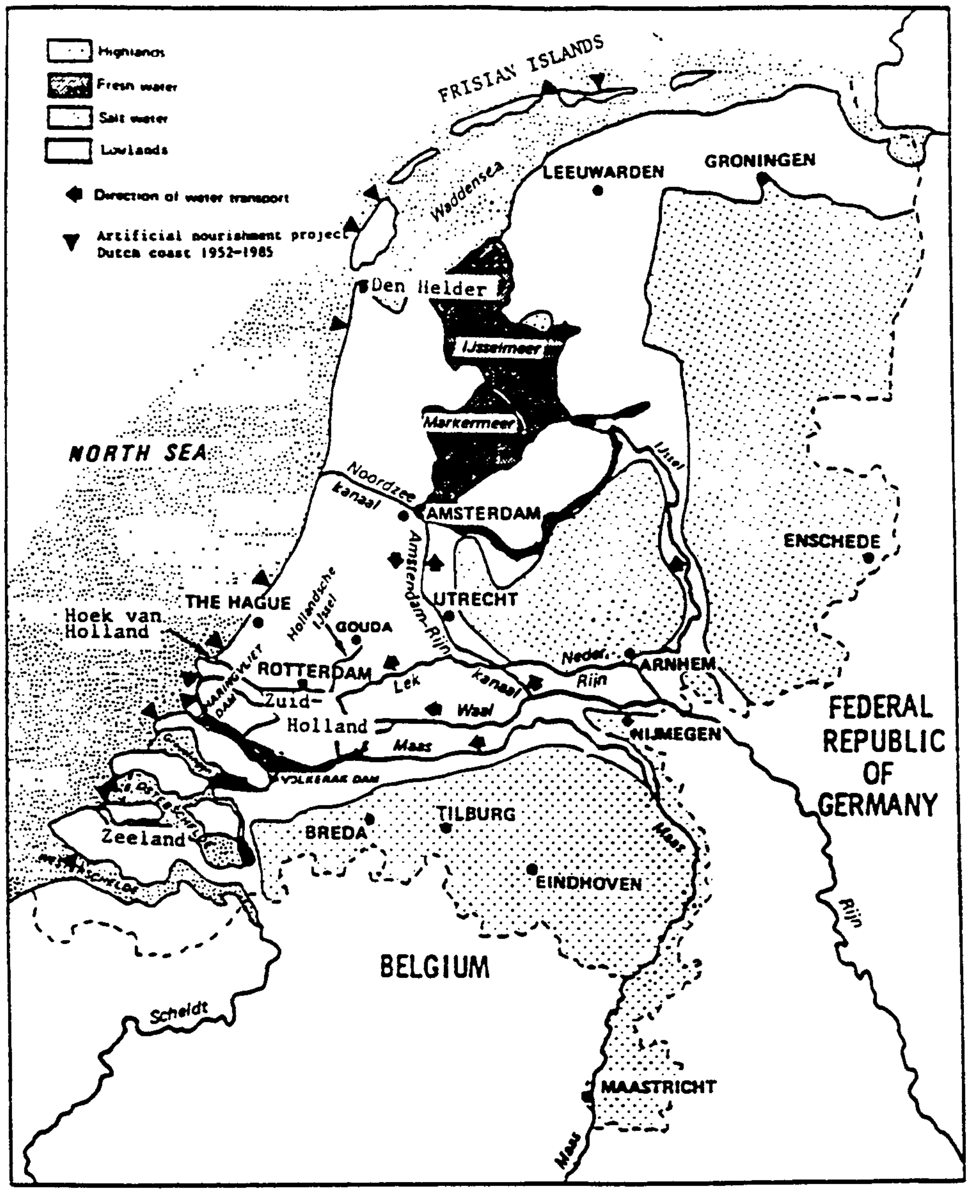

Figure 1.2. **Locations of Artificial Nourishment Along the Dutch Coast (Dutch Manual, 1986).**

Since the first project in the early 1920's, beach nourishment practice has developed from a simple sand dumping exercise into a multi-facet engineering work. We also witnessed significant increases in project activities in the last two decades. The trend is most certainly to continue perhaps at an accelerated rate. The reasons behind the projected increase in activities are:

1. Shorelines are deteriorating at a national scale.

2. Shoreline hardening practice becomes increasingly undesirable and, at certain instances, is no longer permitted.

3. Spreading the coast over a period is politically more palatable than one-time large expenditure.

In the State of Florida, a coastal restoration task force was organized by the Governor in 1985 to examine the existing coastal condition and to provide guidance in the long term strategy of coastal restoration. Of the 800 miles of sandy shoreline around Florida, 543 miles were identified as erosional, again of which 140 miles (224 Km) were considered critically eroding, (Figure 1.3). A ten-year program for the restoration and maintenance of Florida's critically-eroded beaches was proposed by the Florida Department of Natural Resources (DNR) at an initial estimated cost of \$362 million with an additional \$110 million during that ten-year period to be used for periodic renourishment of restored beaches (DNR, 1985, 1986). Similar programs are also expected in other coastal states and in other countries. Germany, for instance, has a five-year program to preserve the beach and dunes for the island of Sylt requiring 20 million m^3 of material at a cost of \$80 million. Japan, where coastal protection is of national priority but presently has no or very limited beach nourishment programs, is also aggressively looking into the soft structure approach as the future solution.

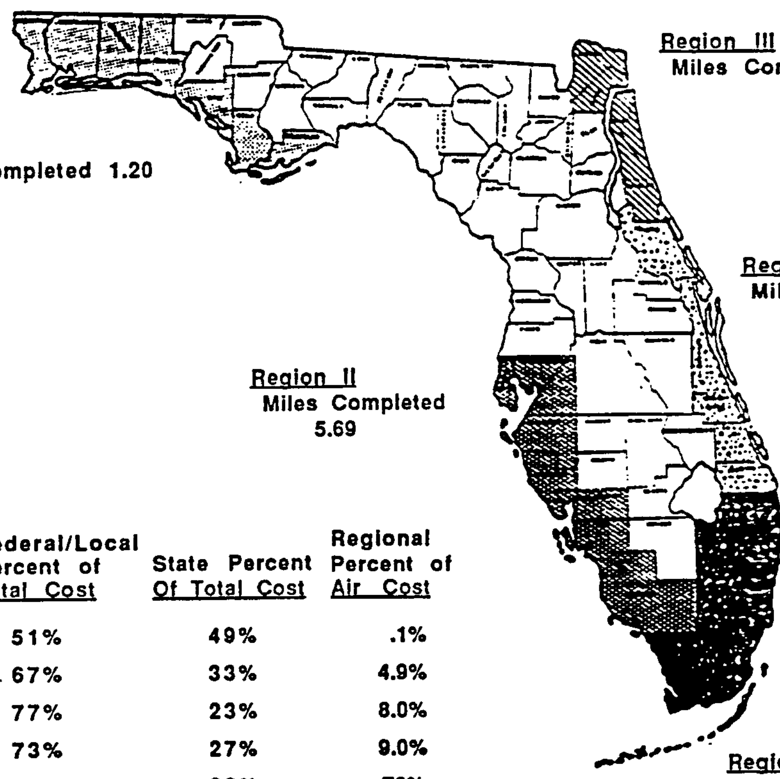

Region	Federal/Local Percent of Total Cost	State Percent Of Total Cost	Regional Percent of Air Cost
I	51%	49%	.1%
II	67%	33%	4.9%
III	77%	23%	8.0%
IV	73%	27%	9.0%
V	71%	29%	78%
Total	71%	29%	100.9%

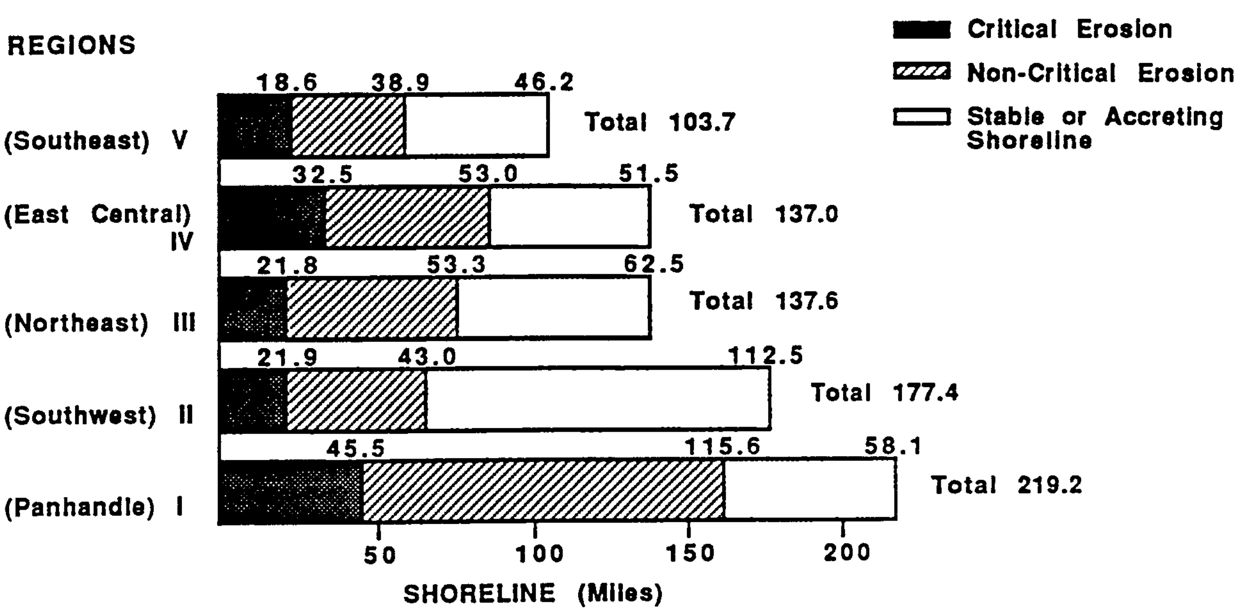

Figure 1.3. Present Erosional Condition Along Florida Coast (DNR, 1985).

MAJOR STEPS IN PROJECT PLANNING

Beach nourishment project planning is still by and large a trial and error process requiring numerous iterations. It is complex and time consuming and it is not uncommon that a project from its incipiency to its implementation could take 5 to 10 years. Planning is, however, critical to the success or even the survival of the project.

In the State of Florida, dredge and fill operations, such as beach restoration which are conducted on the sovereignty lands of the State must be authorized by various regulatory agencies including the Department of Natural Resources, Department of Environmental Regulations, Department of State, Board of Trustees of the Internal Improvement Trust Fund and the U.S. Army Corps of Engineers. If the beach is in the county or city jurisdiction local permits have to be obtained as well. The process of obtaining all the various approval and the collecting and providing of the necessary information to obtain these approvals is time consuming. If the project is to be coast shared by the Federal dollars, a feasibility study must be conducted to show justifiable cost/benefit from the Federal level for project authorization. Projects needing State and Federal fundings can then be submitted to the State Legislature or to the Congress for appropriation. During the process, if excessive funds are expended for project preparation, cost overruns could dissuade the Legislators for project fundings. Furthermore, certain aspects of the project such as shoreline position and sand sources could change or become outdated requiring costly restudy. Therefore, timely and controlled project planning is essential to insure successful project implementation.

The major steps involved in a beach nourishment project are illustrated by the following block diagram:

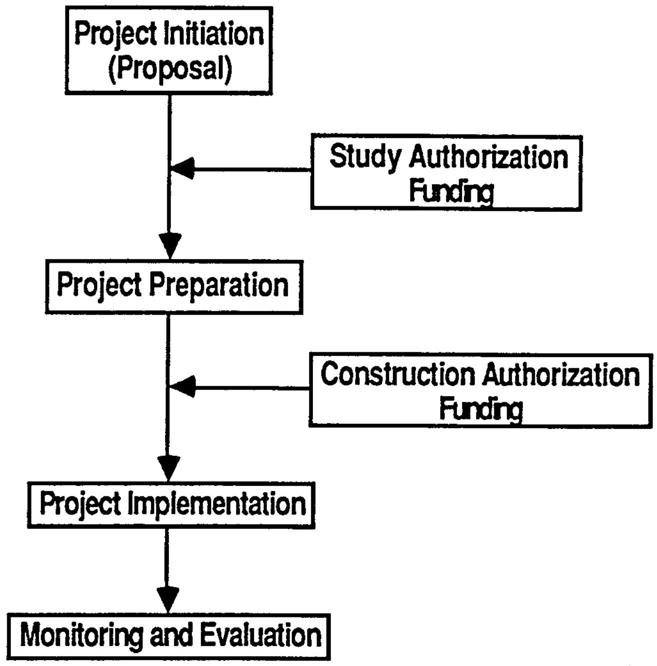

Elements required to accomplish each step are given as follows:

1. Problem Proposal

A). Problem Evaluation

Existing erosion problem

History of efforts and their effectiveness

B). Alternative Solutions

C.) Project Definition

- Requirements - storm protection, recreation, shoreline restoration
- Alternative sand sources - offshore borrow areas, inlet by-passing, etc.

D). Preliminary Cost Analysis

E). Beach Access Analysis

F). Cost/Benefit Analysis

G). Environmental Statement

2. Project Preparation

   A). Engineering

   B). Environmental Impact Study

   C). Cost Estimation

   D). Financing

   E). Permitting

   F). Project Authorization and Documentation

3. Project Implementation

   A). Bidding and Tendering

   B). Pre-Construction Survey

   C). Construction Management and Monitoring

   D). Acceptance

   E). Post-Project Monitoring and Evaluation

   F). Maintenance

The elements listed in each step are usually not independent of each other. Therefore, iterations are expected within each step and sometimes across the steps.

Of course, the tangible product of the whole exercise is the engineering work of a nourished beach. This is also the main topic of the short course. An engineering design is influenced by many factors, such as environmental effects, cost, sand sources, delivery systems, etc. The intent of the course is to provide an overview of a complete engineering design practice. A flow chart such as presented in the Dutch Manual on Beach Nourishment (1986) can be used to aid in the design process. Figure 1.4 presents a flow chart for beach nourishment engineering.

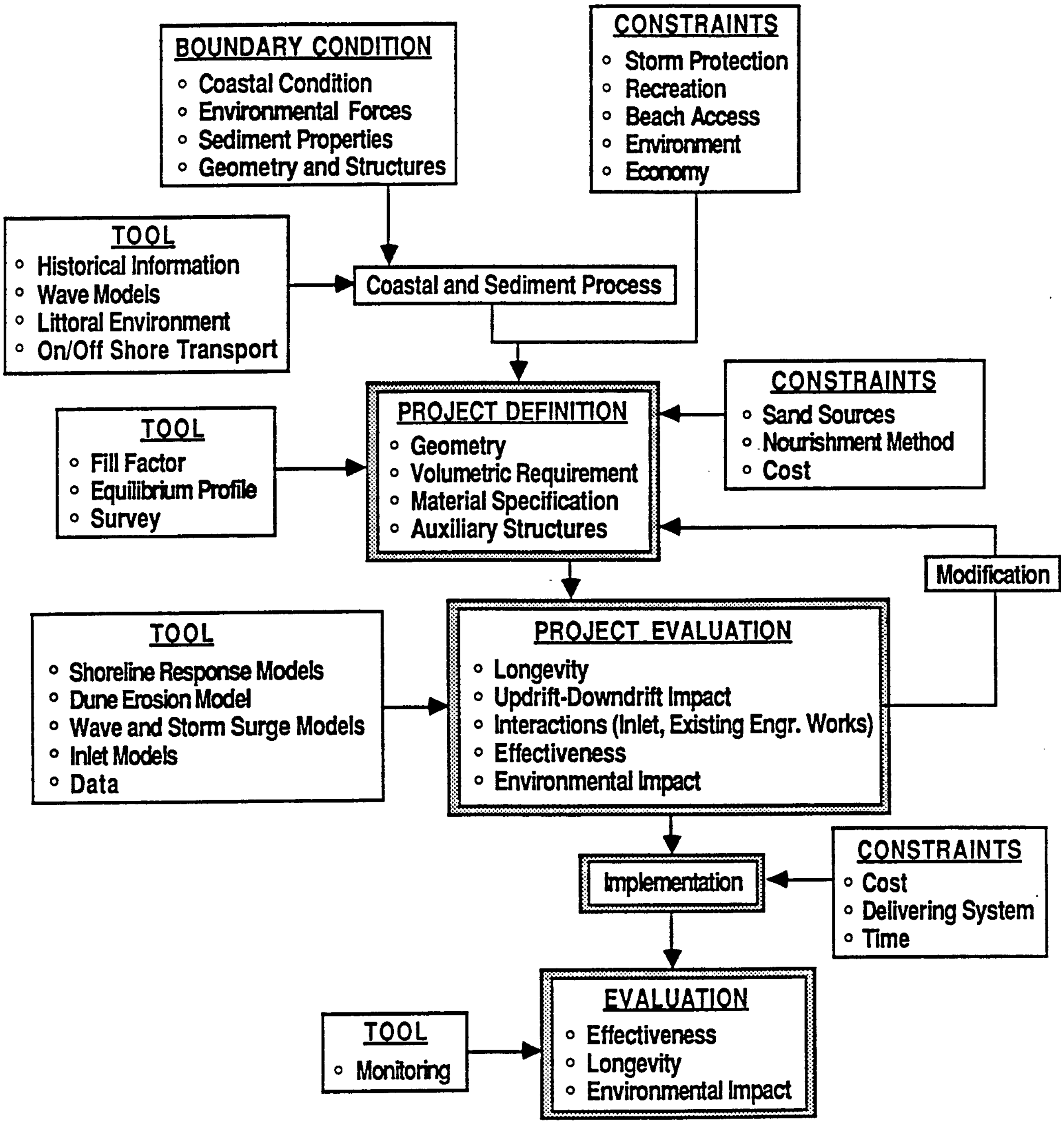

Figure 1.4. Beach Nourishment Design Flow Chart.

REFERENCES

Bruun, P. (1954) Coast Erosion and the Development of Beach Profiles, *U.S. Army Beach Erosion Board* Tech. Memo. No. 44.

Dean, R. G. (1974) Compatibility of Borrow Material for Beach Fills, *Proc. 14th Coastal Engineering Conf.*, ASCE, Copenhagen, Denmark.

Dean, R. G. (1977) Equilibrium Beach Profiles: U.S. Atlantic and Gulf Coasts, Tech. Rep. No. 12, *University of Delaware*, Newark.

DNR (1984) Beach Restoration: A State Initiative, *Florida Department of Natural Resources* Tallahassee, FL.

DNR (1986) A Proposed Comprehensive Beach Management Program for the State of Florida, *Florida Department of Natural Resources*, Tallahassee, FL.

Dutch Manual (1986) *Manual on Artificial Beach Nourishment*, Rijkswaterstaat (Dutch Public Works Department) Delft, The Netherlands.

Fuhrboter, A. (1974) A Refraction Groin Built by Sand, *Proc. 147th Coastal Engineering Conf.*, Copenhagen, Denmark.

Gartner, J., and Dette, H. H. (1987) Design and Performance of Large Scale Nourishments, *Proc. Coastal & Engineering in Developing Countries*, Beijing, China, pp 181-196.

Hall, Jr., J.V. (1952) *Artificially Nourished and Constructed Beaches* Beach Erosion Board, Tech. Memo, No. 29.

Hanson, H. (1987) GENESIS, A Generalized Shoreline Change Numerical Model for Engineering Use, *Lund Univ.*, Pep. No. 1007, Lund, Sweden.

Hobson, R. D. (1977) Sediment Handling and Beach Fill Design, *Coastal Sediments 77*, ASCE, Charleston, S.C.

James, W. R. (1975) Techniques in Evaluating Suitability of Borrow Material for Beach Nourishment, *U.S. Army Coast al Engineering Research Ctr.*, Tech. Memo, No. 60.

Kramer, J. (1972) Artificial Beach Nourishment on the German North Sea Coast, *Proc. 137th Coastal Eng. Conf.*, Vancouver, B.C., Canada.

Krumbein, W. C. (1975) A Method for Specification of Sand for Beach Fills, *Beach Erosion Board*, Tech. Memo, No. 102.

Krumbein, W. C., and James, W. R. (1965) A Log-Normal Size Distribution Model for Estimating Stability of Beach Fill Material, *U.S. Army, Coastal Eng. Res. Ctr.*, Tech. Memo. No. 16.

Moore, B. (1982) Beach Profile Evolution in Response to Changes in Water Level and Wave Height, *M.S. Thesis*, Dept. of Civil Engr., Univ. of Del., Newark, DE.

Roelse, P. (1986) Artificial Nourishment as Coastal Defense in the Netherlands Previous Fills, Future Development, Amex IV *Artificial Beach Nourishment Manual*, Ministry of Transport and Public Work, The Netherlands.

Wang, W. C. (1988) List of Literature Related to the Beach Restoration Projects in the State of Florida. *Technical Rep.*, Coastal Engr. Dept., Univ. of Florida, Gainesville, FL (in preparation).

Walton, Jr., T. L. (1977) Beach Nourishments in Florida and on the Lower-Atlantic and Gulf Coasts. *UFL/COEL-77/031*, Coastal and Oceano. Engr. Dept., Univ. of Florida, Gainesville, FL.

Tonya, C. and Pilkey, O. (1988) An Historical Survey of Beach Replenishment on the U.S. Atlantic Barrier Coast: Good News for Florida, *Beach Preservation Technology Conf.*, Gainesville, FL.

Chapter 2

ENGINEERING DESIGN PRINCIPLES: PART I - DESIGN

Robert G. Dean
Coastal & Oceanographic Engineering Department
University of Florida, Gainesville

INTRODUCTION

It is convenient to discuss the physical performance of beach nourishment projects in terms of the cross-shore response (or profile adjustment) and longshore response, i.e. transport of sand out of the area placed. it is also convenient in exploring performance at the conceptual level to utilize idealized considerations and simplified (linearized) equations in some cases. This allows one to obtain a grasp or overview of the importance of the different variables without the problem of being clouded by complications which may be significant at the 10% - 20% level. To simplify our cross-shore considerations, we will use the so- called equilibrium beach profile concept in which the depth $h(y)$ is related to the distance offshore, y, by the scale parameter, A, in the form

$$h(y) = Ay^{2/3} \tag{2.1}$$

Although this is not a universally valid form, it serves to capture many of the important characteristics of equilibrated beach profiles. To assist in providing an overview of transport in the longshore direction, we will utilize the linearized combined form of the transport and continuity equations first developed by Pelnard Consideré

$$\frac{\partial y}{\partial t} = G\frac{\partial^2 y}{\partial x^2} \tag{2.2}$$

where x is the longshore distance, t is time, G is a "longshore diffusivity" which depends strongly on the wave height mobilizing the sediment and Eq. (2.2) is recognized as the "heat conduction equation".

CROSS-SHORE RESPONSE

Beach Width Gained vs. Sediment Quality

From Fig. 2.1, it is seen that the scale parameter, A, in Eq. (2.1) increases with increasing sediment size. Thus, as presented in Fig. 2.2, a finer sediment will be associated with a milder sloped profile than one composed of coarse sediment. We will denote the native and fill profile scale parameters as A_N and A_F, respectively. The consequence of sand size to beach nourishment is that the coarser the nourishment material, the greater the dry beach width per unit volume placed.

Nourished beach profiles can be designated as "intersecting", "non-intersecting", and "submerged" profiles. Figure 2.3 presents examples of these. Referring to the top panel in this figure of intersecting profiles, a necessary but not sufficient requirement for intersecting profiles is that the fill material be coarser than the native material. One can see that an advantage of such a profile is that the nourished profile "toes in" to the native profile thereby negating the need for material to extend out to the closure depth. The second type of profile is one that would usually occur in most beach nourishment projects. Nonintersecting profiles occur if the nourished material grain size is equal to or less than the native grain size. Additionally, this profile always extends out to the closure depth, h_*. The third type of profile that can occur is the submerged profile (Fig. 2.3c) the characteristics of which are shown in greater detail in Fig. 2.4. This profile type requires the nourished material to be finer than the native. It can be shown that if only a small amount of material is used then all of this material will be mobilized by the breaking waves and moved offshore to form a

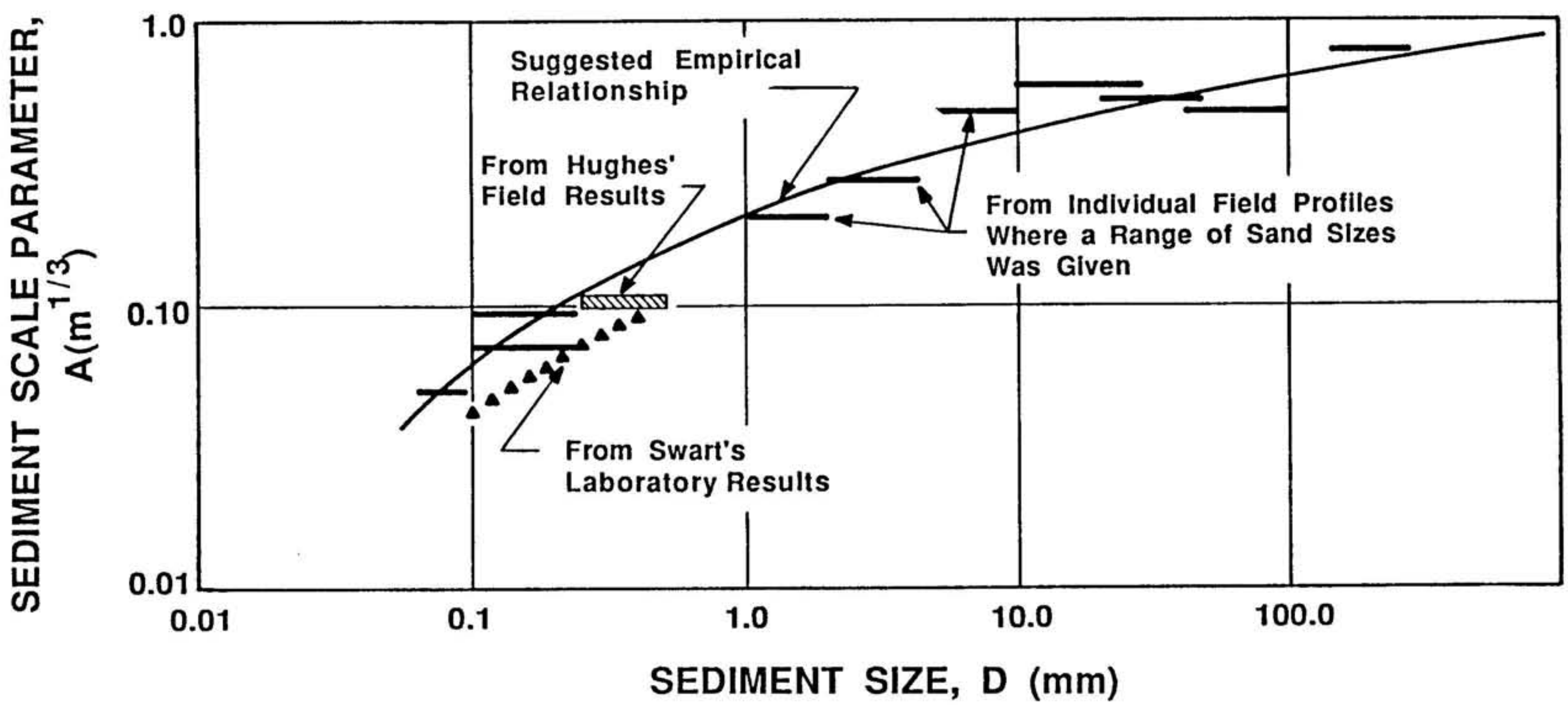

Figure 2.1. Beach Profile Factor, A, vs. Sediment Diameter, D, in Relationship $h = Ay^{2/3}$ (Modified from Moore, 1982).

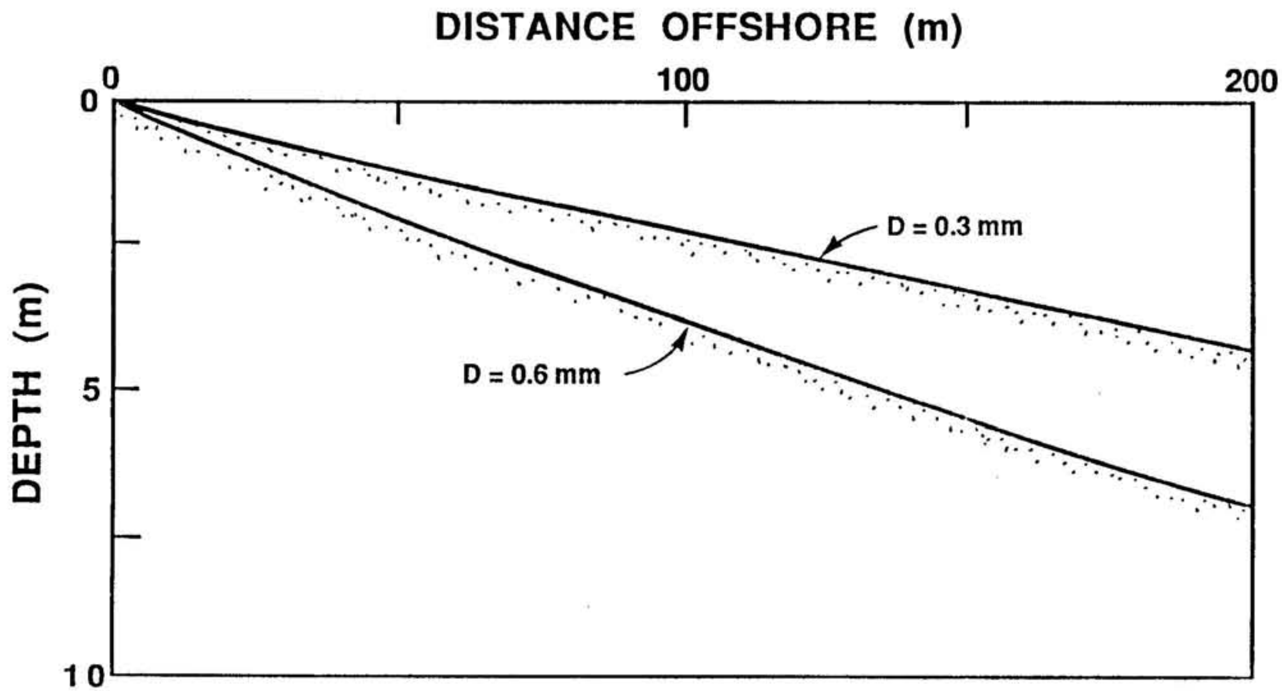

Figure 2.2 Equilibrium Beach Profiles for Sand Sizes of 0.3 mm and 0.6 mm
$A(D = 0.3\ mm) = 0.12\ m^{1/3}$; $A(D = 0.6\ mm) = 0.20\ m^{1/3}$.

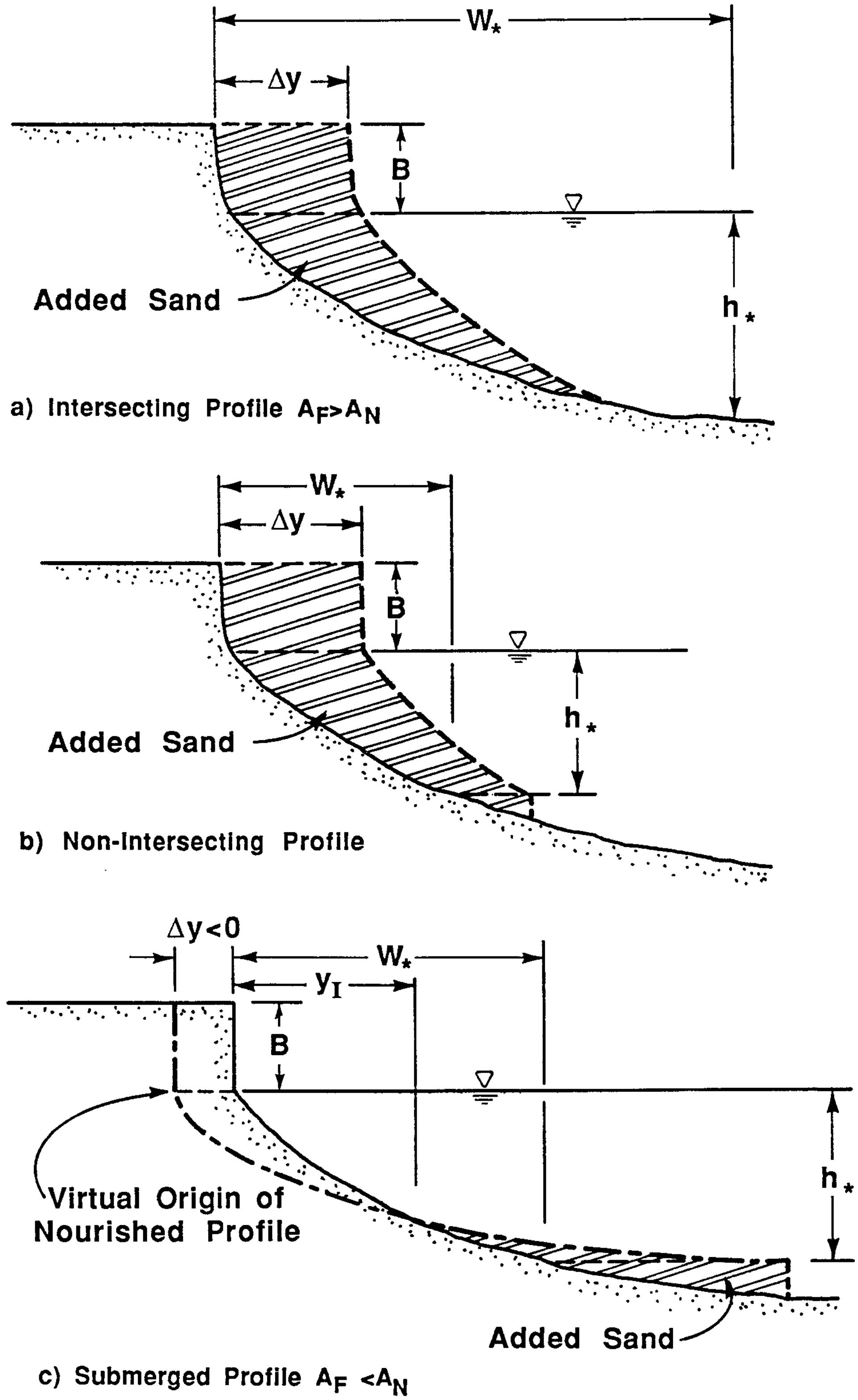

Figure 2.3. Three Generic Types of Nourished Profiles.

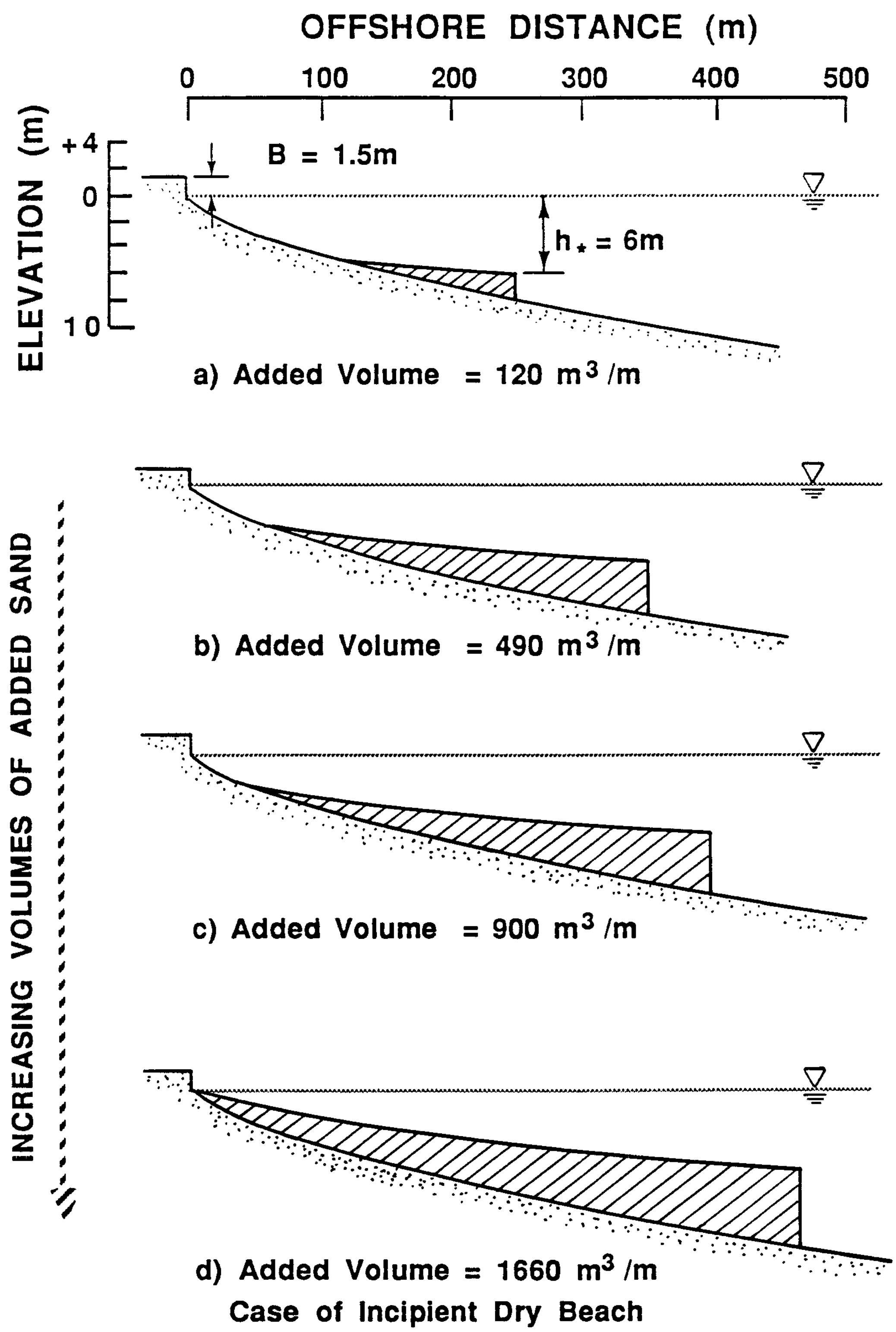

Figure 2.4 Effect of Increasing Volume of Sand Added on Resulting Beach Profile. A = 0.1 $m^{1/3}$, A = 0.2 $m^{1/3}$, h_* = 6 m, B = 1.5 m.

small portion of the equilibrium profile associated with this grain size as shown in the upper panel. With increasing amounts of fill material, the intersection between the nourished and the original profile moves landward until the intersection point is at the water line. For greater quantities of material, there will be an increase in the dry beach width, Δy, resulting in a profile of the second type described.

Figure 2.5 illustrates the effect of placing the same volume of four different sized sands. In Fig. 2.5a, sand coarser than the native is used and a relatively wide beach Δy is obtained. In Fig. 2.5b, the same volume of sand of the same size as the native is used and the dry beach width gained is less. More of the same volume is required to fill out the milder sloped underwater profile. In Fig. 2.5c, the placed sand is finer than the native and much of the sand is utilized in satisfying the milder sloped underwater profile requirements. In a limiting case, shown in Fig. 2.5d, no dry beach is yielded with all the sand being used to satisfy the underwater requirements.

We can quantify the results presented in Fig. 2.5 for beach widening through nourishment by utilizing equilibrium profile concepts. It is necessary to distinguish two cases. The first is with intersecting profiles such as indicated in Fig. 2.3a and requires $A_F > A_N$. For this case, the volume placed per unit shoreline length, $\mathcal{V}_1$ associated with a shoreline advancement, Δy, is presented in non-dimensional form as

$$\frac{\mathcal{V}_1}{BW_*} = \frac{\Delta y}{W_*} + \frac{3}{5}\frac{h_*}{B}\left(\frac{\Delta y}{W_*}\right)^{5/3} \frac{1}{\left[1 - \left(\frac{A_N}{A_F}\right)^{3/2}\right]^{2/3}} \tag{2.3}$$

in which B is the berm height, W_* is a reference offshore distance associated with the breaking depth, h_*, on the original (unnourished) profile, i.e.

$$W_* = \left(\frac{h_*}{A_N}\right)^{3/2} \tag{2.4}$$

and the breaking depth, h_* and breaking wave height, H_b are related by

$$h_* = H_b/\kappa$$

with $\kappa(\approx 0.78)$, the spilling breaking wave proportionality factor. Figure 2.6 presents an estimate of h_* around the Florida shoreline.

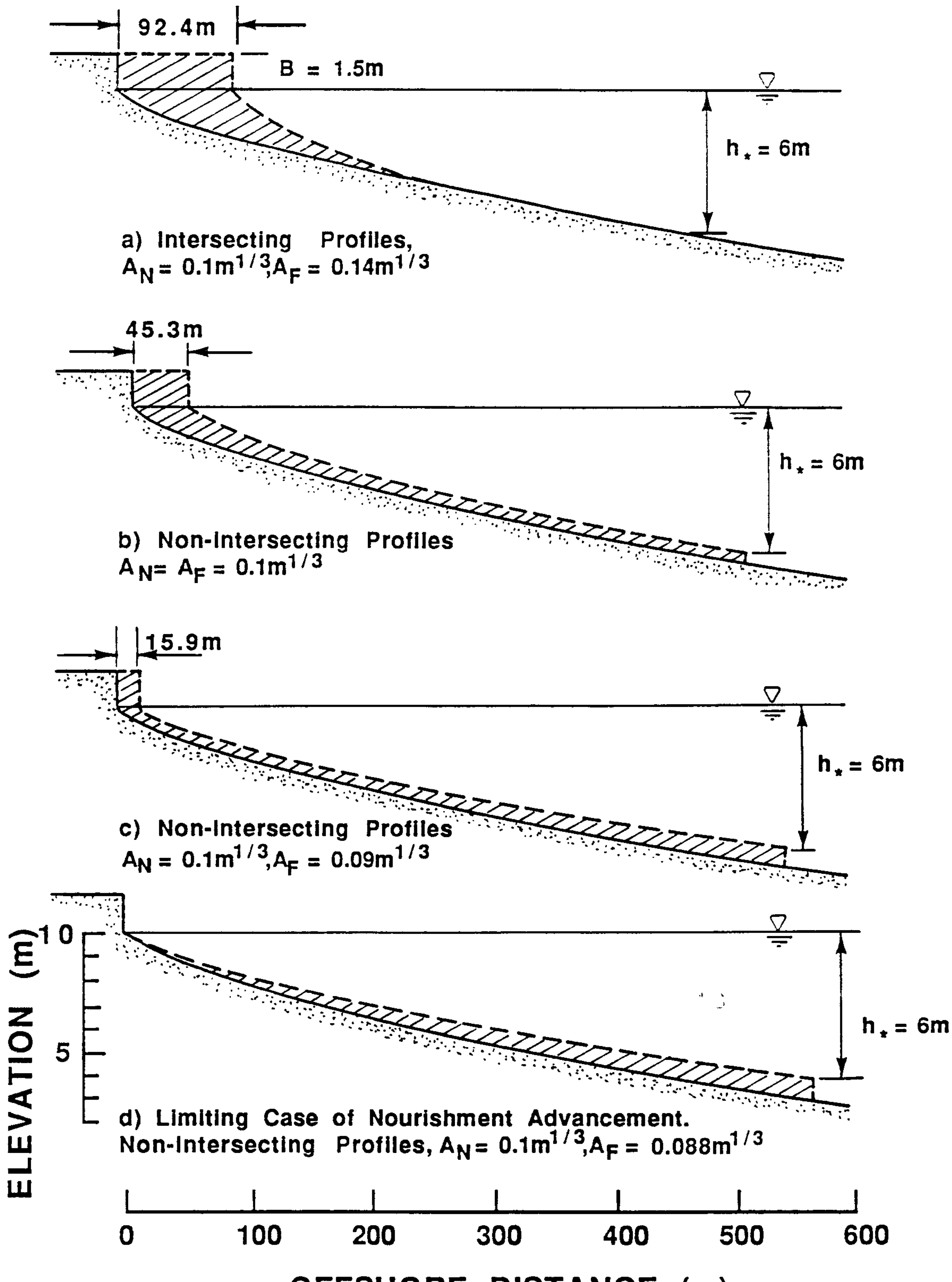

Figure 2.5. Effect of Nourishment Material Scale Parameter, A_F, on Width of Resulting Dry Beach. Four Examples of Decreasing A_F.

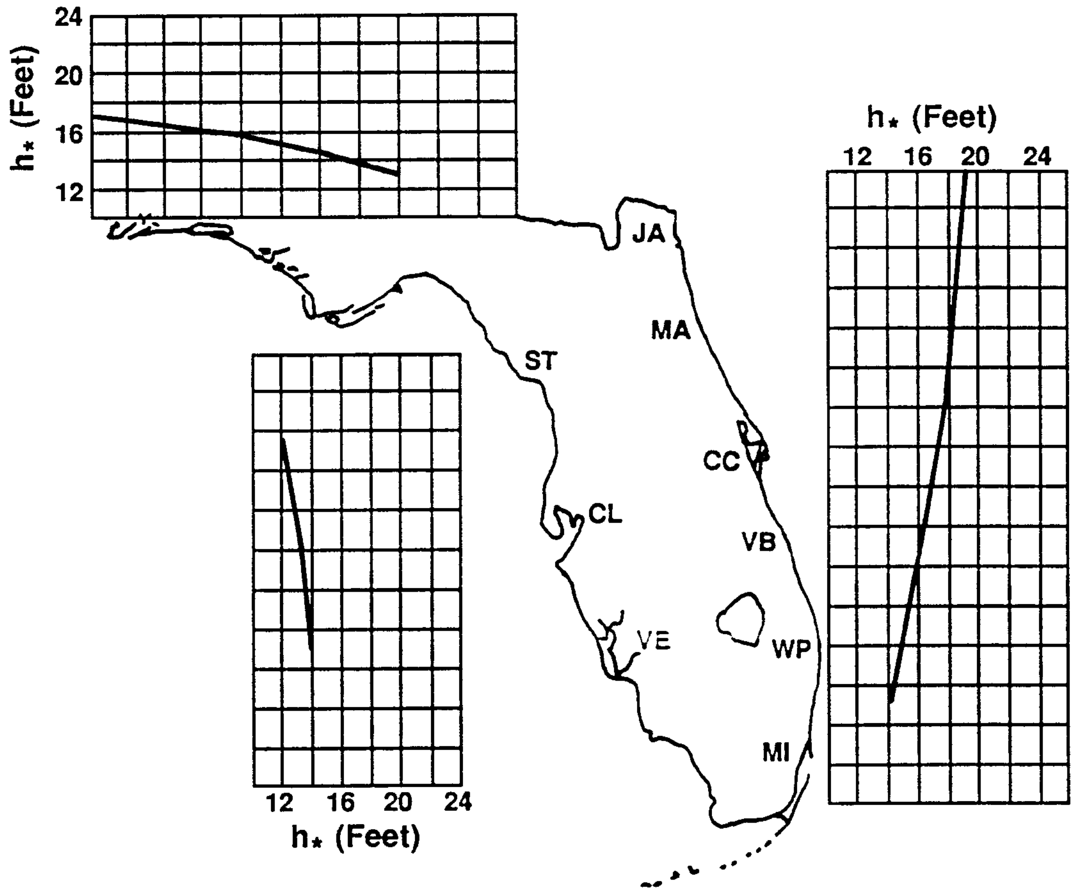

Figure 2.6 Recommended Distribtuion of h_* Along the Sandy Shoreline of Florida.

For non-intersecting profiles, Figures 2.3b and 2.5b,c and d, the corresponding volume $\text{\textit{V}}_2$ in non-dimensional form is

$$\frac{\text{\textit{V}}_2}{W_* B} = \left(\frac{\Delta y}{W_*}\right) + \frac{3}{5}\left(\frac{h_*}{B}\right)\left\{\left[\frac{\Delta y}{W_*} + \left(\frac{A_N}{A_F}\right)^{3/2}\right]^{5/3} - \left(\frac{A_N}{A_F}\right)^{3/2}\right\} \tag{2.5}$$

It can be shown that the critical value $(\Delta y/W_*)_c$ for intersection/non-intersection of profiles is given by

$$\left(\frac{\Delta y}{W_*}\right)_c = 1 - \left(\frac{A_N}{A_F}\right)^{3/2} \tag{2.6}$$

with intersection occurring if $\Delta y/W_*$ is less than the critical value.

The critical volume associated with intersecting/non- intersecting profiles is

$$\left(\frac{\text{\textit{V}}}{BW_*}\right)_{c1} = \left(1 + \frac{3}{5}\frac{h_*}{B}\right)\left[1 - \left(\frac{A_N}{A_F}\right)^{3/2}\right] \tag{2.7}$$

and applies only for $(A_F/A_N) > 1$. Also of interest, the critical volume of sand that will just yield a finite shoreline displacement for non-intersecting profiles ($A_F/A_N < 1$), is

$$\left(\frac{\text{\textit{V}}}{BW_*}\right)_{c2} = \frac{3}{5}\frac{h_*}{B}\left(\frac{A_N}{A_F}\right)^{3/2}\left\{\frac{A_N}{A_F} - 1\right\} \tag{2.8}$$

Figure 2.7 presents these two critical volumes versus the scale parameter ratio A_F/A_N for the special case $h_*/B = 4.0$.

The results from Eqs. (2.3), (2.5) and (2.6) are presented in graphical form in Figs. 2.8 and 2.9 for cases of $(h_*/B) = 2$ and 4 respectively. Plotted is the non-dimensional shoreline advancement $(\Delta y/W_*)$ versus the ratio of fill to native sediment scale parameters, A_F/A_N, for various isolines of dimensionless fill volume $\text{\textit{V}}' \left(= \frac{\text{\textit{V}}}{W_* B}\right)$ per unit length of beach. It is interesting that the shoreline advancement remains more or less constant for $A_F/A_N > 1$; for smaller values the additional shoreline width decreases rapidly. For A_F/A_N values slightly smaller than plotted, there is no beach width gain, i.e. as in Fig. 2.5d.

Effects of Sea Level Rise on Beach Nourishment Quantities

Recently developed future sea level scenarios developed based on assumed fossil fuel consumption and other relevant factors have led to concern over the viability of the beach

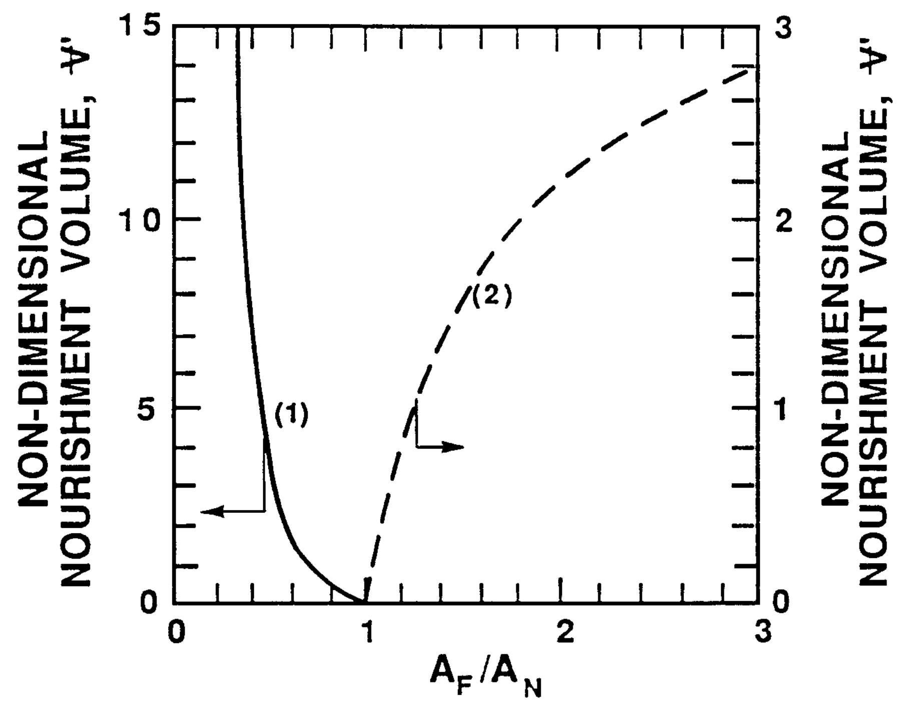

Figure 2.7. (1) Volumetric Requirement for Finite Shoreline Advancement (Eq. 2.8); (2) Volumetric Criterion for Intersecting Profiles (Eq. 2.7). Variation with A_F/A_N. Results Presented for $h_*/B = 4.0$

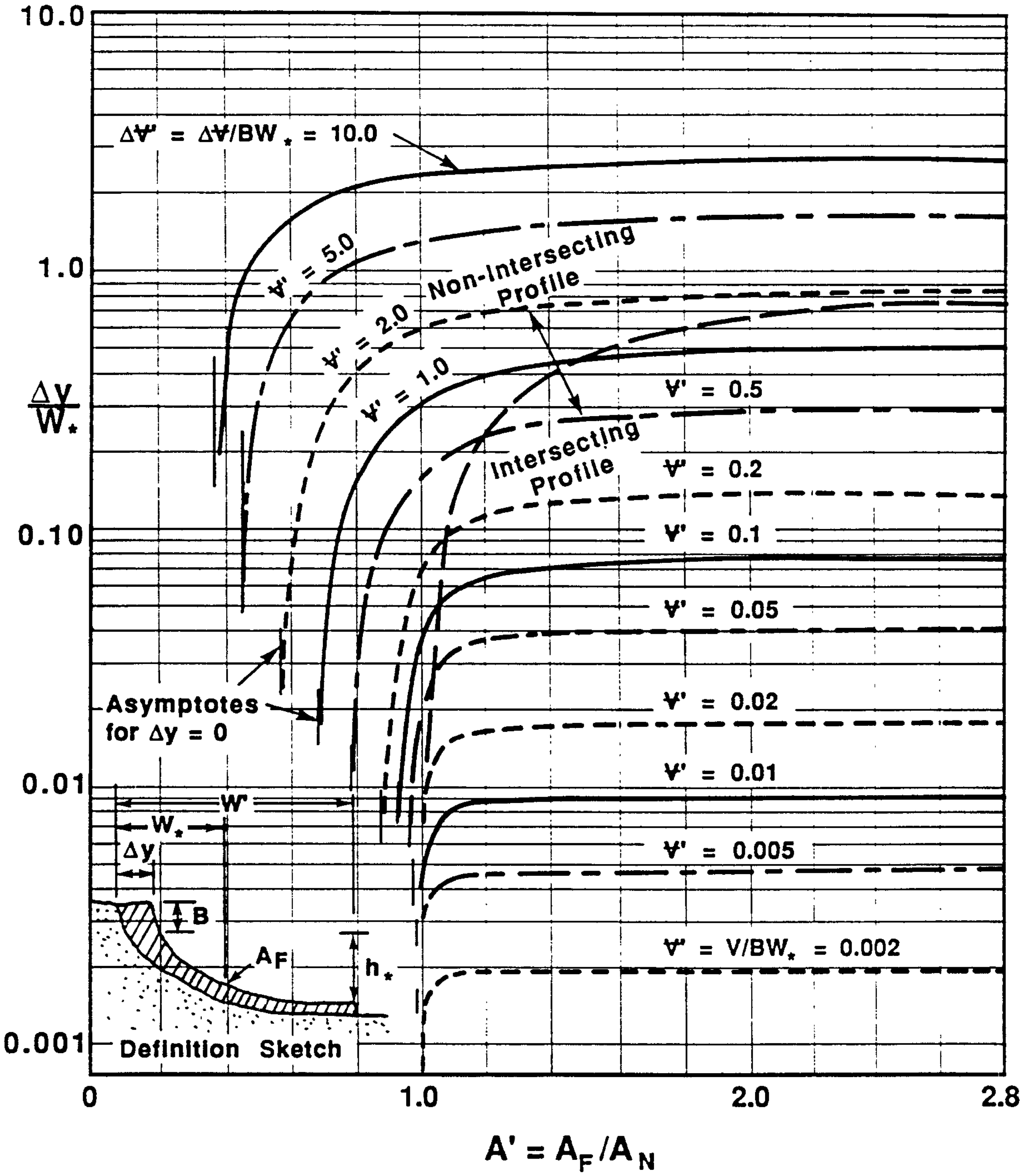

Figure 2.8. Variation of Non-Dimensional Shoreline Advancement $\Delta y/W_*$ With A' and $\forall'$. Results Shown for $h_*/B = 2.0$

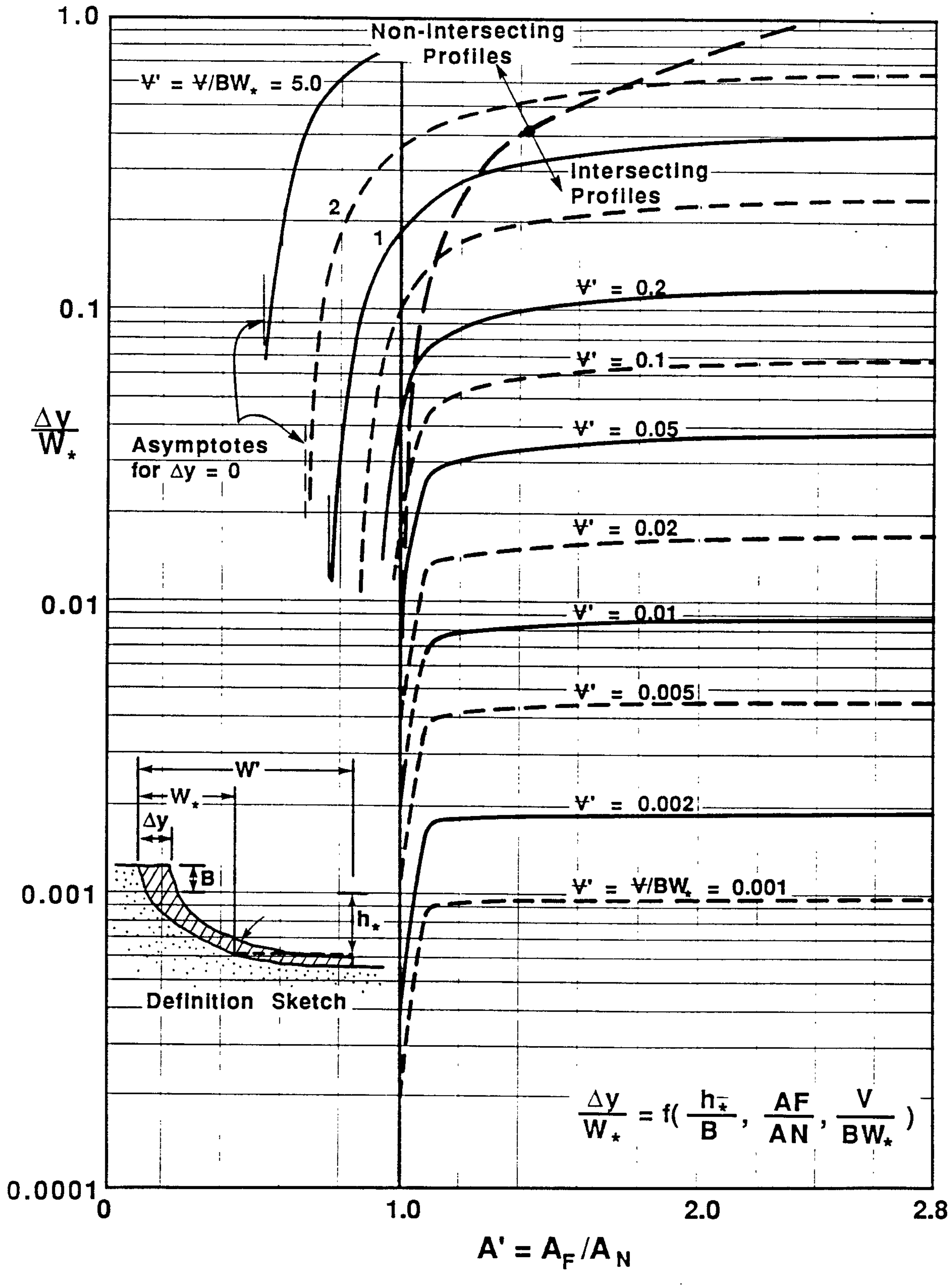

Figure 2.9. Variation of Non-Dimensional Shoreline Advancement $\Delta y/W_*$ With A' and ∀'. Results Shown for $h_*/B = 4.0$

nourishment option. First, in the interest of objectivity, it must be said that the most extreme of the scenarios published by the Environmental Protection Agency (EPA) which amounts to over 11 ft. by the year 2100 are extremely unlikely. While it is clear that worldwide sea level has been rising over the past century and is highly likely to increase in the future, the future rate is very poorly known. Moreover, probably at least 20 to 40 years will be required before our confidence level of future sea level rise rates will improve substantially. Within this period, it will be necessary to assess the viability of beach restoration on a project-by-project basis in recognition of possible future sea level increases. Presented below is a basis for estimating nourishment needs for the scenario in which there is no sediment supply across the continental shelf and there is a more-or-less well-defined seaward limit of sediment motion; in the second case the possibility of onshore sediment transport will be discussed.

Case I - Nourishment Quantities for the Case of No Onshore Sediment Transport

Bruun's Rule (1962) is based on the consideration that there is a well-defined depth limit of sediment transport. With this assumption, the only response possible to sea level rise is seaward sediment transport. Considering the shoreline change Δy, to be the superposition of recession due to sea level rise Δy_S and the advancement due to beach nourishment, Δy_N,

$$\Delta y = \Delta y_S + \Delta y_N \tag{2.9}$$

and, from Bruun's Rule

$$\Delta y_S = -S \frac{W_\star}{h_\star + B} \tag{2.10}$$

in which S is the sea level rise, $W_\star$ is the distance from the shoreline to the depth, $h_\star$, associated with the seaward limit of sediment motion and B is the berm height. Assuming that compatible sand is used for nourishment (i.e. $A_F = A_N$)

$$\Delta y_N = \frac{\mathcal{V}}{h_\star + B} \tag{2.11}$$

and $\mathcal{V}$ is the beach nourishment volume per unit length of beach. Therefore

$$\Delta y_N = \frac{1}{(h_\star + B)} \left[\mathcal{V} - S W_\star\right] \tag{2.12}$$

The above equation can be expressed in rates by,

$$\frac{dy}{dt} = \frac{1}{(h_* + B)}\left[\frac{dV}{dt} - W_*\frac{dS}{dt}\right] \tag{2.13}$$

where $\frac{dS}{dt}$ now represents the rate of sea level rise and $\frac{dV}{dt}$ is the rate at which nourishment material is provided. It is seen from Eq. (2.13) that in order to maintain the shoreline stable due to the effect of sea level rise the nourishment rate $\frac{dV}{dt}$ is related to the rate of sea level rise $\frac{dS}{dt}$ by

$$\frac{dV}{dt} = W_*\frac{dS}{dt} \tag{2.14}$$

Of course, this equation only applies to cross-shore mechanisms and therefore does not recognize any background erosion, or longshore transport (so-called "end losses"). It is seen that W_* behaves as an amplifier of material required. Therefore, it is instructive to explore the nature of W_* and it will be useful for this purpose to consider an equilibrium profile given by

$$h = Ay^{2/3}$$

in which A is the scale parameter presented in Fig. 2.1. Using the spilling breaking wave approximation

$$h_* = \frac{H_b}{\kappa} = A\,W_*^{2/3}$$

then

$$W_* = \left(\frac{H_b}{\kappa A}\right)^{3/2} \tag{2.15}$$

i.e. W_* increases with breaking wave height and with decreasing A (or sediment size).

Case II - Nourishment Quantities for the Case of Onshore Sediment Transport

Evidence is accumulating that in some locations there is a substantial amount of onshore sediment transport. Dean (1987) has noted the consequences of the assumption of a "depth of limiting motion" in allowing only offshore transport and proposed instead that if this assumption is relaxed, onshore transport can occur leading to a significantly different response to sea level rise. Recognizing that there is a range of sediment sizes in the active profile and adopting the hypothesis that a sediment particle of given hydraulic characteristics is in equilibrium under certain wave conditions and at a particular water depth, if sea level rises, then our reference particle will seek equilibrium which requires landward rather than seaward transport as resulting from the Bruun Rule. Figure 2.10 summarizes some of the elements of this hypothesis.

Turning now to nourishment requirements in the presence of onshore sediment transport, the conservation of cross-shore sediment yields

$$\frac{\partial Q}{\partial y} = \frac{\partial h}{\partial t} + \text{sources} - \text{sinks} \tag{2.16}$$

in which h is the water depth referenced to a fixed vertical datum and the sources could include natural contributions such as hydrogenous or biogenous components, and suspended deposition or human related contributions, i.e. beach nourishment. Sinks could include removal of sediment through suspension processes. Eq. (2.16) can be integrated seaward from a landward limit of no transport to any location, y

$$Q(y) - \int_0^y (\text{sources - sinks})dy = \int_0^y \frac{\partial h}{\partial t} dy \tag{2.17}$$

If only natural processes are involved and there are no gradients of longshore sediment transport, the terms on the left hand side of Eq. (2.17) represent the net rate of increase of sediment deficit as a function of offshore distance, y. For y values greater than the normal width, W_*, of the zone of active motion, the left hand side can be considered as representing the "ambient" deficit rate due to cross-shore sediment transport resulting from long-term disequilibrium of the profile and source and sink terms.

In attempting to apply Eq. (2.17) to the prediction of profile change and/or nourishment needs under a scenario of increased sea level rise, it is reasonable to assume that over the next several decades the ambient deficit rate (or surplus) of sediment within the active zone will remain constant. However, an increased rate of sea level rise will cause an augmented demand which can be quantified as $W_* \left[\left(\frac{dS}{dt}\right) - \left(\frac{dS}{dt}\right)_0\right]$ in which $\left(\frac{dS}{dt}\right)_0$ is the reference sea level change rate during which time the ambient demand rate is established. Thus the

POSSIBLE MECHANISM OF SEDIMENTARY EQUILIBRIUM

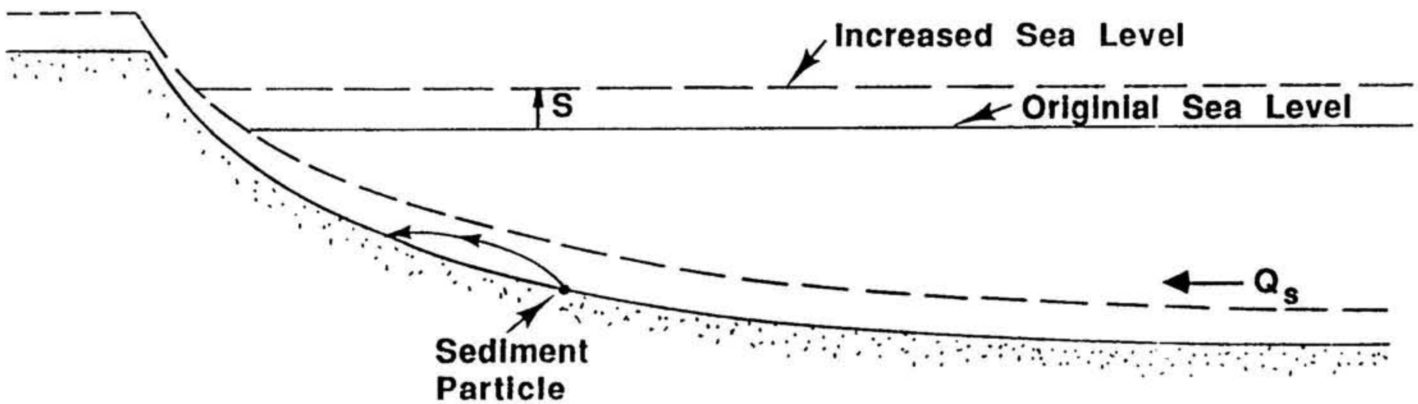

"Subjected to a Given Statistical Wave Climate, A Sediment Particle of a Particular Diameter is in Statistical Equilibrium When in a Given Water Depth"

Thus When Sea Level Increases, Particle Moves Landward

Figure 2.10. Possible Mechanism of Sedimentary Equilibrium (After Dean, 1987).

active zone sediment deficit rate will be

$$\text{New Deficit Rate} = \left[\int_0^{W_*} \frac{\partial h}{\partial t} dy\right]_0 + W_* \left[\left(\frac{dS}{dt}\right) - \left(\frac{dS}{dt}\right)_0\right] - \frac{d\mathcal{V}}{dt} \tag{2.18}$$

in which $\frac{d\mathcal{V}}{dt}$ represents the nourishment rate and the subscript "0" on the bracket represents the reference period before increased sea level rise. In order to decrease the deficit rate to zero, the required nourishment rate is

$$\frac{d\mathcal{V}}{dt} = \left[\int_0^{W_*} \frac{\partial h}{\partial t} dy\right]_0 + W_* \left[\left(\frac{dS}{dt}\right) - \left(\frac{dS}{dt}\right)_0\right] \tag{2.19}$$

These models may assist in evaluating the vulnerability of various shoreline systems to increased rates of sea level rise. For Florida, long-term trend estimates of $\frac{dS}{dt}$ over the last 60 or so years are 0.01 ft./year although there is considerable variability in the year-to-year values of sea level changes, including interannual increases and changes which can amount of 40 times the annual trend value.

PLANFORM EVOLUTION OF BEACH NOURISHMENT PROJECTS

To a community that has allocated substantial economic resources to nourish their beach, there is considerable interest in determining how long those beaches can be expected to last. Prior to addressing this question, we will develop some tools.

The Linearized Equation of Beach Planform Evolution

The linearized equations for beach planform evolution were first combined and applied by Pelnard Consideré in 1956. The combined equation is the result of the sediment transport equation and the equation of continuity.

Governing Equations

Transport Equation - Utilizing the spilling breaker assumption, the equation for longshore sediment transport has been presented as

$$Q = \frac{K}{8} \frac{H_b^{5/2}\sqrt{g/\kappa}}{(1-p)(s-1)} \frac{\sin 2\theta_b}{2} \tag{2.20}$$

in which p is the sediment porosity ($\approx$ 0.35-0.40) and s is the sediment specific gravity (= 2.65). Equation (2.20) will later be linearized by considering the deviation of the shoreline planform from the general shoreline alignment to be small. Referring to Fig. 2.11, denoting μ as the azimuth of the general alignment of the shoreline as defined by a baseline, β as the azimuth of an outward normal to the shoreline, α_b as the azimuth of the direction from which the breaking wave originates, then

$$Q = \frac{K\, H_b^{5/2}\sqrt{g/\kappa}}{8(1-p)(s-1)} \frac{\sin 2(\beta - \alpha_b)}{2} \tag{2.21}$$

where $\beta = \mu - \frac{\pi}{2} - \tan^{-1}\left(\frac{\partial y}{\partial x}\right)$

Equation of Sediment Conservation - The one-dimensional equation of sediment conservation is

$$\frac{\partial y}{\partial t} + \frac{1}{(h_* + B)} \frac{\partial Q}{\partial x} = 0 \tag{2.22}$$

Combined Equation of Beach Planform Evolution

Differentiating with respect to x, the equation of longshore sediment transport, Eq. (2.21), we find

$$\frac{\partial Q}{\partial x} = \frac{K\, H_b^{5/2}\sqrt{g/\kappa}}{8(1-p)(s-1)} \cos 2(\beta - \alpha_b) \frac{\partial \beta}{\partial x} \tag{2.23}$$

Recalling the definition of β and linearizing

$$\beta = \mu - \frac{\pi}{2} - \tan^{-1}\left(\frac{\partial y}{\partial x}\right) \approx \mu - \frac{\pi}{2} - \frac{\partial y}{\partial x} \tag{2.24}$$

and considering the wave approach angle $(\beta - \alpha_b)$ to be small such that $\cos 2(\beta - \alpha_b) \approx 1$, the final result is

$$\frac{\partial Q}{\partial x} = -\frac{K \quad H_b^{5/2}\sqrt{g/\kappa}}{8(1-p)(s-1)} \frac{\partial^2 y}{\partial x^2} \tag{2.25}$$

Combining Eqs. (2.22) and (2.25), a single equation describing the planform evolution for a shoreline which is initially out of equilibrium is obtained as

$$\frac{\partial y}{\partial t} = G \frac{\partial^2 y}{\partial x^2} \tag{2.26}$$

where

$$G \equiv \frac{K \quad H_b^{5/2}\sqrt{g/\kappa}}{8(s-1)(1-p)(h_* + B)} \tag{2.27}$$

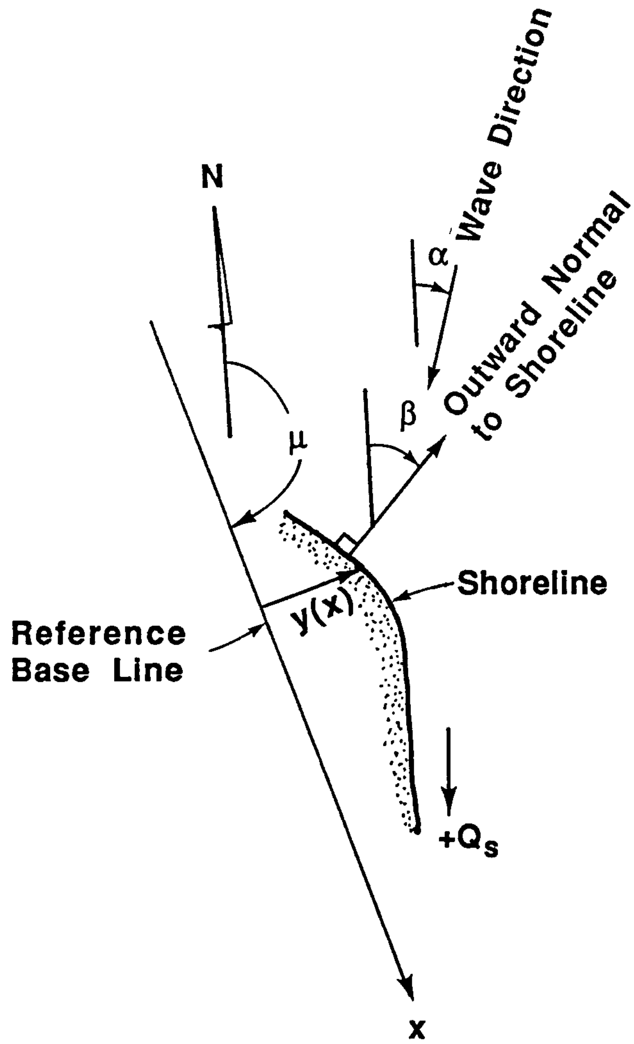

Figure 2.11. Definition Sketch.

The parameter G may be considered as a "shoreline diffusivity" with dimensions of $(\text{length})^2/\text{time}$. Field studies have documented the variation of K with sediment size, D, as presented in Fig. 2.12. A more detailed evaluation demonstrates that a more appropriate expression for G can be developed and expressed in terms of deep water conditions

$$G = \frac{K\, H_0^{2.4} C_{G_0}^{1.2} g^{0.4} \cos^{1.2}(\beta_0 - \alpha_0)\cos 2(\beta_0 - \alpha_*)}{8(s-1)(1-p)C_* \kappa^{0.4}(h_* + B)\cos(\beta_0 - \alpha_*)} \tag{2.28}$$

where the subscript "0" denotes deep water conditions and C_* is the wave celerity in water depth, h_*. Figure 2.13 presents estimates of G around the Florida peninsula and Figs. 2.14 and 2.15 present estimates of effective deep water wave height and period.

It is recognized that the form of Eq. (2.26) is the heat conduction or diffusion equation for which a number of analytical solutions are available. Several of these will be explored in the next section.

It is of interest to know approximate values of the shoreline diffusivity, G. It is seen that G depends strongly on H_b, and secondarily on H_b, $(h_* + B)$ and κ. Table 2.1 presents values of G for various wave heights in several unit systems where it is noted that the reference wave height is the breaking wave height.

Table 2.1: Values of G for Representative Wave Heights

H_b	Value of G in			
(ft.)	ft^2/s	mi^2/yr	m^2/s	km^2/yr
1	0.0214	0.0242	0.00199	0.0626
2	0.121	0.137	0.0112	0.354
5	1.194	1.350	0.111	3.50
10	6.753	7.638	0.628	19.79
20	38.2	43.2	3.55	111.9

Note: In this table the following values have been employed: $K = 0.77$, $\kappa = 0.78$, $g = 32.2$ ft/s^2, $s = 2.65$, $p = 0.35$, $h_* + B = 27$ ft.

Analytical Solutions for Beach Planform Evolution

Examples which will be presented and discussed include: (1) the case of a narrow strip of sand protruding a distance, Y, from the general shoreline alignment, and (2) a rectangular

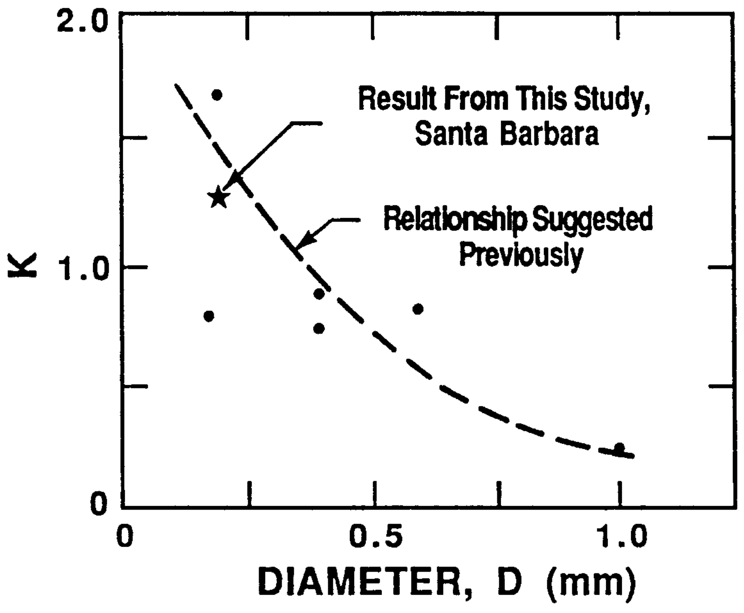

Figure 2.12. Plot of K vs. D. Results of Present and Previous Studies (Modified From Dean, 1978).

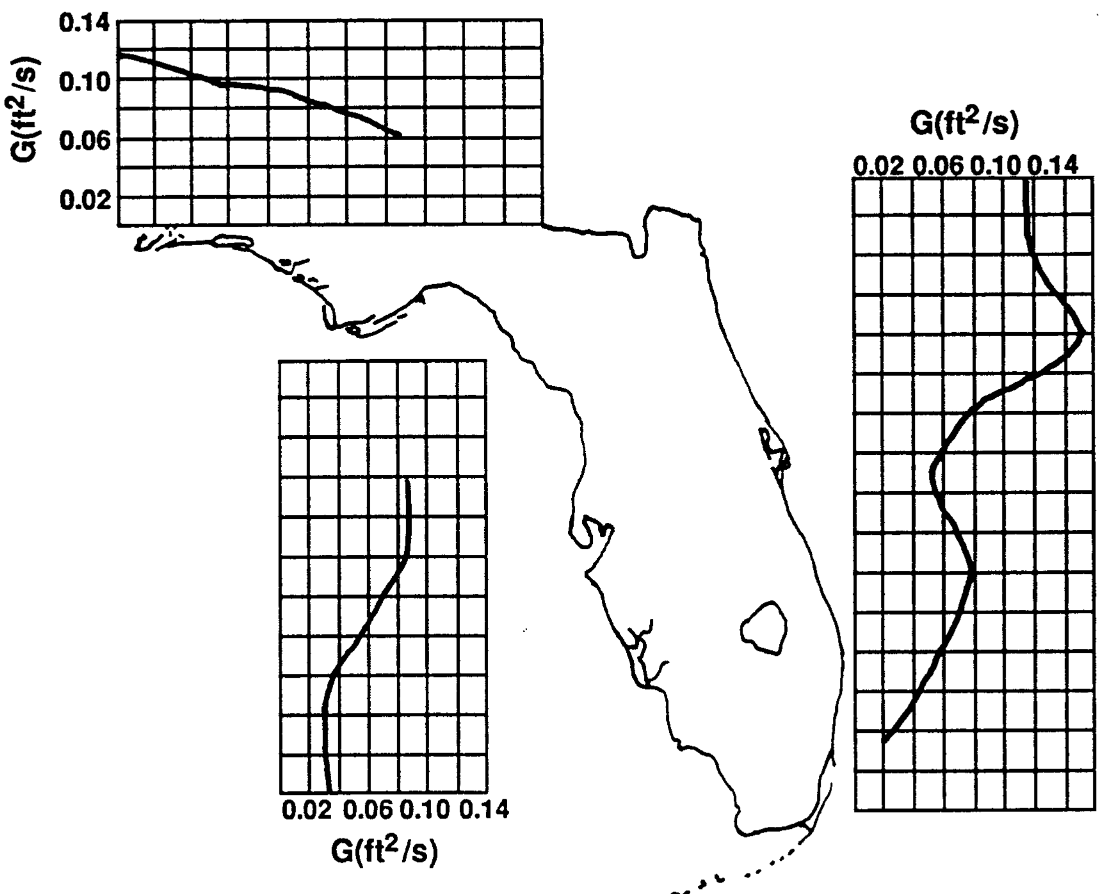

Figure 2.13. Approximate Estimates of G(ft^2/s) Around the Sandy Beach Shoreline of the State of Florida. Based on the Following Values: K = 0.77, g = 32.2 ft/sec^2, S = 2.65, p = 0.35, κ= 0.78, h_* From Fig. 8., B Estimates Ranging from 6 to 9 ft, H_o from Fig. 23, T from Fig. 24.

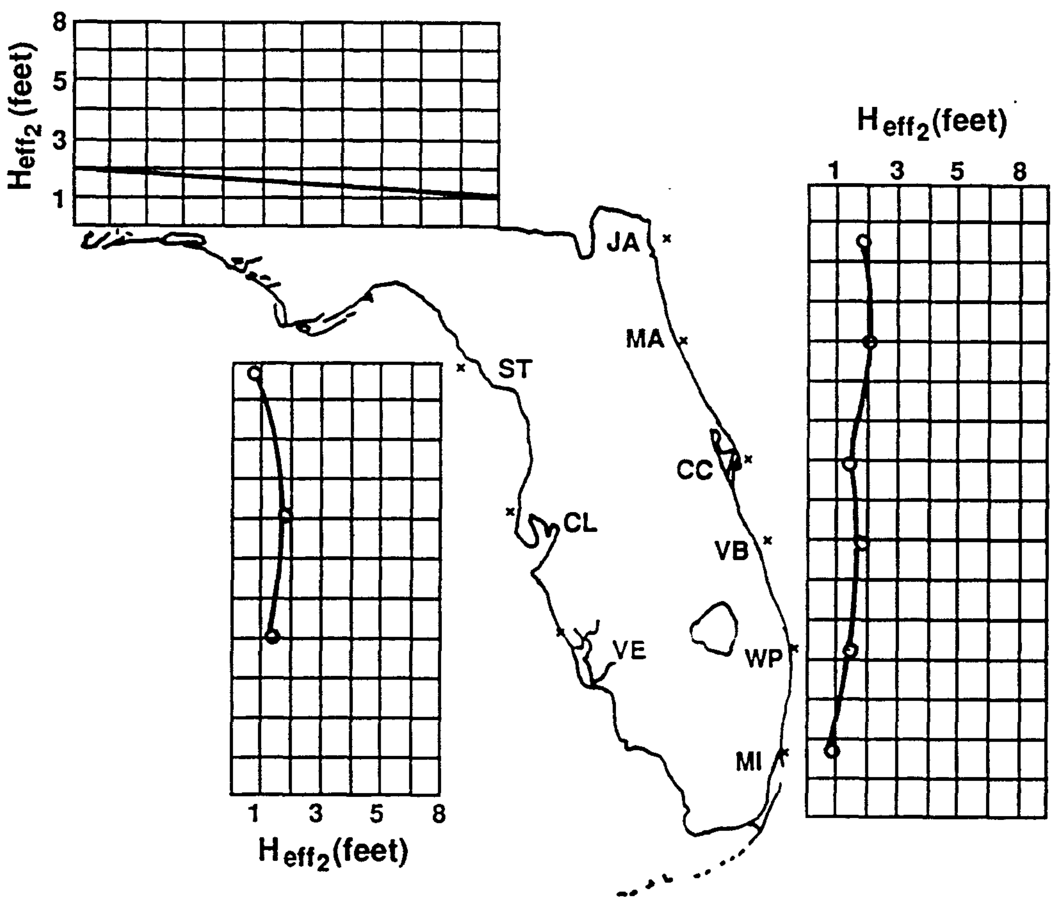

Figure 2.14. Recommeneded Values of Effective Deep Water Wave Height, H_O, Along Florida's Sandy Shoreline.

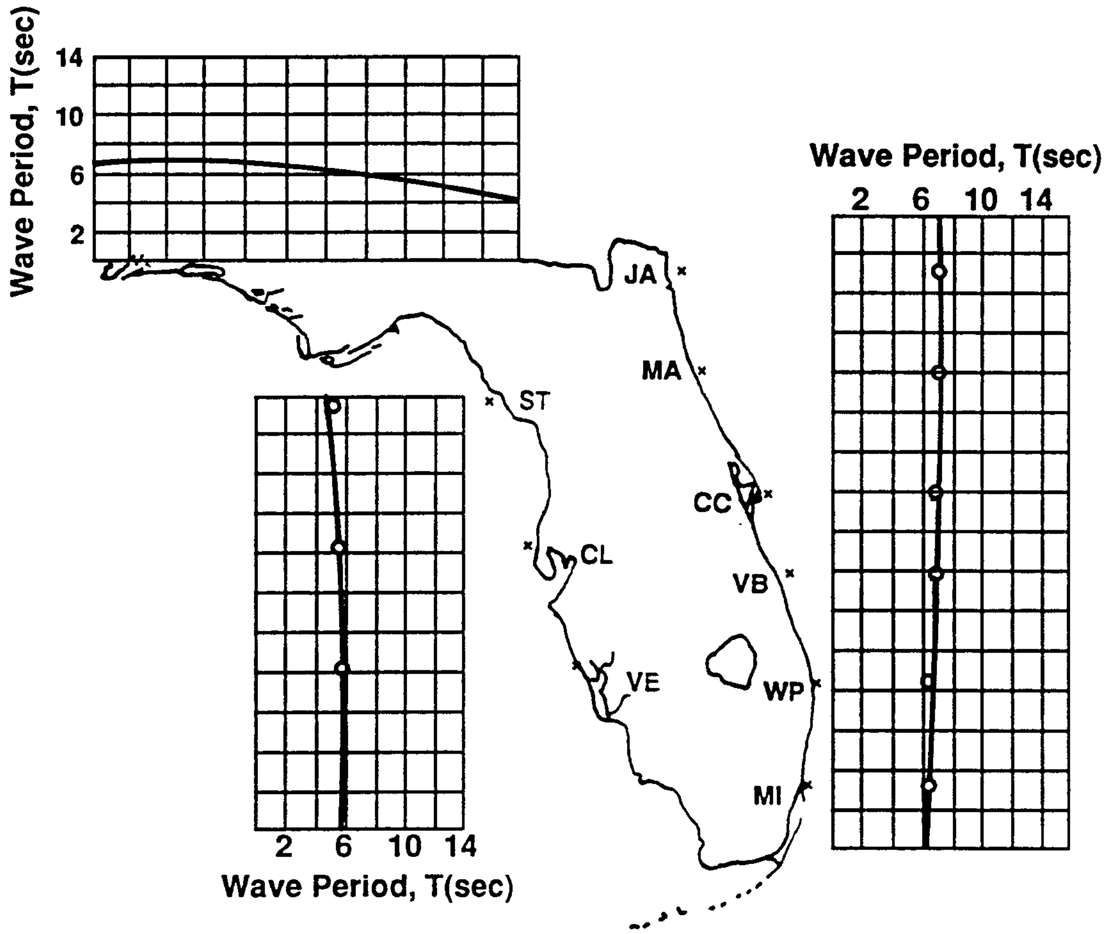

Figure 2.15. Recommended Values of Effective Wave Period, T, Along Florida's Sandy Shoreline.

distribution of sand extending into the ocean which could provide a reasonably realistic representation of a beach nourishment project.

(1). A Narrow Strip of Sand Extending into the Ocean

Consider the case of a narrow strip of sand extending a distance, Y into the ocean and of width Δx such that $m = Y\Delta x$, Fig. 2.16. The total area of the sand is designated m and the solution for this initial condition and the differential equation described by Eq. (2.26) is the following

$$y(x,t) = \frac{m}{\sqrt{4\pi Gt}} \exp\left(-\frac{x^2}{4Gt}\right) \qquad (2.29)$$

which is recognized as a normal distribution with increasing standard deviation or "spread" as a function of time. Figure 2.17 shows the evolution originating from the initial strip configuration. Examining Eq. (2.29), it is seen that the important time parameter is Gt. The quantity, G, which is the constant in Eq. (2.27) serves to hasten the evolution toward an unperturbed shoreline. In Eq. (2.29) it is seen that the quantity, G, is proportional to the wave height to the 5/2 power which provides some insight into the significance of wave height in remolding beach planforms which are initially out of equilibrium.

It is interesting that, contrary to intuition, as the planform evolves it remains symmetric and centered about the point of the initial shoreline perturbation even though waves may arrive obliquely. Intuition would suggest that sediment would accumulate on the updrift side and perhaps erosion would occur on the downdrift side of the perturbation. It is recalled that the solution described in Fig. 2.17 applies only for the case of small deviations of the shoreline from the original alignment and may be responsible for the difference between the linear solution and intuition.

For purposes of the following discussion, we recover one of the nonlinearities removed from the definition of the "constant" G from Eqs. (2.23) and (2.26)

$$G = \frac{K\, H_b^{5/2}\sqrt{g/\kappa}}{8(s-1)(1-p)(h_* + B)} \cos 2(\beta - \alpha_b) \qquad (2.30)$$

and it is seen that if the difference between the wave direction and the shoreline orientation exceeds 45°, then the quantity, G, will be negative. Examining the results presented earlier,

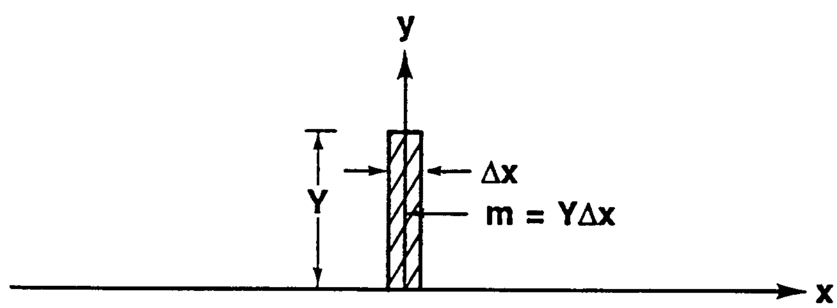

Figure 2.16. Initial Beach Planform. Narrow Strip of Sand Extending From Unperturbed Shoreline.

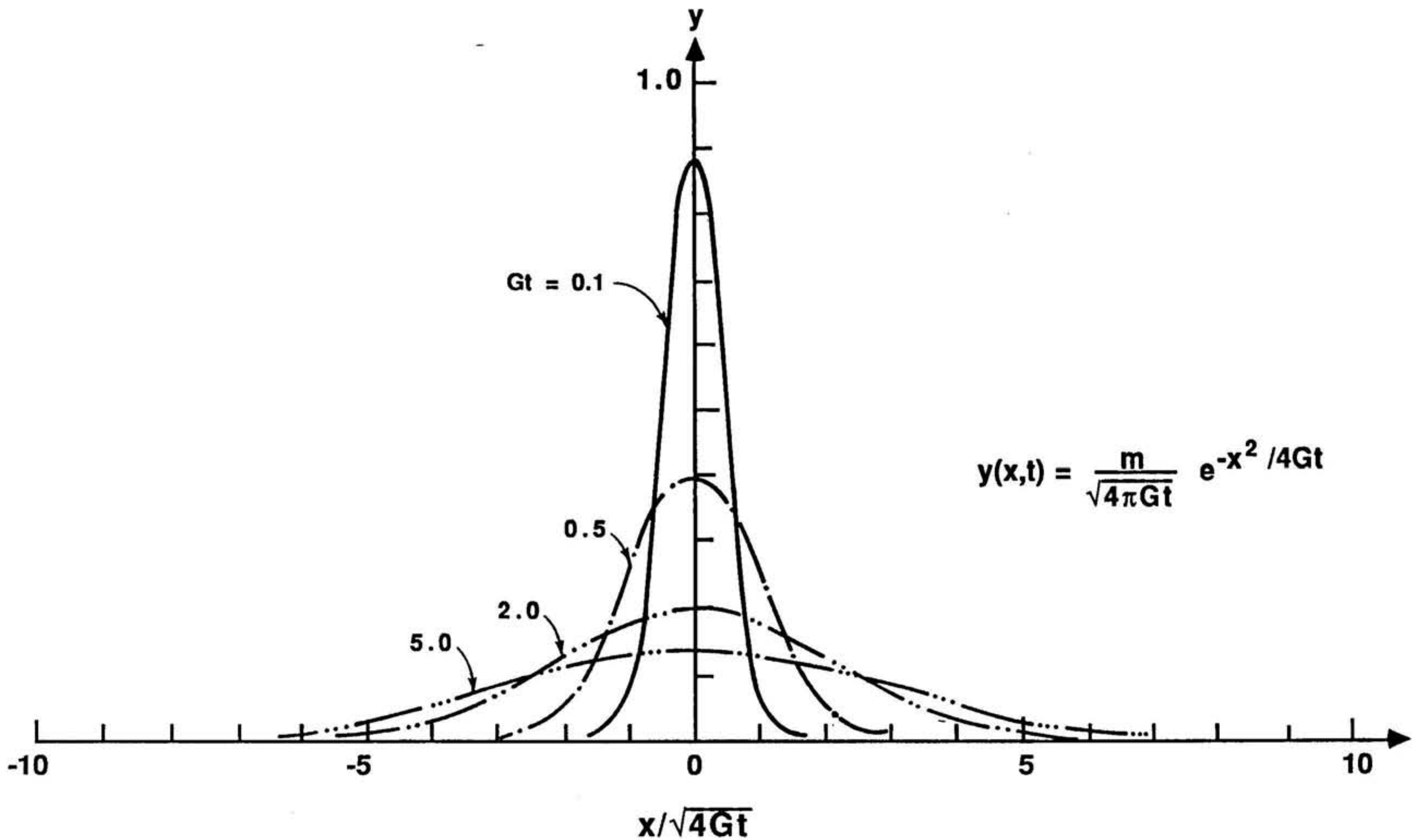

Figure 2.17. Evolution of an Initially Narrow Shoreline Protuberence.

it is clear that if this should occur then it is equivalent to "running the equation backwards" in time. That is, if we were to commence with a shoreline which had a perturbation represented by a normal distribution then rather than smoothing out, the perturbation would tend to grow, with the ultimate planform being a very narrow distribution exactly as was our initial planform! In fact, regardless of the initial distribution one would expect the shoreline to grow into one or more accentuated features. Shorelines of this type ($\cos 2(\beta - \alpha_b)$ less than zero) can be termed "unstable" shorelines and may provide one possible explanation for certain shoreline features including cuspate forelands.

(2). Initial Shoreline of Rectangular Planform

Consider the initial planform presented in Fig. 2.18 with a longshore length, ℓ, and extending into the ocean a distance, Y. This planform might represent an idealized configuration for a beach restoration program and thus its evolution is of considerable interest to coastal engineers, especially in interpreting and predicting the behavior of such projects.

It is seen that in a conceptual sense it would be possible to consider the problem of interest to be a summation of the narrow small strip planforms presented in the previous example. In fact, this is the case and since Eq. (2.26) is linear, the results are simply a summation or linear superposition of a number of normal distributions. The analytic solution for this initial planform can be expressed in terms of two error functions as

$$y(x,t) = \frac{Y}{2}\left\{erf\left[\frac{\ell}{4\sqrt{Gt}}\left(\frac{2x}{\ell}+1\right)\right] - erf\left[\frac{\ell}{4\sqrt{Gt}}\left(\frac{2x}{\ell}-1\right)\right]\right\} \tag{2.31}$$

where the error function "erf{}" is defined as

$$erf(z) = \frac{2}{\sqrt{\pi}}\int_0^z e^{-u^2}du \tag{2.32}$$

and here u is a dummy variable of integration. This solution is examined in Fig. 2.18 where it is seen that initially the two ends of the planform commence spreading out and as the effects from the ends move towards the center, the planform distribution becomes more like a normal distribution. There are a number of interesting and valuable results that can be

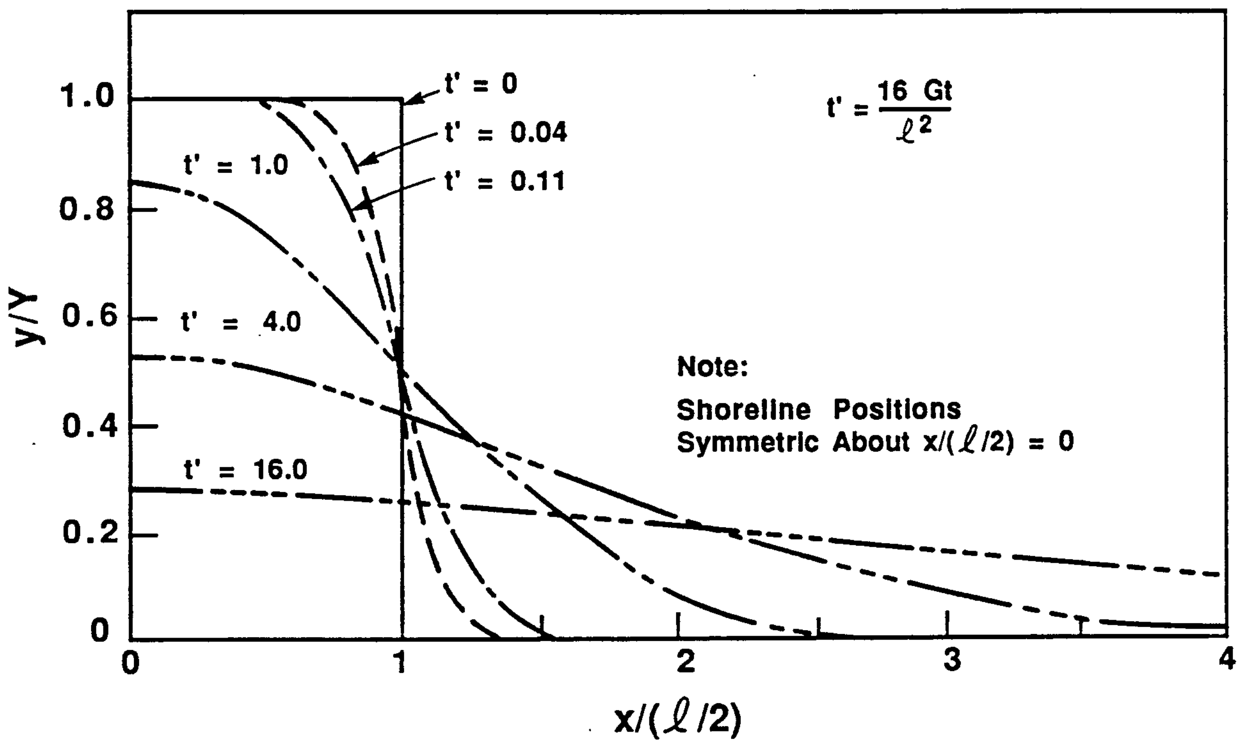

Figure 2.18. Evolution of an Initally Rectangular Beach Planform on an Otherwise Straight Beach. Only One-Half of Project is Shown.

obtained by examining Eq. (2.31). First, it is seen that the important parameter is

$$\frac{\ell}{\sqrt{Gt}} \tag{2.33}$$

where ℓ is the length of the rectangle and G is the parameter in the diffusion equation as discussed earlier. If the quantity $\left(\frac{\ell}{\sqrt{Gt}}\right)$ is the same for two different situations, then it is clear that the planform evolutions are also the same. Examining this requirement somewhat further, if two nourishment projects are exposed to the same wave climate but have different lengths, then the project with the greater length would tend to last longer. In fact, the longevity of a project varies as the square of the length, thus if Project A with a shoreline length of one mile "losses" 50 percent of its material in a period of 2 years, Project B subjected to the same wave climate but with a length of 4 miles would be expected to lose 50 percent of its material from the region where it was placed in a period of 32 years. Thus the project length is very significant to its performance.

Considering next the case where two projects are of the same length but located in different wave climates, it is seen that the G factor varies with the wave height to the 5/2 power. Thus if Project A is located where the wave height is 4 ft and loses 50 percent of its material in a period of 2 years then Project B with a similarly configured beach planform located where the wave height is 1 foot would be expected to lose 50 percent of its material in 64 years.

Figure 2.19 presents a specific example of beach evolution and Fig. 2.20 presents results in terms of the proportion of sediment remaining in front of the beach segment where it was placed as a function of time. These results are presented for several examples of combinations of wave height and project lengths. As an example of the application of Fig. 2.20, a project of 4 miles length in a location where the wave height is 4 feet would lose 60 percent of its material in 7 years and a second project in a location where the wave height is 2 ft and the project length is 16 miles would lose only 10 percent of its material in a period of 40 years. Figure 2.20 was developed based on the solution presented in Eq. (2.31).

It is possible to develop an analytical expression for the proportion of sand, $M(t)$,

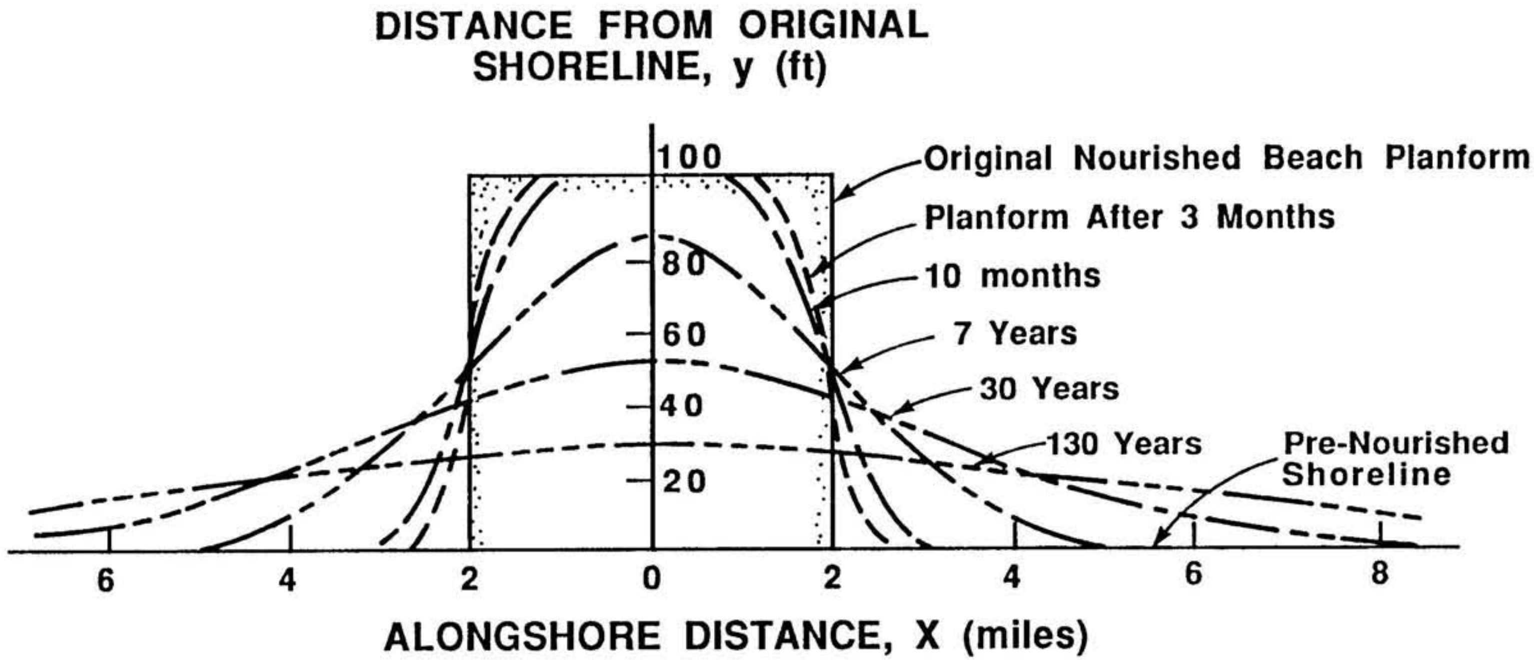

Figure 2.19. **Example of Evolution of Initially rectangular Nourished Beach Planform. Example for Project Length, ℓ, of 4 Miles and Effective Wave Height, H, of 2 feet and Initial Nourished Beach Width of 100 Feet.**

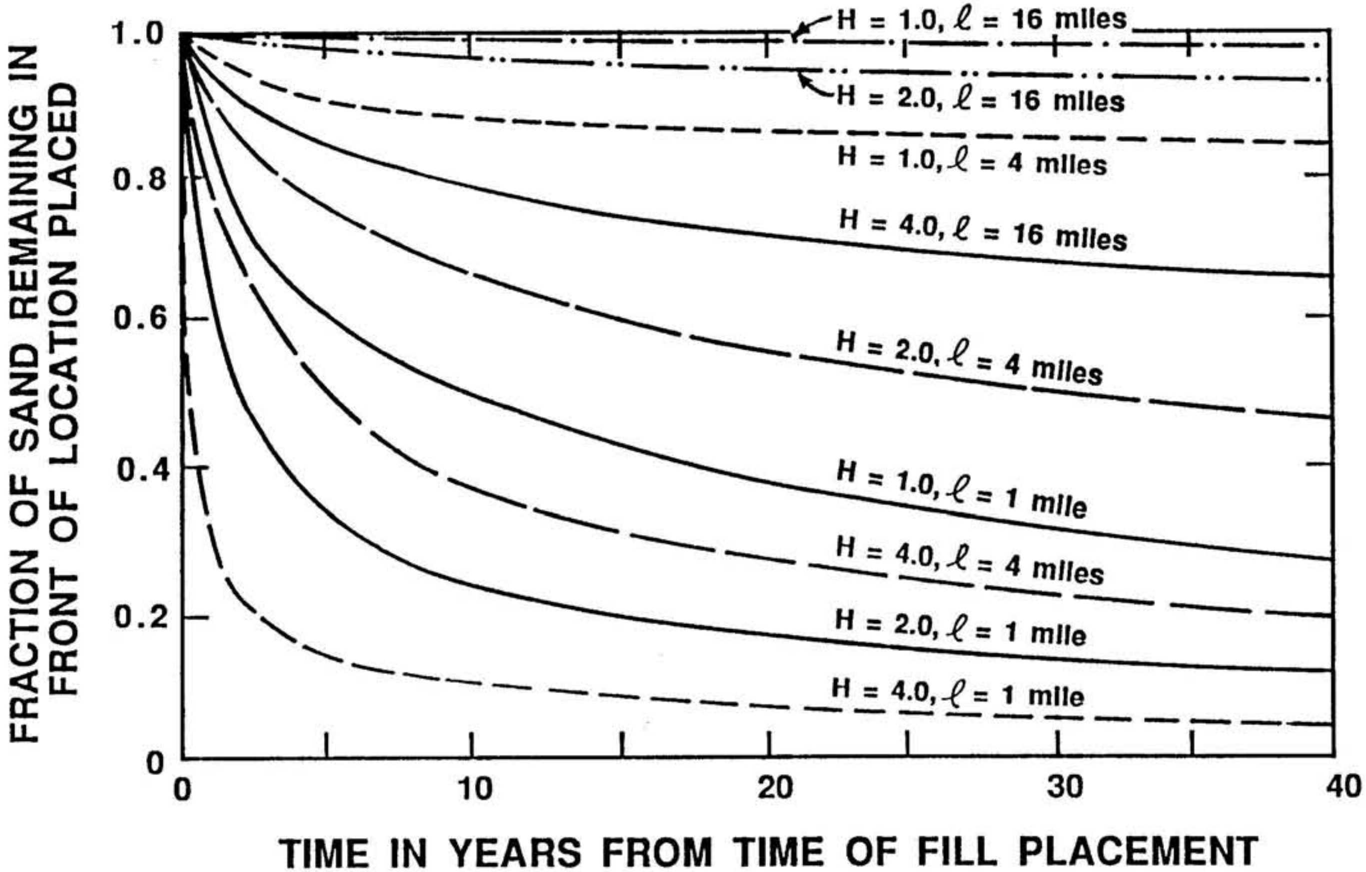

Figure 2.20. Fraction of Material Remaining in Front of Location Placed for Several Wave Height, H, and Project Lengths, ℓ . Effect of Longshore Transport.

remaining in the location placed, as defined by

$$M(t) = \frac{1}{Y\ell}\int_{-\ell/2}^{\ell/2} y(x,t)dx \tag{2.34}$$

to yield

$$M(t) = \frac{2\sqrt{Gt}}{\ell\sqrt{\pi}}\left(e^{-(\ell/2\sqrt{Gt})^2} - 1\right) + erf\left(\frac{\ell}{2\sqrt{Gt}}\right) \tag{2.35}$$

which is plotted in Fig. 2.21 along with the asymptote for small times

$$M(t) \cong 1 - \frac{2}{\sqrt{\pi}}\frac{\sqrt{Gt}}{\ell} \tag{2.36}$$

which appears to fit reasonably well for

$$\sqrt{Gt}/\ell < 0.5 \tag{2.37}$$

A useful approximation for estimating the "half-life" of a project is obtained by noting that $M = 0.5$ for $\sqrt{Gt}/\ell \cong 0.46$. Thus the half-life, t_{50}, is

$$t_{50} = (0.46)^2\frac{\ell^2}{G} = 0.21\frac{\ell^2}{G} \tag{2.38}$$

in which all variables are in consistent units. A more readily applied form is developed from Eq. (2.27) as

$$t_{50} = 8.7\frac{\ell^2}{H_b^{5/2}} \tag{2.39}$$

where t_{50} is in years, ℓ in miles and H_b is the breaking wave height in ft.

Effect on Retention of Setting Back the Fill Ends from Project Boundaries

As noted earlier, there is an understandable interest by a community or other entity which is funding a project in retaining the sand within their boundaries as long as practical. One approach to this concern would be to install retaining or stabilization structures near the ends of the fill. A second would be to simply set-back the limits of the fill from the project boundaries with the understanding that the sand would soon "spread out". Omitting the details, Fig. 2.22 presents results for relative end set-backs $\Delta/\ell = 0$, 0.2 and 0.5. It is seen that the effects are greatest early in the project life (say $\sqrt{Gt}/\ell = 0.6$ or 0.8) where a set back $\Delta/\ell = 0.5$ would increase the percent material retained from 42% to 73%.

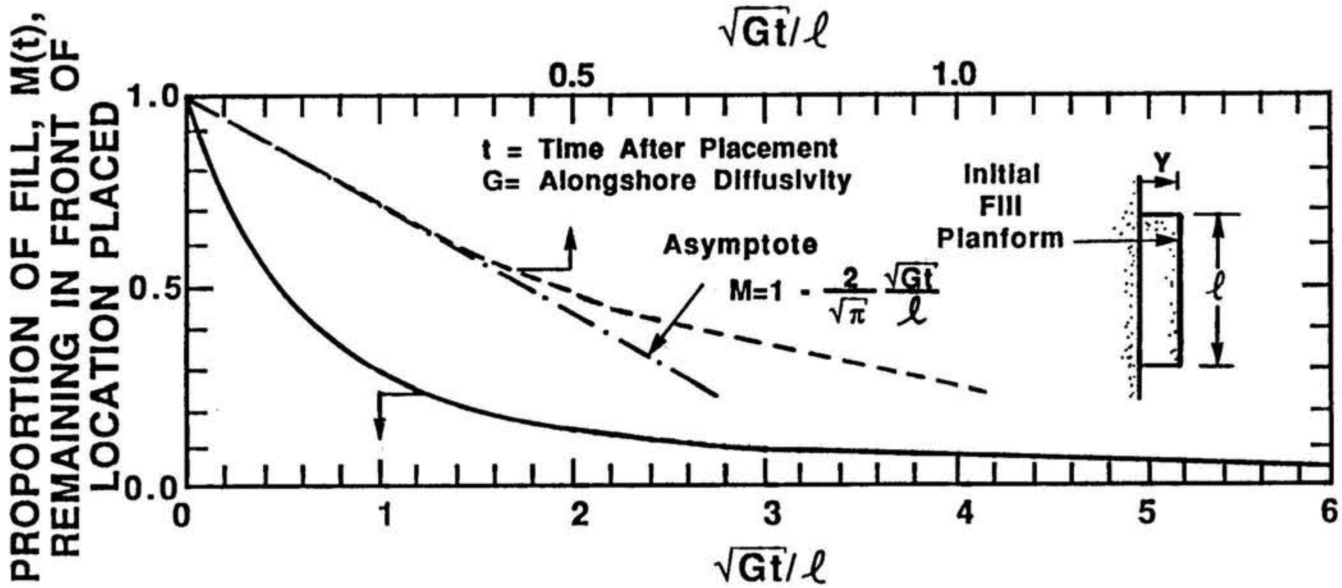

Figure 2.21. Percentage of Material Remaining in Region Placed vs. the Parameter $\sqrt{Gt}/\ell$.

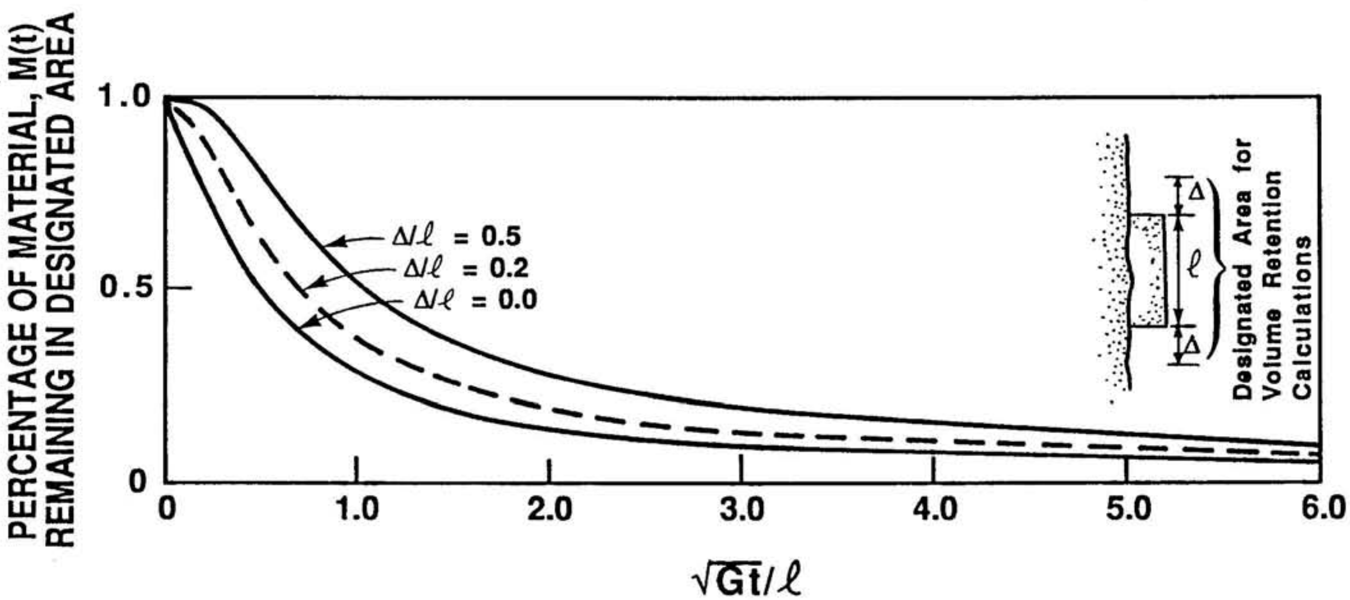

Figure 2.22. Percentage of Material Remaining in Designated Area of Length, $\ell + 2\Delta$. Rectangular Beach Fill of Length, ℓ.

Effect of Ends on a Beach Fill

It is somewhat interesting to evaluate the effect on longevity of providing a fillet at the two ends of a fill which is otherwise rectangular in planform. Basing the longevity on the retention of sand within the placed planform, it is interesting that tapered- end planforms have a substantially greater longevity than rectangular planforms. The reasons is apparent by examining Fig. 2.19. The loss rates of a rectangular planform fill are higher over the first increment of time than over the same increment of time but later in the project history. It is seen from Fig. 2.19 that the evolution of the planform occurs with the early changes occurring where the planform changes are the most extreme. This is not surprising when one recalls that the governing equation (Eq. (2.26)) is the heat conduction equation and that the fill planform is equivalent to a temperature distribution above background of the same form in an infinitely long rod. Returning again to the tapered end planform, which approximates the evolved rectangular planform at a later stage, the evolution of the tapered end fill at an early stage approximates that of a rectangular fill at a later stage.

Figures 2.23 and 2.24 present calculated evolutions for rectangular and tapered end planforms, respectively and Table 2.2 summarizes the cumulative losses from the region placed over the first five years. It is seen that the tapered end fills have reduced the end losses by about 33%.

Table 2.2: Comparison of Cumulative Percentage Losses from Rectangular and Tapered Fill Planforms ($G = 0.02$ ft^2/sec; $\ell = 3$ miles; $Y = 55$ ft)

Years After Placement	Cumulative Percentage Losses With: Rectangular Planform	Cumulative Percentage Losses With: Rectangular Planform With Triangular Fillets
1	5.7	2.4
2	9.5	4.6
3	11.8	6.6
4	13.8	8.3
5	15.5	9.8

A Case Example - Bethune Beach

In 1985, shorefront property owners in Bethune Beach, Volusia County, FL applied

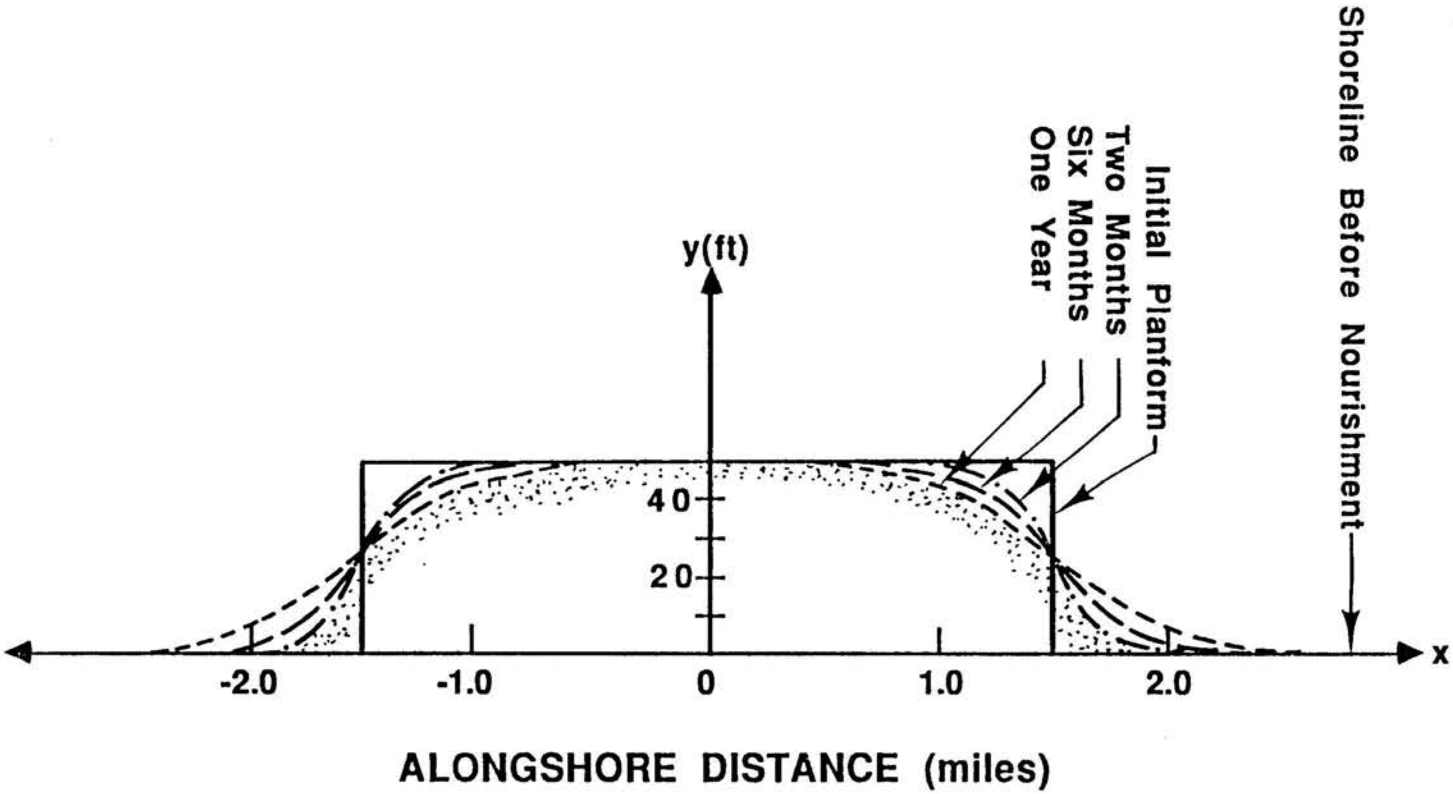

Figure 2.23. Calculated Evolution of a Rectangular Planform Beach Nourishment Project. Planforms Presented for Initial Conditions and 1,2 and 5 Years After Placement.

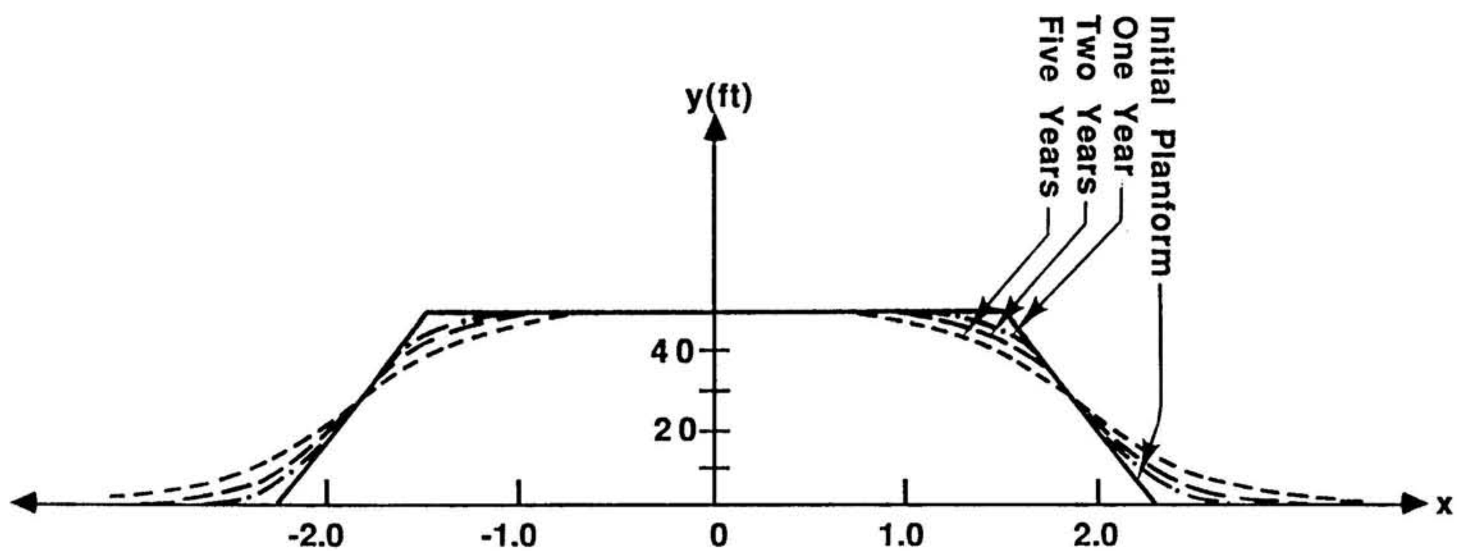

Figure 2.24. Calculated Evolution of a Rectangular Planform with Triangular End Fillets. Planforms Presented for Initial Conditions and 1,2 and 5 Years After Placement.

for a permit to construct two segments of armoring. The Governor and Cabinet initially deferred a decision requesting that consideration be given to utilizing the same funds for beach nourishment. The two segment lengths were 925 ft and 3,850 ft, as presented in Fig. 2.25. The designation beside each segment (e.g. VO 353) is the identifier given by the Division of Beaches and Shores to the permit application. The cost of the revetments was about $200 per foot which at a nourishment cost of $6 per cubic yard would purchase approximately 33 cubic yards per front foot or a total of 160,000 cubic yards for the two segments combined.

Rather simple numerical modeling was carried out using Eqs. (2.26) and (2.27) with monthly averaged wave heights as determined by the University of Florida's wave gage at nearby Marineland, FL. The results of this numerical modeling are presented in Figs. 2.25 and 2.26. Figure 2.25 presents the planform evolution after one month and one year. It is seen in accordance with earlier discussions, that due to the relative short lengths of these segments, the sand spreads out rapidly in an alongshore direction. Figure 2.26 presents, as a function of time, the volume of sand remaining in front of the two segments where the nourishment would have been placed.

Project Downdrift of a Partial or Complete Littoral Barrier

In this case the project is located downdrift of a partial or complete littoral barrier, such as a jettied inlet. We will denote the net longshore transport as Q_o and the bypassed quantities as $FQ_o(0 < F < 1)$, see Fig. 2.27. In this case, the fraction remaining, $M_2(t)$, is

$$M_2(t) = \frac{\int_o^\ell V(x,t)dx}{V_o \ell} \tag{2.40}$$

and can be shown to be

$$M_2(t) = erf\left(\frac{\ell}{\sqrt{Gt}}\right) + \frac{1}{\sqrt{\pi}}\frac{\sqrt{GT}}{\ell}\left(e^{-(\ell/\sqrt{GT})^2} - 1\right) - \frac{(1-F)Q_o t}{V_o \ell} \tag{2.41}$$

in which V_o is the volume placed. Eq. (2.41) is presented vs $\sqrt{Gt}/\ell$ in Fig. 2.27 for various values of $(1-F)Q_o\ell/V_oG$. This latter parameter presents the ratio of longshore

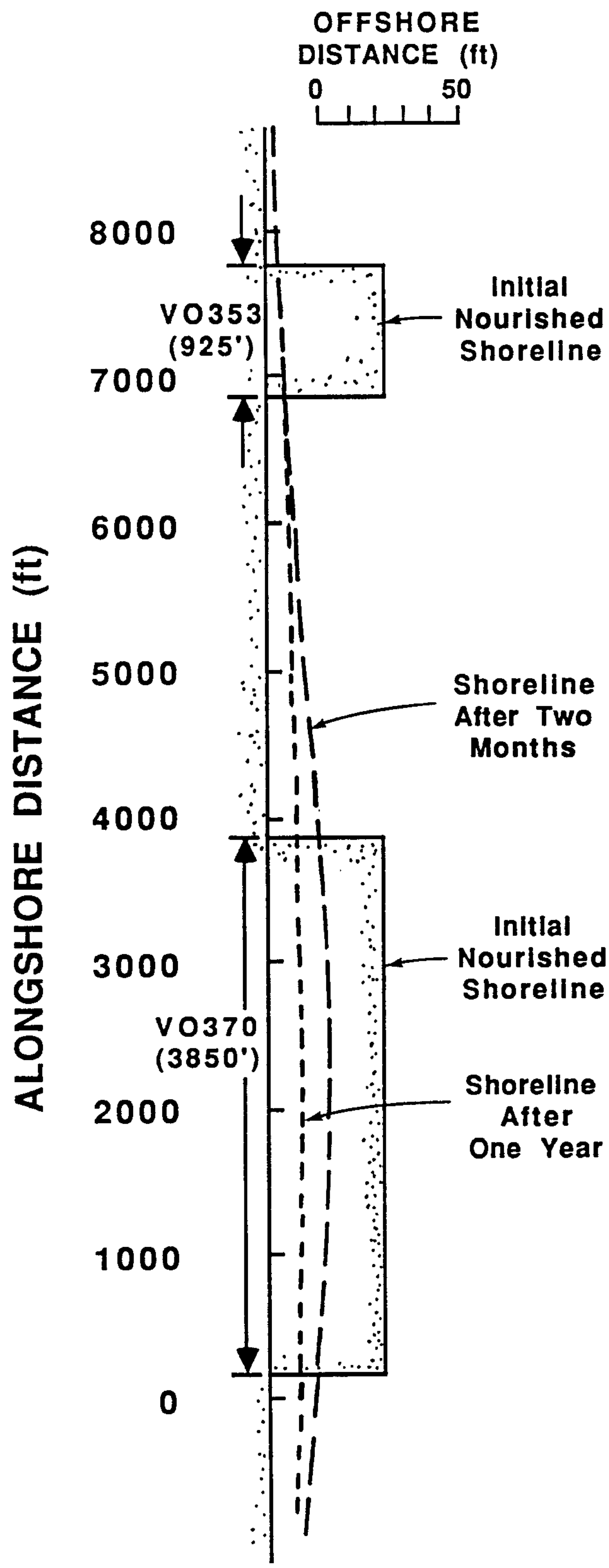

Figure 2.25. Initial and Subsequent Planforms of Nourished Beach. Bethune Beach, Florida, Example.

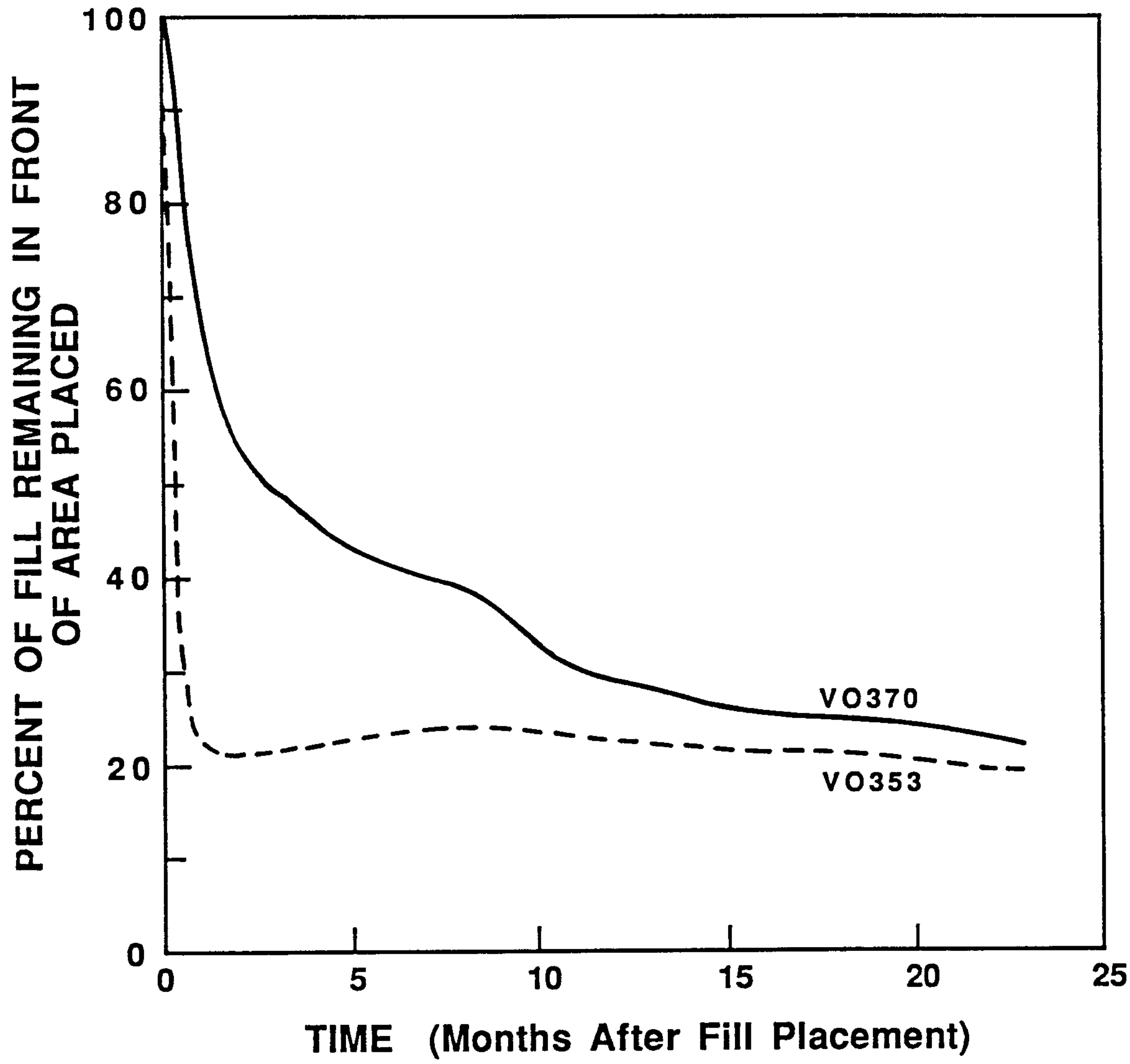

Figure 2.26. "Loss" of Beach Fill From Infront of Area Placed as a Result of Longshore Transport. Bethune Beach, Florida, Example.

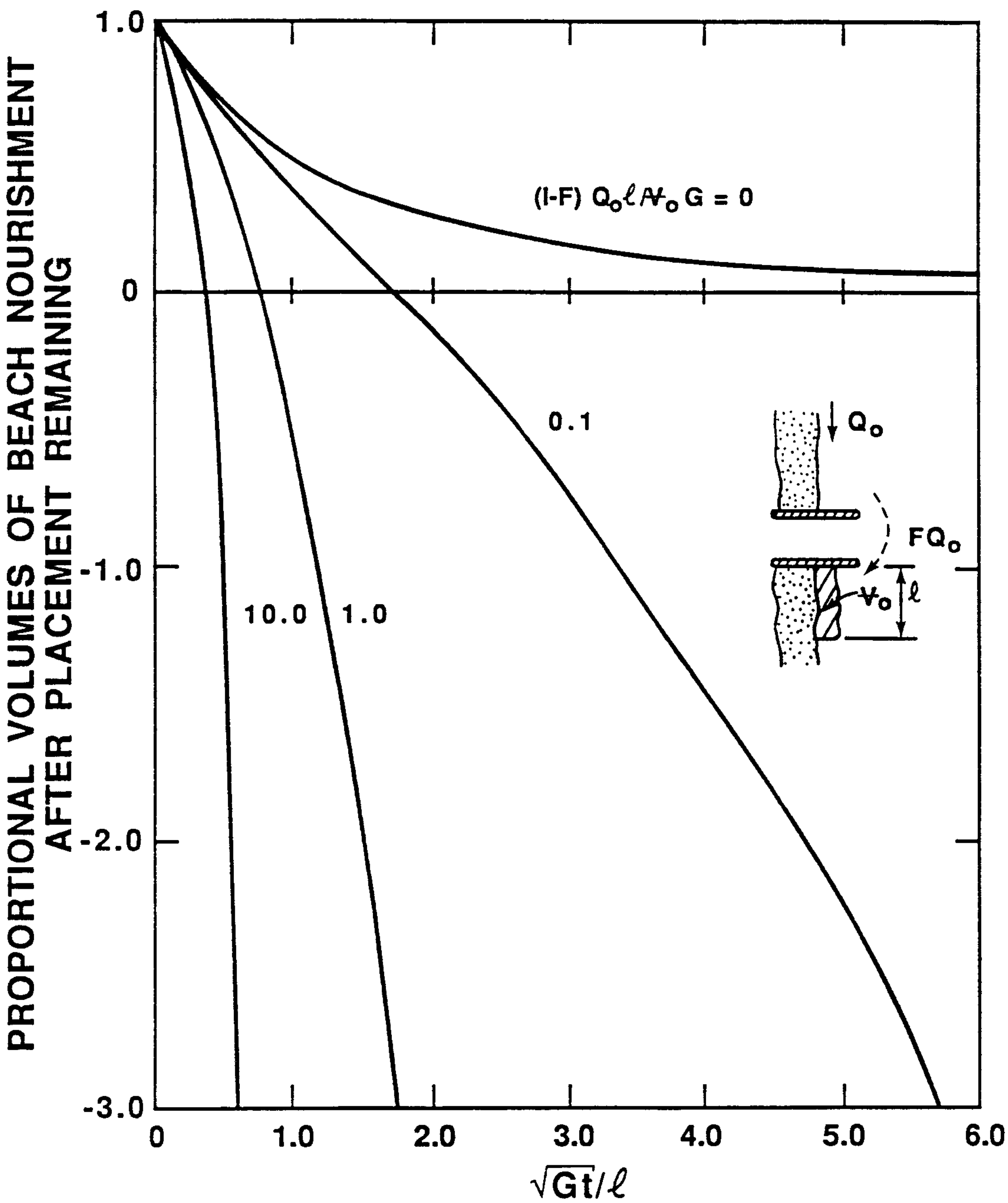

Figure 2.27. **Proportional Volumes of Beach Nourishment Remaining After Placement vs, $\sqrt{Gt}/\ell$ and $(1\text{-}F)Q_o/\forall_o G$.**

transport losses due to a bypassing deficit to those losses resulting from the anomalous planform.

DAMAGE REDUCTION DUE TO BEACH NOURISHMENT

The concept of reduction in storm damage by beach nourishment will be illustrated by two approaches. First, data collected and summarized by Shows (1978) documented the relationship between average damage costs suffered by a structure as a function of the proximity of that structure to the shoreline set-back line in Bay County. The set-back

line is approximately parallel to the shoreline. Figure 2.28 presents these results for 540 structures in Bay County following Hurricane Eloise in 1975. The horizontal axis is the structure location relative to the set-back line which is more or less parallel to the shoreline. Relative to beach nourishment, the two most significant features of Fig. 2.28 are: (1) the steeply rising damage function with proximity to the set-back line (or shoreline), and (2) the possibility of displacing the damage function seaward by beach nourishment which would translate the curve in Fig. 2.28 horizontally to the left by the width of beach added. As a second illustration consider the situation in Fig. 2.28 which corresponds to a profile off Sand Key, Florida. A peak storm tide of 11 ft and an offshore breaking wave height of 20 ft will be assumed for purposes of this example. These conditions are believed to be reasonably representative of a 100 year return period. Considering the pre-nourishment condition and utilizing the breaking wave model reported by Dally, Dean and Dalrymple (1985), the wave height distribution is presented in Fig. 2.29. Considering now a beach nourishment project which advances the shoreline gulfward a distance of 40 ft, the wave height distribution is as presented in Fig. 2.29. Table 2.3 summarizes the wave height at the seawall for the original and nourished conditions and also presents a measure of the damage potential for the two cases with and without nourishment. In these results the damage potential is considered to be proportional to the cube of the wave height. The presence of the nourishment project reduces the damage potential by nearly a factor of four!

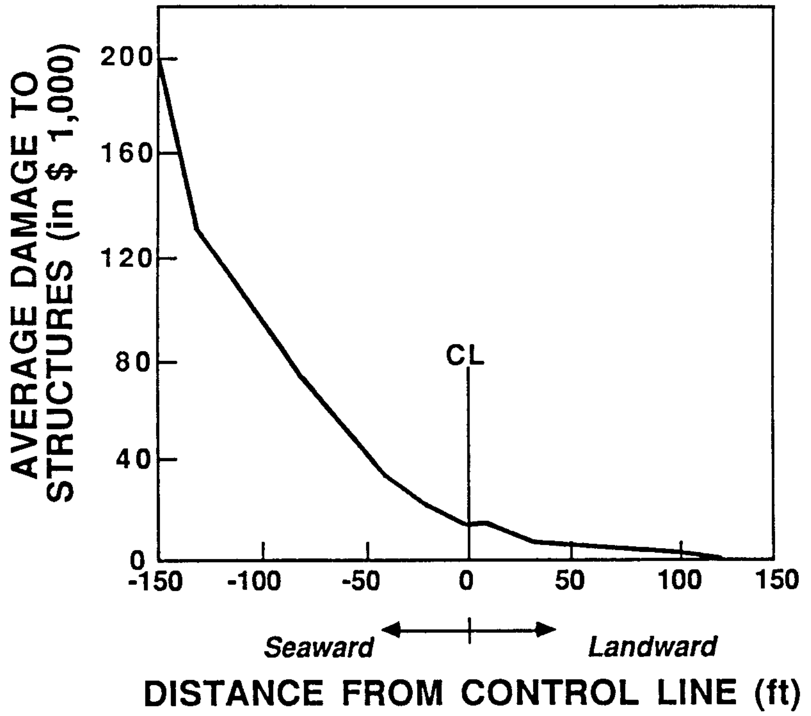

Figure 2.28. Damage to Structure in Relation to its Location with Control Line (Resulting From Study of 540 Structures in Bay County After Hurricane Eloise, by Shows, 1978).

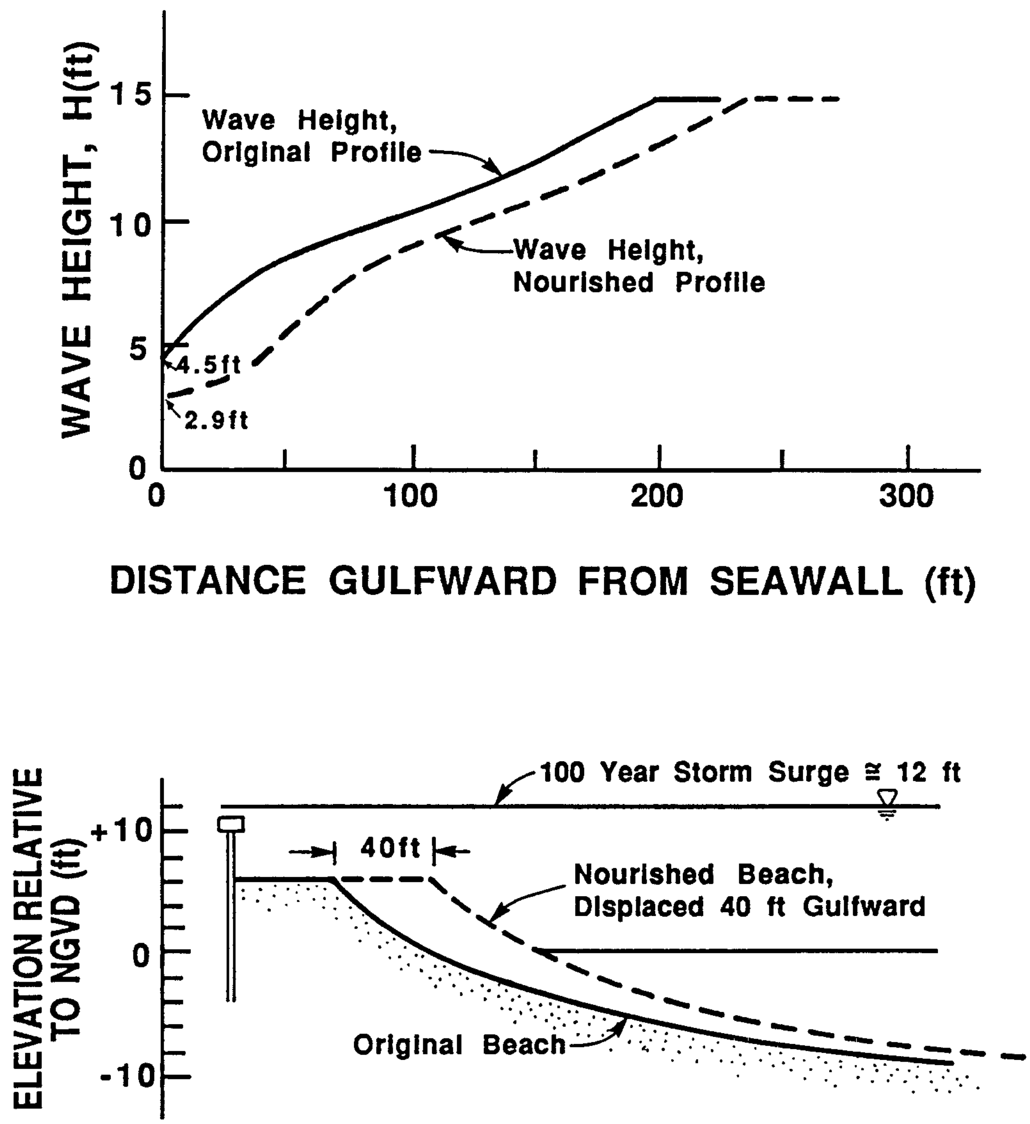

Figure 2.29. Wave Height Reduction at Seawall Due to Presence of a Beach Nourishment Project.

Table 2.3: Summary of Wave Height and Damage Potential Reduction at Seawall with Beach Nourishment Project*

Case	Wave Heights (ft)	Damage Potential αH^3
Without Nourishment	4.5	90
With Nourishment	2.9	24

*Refer to Fig. 2.29.

Table 2.4: Present Worth Damage Factor, $F(w, I)$ as a Function of Interval Considered and Beach Width

Interest Rate, I	Present Worth Damage Factor, $F(w, I)$, for Various Beach Widths, w			
	$w = 0$ ft	$w = 50$ ft	$w = 100$ ft	$w = 150$ ft
6%	1.84	0.89	0.59	0.37
8%	1.39	0.56	0.44	0.27
10%	1.07	0.49	0.44	0.27

There are various general approaches to developing estimates of damage reduction due to beach nourishment. One approach is to attempt to carry out a structure-by-structure damage analysis due to a storm of a certain severity as characterized by a storm tide, wave height and duration. The damage due to many such storms weighted by their probability of occurrence can then be combined to yield the total expected damage. A second approach and that which will be employed here is to recognize that during a particular storm, it is appropriate to consider (1) relative alongshore uniformity of wave attack, and (2) a representative proportional damage as a function of storm severity and beach width, W.

Having demonstrated qualitatively the damage reduction due to beach nourishment, we will proceed to a formalized procedure, making assumptions and simplifying as necessary.

The methodology will assume that a proportional structural damage curve is available as a function of storm return period, T_R, and additional beach width, w. Curves of this type would be site specific depending on the location of the existing structure relative to the shoreline, and the design and quality of the structures. Figure 2.29 presents one example of such a set of relationships. The cumulative probability, $P(T_R)$ of encountering a storm of return period T_R in any given year is

$$P(T_R) = \frac{1}{T_R} \tag{2.42}$$

The information presented in Fig. 2.30 can be developed with varying degrees of realism through Monte Carlo simulation methodology such that the result is applied directly and easily. One approach is to assume that the damage from one storm is repaired prior to the occurrence of a succeeding storm. The present worth damage factor, $F(w, I, J)$ in a period of J years, depends on the interest rate, I, the maintained beach width, w, and represents the ratio of present worth of all damage values over the J year to the present structure value.

This method obviously embodies many approximations, but does provide a rational framework for a very complex problem. One realization of the present worth damage factor for storms over the next J years if the beach width is maintained constant can be shown to

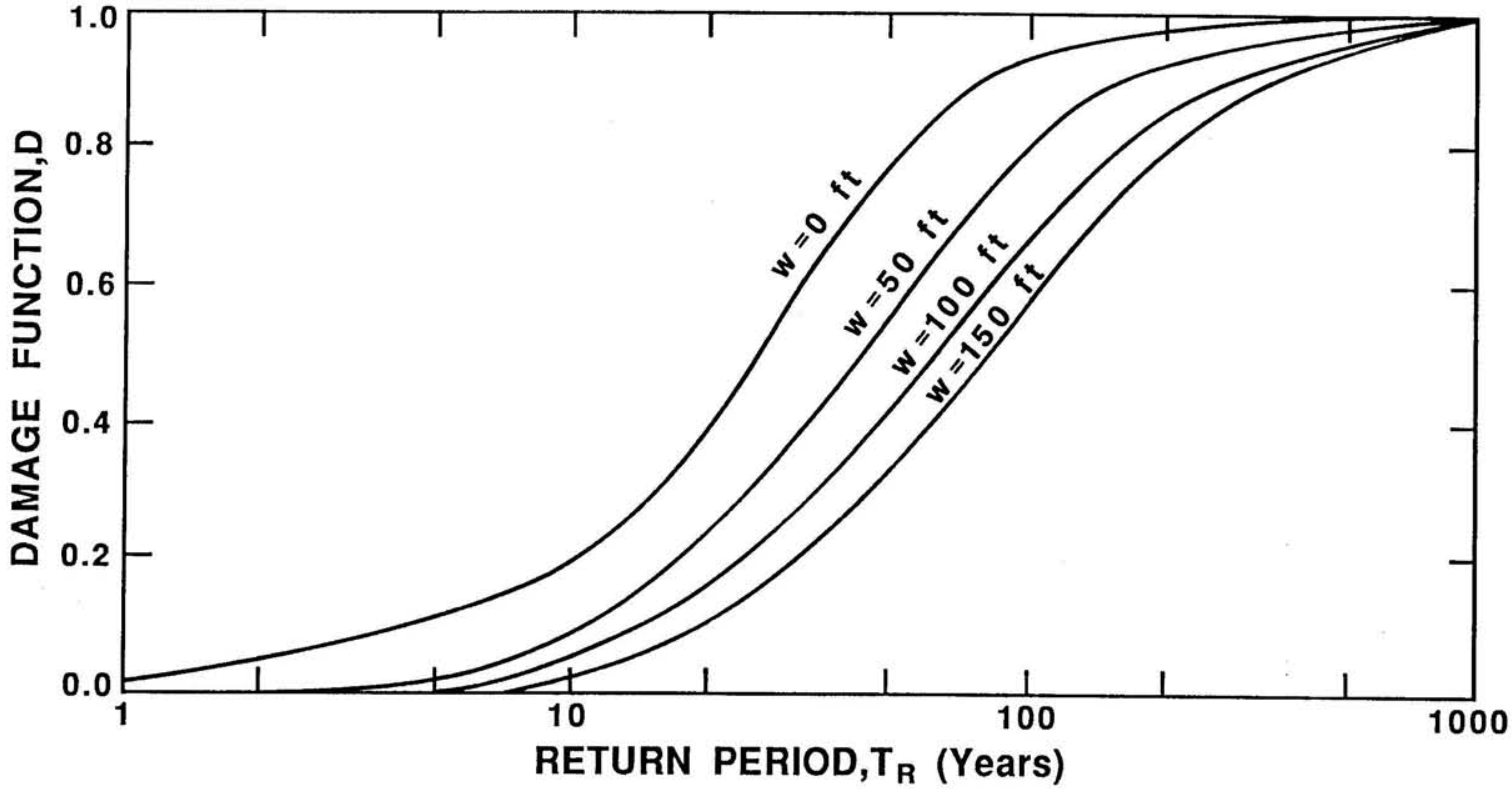

Figure 2.30. Assumed Damage Function, D, for Various Beach Widths, w, and Storm Return Periods, T_R.

be

$$F^K(w,I,J) = \sum_{j=1}^{J} D(w,T_R)\frac{1}{(1+I)^j} \tag{2.43}$$

Hear the superscript K denotes the K^{th} realization and the selection of the J storms is carried out through Monte Carlo simulation in accordance with the cumulative probability distribution, $P\left(=\frac{1}{T_R}\right)$. Thus, in addition to the most probable damage, it is possible to develop probability distributions of the present worth damage factor.

Table 2.4 presents the values of the average present worth damage factor $\bar{F}(w,I,\infty)$ for all future damages and constant beach width, w. As expected, for the higher interest rates, the present worth values are less. Of relevance is that the greatest incremental benefits occur for the beaches that are initially the most narrow, i.e. for the situation in which the structures are in greatest jeopardy. This reinforces the earlier statement that sand transported from a nourishment project that widens adjacent beaches should be recognized as a financial benefit of not loss to that project.

A somewhat more realistic approach would be to recognize that due to erosional processes, it would be necessary to renourish every $j_\star$ years during which the beach would narrow from w_o to w' at an annual recession rate, r,

$$r = \frac{w_o - w'}{j_\star} \tag{2.44}$$

For this case, one realization of the present worth damage function, $F(w_o, j_\star, r, I, J)$, is determined as

$$F^K(w_o, j_\star, r, I, \varsigma) = \sum_{n=o}^{\infty} \sum_{j+nj_\star+1}^{(n+1)j_\star} D\left(w_o - r\left(nj_\star + \frac{3}{2} - j\right)_o T_R\right)\frac{1}{(1+I)^j} \tag{2.45}$$

Each of the inner summations represents the contributions to the present worth damage factor during one nourishment interval. Damage reductions employing Eq. (2.42) can assist in identifying the optimal renourishment interval, $j_\star$.

REFERENCES

Bruun, P. (1962) "Sea Level Rise as a Cause of Shore Erosion", *ASCE Journal of Waterways and Harbors Division,* Vol. 1, p. 116-130.

Dally, W.R., R.G. Dean and R.A. Dalrymple (1985) "Wave Height Variation Across Beaches of Arbitrary Profile", *Journal of Geophysical Research*, Vol. 90, No. C6, pp. 11917-11927.

Dean, R.G. (1987) "Additional Sediment Input to the Nearshore Region", *Shore and Beach*, Vol. 55, Nos. 3- 4, p. 76-81.

Shows, E.W. (1978) "Florida's Coastal Setback Line - An Effort to Regulate Beachfront Development", Vol. 4, Nos. 1/2, *Coastal Zone Management Journal*, p. 151-164.

Chapter 3

ENGINEERING DESIGN PRINCIPLES: PART II - BOUNDARY CONDITIONS

Hsiang Wang

HISTORICAL SHORELINE INFORMATION

In beach nourishment engineering, historical shoreline change information is needed to assess the dynamics of the sediment process and the effects of man-made structures and constructions such as inlet improvement, jetties, groins, harbors, etc.This information is also needed for the prediction of the performance of a beach nourishment project and estimating the quantity and frequency of renourishment.

Historical shoreline changes can be deduced from three sources: hydrographic and beach surveys, maps and charts and aerial photographs. In the state of Florida, shoreline maps from the U.S. Coastal and Geodetic Survey (U.S. C&GS.) of reliable quality can be found as early as 1850s. The so-called T-sheet map series is available at varying scales from 1:10000 to 1:40000. One set of these T-sheet maps, the 7. 5 minute series of Standard Topographic Quadrangle Maps (scale 1:24000), is the most complete one. The shorelines are expressed as the Mean High Waterline (MHW).

Another map source is the TP-sheet series of Coastal Zone Ortho Maps (scale 1:10000), produced by the National Ocean Survey. This series of maps was constructed from aerial photos and covered the period of the 1970's only. These maps were rectified for both the horizontal and vertical distortions and the shorelines were rectified for both the horizontal and vertical distortions and the shorelines were given as Mean High Waterline also.

The second source of shoreline information is the aerial photos. Usually only vertically controlled photographs should be used. In the state of Florida, the most complete set was collected by the Florida Department of Natural Resources (DNR) from 1970s on.

They were at scale of 1:1200 and/or 1:2400 and were used to produce the states' Coastal Construction Control Line maps.

The third and perhaps the most reliable source of shoreline information is the actual ground truth survey. The sources of this type of information are quite scattered from, for instance, U.S. C&GS, U.S. Corps of Engineers (C.O.E.), state, county and city agencies and engineering consulting firms. The most systematic beach surveys are conducted by DNR. They are available since mid 1970s at approximately six year intervals. These data consists of beach face surveys to wading depth at 1000 ft intervals and hydrographic surveys to 3000 ft offshore at 3000 ft intervals.

DNR has just completed an effort to digitize and map historical shoreline changes for the entire coast of Florida. These data set should consists of the following information (Wang and Wang, 1987).

a. Digitized shoreline and offshore bathymetry at 6 ft, 12 ft, 18 ft, 24 ft, and 30 ft contours whenever available. All the data are referred to DNR monuments which, in turn, are referenced to State Plane Coordinates.

b. Composite historical shoreline change maps at a scale of 1:24000 and 1:24000.

c. Composite historical offshore depth-contour change maps at a 1:24000 scale.

Figure 3.1 is an example of the data file of the digitized shoreline information stored in DNR. Based upon our experience, the digitization error is within 0. 01 inch if done properly, which translates to 20 ft at 1:24000 scale.

BREVARD COUNTY, FLORIDA

* SHORELINE POISITION DATA FILE

DNR MONUMENT I.D.	SURVEY DATE(S)	SURVEY MONTH	STATE PLANE COORDINATES FOR DNR MONUMENT NORTHING (FEET)	STATE PLANE COORDINATES FOR DNR MONUMENT EASTING (FEET)	AZIMUTH (DEG.)	SHORELINE DISTANCE FROM DNR MONUMENT (FEET)	REFERENCE SHORELINE	SHORELINE NORTHING (FEET)	SHORELINE EASTING (FEET)	SOURCE SCALE	SOURCE
R-1T	1877-1879		1480906.50	631108.50	90	256.38	MHW	1480906.50	631364.88	20000	U.S.C&GS.
R-1T	1929		1480906.50	631108.50	90	760.81	MHW	1480906.50	631869.31	20000	U.S.C&GS.
R-1T	1947-1948		1480906.50	631108.50	90	747.19	MHW	1480906.50	631855.69	24000	U.S.G.S.
R-1T	1966		1480906.50	631108.50	90	244.81	MHW	1480906.50	631353.31	20000	U.S.C&GS.
R-1T	1969-1971		1480906.50	631108.50	90	315.44	MHW	1480906.50	631423.94	10000	U.S.N.O.S.
R-1T	1974	5	1480906.50	631108.50	90	417.38	MHW	1480906.50	631525.88	2400	DNR(PHOTO)
R-1T	1976	1	1480906.50	631108.50	90	822.44	MHW	1480906.50	631930.94	24000	U.S.G.S.
R-1T	1980	5	1480906.50	631108.50	90	579.88	MHW	1480906.50	631688.38	2400	DNR(PHOTO)
R-1T	1985	8	1480906.50	631108.50	90	527.50	MHW	1480906.50	631636.00		DNR(SURVEY)
R-1T	1985	10	1480906.50	631108.50	90	472.38	MHW	1480906.50	631580.88	2400	DNR(PHOTO)
R-2	1877-1879		1480068.00	631057.50	90	-23.37	MHW	1480068.00	631034.13	20000	U.S.C&GS.
R-2	1929		1480068.00	631057.50	90	427.81	MHW	1480068.00	631485.31	20000	U.S.C&GS.
R-2	1947-1948		1480068.00	631057.50	90	448.06	MHW	1480068.00	631505.56	24000	U.S.G.S.
R-2	1966		1480068.00	631057.50	90	120.69	MHW	1480068.00	631178.19	20000	U.S.C&GS.
R-2	1969-1971		1480068.00	631057.50	90	176.44	MHW	1480068.00	631233.94	10000	U.S.N.O.S.
R-2	1974	5	1480068.00	631057.50	90	185.63	MHW	1480068.00	631243.13	2400	DNR(PHOTO)
R-2	1976	1	1480068.00	631057.50	90	701.69	MHW	1480068.00	631759.19	24000	U.S.G.S.
R-2	1980	5	1480068.00	631057.50	90	445.75	MHW	1480068.00	631503.25	2400	DNR(PHOTO)
R-2	1985	8	1480068.00	631057.50	90	345.81	MHW	1480068.00	631403.31		DNR(SURVEY)
R-2	1985	10	1480068.00	631057.50	90	316.38	MHW	1480068.00	631373.88	2400	DNR(PHOTO)
R-3	1077-1879		1479006.50	630673.00	90	-20.25	MHW	1479006.50	630652.75	20000	U.S.C&GS.
R-3	1929		1479006.50	630673.00	90	390.81	MHW	1479006.50	631063.81	20000	U.S.C&GS.
R-3	1947-1948		1479006.50	630673.00	90	364.63	MHW	1479006.50	631037.63	24000	U.S.G.S.
R-3	1966		1479006.50	630673.00	90	117.88	MHW	1479006.50	630790.88	20000	U.S.C&GS.
R-3	1969-1971		1479006.50	630673.00	90	155.75	MHW	1479006.50	630828.75	10000	U.S.N.O.S.
R-3	1974	5	1479006.50	630673.00	90	172.38	MHW	1479006.50	630845.38	2400	DNR(PHOTO)
R-3	1976	1	1479006.50	630673.00	90	722.94	MHW	1479006.50	631395.94	24000	U.S.G.S.
R-3	1980	5	1479006.50	630673.00	90	488.63	MHW	1479006.50	631161.63	2400	DNR(PHOTO)
R-3	1985	8	1479006.50	630673.00	90	366.94	MHW	1479006.50	631039.94		DNR(SURVEY)
R-3	1985	10	1479006.50	630673.00	90	320.13	MHW	1479006.50	630993.13	2400	DNR(PHOTO)
R-4T	1877-1879		1478094.00	630366.50	90	-20.75	MHW	1478094.00	630345.75	20000	U.S.C&GS.
R-4T	1929		1478094.00	630366.50	90	330.13	MHW	1478094.00	630696.63	20000	U.S.C&GS.
R-4T	1947-1948		1478094.00	630366.50	90	343.25	MHW	1478094.00	630709.75	24000	U.S.G.S.
R-4T	1966		1478094.00	630366.50	90	94.56	MHW	1478094.00	630461.06	20000	U.S.C&GS.
R-4T	1969-1971		1478094.00	630366.50	90	169.38	MHW	1478094.00	630535.88	10000	U.S.N.O.S.
R-4T	1974	5	1478094.00	630366.50	90	139.50	MHW	1478094.00	630506.00	2400	DNR(PHOTO)
R-4T	1976	1	1478094.00	630366.50	90	708.94	MHW	1478094.00	631075.44	24000	U.S.G.S.
R-4T	1980	5	1478094.00	630366.50	90	497.13	MHW	1478094.00	630863.63	2400	DNR(PHOTO)
R-4T	1985	8	1478094.00	630366.50	90	311.31	MHW	1478094.00	630677.81		DNR(SURVEY)
R-4T	1985	10	1478094.00	630366.50	90	270.38	MHW	1478094.00	630636.88	2400	DNR(PHOTO)
R-5	1877-1879		1477176.50	630103.00	90	-60.81	MHW	1477176.50	630042.19	20000	U.S.C&GS.
R-5	1929		1477176.50	630103.00	90	269.44	MHW	1477176.50	630372.44	20000	U.S.C&GS.
R-5	1947-1948		1477176.50	630103.00	90	289.00	MHW	1477176.50	630392.00	24000	U.S.G.S.
R-5	1966		1477176.50	630103.00	90	90.31	MHW	1477176.50	630193.31	20000	U.S.C&GS.
R-5	1969-1971		1477176.50	630103.00	90	145.56	MHW	1477176.50	630248.56	10000	U.S.N.O.S.
R-5	1974	5	1477176.50	630103.00	90	99.19	MHW	1477176.50	630202.19	2400	DNR(PHOTO)
R-5	1976	1	1477176.50	630103.00	90	653.31	MHW	1477176.50	630756.31	24000	U.S.G.S.
R-5	1980	5	1477176.50	630103.00	90	427.56	MHW	1477176.50	630530.56	2400	DNR(PHOTO)
R-5	1985	8	1477176.50	630103.00	90	277.50	MHW	1477176.50	630380.50		DNR(SURVEY)
R-5	1985	10	1477176.50	630103.00	90	224.88	MHW	1477176.50	630327.88	2400	DNR(PHOTO)
R-6T	1877-1879		1476239.01	629838.12	90	-102.93	MHW	1476239.01	629735.19	20000	U.S.C&GS.
R-6T	1929		1476239.01	629838.12	90	215.69	MHW	1476239.01	630053.81	20000	U.S.C&GS.
R-6T	1947-1948		1476239.01	629838.12	90	252.82	MHW	1476239.01	630090.94	24000	U.S.G.S.
R-6T	1966		1476239.01	629838.12	90	101.13	MHW	1476239.01	629939.25	20000	U.S.C&GS.
R-6T	1969-1971		1476239.01	629838.12	90	173.13	MHW	1476239.01	630011.25	10000	U.S.N.O.S.
R-6T	1974	5	1476239.01	629838.12	90	108.51	MHW	1476239.01	629946.63	2400	DNR(PHOTO)
R-6T	1976	1	1476239.01	629838.12	90	628.01	MHW	1476239.01	630466.13	24000	U.S.G.S.
R-6T	1980	5	1476239.01	629838.12	90	397.63	MHW	1476239.01	630235.75	2400	DNR(PHOTO)

Figure 3.1. Example of Data File of the Digitized Shoreline Information Stored In DNR.

For beach nourishment design, two kinds of information are useful–shoreline changes and volumetric changes. The problems associated with the computations of shoreline and volumetric changes are discussed in the following sections.

COMPUTATION OF SHORELINE CHANGES

For beach nourishment design shoreline change information are useful to assess background erosion or accretion rate and the effects of structure on updrift and downdrift shorelines. An example is used here to illustrate the procedures.

The example used here is the stretch of shoreline centered around Sebastian Inlet which is located at the Brevard/Indian River County line on the east coast of Florida (Fig.3.2). Attempts to open the inlet by hand labor started in 1886 but the inlet was never remained open for any extended period until 1948 when the inlet was stabilized by the construction of permanent jetties. Therefore, it serves as an good example as how the structure effects the shoreline change through examining historical data.

Figure 3.3 plots the historical shoreline changes for three different period from 1929 to 1947, prior to inlet stabilization, from 1947-70, the initial stage of inlet stabilization and from 1970-1986, the later stage of inlet stabilization. As can be seen, prior to inlet stabilization by jetty structure, the shoreline overall advanced during this period. During the period of 1947-70, the effects of the post stabilized inlet was quite pronounced with updrift accretion and downdrift erosion of approximately 5 miles on each side. The estimated updrift accretion was about 3 ft/yr. whereas the downdrift erosion was about 5 ft/yr. Clearly, the littoral drift was not only impounded on the updrift side but also on the ebb tidal shoal and transported into the inlet. From 1970-86, the rate of shoreline changes slowed down considerably to approximately 1.5 ft/yr. erosional on the south side and 1.0 ft/yr. accretional on the north side. This was probably due to the fact that ebb tidal shoal became more matured during the later stage, thus, impounded less material.

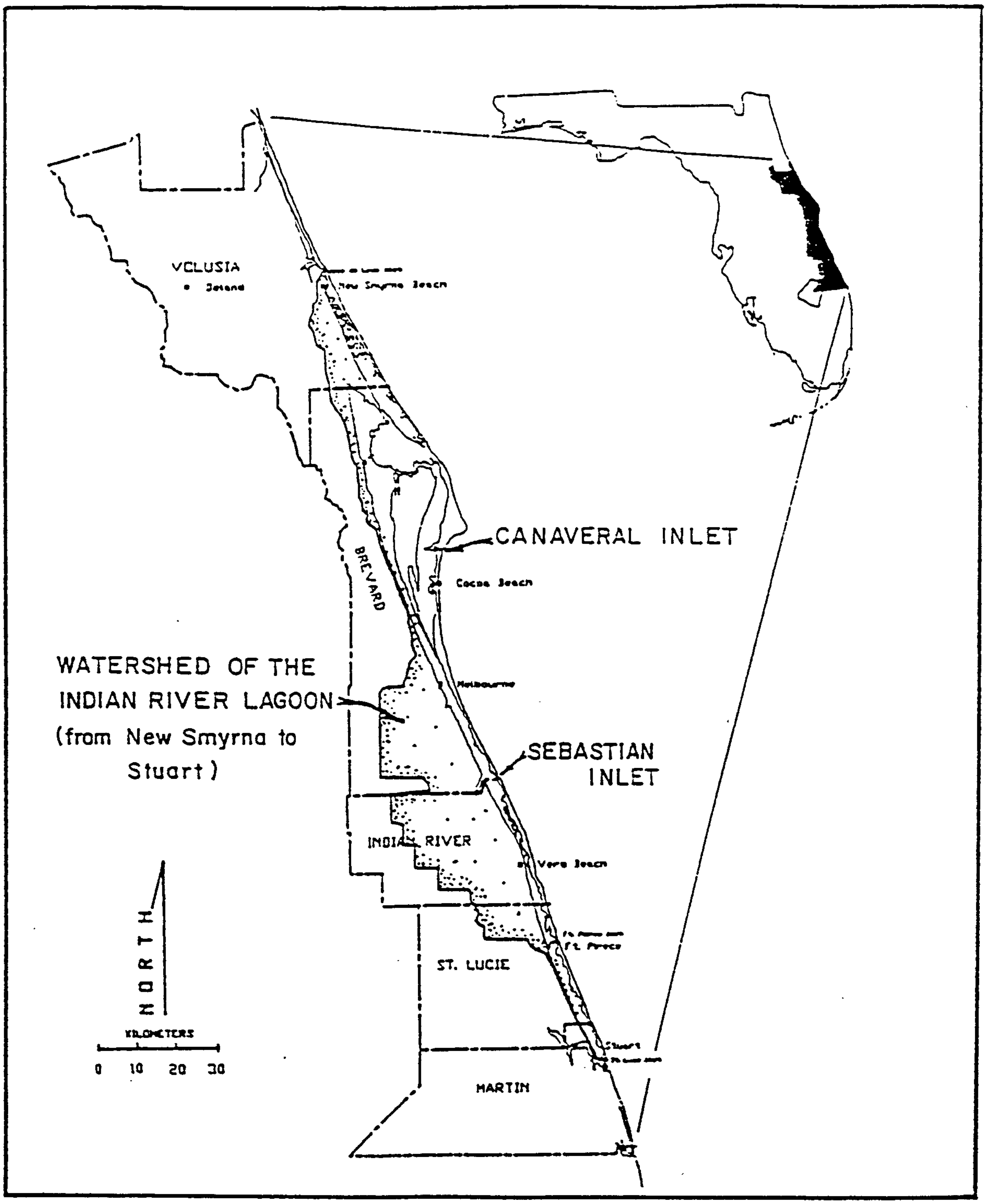

Fig. 3.2. Location of Sebastian Inlet, FL., and the watershed of Indian River Lagoon.

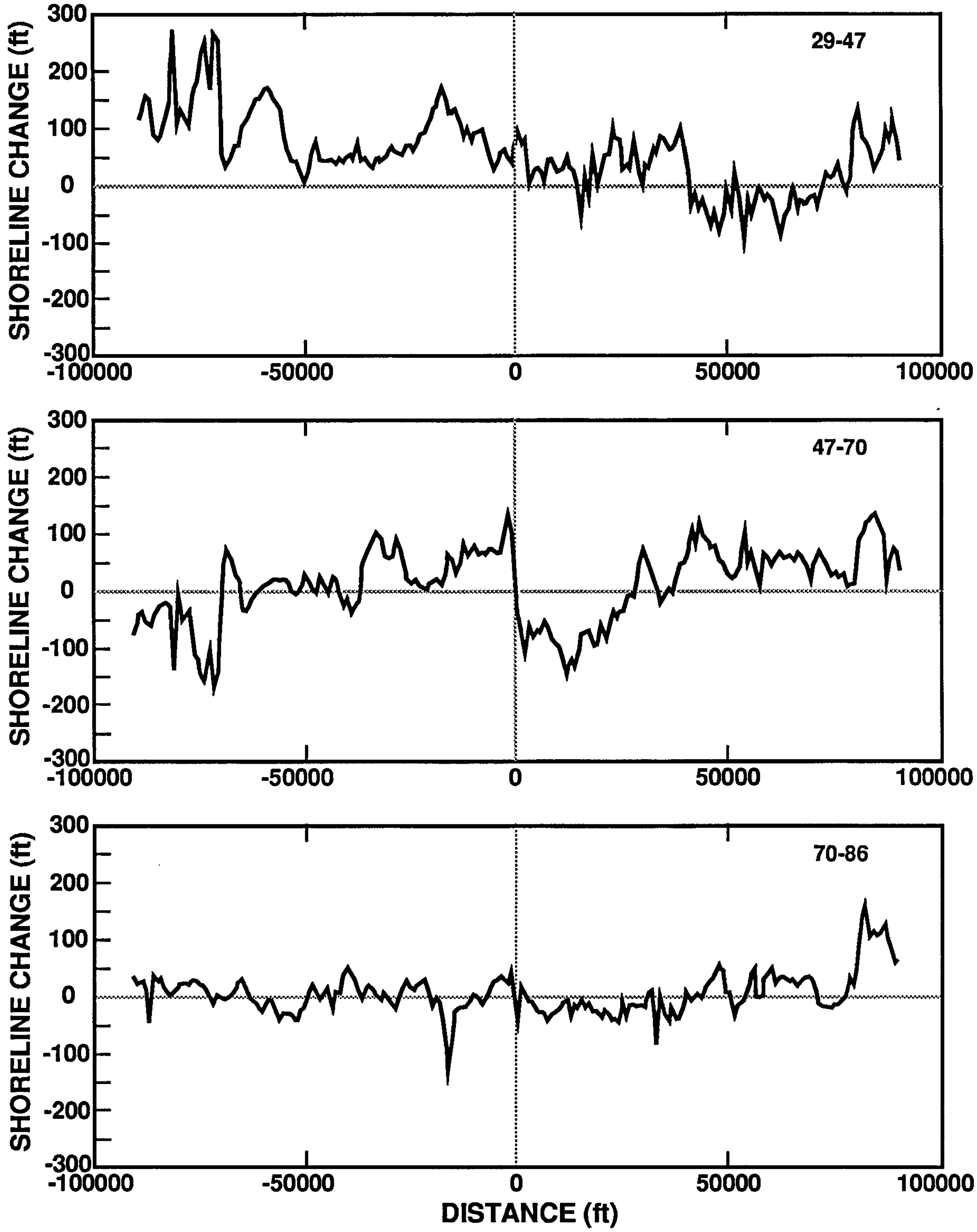

Fig. 3.3. Historical shoreline changes near Sebastian Inlet during three different periods (Inlet stabilized in 1946).

By examining historical data, one can also identify the locations of critical erosion. In the present case, the most severe erosion occurs immediately on the downdrift of the downdrift jetty and at three miles downdrift of the inlet.

The data of shoreline change is often quite noisy. Usually some form of smoothing is required such as running average or harmonic analysis. To separately identify the background shoreline change and the change due to shore-perpendicular structures, two techniques can be used; the so-called odd-even analysis proposed recently by Douglas and Dean (1990) and the well known harmonic analysis.

The odd-even analysis was based on the reasoning that in the absence of structure, the shoreline change should be more or less spatially uniform, therefore, manifests even function change. The presence of shore-perpendicular structure, on the other hand, would cause opposite effects on the updrift and the downdrift shorelines; therefore, the resulting shoreline change should appear as odd function. Mathematically, the even and odd components of the shoreline changes can be established by the following equations:

$$\Delta V_e(x) = \frac{1}{2}[\Delta V(+x) + \Delta V()x)] \tag{3.1}$$

$$\Delta V_o(x) = \frac{1}{2}[\Delta V(+x) + \Delta V(V_x)] \tag{3.2}$$

where V can be shoreline position change or volumetric change; the subscripts e and o refer to even and odd, respectively. The net change is then:

$$\Delta V = V_e + V_o \tag{3.3}$$

The results of odd and even analysis for the period of 1947-70 for the Sebastian Inlet region while the effects of the inlet was most pronounced was illustrated in Fig 3.4.

The harmonic analysis serves similar purpose. The shoreline is expressed as a series of harmonic functions which contain even and odd functions as follows:

$$V(x) = a_0 + \sum_1^n a_n \cos k_n x + \sum_1^n b_n \sin k_n x \tag{3.4}$$

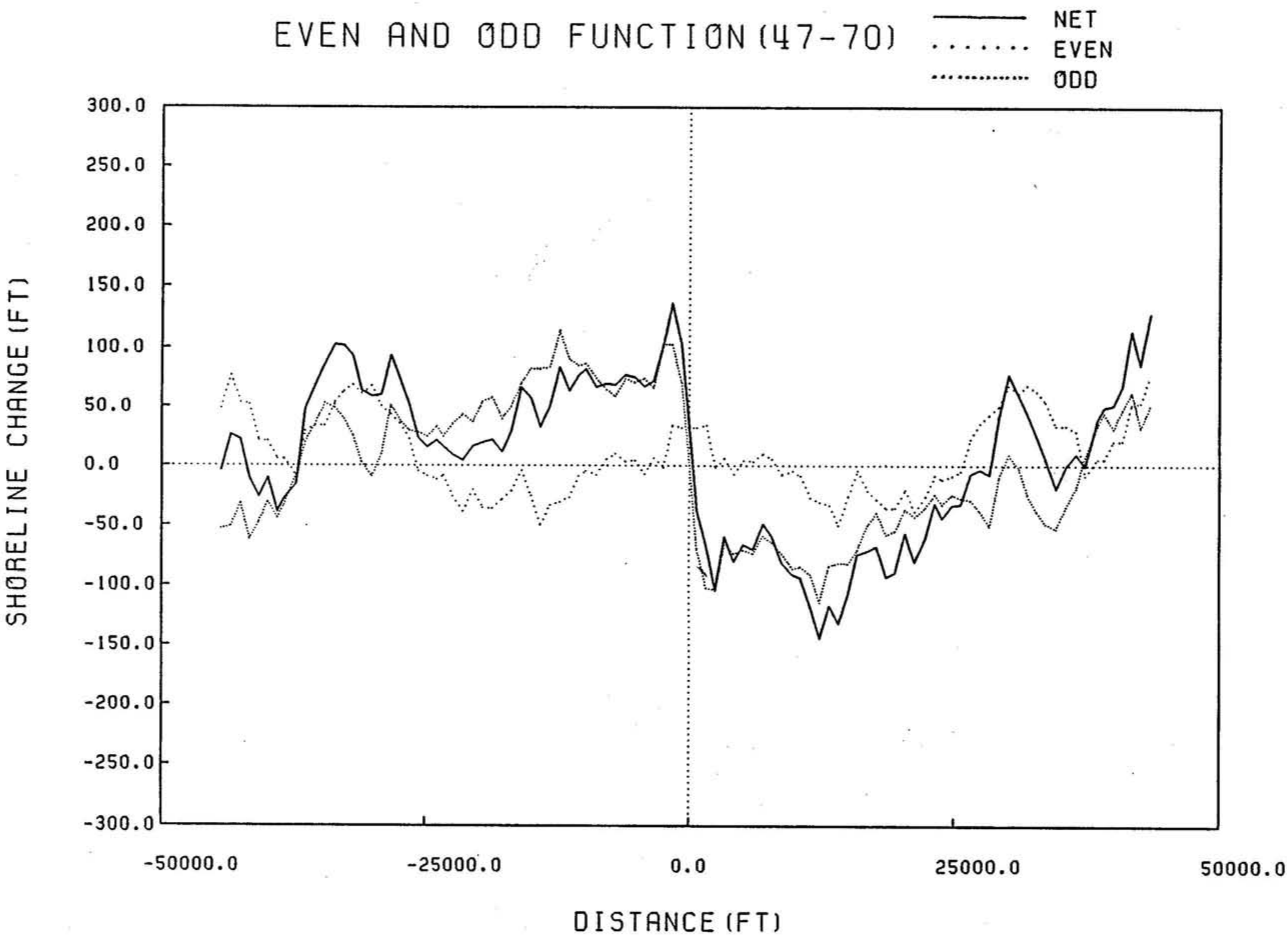

Fig. 3.4. Even-odd function analysis near Sebastian Inlet for shoreline changes between 1947-1970 (Inlet location at origin).

where $k_0 = \frac{2\pi}{L}$ with L being the length of the shoreline, and $k_n = nk$. The coefficients a's and b's can be determined by conventional Fourier analysis. The coefficient a_0 represents the mean shoreline movement. All the cosine terms are even functions representing background shoreline changes whereas all the sine terms are odd functions representing shoreline changes due to structure effects. This harmonic analysis tends to smooth the data and also brings out the rhythmic feature, if any, of the shoreline change. This method is, however, not suitable for short shoreline length.

Other data analysis techniques such as Eigen function analysis are also used to bring out various features of shoreline changes such as shoreline rotations, etc.

To compute volumetric change requires hydrographic and topographic information in addition to shoreline position. It is useful to compute the volumetric changes above the MHW and below the MHW separately. In theory, this can be done simply through integrating the area between measured profiles. In practice, a number of problems are involved which are discussed here:

A. Estimation of offshore depth limit

There are a number of conventional offshore control depths as defined in Fig. 3.5.: the breaking depth, d_b, is where the wave breaks, the depth of active profile, d_e, is defined as the seaward depth of littoral zone, the shoaling zone depth, d_s, also known as the buffer zone depth, is the offshore depth of a zone within which the sediment motion is mainly onshore due to wave induced bottom drift and the closure depth, d_c, is defined as the limiting water depth beyond which the sediment motion can be considered to be minimal in a time scale of engineering interest.

These depths are functions of many variables including, among other, wave and current environment, tidal range, offshore slope and topography, presence of structures and sediment characteristics. As just which depth we should select as depth of computation depends on the purpose.

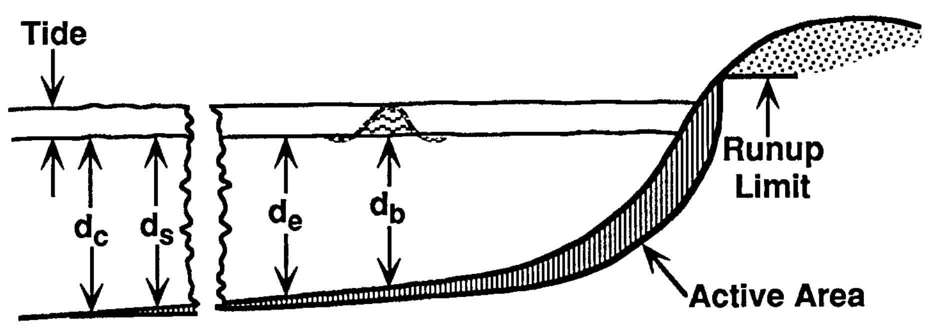

Fig. 3.5. Definitions of offshore control depths.

To determine long term volumetric changes the closure depth is the logical choice. For the Atlantic coast, a depth of 27 ft (9m) measured from the berm elevation has been suggested as the representative value. Owing to the very mild slope along the Atlantic coast, this depth could be way offshore (typically from 1000 to 4000 ft offshore but could be considerably further of offshore rock crops or reefs exist). At such a distance accurate profile data may not exist. The hydrographic survey by DNR, for instance, was carried out to approximately 3000 ft offshore at 3000 ft longshore intervals (every fourth monument).

Using Indian River County as an example, Figure 3.6 shows the offshore topographies. The 30 ft contour line grows wider toward the south partially owing to the existence of a reef system (shown by hatched area). Therefore, in the northern end, the DNR survey reached beyond -27 ft but in the southern part of the county, the closure depth was never reached in either 1972 or 1986 survey series. A number of representative survey profiles in the county are shown in Figure 3.7.

The effects of choosing different offshore closure depths are further illustrated in Figure 3.8. In this figure, volume changes along the shoreline computed to different elevations were shown. The solid line marked <u>all</u> means the closure depth was at the end point of the survey irrespective the depth at this point. This point roughly (but not always) corresponds to the -30 ft depth. The total volumetric changes for the entire county which is the integration of volume along the shoreline are tabulated here:

Above NGVD	1.4×10^6 yd^3
From NGVD to 5′	0.6×10^6 yd^3
From NGVD to 10′	0.8×10^6 yd^3
From NGVD to 15′	0.1×10^6 yd^3
Total below NGVD	-4.7×10^6 yd^3

Therefore, depending upon the selection of offshore boundary, this coast could appear to be accretional down to -15 ′ NGVD. But this coast is erosional if the closure depth was used as the offshore boundary by losing about 4.7×10^6 yd ^{3} of sand during 1972-86.

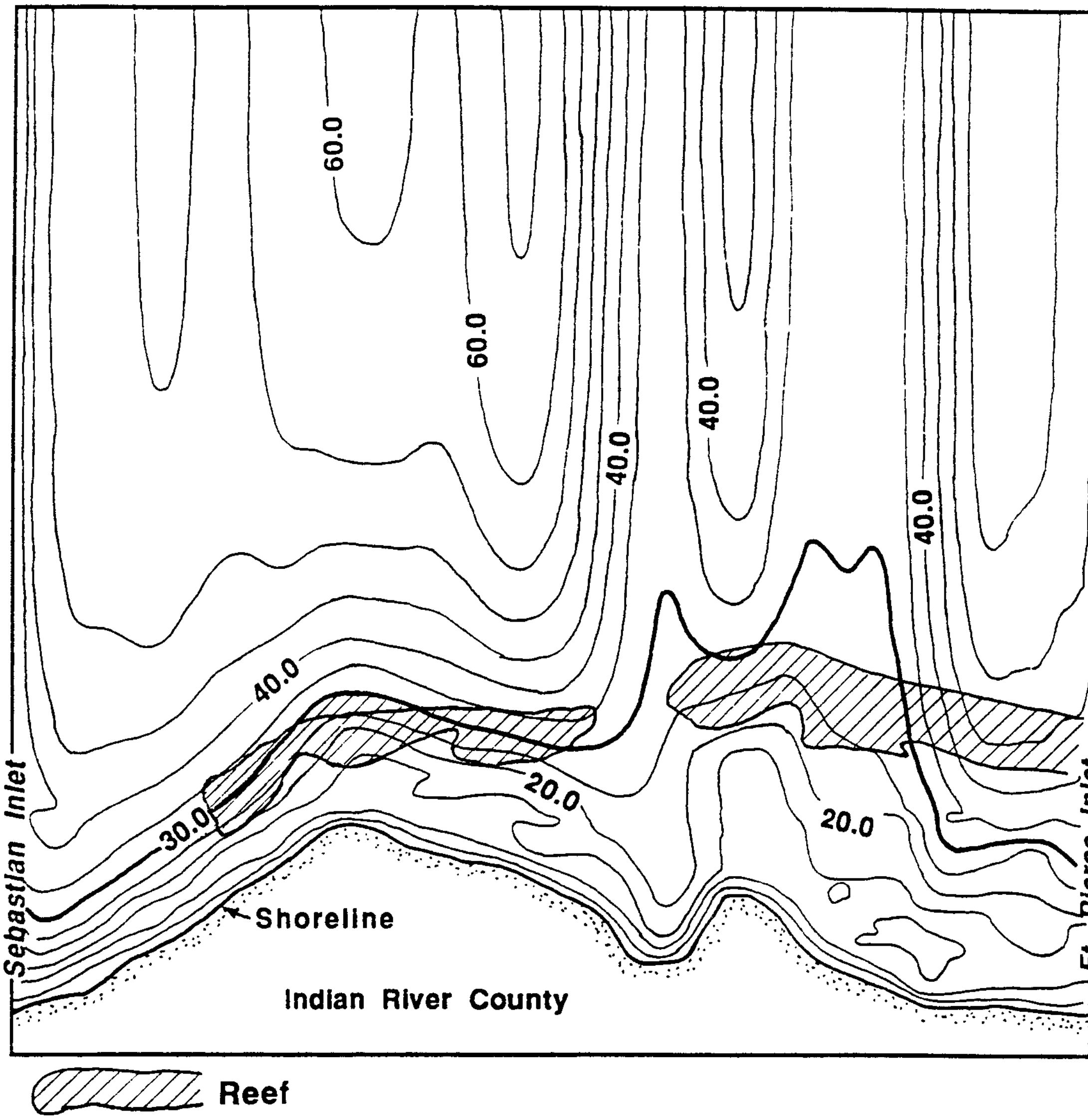

Figure 3.6. **Offshore Depth Contour of Indian River County (1972 DNR Survey).**

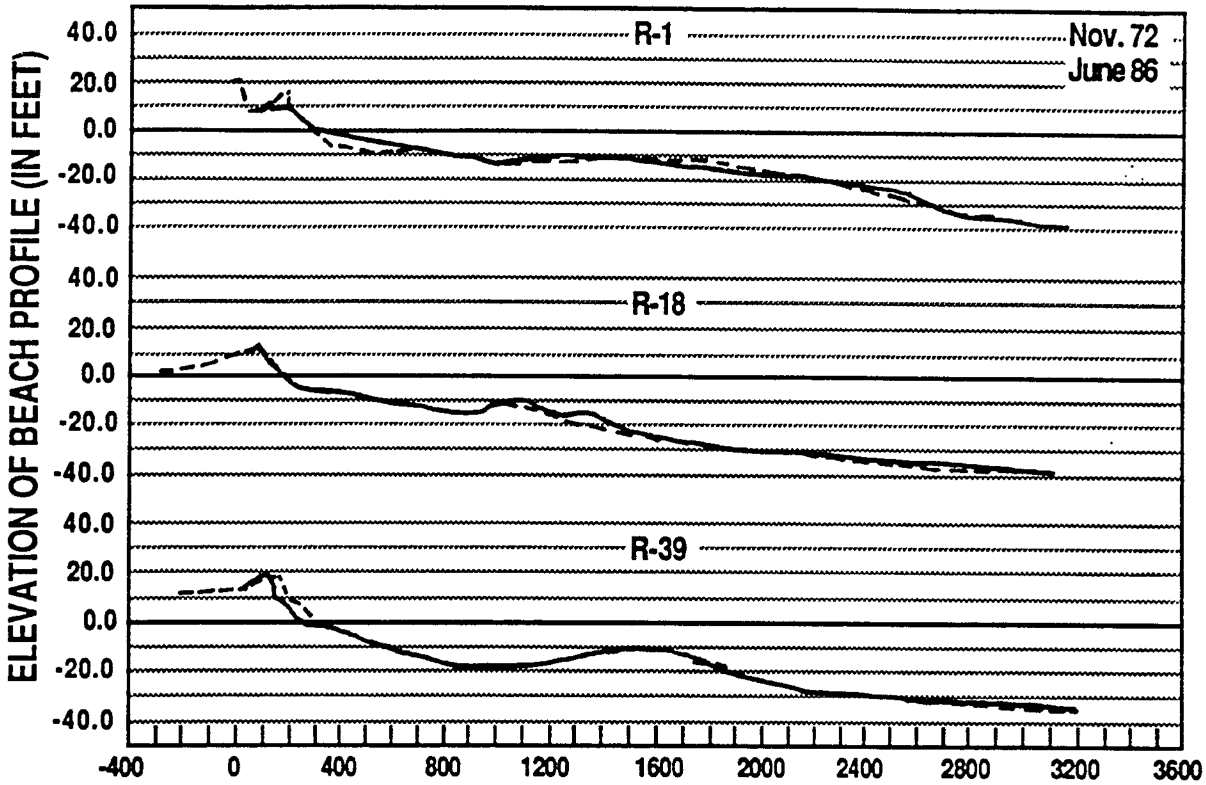

(A) Profiles at North End

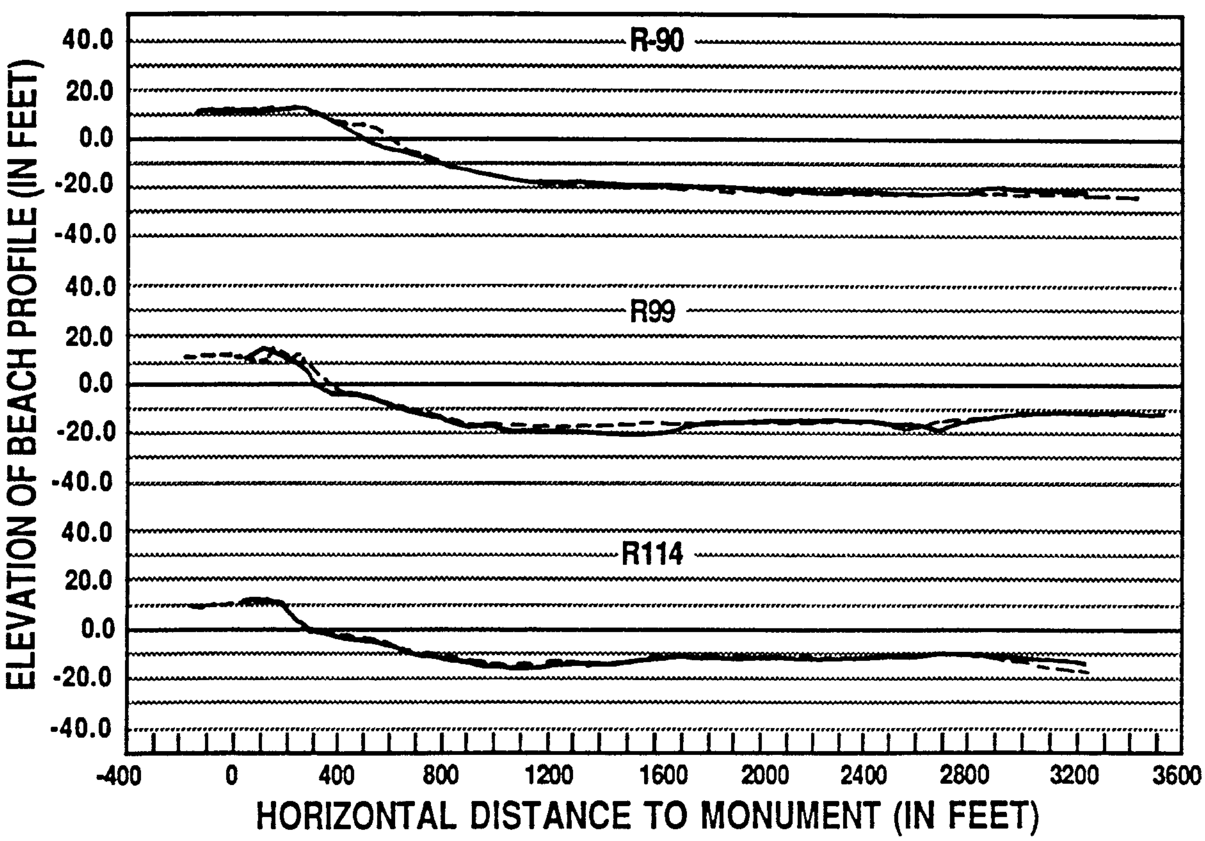

(B) Profiles at South End

Figure 3.7. **Representative Survey Profiles Along Indian River County Shoreline (R1, R18, R39 in North) (R90, R99, R114 in South)**

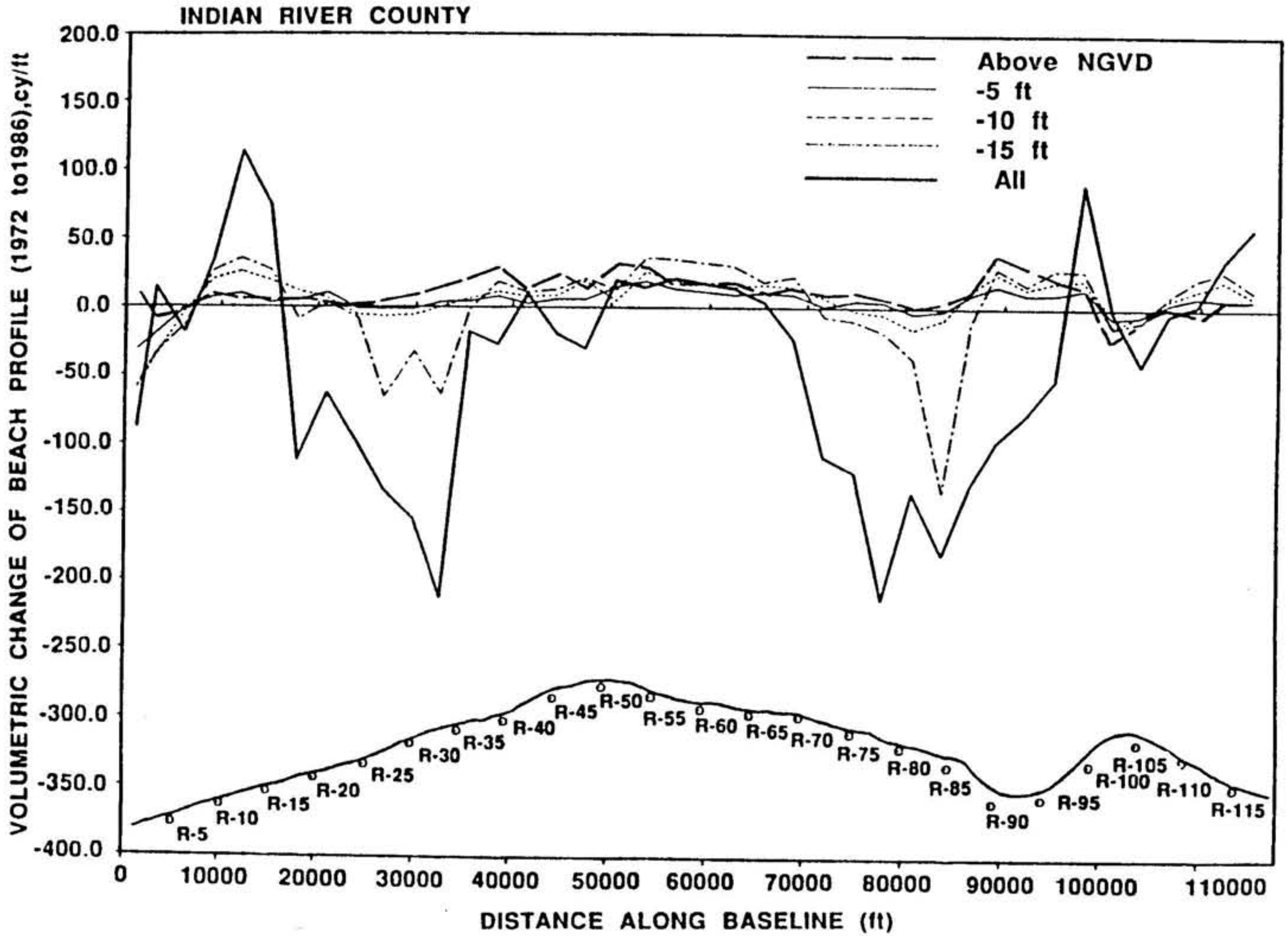

Figure 3.8. **Volumetric Changes as Influenced by Different Offshore Closure Depths (Indian River County).**

The selection of beach nourishment offshore depth limit is another important task as this depth greatly affects the nourishment volumetric requirement computation which, in turn, affects the project evolution and the performance of the project.

Clearly, it is impractical to use the closure depth as the nourishment limit for it will require too large a nourishment volume. Furthermore, at such a distance accurate profile data may not exist as mentioned earlier.

The depth of the active profile can be argued, and certainly is more practical, as a reasonable choice. This depth can be computed on the concept of critical shear stress, or as a solution of

$$U_c^2 = K_c(S-1)gd \tag{3.5}$$

where U_c is the critical near-bed velocity, S is the ratio of sediment to fluid density, g is gravitational acceleration and d is the water depth. The coefficient K_c is in the order of 0.03 for median sand. Hallermeier (1983) proposed the following empirical equation

$$d_e = 2.9H(S-1)^{-0.5} - 110\frac{H^2}{(S-1)gT^2} \tag{3.6}$$

For field application it was also suggested that an annual value of d_e can be established by using H value exceeded 12 hrs per year, or,the local significant wave height with frequency of exceedance of 0.137%. Birkermier(1988) found the value from Eq.(3.6) to be too high and suggested the following modified equation:

$$d_e = 1.75(h_s)_{0.137} - 57.9\frac{(H_{s,0.137})^2}{gT_s^2} \tag{3.7}$$

For random waves with P-M spectrum and with JONSWAP spectrum, the values of $\frac{H_s}{gT_s^2}$ are 0.004 and 0.005, respectively. When these values are used, Eq.(3.6) gives

$$d_e = 1.95 \ \ to \ \ 2.00(H_s)_{0.137} \tag{3.8}$$

and from Eq.(3.7)

$$d_e = 1.45 \ \ to \ \ 1.51(H_s)_{0.137} \tag{3.9}$$

A value of d_e equal to 1.5 to 1.75 $(h_S)_{0.137}$ has been recommended as a practical range.

B. Errors induced by survey inaccuracy

The most serious survey error is the shift of horizontal and vertical datums between surveys as this error is cumulative. Because of the mild slope and long horizontal distance, a small shift in either horizontal or vertical datum could translate into thousands cubic feet of sediment volume per lineal foot of beach front. Thus, the error could be in the same order of magnitude as the total volumetric change. A sensitivity analysis such as illustrated in Figure 3.9 would be helpful to establish the confidence level of the results. From this figure, it can be seen that if the volumetric change is small (mild erosion or accretion), the survey induced error (relative) could be very large. On the other hand, if the volumetric change is large (strong erosion or accretion) the survey induced error, relatively speaking, is usually small. The other source of error which by its nature is less serious is due to the motion of the survey vessel. Over a long distance the errors of this type tend to compensate each other as oppose to cumulative.

C. Seasonal variations

The shape of the beach is known to vary seasonally. Therefore, comparisons of beach profiles surveyed at two different seasons could lead to wrong conclusions. Figure 3.10 shows that from 1972 (winter profile) to 1986 (summer profile), Indian River County had an apparent shoreline advance. St. Lucie County which is next to the Indian River County on the south also had two hydrographic surveys by DNR, one in 1972 and the other in 1987. However, the survey in 1972 was carried out in the summer whereas the 1987 survey was completed in the winter, exactly the opposite to the Indian River County case. Now as shown in Figure 3.9, the shoreline had an apparent retreat downdrift from the Fort Pierce Inlet; the volumetric change to the near-closure depth was actually accretional. This is, of course, exactly opposite to the situation in the Indian River County. These two counties are adjacent to each other; yet, during the same period the shoreline in one county advanced while the other retreated. Thus, the possibility of false signals due to seasonal variations must be examined.

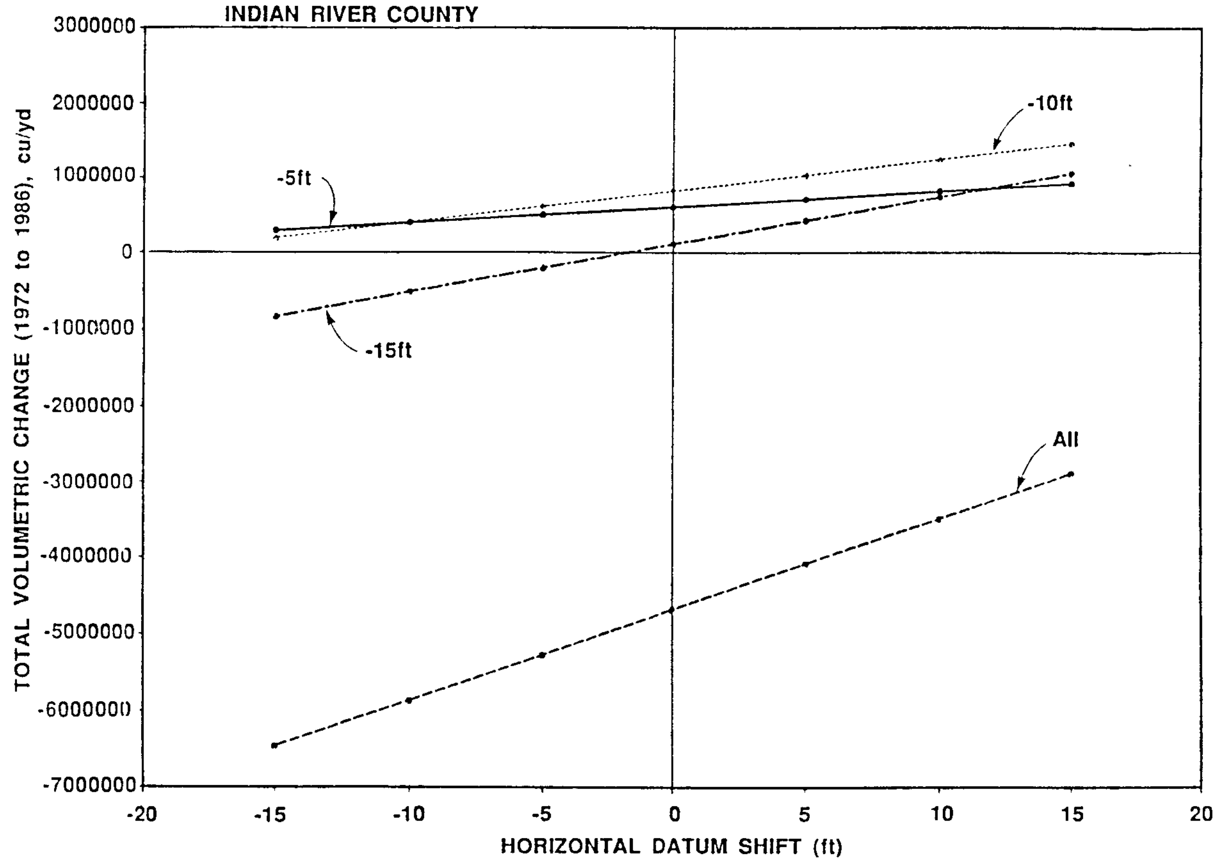

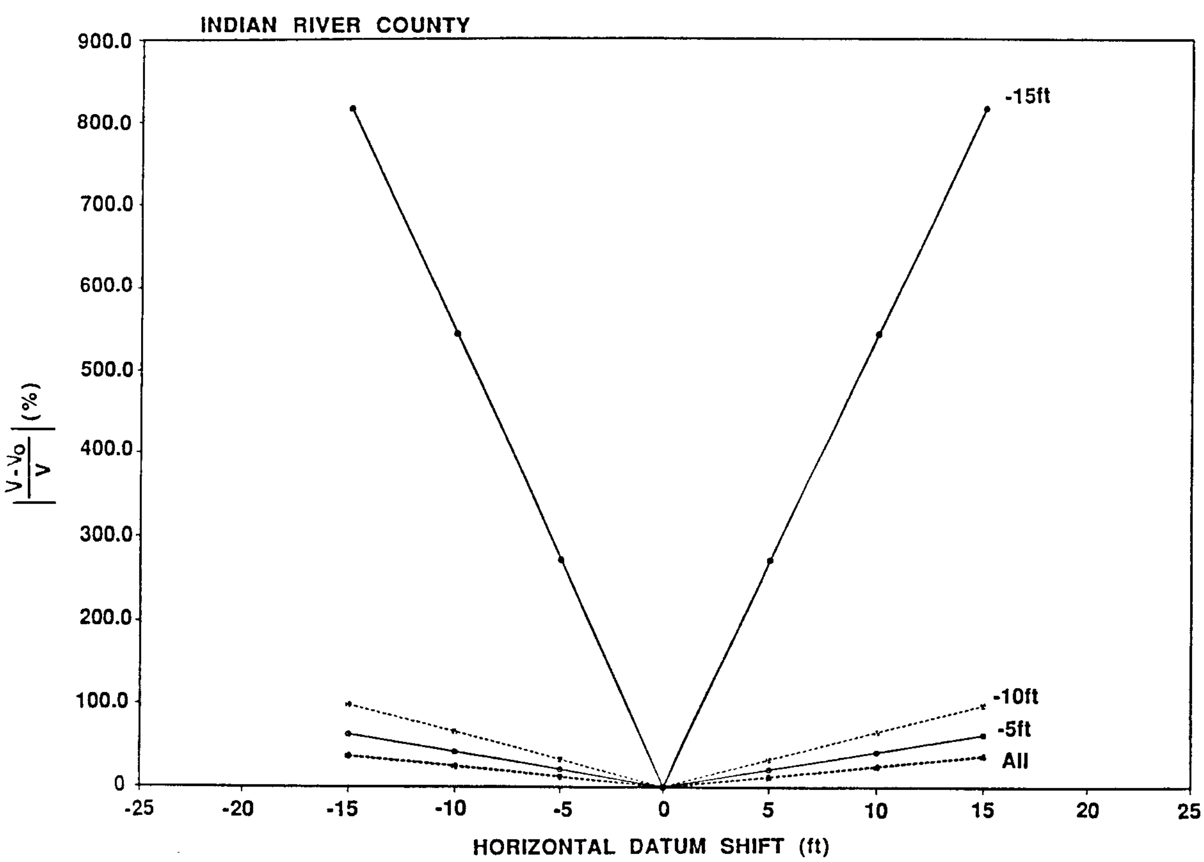

Figure 3.9. **Errors Induced by Shifting of Datum (1972 is used as reference; Positive Value means 1986 Profile Shifted Seaward).**

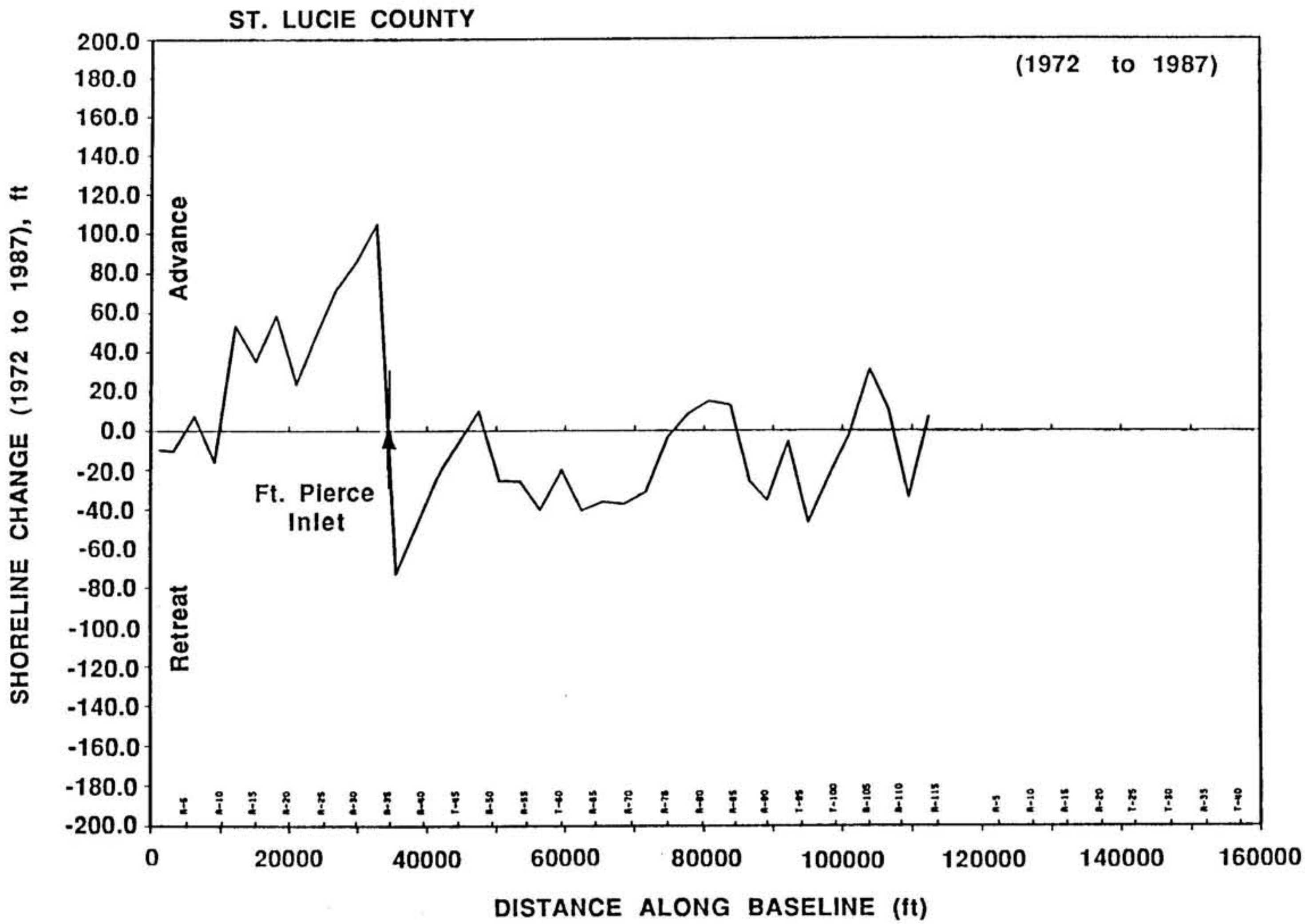

Figure 3.10. **Total Shoreline Change of St. Lucie County.**

LONG-TERM AND EXTREME SEA CONDITIONS

Wave is the prime mover of coastal sediment. Long-term wave information is the necessary input for computing littoral drift quantity and shoreline evolution which, in turn, governs the effectiveness of beach nourishment and the required frequencies of renourishment. The extreme sea conditions are needed to estimate short-term shoreline retreat and dune erosion due to design storm; both are important boundary conditions for beach nourishment design.

Long-term wave information along the Florida Coast can be derived from a number of sources:

A. Summary of Synoptic Meteorological Observations (SSMO)

SSMO was prepared under the direction of the U.S. Naval Weather Service Command by the National Climatic Center. All the data were obtained from Marine surface observations by ships. It is one of the most commonly cited data sources for surface winds and ocean waves. Along the Florida coast these marine conditions are divided into five regions - Jacksonville, Miami, Key West, Fort Myers, Apalachicola and Pensacola. Statistics of percent frequency of wind speed and direction versus sea height were given on a monthly basis as were the percent frequency of wave height versus wave period.

Based upon these data, the statistics of wave height versus wave direction in deep water condition can be inferred. The joint distribution of wave height, wave period and direction cannot be established with this set of data without further assumptions. Since SSMO data are biased to calm weather they are not suitable for extreme condition analysis.

B. Measured Wave Data

The National Oceanic and Atmospheric Administration (NOAA) maintained a number of meteorological buoys along the coast of the United States. The locations of the North Atlantic and Gulf coast buoys are shown in Figure 3.11. They are all in deep water with

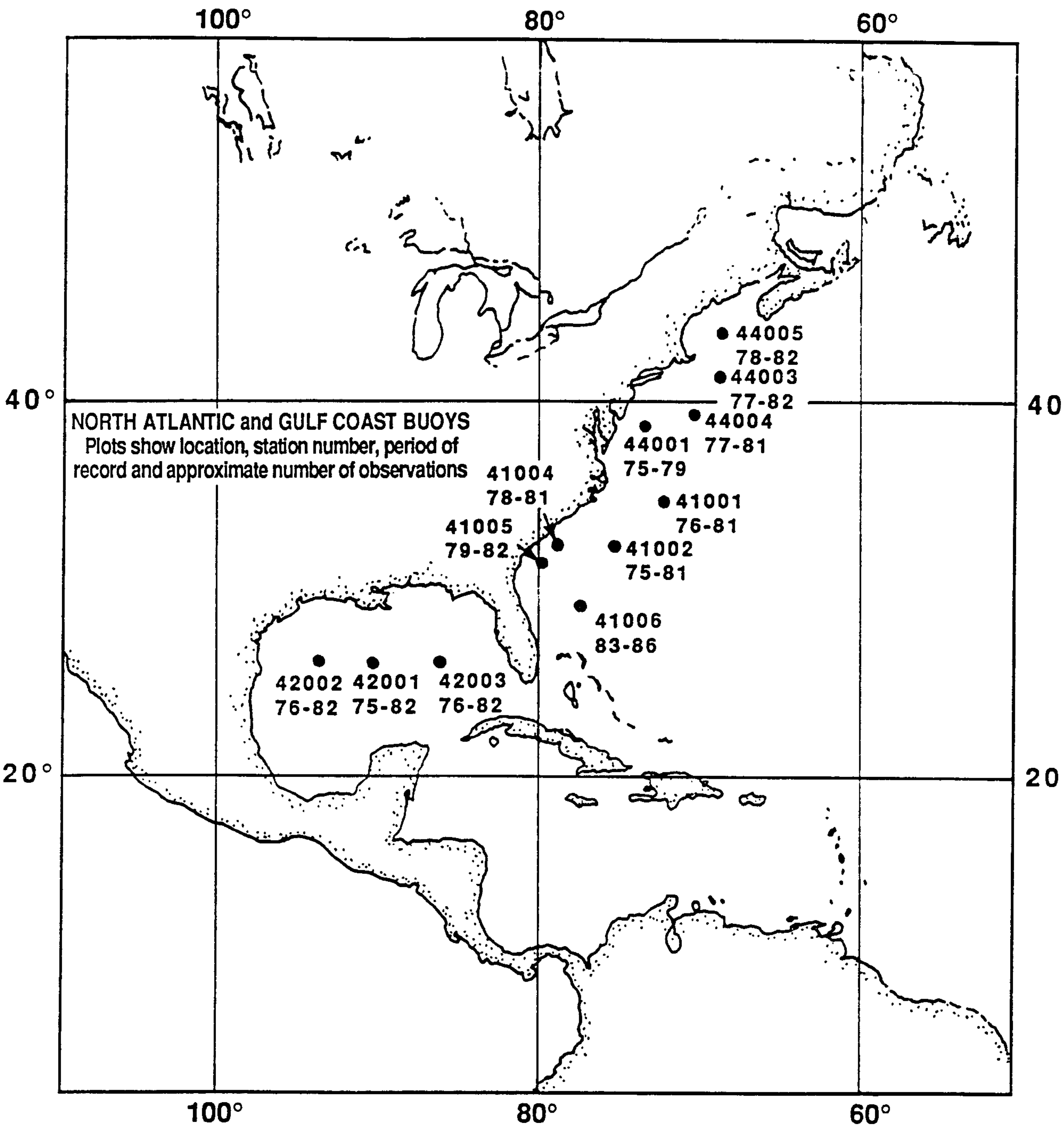

Figure 3.11. **North Atlantic and Gulf of Mexico Buoys.**

water depths ranging from 120 m to 4,000 m (Wilson, 1975-1986). These buoys record wave height and period as well as wind conditions at the 5-meter level. The wave directions have to be inferred from wind information.

Along the coast of Florida, the Department of Coastal and Oceanographic Engineering (COE), University of Florida, maintains a coastal data network (CDN) that contains twelve gage stations at present. Their water depths range from 5. 8 m to 18. 0 m. These gages record wave height, wave period and water level variations. A few of the gages also can provide wave directional information by simultaneously measuring oscillatory current velocities in the horizontal plane. The locations of these gages are also shown in Figure 3.12. At certain locations, up to 10 years of data have been recorded. All the data are archived in COE and monthly summary reports are available. Table 3.1 illustrates the format of the monthly wave information summary and Figure 3.13 shows the graphic display of the monthly wave information.

A list of information concerning the wave data lengths, types, and mean water depths and locations where data are being collected by the CDN wave gages and the NOAA buoys is given in Table 3.2. The CDN wave gages are identified by the names of the nearby cities or bay systems. The NOAA buoys are identified by the location identification numbers. Most of the wave data retrieved from the CDN wave gages have data length more than five years while most of the buoy data have data length longer than ten years.

C. Wave Hindcasting Information

At present, there are a number of operational wave hindcast models for the Atlantic Ocean along the eastern seaboard of the United States. The Fleet Numerical Oceanography Center (FNOC), U.S. Navy, for instance, provides routine wave hindcasting based upon their Global Spectral Ocean Wave Model (GSOWM). The GSOWM is based on a 2. 5 by 2. 5 degree latitude/longitude grid. It provides deepwater wave information in terms of wave energy- frequencies versus direction. This hindcast information is available on magnetic

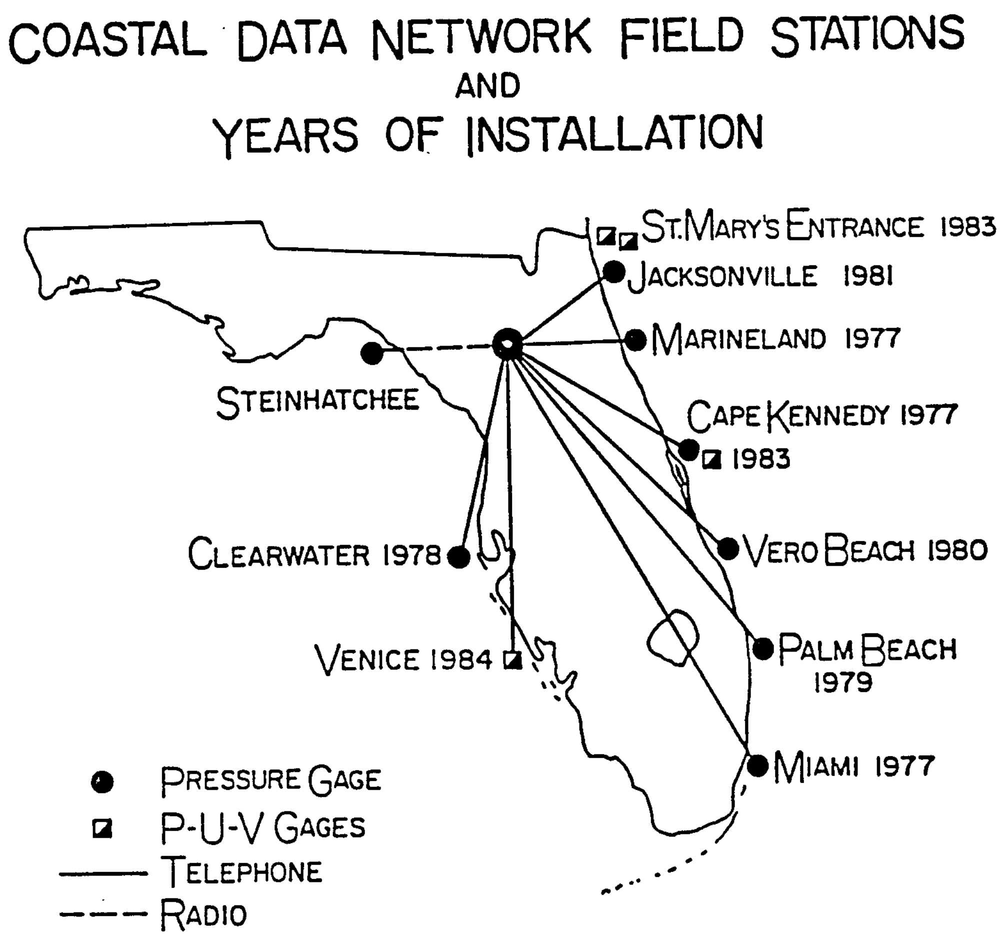

Figure 3.12. **COE Wave Stations.**

COASTAL DATA NETWORK

Station: MARINELAND
JANUARY, 1988 — Monthly Wave Data Analysis Report

% Wave Energy Distribution

(Period Bandwidth Limit -in sec)

Time: Day/Hr	Rel. Depth: (m)	Hs: (m)	Tm: (sec)	21+	21-16	16-13	13-10.7	10.7-9.1	9.1-8	8-7.1	7.1-5.8	5.8-4
1 / 0	10.8	1.43	12.8	3.1	2.6	19.8	9.5	6.9	5.7	4.9	16.	31.
1 / 6	12.3	1.16	12.8	2.4	6.8	16.6	8.0	9.5	6.3	8.3	24.	18.
1 /12	10.8	1.18	6.4	1.3	2.5	11.1	6.4	6.9	8.9	13.1	33.	17.
1 /18	11.8	1.09	5.8	1.5	1.6	8.4	9.1	7.0	8.6	14.4	32.	18.
2 / 0	10.6	0.88	7.1	1.6	1.6	12.6	8.2	5.3	9.4	14.5	21.	26.
2 / 6	12.2	0.84	7.1	1.6	1.5	5.6	6.3	6.8	10.0	16.4	29.	23.
2 /12	11.0	0.77	8.0	1.6	2.2	6.2	8.8	7.8	15.6	11.5	22.	24.
2 /18	12.0	1.23	5.3	1.2	1.1	1.8	2.8	4.7	8.4	11.7	34.	34.
3 / 0	11.0	1.47	5.8	0.7	0.5	0.9	1.9	4.5	6.7	10.2	36.	39.
3 / 6	12.4	1.64	8.0	1.0	0.7	0.8	2.4	8.5	15.8	14.7	29.	27.
3 /12	11.3	1.54	7.1	1.1	1.1	6.3	13.8	12.1	12.5	15.1	19.	19.
3 /18	11.9	1.68	6.4	1.1	0.6	4.2	12.6	11.7	11.2	12.5	30.	16.
4 / 0	11.0	1.25	8.0	1.2	0.6	3.0	12.8	13.9	14.8	10.2	24.	20.
4 / 6	12.0	1.12	9.1	1.8	1.4	1.7	10.8	24.2	15.9	10.8	20.	13.
4 /12	11.3	0.82	8.0	1.4	1.6	2.6	15.6	16.9	17.3	8.3	19.	18.
4 /18	11.6	0.89	9.1	1.3	1.6	2.4	8.8	20.5	17.7	9.8	16.	22.
5 / 0	11.0	0.74	9.1	1.4	1.6	2.6	14.6	18.0	15.4	5.6	12.	29.
5 / 6	11.7	1.45	5.8	0.6	0.5	0.7	2.1	8.5	7.8	8.3	44.	28.
5 /12	11.5	1.23	6.4	0.7	0.5	1.0	3.4	7.7	8.4	8.2	38.	32.
5 /18	11.4	1.29	6.4	0.9	0.6	1.0	3.9	12.8	9.5	7.6	32.	32.
6 / 0	11.3	0.93	4.9	1.1	1.4	2.6	7.3	9.2	9.2	9.9	20.	40.
6 / 6	11.5	1.25	5.8	0.6	1.3	1.6	4.9	9.8	6.4	7.6	31.	37.
6 /12	11.6	1.28	5.3	0.6	0.8	2.2	6.3	7.6	7.2	6.9	31.	38.
6 /18	11.3	1.22	5.8	0.7	1.0	2.3	5.4	7.8	4.4	7.7	36.	35.
7 / 0	11.5	1.12	5.8	0.9	0.9	2.5	11.2	6.7	6.1	7.3	31.	33.
7 / 6	11.4	1.24	5.3	0.7	0.5	1.7	6.3	5.0	3.6	7.4	35.	40.
7 /12	11.9	1.38	6.4	0.7	0.6	2.0	7.6	6.1	6.4	12.4	41.	23.
7 /18	11.2	1.74	7.1	0.7	0.3	0.9	3.9	8.1	18.6	25.7	24.	18.

CDN.FORMAT A/Version 1987.1
COEL.University of Florida.Gainesville.Florida 32611

Table 3.1. Format for monthly Wave Data Analysis from Coastal Data Network, COE, University of Florida.

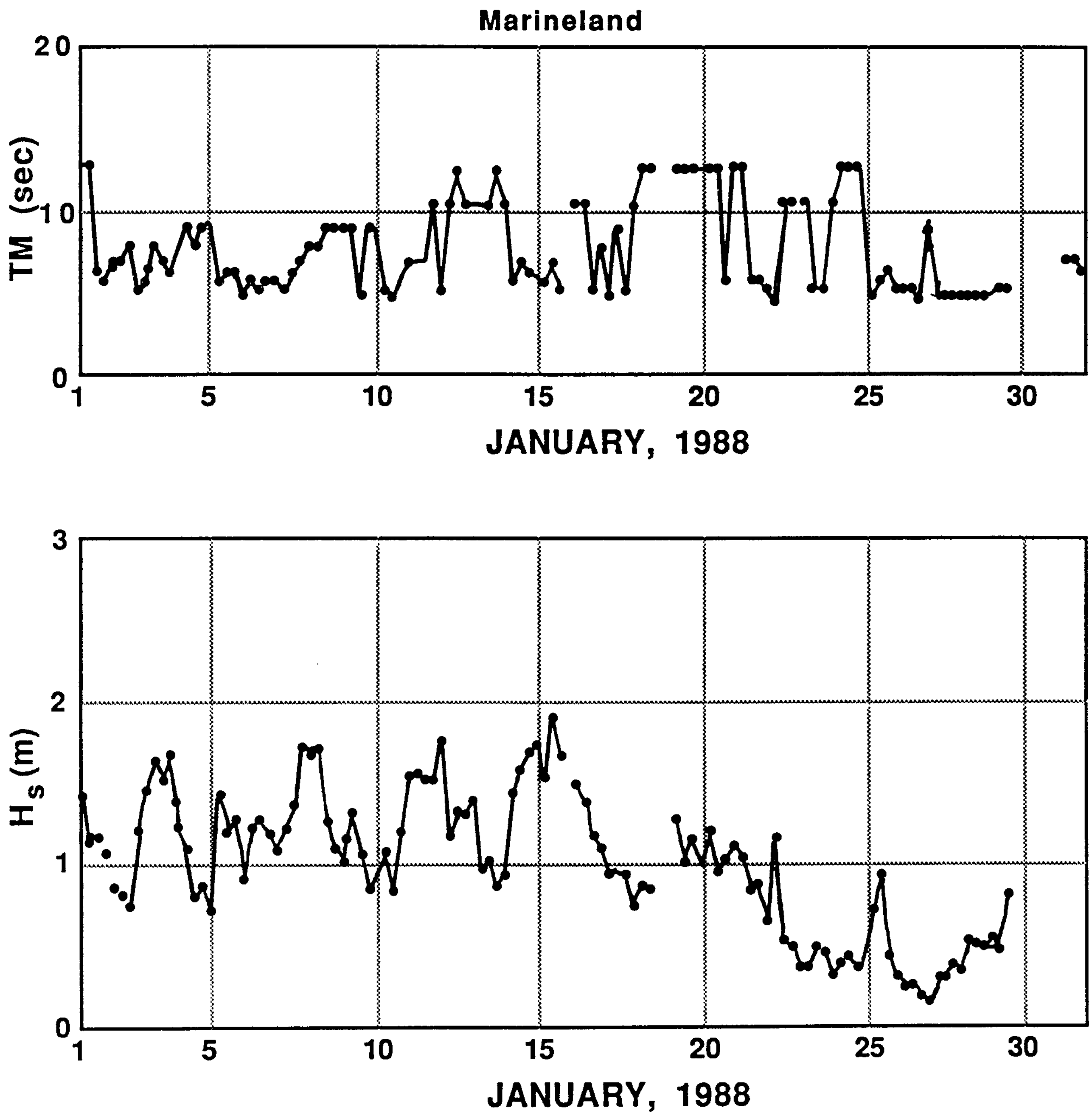

Figure 3.13. **Graphic Display of Monthly Wave Information.**

Table 3.2 Summary of wave gage and floating buoy data informations

CDN underwater wave gage data				
station or ID.#	data length (from – to)	latitude and longitude	water depth(m)	directional data
St. Mary's entrance #4	11/83– 5/84	30°43'N, 81°19'W	14.2	yes
	6/86– 7/86	"	"	yes
	8/87– 1/88	"	"	yes
St. Mary's entrance #5	11/83– 5/84	30°40'N, 81°16'W	17.5	yes
	7/84–12/84	"	"	yes
	3/85– 4/85	"	"	yes
	7/85– 9/85	"	"	yes
	8/87– 1/88	"	"	yes
Jacksonville	6/84–12/87	30°18'N, 81°22'W	10.1	no
Marineland	1/81– 4/86	29°40'N, 81°12'W	11.4	no
Cape Canaveral	3/82–12/87	28°25'N, 80°35'W	8.0	no
Cape Canaveral (offshore)	5/84– 9/84	28°20'N, 80°25'W	18.0	yes
	12/85– 5/86	"	"	yes
Vero Beach	10/86–12/87	27°40'N, 80°21'W	7.8	no
West Palm Beach	3/82–12/86	26°42'N, 80°02'W	9.9	no
Miami Beach	7/83–12/87	25°46'N, 80°07'W	6.5	no
Venice	2/86– 3/87	27°04'N, 82°27'W	7.5	no
	4/87– 5/87	"	"	yes
	6/87–12/87	"	"	no
Clearwater	3/82–12/87	27°59'N, 82°51'W	5.8	no
Steinhatchee	2/86– 7/86	29°42'N, 83°46'W	9.2	no

NOAA maintained buoy data				
station or ID.#	data length (from – to)	latitude and longitude	water depth(m)	directional data
41001	6/76– 4/86	35°00'N, 72°18'W	4000	no
41002	11/75– 4/86	32°18'N, 75°12'W	3900	no
41006	5/82– 4/86	29°18'N, 77°18'W	1200	no
44003	3/79– 4/86	40°48'N, 68°30'W	150	no
44004	9/75– 4/86	39°00'N, 70°00'W	1300	no
44005	1/79– 4/86	42°42'N, 68°18'W	120	no
42001	8/75– 4/86	25°54'N, 89°42'W	3300	no
42002	3/77– 4/86	26°00'N, 93°00'W	2400	no
42003	7/77– 4/86	26°00'N, 86°18'W	3250	no

tape for the period from October 1, 1975 to present (from National Climatic Data Center in Asheville, N.C.).

The other main operational model is the discrete spectral model developed by the Wave Information Study (WIS) group of the Waterways Experiment Station (WES), U.S. Army. The modeling was originally designed to have three separate phases: deepwater wave hindcasting, wave modification in shelf zone, and finally, transformation into nearshore shallow water zone. The main intent of the model is to provide hindcast wave information along the coastal waters on both sides of the continent of the United States. A 20-year hindcast information was generated at 13 stations along the edge of the continental shelf of the eastern United States. The hindcast was further extended to shallow water through linear shoaling and refraction by assuming plane beach (Jensen, 1983). A similar 20-year wave hindcasting is just becoming available for the Gulf Coast also.

Recently, the Department of COE has just modified the WIS model for the Florida coast along the Atlantic seaboard (Lin, 1988). The model is more rigorous in shallow water wave hindcasting and was calibrated using shallow water directional wave data collected by COE. The model has been applied to hindcasting wind waves along the east coast of Florida and it performed well for both low- and high-pressure weather systems. Figure 3.14 shows the comparisons between the hindcasted and the measured waves at Marineland station for a two months period in 1984 (September and October) when three hurricanes and two northeasters hit the coast. Based upon the actual wave data collected at those stations with duration of more than four years, extreme wave height analysis was performed by Lin and Wang (1988). Using monthly maximum waves as data base, they have shown that Fisher-Tippett Type I distribution, or commonly known as the Gumbel distribution, to have the best fit for both east coast and west coast waves and in both deep and shallow water.

By denoting the significant wave height as H_s, the Type I distribution of the significant wave height is expressed as

$$\phi_1(H_s) = \exp\left[-\exp\left(-\frac{H_s - d}{c}\right)\right] = \exp[-exp(-y)], \qquad c \geq 0, d \geq 0 \qquad (3.10)$$

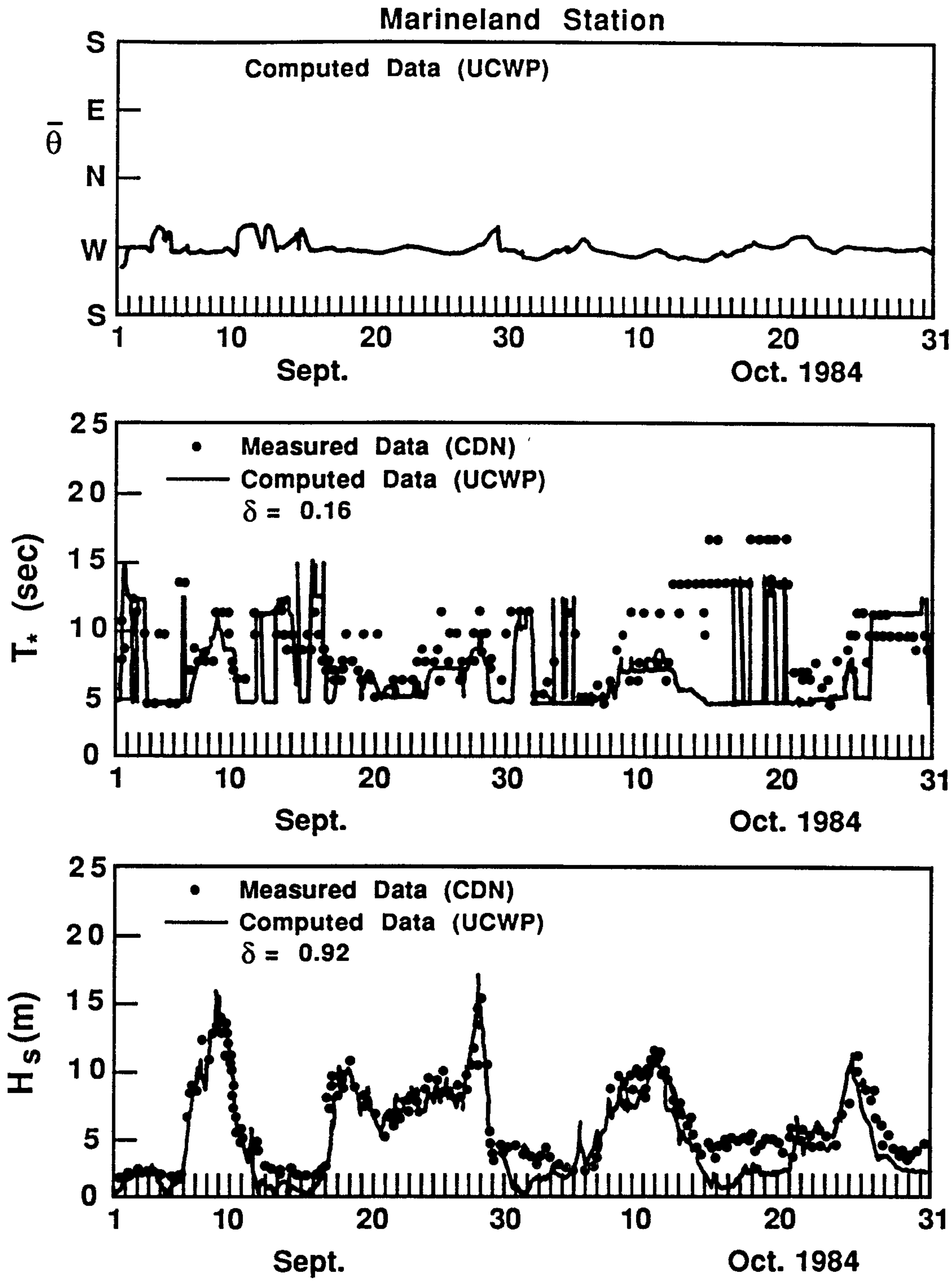

Figure 3.14. **Comparisons of CDN and UCWP Average Wave Direction, Significant Wave Heights and Peak Energy Frequencies at the Marineland Gage Location.**

where c and d are the data-dependent shape factors and y is known as the reduced variate. Table 3.3 summarizes the values of c and d for the best fit at 15 selected study sites (9 deep water and 6 shallow water). All these data sets are found to lie within a 99 percent confident limit. An example is given in Fig. 3.15.

It is observed that the estimated values of both parameters c and d are at water depth. Figure 3.16 shows the values of c and d plotted against the mean water depth. Knowing that both c and d should be zero when the water depth is zero and that the upper bound values of c and d should approach the deepwater values from the NOAA buoy data empirical formulas can be developed. For the east coast the following formulas are proposed:

$$c = 1.56 \bullet \left(\tanh \frac{h}{160}\right)^{3/7}, \text{and } d = 4.15 \bullet \tanh \frac{h}{25} \text{ (in metric units)} \tag{3.11}$$

based on the mean values obtained by the deepwater buoy data. For the west coast of Florida, the c and d parameters in the extreme wave height statistics can be approximated by the following formulas:

$$c = 1.25 \bullet \left(\tanh \frac{h}{100}\right)^{3/7}, \text{and } d = 2.63 \bullet \left(\tanh \frac{h}{11}\right)^{3/2} \text{ (in metric units)} \tag{3.12}$$

Estimates of 20, 50, and 100 year return values of H_s, at the different water depths of 5, 10, 20, and 50 m, based on Eqs. 3.1, 3.2 and 3. 3, are given in Table 3.4. The significant wave heights predicted to the west coast of Florida are in general smaller than those to the east coast of Florida. This is because the fetch is limited in the Gulf of Mexico.

NEARSHORE WAVE INFORMATION

In the nearshore region waves usually have onshore directions. Even under the offshore winds, the waves may still have overall onshore direction due to propagation of distant waves. This is often the case for the waves observed near the Florida coast at the CDN wave gages. Examples displaying the wave roses, which show the information of percentage wave energies found in each of the 32 evenly-divided circular directional bands, at the location of St. Mary's entrance near Georgia and Florida border and the Venice gage are given in Figure 3.17.

Table 3.3 Summary of the values of c and d at the 15 selected study sites

CDN wave gage data				
station or ID#	data length (from – to)	c (m)	d (m)	water depth (m)
Jacksonville	6/84–12/87	0.457	1.59	10.1
Marineland	1/81–12/87	0.497	1.80	11.4
Cape Canaveral	3/82–10/87	0.412	1.23	8.0
West Palm Beach	3/82–12/86	0.444	1.55	9.9
Miami Beach	7/83–12/87	0.394	1.02	6.5
Clearwater	3/82–12/87	0.373	0.92	5.8
WIS hindcasted wave data				
station or ID#	data length (from – to)	c (m)	d (m)	water depth (m)
Jacksonville	1/56–12/75	0.472	1.80	10.0
Cape Canaveral	1/56–12/75	0.450	1.62	10.0
West Palm Beach	1/56–12/75	0.456	1.57	10.0
mean: (±s.d.*)		0.459 (±0.011)	1.66 (±0.12)	10.0
NOAA buoy data (Atlantic Ocean)				
station or ID#	data length (from – to)	c (m)	d (m)	water depth (m)
41001	6/76– 4/86	1.639	4.21	4000
41002	11/75– 4/86	1.587	4.00	3900
41006	5/82– 4/86	1.563	4.16	1200
44003	3/79– 4/86	1.563	4.20	150
44004	9/75– 4/86	1.538	4.21	1300
44005	1/79– 4/86	1.471	4.12	120
mean: (±s.d.*)		1.560 (±0.055)	4.15 (±0.08)	
NOAA buoy data (Gulf of Mexico)				
station or ID#	data length (from – to)	c (m)	d (m)	water depth (m)
42001	8/75– 4/86	1.250	2.59	3300
42002	3/77– 4/86	1.282	2.71	2400
42003	7/77– 4/86	1.235	2.59	3250
mean: (±s.d.*)		1.256 (±0.024)	2.63 (±0.07)	

* s.d. stands for standard deviation.

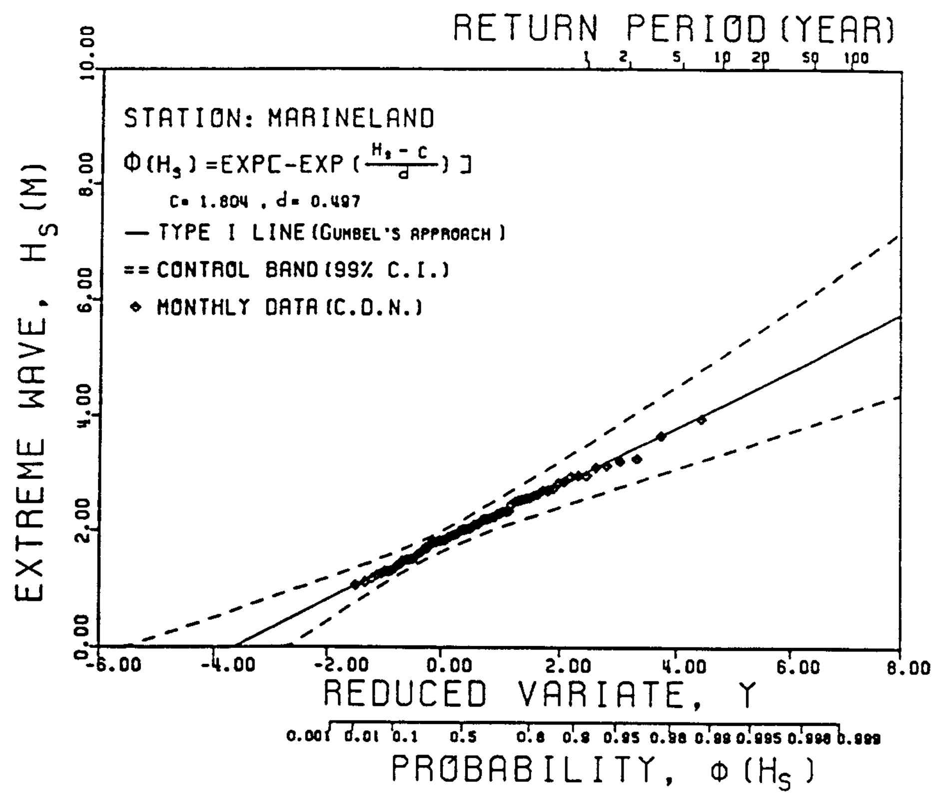

Figure 3.15. **Probability Distributions of the Monthly Largest Wave Heights at the Wave Gage Location near Marineland, Florida.**

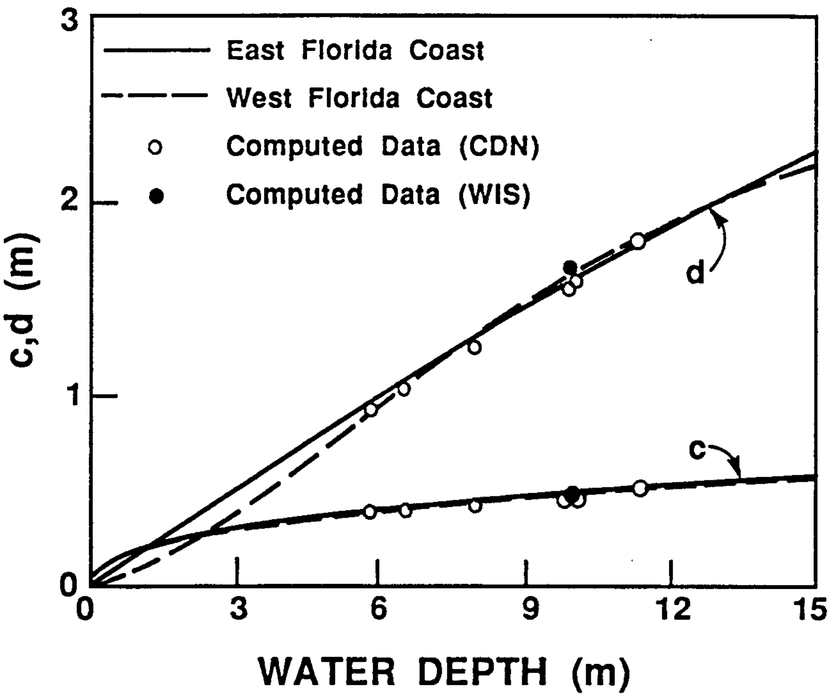

Figure 3.16. **Plots of the Proposed and Esitmated Values of c and d.**

Design H_s (m) at the east coast of Florida				
water depth return period	5 (m)	10 (m)	20 (m)	50 (m)
20 (year)	2.75	4.18	6.25	9.12
50 (year)	3.08	4.62	6.84	9.98
100 (year)	3.32	4.94	7.28	10.63
Design H_s (m) at the west coast of Florida				
water depth return period	5 (m)	10 (m)	20 (m)	50 (m)
20 (year)	2.63	4.16	5.85	7.55
50 (year)	2.94	4.58	6.42	8.37
100 (year)	3.18	4.91	6.85	9.00

Table 3.4. Predictions of 20, 50, and 100 year return values of H_s

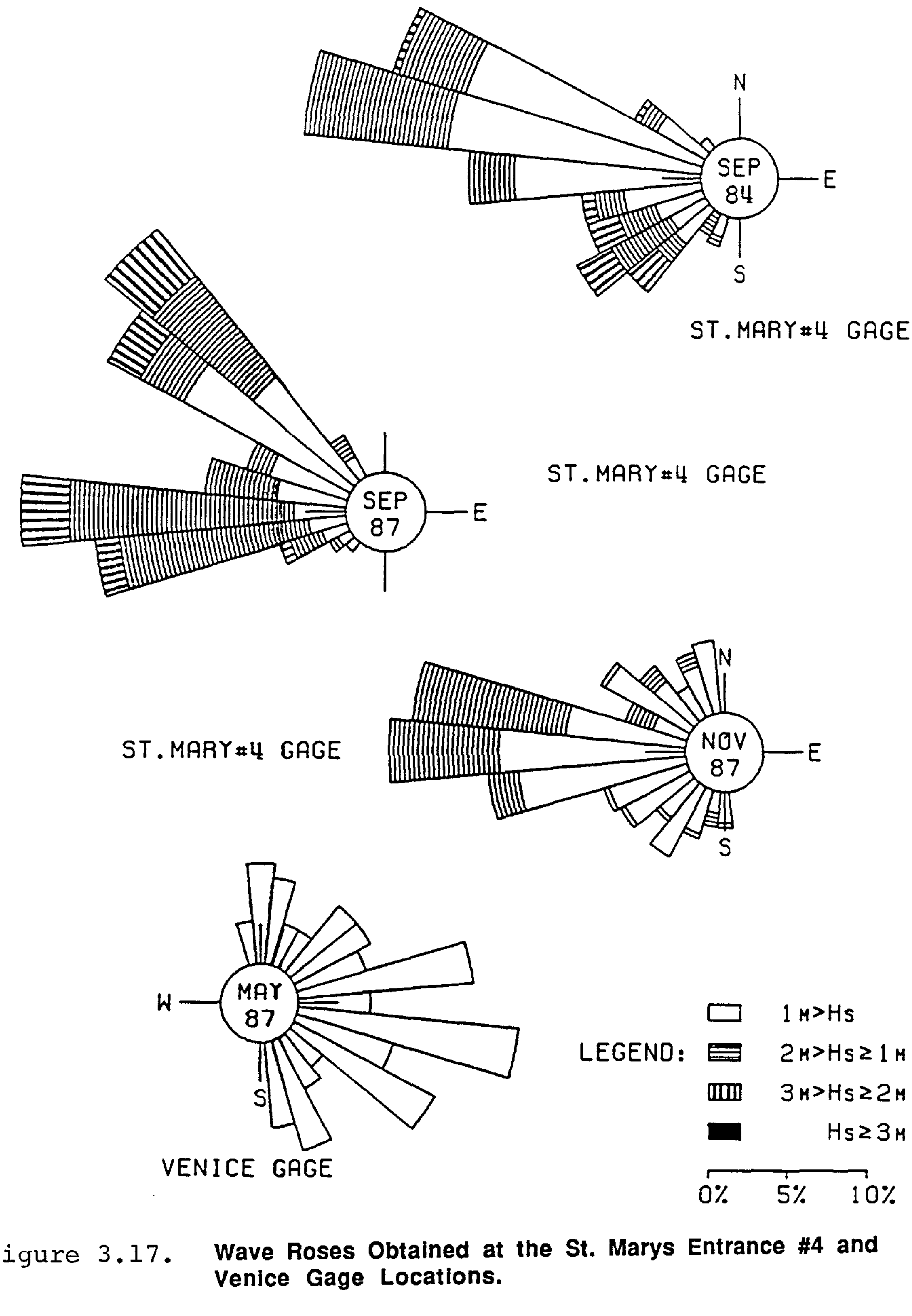

Figure 3.17. **Wave Roses Obtained at the St. Marys Entrance #4 and Venice Gage Locations.**

At present, the directional wave data collected by the CDN wave gages are not of sufficient duration to facilitate the long-term statistical study. The hindcasted directional wave information is available from the 20-year hindcast data by the WIS group of the Waterways Experiment Station, the U.S. Army Corps of Engineers (Jensen, 1983). The information does not include the hurricane waves.

To determine littoral drift environment, the most pertinent wave information is the wave height versus direction distributions just outside the surf zone (wave period only plays a minor role in the littoral drift equation). To establish such information, the following simplified procedures are suggested:

a. Prepare a joint probability table of wave direction. Establish a grid system encompassing the coastline of interest and extend the grid to offshore to deep water condition or to the location where the offshore wave information is available. The grid size depends on offshore topography. In general, a half mile should be a reasonable choice to 30 ft contour. Within the 30 ft contour, the grid size should be reduced further.

b. Based upon the shoreline orientation, select wave directions that will impact the shoreline. For the east coast of Florida, waves from NE, E, SE and S should probably be included. Wave statistics of height-period-direction distributions at the offshore boundary should be established based upon available wave information. An example for the wave conditions, offshore Indian River County, is given in Figure 3.18 based upon WIS model output (30 ft contour line).

c. Construct wave refraction diagram for each of the wave periods used in the wave statistics. For the present example four wave periods -5, 7, 9, and 12 sec. -were used. Wave rays from the four directions, for each of the four periods, were generated using a reference deep water wave height of 1 m. The wave amplification factors for each wave period from each direction can thus be established.

d. Compute shallow water wave height through multiplying deep water wave height by the amplification factor. The distributions of wave height - wave period - direction in the

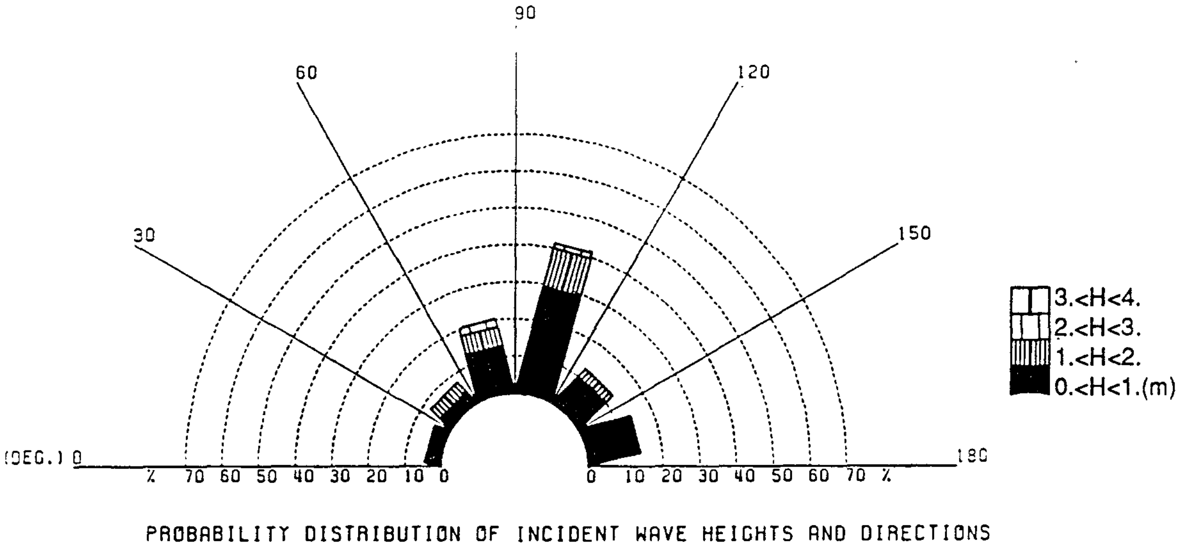

The Location of #152: Riomar, Florida Depth = 10 m

Water Depth = 10 m (WIS # 152)

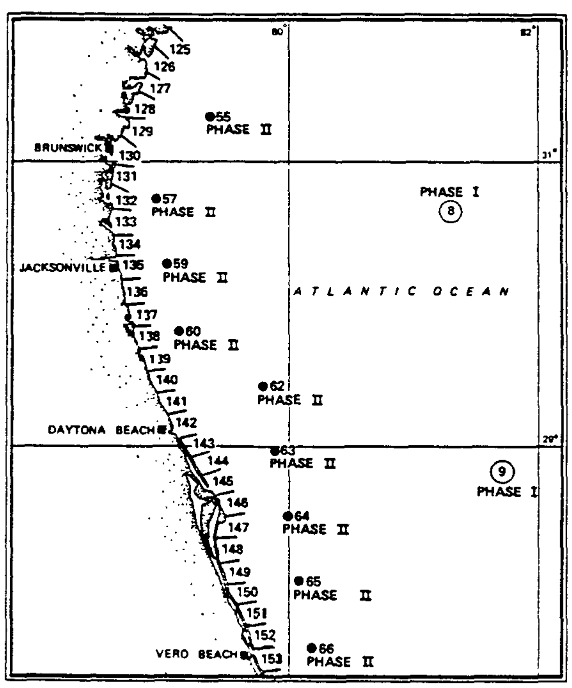

Figure 3.18. **Wave Roses at St. 152 (Offshore Indian River County) Based upon WIS Hindcast at 10 m Depth.**

nearshore area can then be established. Since wave period is not important in littoral drift computation, often only wave height-direction distribution information is required. Figure 3.18 shows the nearshore wave height roses along Indian River County based upon the WIS output at 30 ft. contour given in Figure 3.19.

STORM SURGE AND WATER LEVEL CHANGES

Water level rise is perhaps the most damaging factor causing beach and dune erosion. This is because water level rise will submerge the backshore that is not in a state of equilibrium and will increase wave energy by sustaining larger waves owing to the increase in water depth. Water level change consists of three main components: long term mean sea level change, astronomical tide and meteorological tide. In engineering work such as beach nourishment, the meteorological tide also known as the storm surge is by far the most important factor because of its transient nature, large magnitude and unpredictability.

Along the Florida Coast, storm surges are generated by three types of storms: extratropical cyclone, tropical cyclone and intermediate type of storm.

The extratropical cyclones usually originate in high and mid latitude. They are large scale system of 500 miles to over 1000 miles and are relatively stationary. They are not a major threat to the Florida Coast in terms of high winds. However, because of their scale and duration, they are responsible for most of the severe winter erosions along the east coast of Florida, particularly, in the northern portion of the State.

Most of the severe storm surges recorded in Florida were caused by hurricanes or tropical storms of a severe nature (wind speed exceeds 74 miles per hour). They are intense systems of a much smaller scale, about 10 to 50 miles from the center to maximum wind known as the radius of the hurricane. They are also more rapid-moving than northeasters with widely varying tracks. Along the Florida coast, severe hurricanes and associated storm surges occur somewhere two to three times per decade.

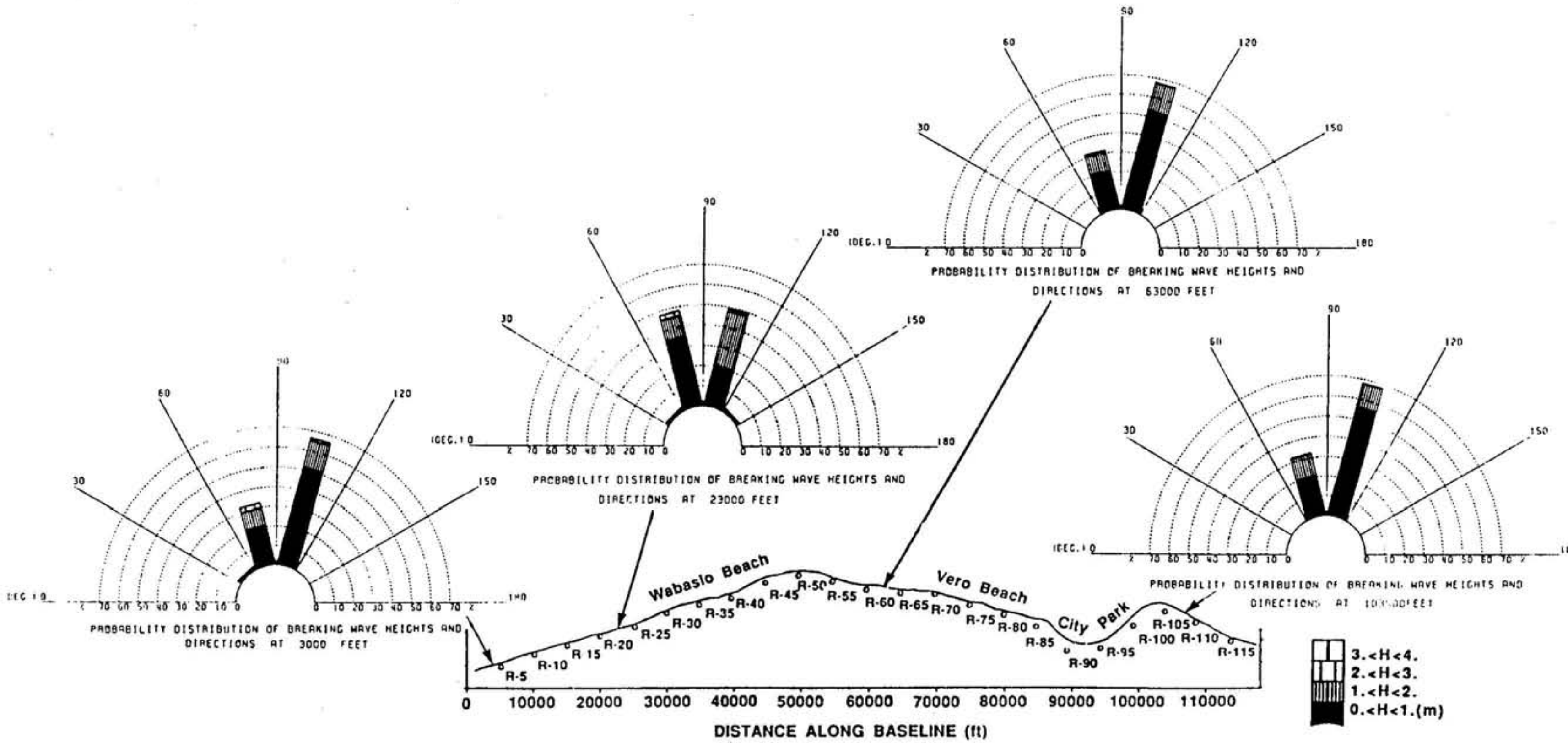

Figure 3.19. **Nearshore Wave Height Roses Along Indian River County Shore.**

The intermediate type of storm, called a "subtropical storm" is a mixed type of extratropical and tropical characteristics. Six subtropical storms have been identified in or near Florida (Harris, 1982). They are infrequent and not a major threat.

Since high storm surges are localized phenomenon induced by infrequent high–intensity landfall or near landfall storms, field record is usually not sufficient to determine the design value through statistical analysis. Numerical simulation coupled with storm surge model is usually employed to generate design information. Storm surge modeling is quite an advanced field.

There are numerous storm surge models; most of them are adequate for their intended area and weather conditions.

In Florida, a Coastal Control Construction Control Line (CCCL) program was instituted in the 1970s that mandates all the new constructions have to set back behind the 100-year coastal flood line. Therefore, adequate storm surge model is available. Federal Emergency Management Administration (FEMA) is also continuously updating their coastal flood levels. The current methodology used by the Florida Department of Natural resources for generating storm surge information is illustrated by the Flow Chart shown in Figure 3.20. The procedure consists of developing and verifying a 2-dimensional hurricane storm surge model for regional application (county by county basis). The model is calibrated and adjusted with real storm surge record. A 1-dimensional simplified model is then calibrated against the 2-dimensional model and used to reduce the cost of computations for a large number of runs simulating a 500-year duration of storm tides. The dynamic waves set-up is also included in the simulation.

The input wind fields are generated by a 5-parameter wind model. The five parameters are: central pressure, radius of maximum wind, forward speed and hurricane translation direction and landfall characteristics. The landfall characteristics are defined as "landfalling" and "along shore" as shown in Figure 3.21. Historical hurricane data from 1871 to the present are then used as the statistical basis for generating these parameters. An example

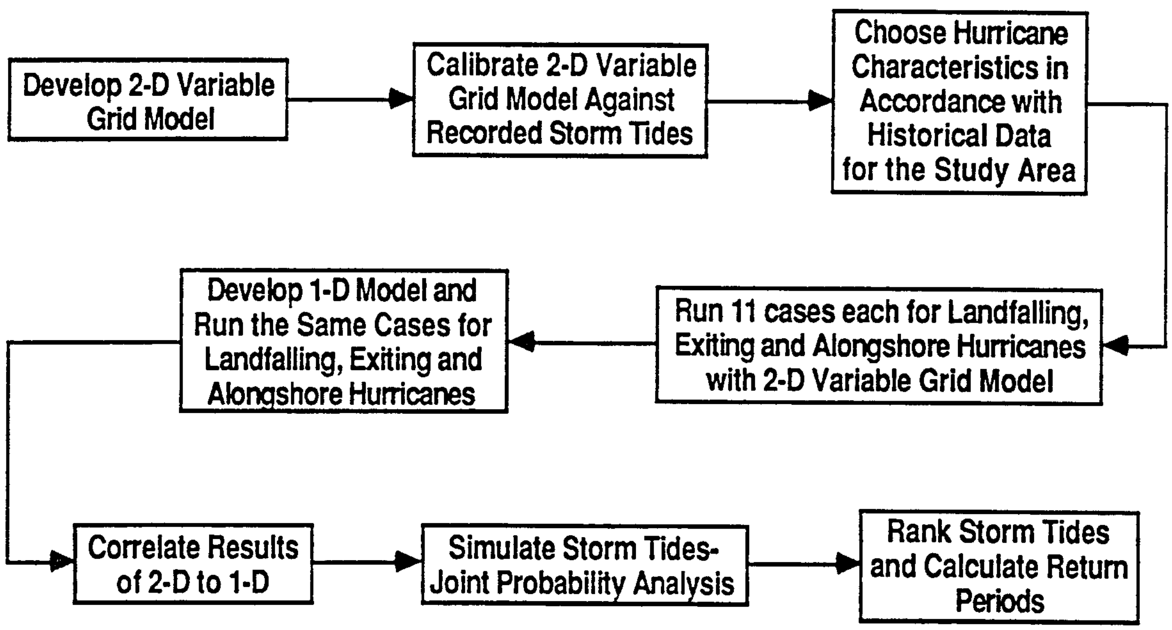

Figure 3.20. **Flow Chart for Storm Surge Simulation (Dean and Chiu, 1981).**

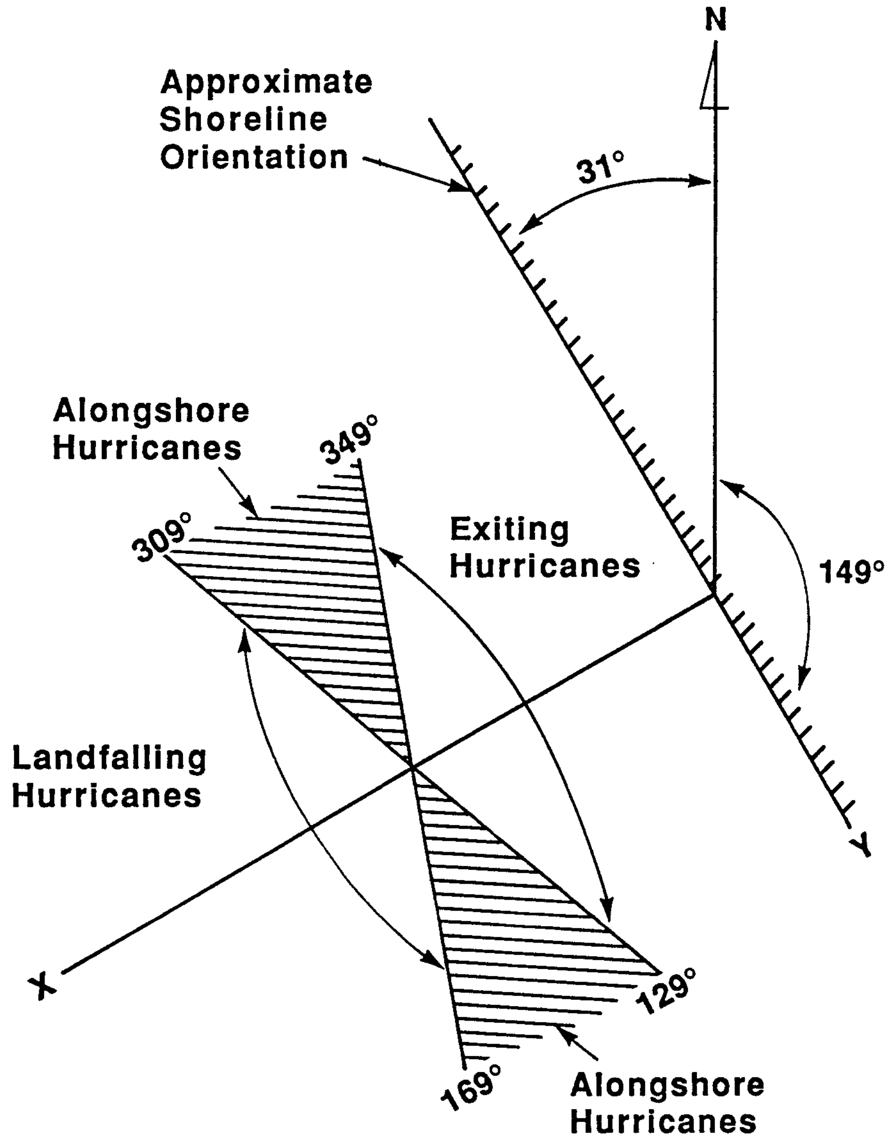

Figure 3.21. **Designation of Alongshore, Landfalling and Exiting Hurricanes depending on Track Directions Relative to Shoreline Orientation (Dean and Chiu, 1981).**

of the simulated storm surge level vs return period is given in Figure 3.22. Detailed description of the storm surge simulation model for the State of Florida can be found in Dean and Chiu (1981).

MORPHOLOGICAL AND SEDIMENTARY CONDITIONS

Morphological conditions and sediment property greatly affect the shore process and the littoral drift environment which, in turn, govern the rate and shape of shoreline changes. Inlets often behave as littoral drift barriers depriving sand to the down drift side; river mouths, on the other hand, often serve as sand sources transporting material from upland to the beach. Headlands and rock outcrops are stable morphological features and often cause abrupt change or reversal of littoral drift pattern. Offshore reefs and outcrops provide natural shields against wave attacks and create discontinuity of offshore profiles. Spits are usually unstable and are commonly associated with adjacent shoreline rotations and/or elongations. The occurrence of large scale sand waves, a not well understood phenomenon, creates a migratory shoreline deformation along the coast. Sand dunes provide added protection for the upland and on the same time supply sand to the beach during storms. Major or drastic shoreline changes are usually related to morphological changes such as opening and closure of inlet, offshore dredging or the construction of man-made structures. Therefore, a survey of morphological condition is essential for the planning of beach nourishment projects and for aid in the interpretation of dynamic processes.

Sediment property is the single most important factor affecting the beach profile shapes, particularly, the so-called equilibrium profile which plays as important role in beach nourishment engineering. Referring to the definition sketch of beach profile in Figure 3.23 the most active portion of the beach is within the foreshore and inshore zones. Under steady wave actions, this portion of the beach tends to reach a stable shape. Based upon field evidence, Bruun (1954) and later Dean (1977) found this stable profile can be expressed by

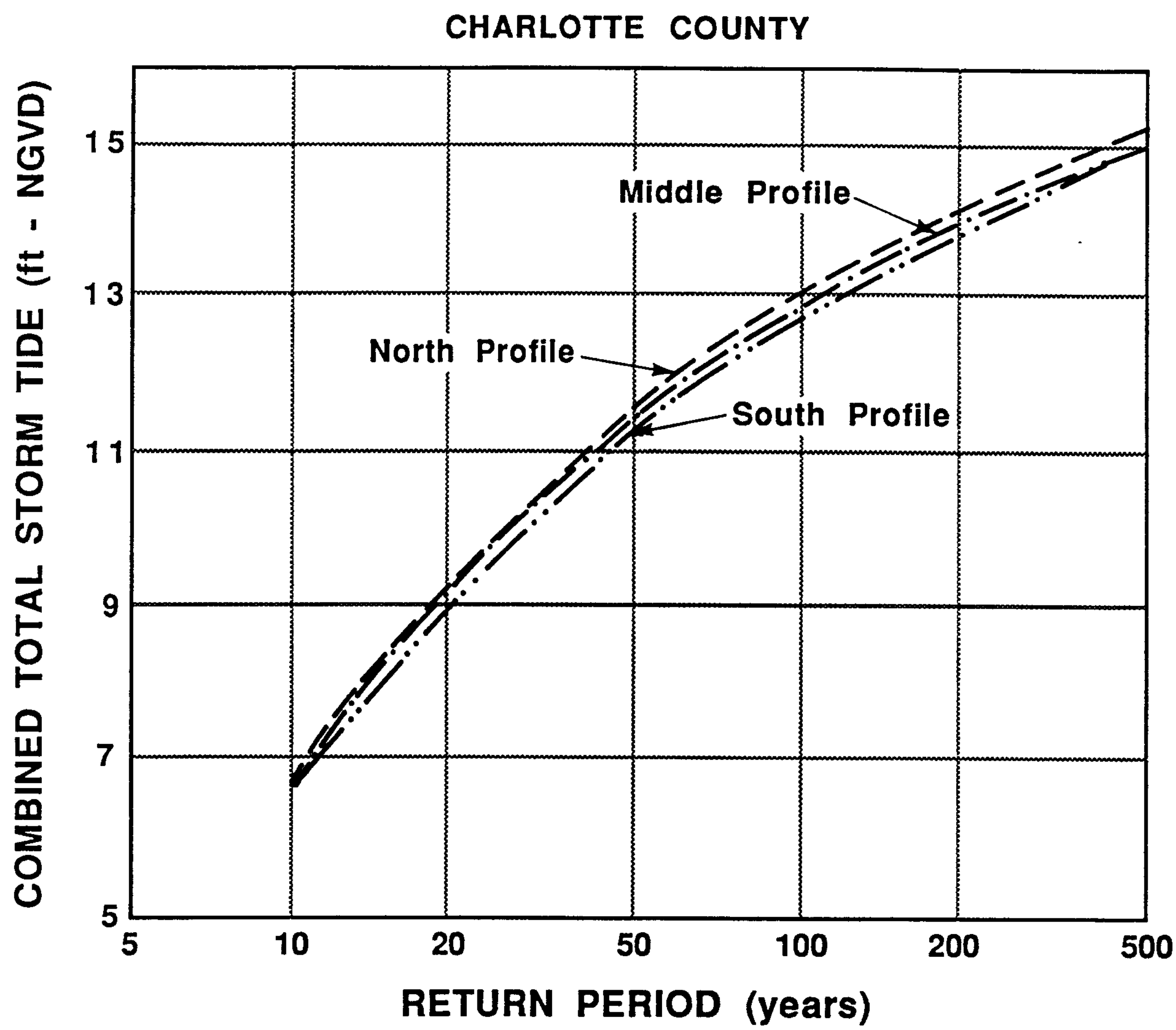

Figure 3.22. **Combined Total Storm Tide Elevation Versus Return Period for Three Repersentative Transect Lines in Charlotte County (DNR, CCCL Program).**

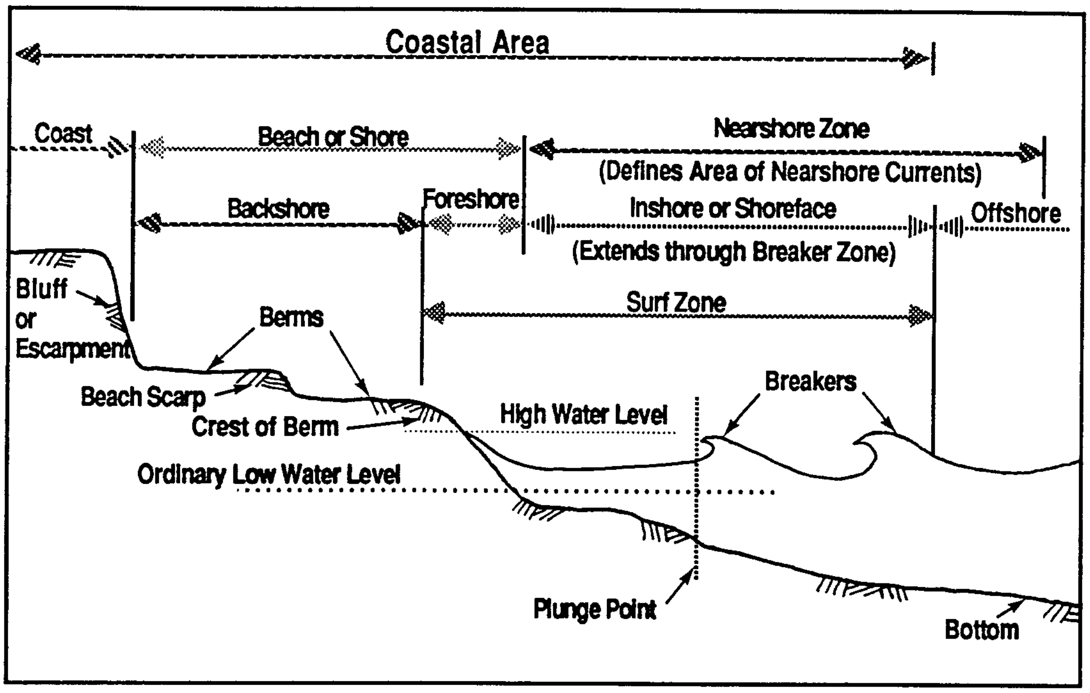

Figure 3.23. **Beach Profile Definition Sketch (CERC, 1973).**

a power function:

$$h(x) = Ax^m \tag{3.13}$$

where x is the axis normal to the shoreline and h is the water depth along the profile. In application, the origin is selected at the mean high water (MHW) with positive axis pointing offshore. The value m is found to be approximately equal to 2/3, which is consistent with a model proposed by Dean (1983) assuming spilling breaker and uniform wave energy dissipation per unit water volume inside the surf zone as the mechanism of sediment suspension. The coefficient A was evaluated by Moore (1982) and Dean (1984) and found to be mainly a function of sediment grain size (or more appropriately sediment particle fall velocity). More detailed treatment on the equilibrium profile and its application to beach nourishment is given in the next chapter.

One should realize that the proposed equation only represents an approximation of a typical beach shape under mild wave condition. Field survey including profiling and sediment sampling is essential to establish correctly the typical profile for the region of interest. It is also important to differentiate the normal and storm profiles of the region and their influence on beach width and storm protection.

Sediment property is also important in determining the compatibility of nourishment material. There is no control data inventory in the State of Florida on beach sand property. Sand sampling and analysis should be an integral part of the nourishment project. U.S. Corps of Engineers, Jacksonville District does maintain records of offshore core samples, which are useful for preliminary analysis of potential borrowing material.

HYDROGRAPHIC SURVEY

Detailed hydrographic survey information is required for the following purposes:

a. To calculate the required quantity of beach fill.

b. To serve as baseline for the future monitoring and performance analysis.

c. To use as input for littoral drift and shoreline change computations.

A number of essential points should be observed, whenever possible:

a. The survey should tie in with the DNR monuments and the state's plan coordinates.

b. The survey should cover from the dune line (or hard structure) to the closure depth, if possible.

c. MHW line should be noted in the survey.

d. The survey should cover both summer and winter seasons and/or at the same season that the DNR survey information in the past is available.

e. Based upon the analysis of historical shoreline and volumetric changes and the accompanying sensitivity analysis as illustrated in the Section "Historical Shoreline Information" areas requiring special attention should be noted. The requirement of survey accuracy and error tolerance should also be established to insure useful survey results.

LITTORAL DRIFT ENVIRONMENT

To estimate the rate of littoral drift in the absence of actual field measurement, the accepted practice is to relate the longshore sediment transport rate to the longshore component of"wave energy flux", or

$$I_\ell = k\ P_{\ell s} \tag{3.14}$$

where I_ℓ is the immersed weight transport rate and $P_{\ell s}$ is the longshore energy flux factor. Based upon linear wave theory, $P_{\ell s}$ at the breaker line can be estimated as:

$$P_{\ell s} = \frac{\gamma}{16} H_b^2 C_{gb} \sin 2(\alpha_b - \beta) \tag{3.15}$$

where γ is the specific weight of sea water; H_b is the breaking wave height; C_{gb} is the wave group velocity at the breaking point; α_b is wave breaking angle and β is shoreline normal. Since I_ℓ and $P_{\ell s}$ have the dimension (force/time), α should, in theory, be unity. Various

K values have been suggested. The value recommended by SPM (1984) is 0. 39 if wave energy is based upon significant wave height. Komar and Inman (1970) recommended $K =$ 0. 77 using wave energy based upon H_{RMS} value. It is often more practical for engineering application to express the sediment transport rate in terms of volumetric transport rate. In this case, the coefficient of proportionality is no longer dimensionless and we have

$$Q_\ell(m^3/yr) = 1290(m^3 - s/N - yr)P_{\ell s}(N - m/m - s)$$

$$Q_\ell(yd^3/yr) = 7500(yd^3 - s/lb - yr)P_{\ell s}(ft - lb/ft - s) \tag{3.16}$$

using H_s as basis for energy computation.

The value of K suggested above is suitable for straight shoreline of normal sandy beach. The actual value of K for a specific shoreline is influenced by the material, foreshore geometry, man-made structures and natural changes, etc., and is, therefore, expected to vary from the suggested value.

Based upon the wave information and the longshore transport equation, long–term or short-term littoral drift environment can be established. Figure 3.24 shows an example of longshore sediment transport computation for the month of December 1987, near Ponce de Leon, Florida. The computation started with wind as input to generate waves in deep water. The waves were then carried into shallow water, which in turn, were the input to the longshore transport equation. In the example given here the time increment in the computation was 10 min. The wind information was reported at 3 hrs interval. Linear interpretation was used to establish wind condition at 10 min. interval. Figure 3.25 shows the cumulative transport rate. The impact of episodic events is clearly seen. Figure 3.26 shows the histogram of longshore transport at the same site for year 1987. Based upon this computation, the annual net littoral drift is estimated to be around 123,000 cu. yd/year.

Long term wave data, if available, can also be used to generate synthesized longshore transport rate which is the statistical representation. The procedures developed by Harris (1991) are given here using Sebastian Inlet region as an example.

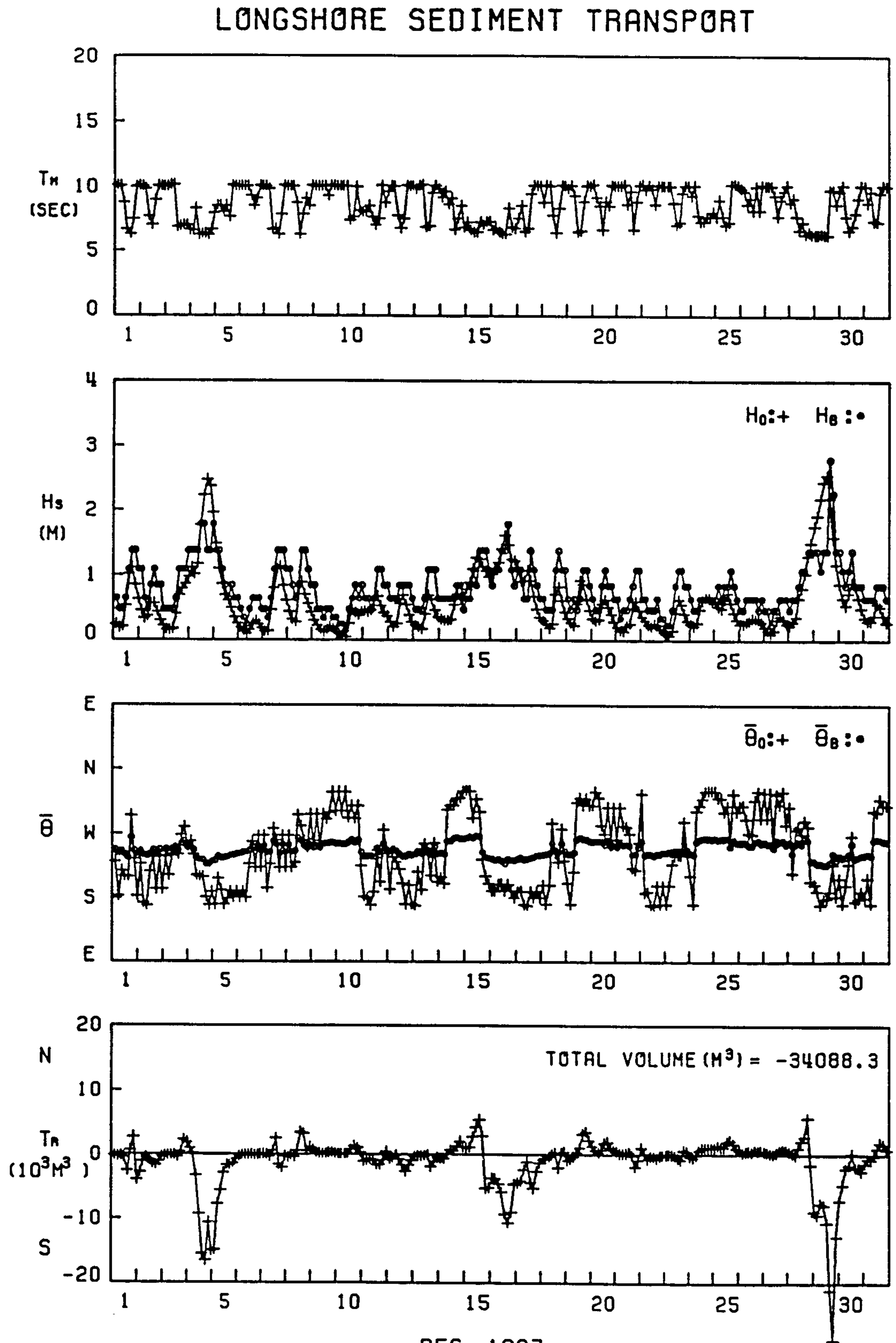

Figure 3.24. **Example of Longshore Transport Computation based upon Wind Information for 1 hour, Month of December 1987, near Ponce de Leon, Florida.**

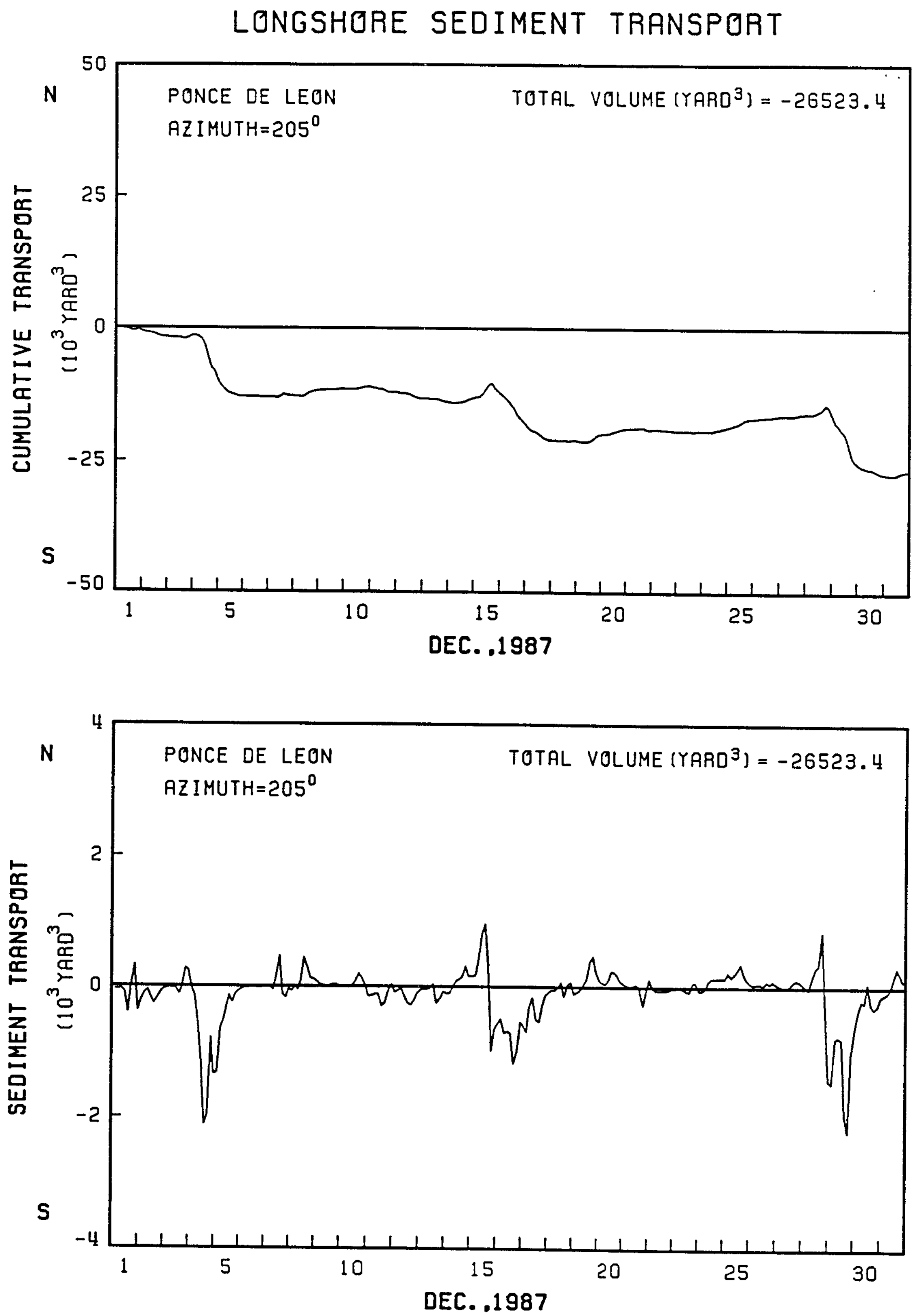

Figure 3.25. **Cumulative Longshore Sediment Transport Rate, December 1987, Ponce de Leon, Florida.**

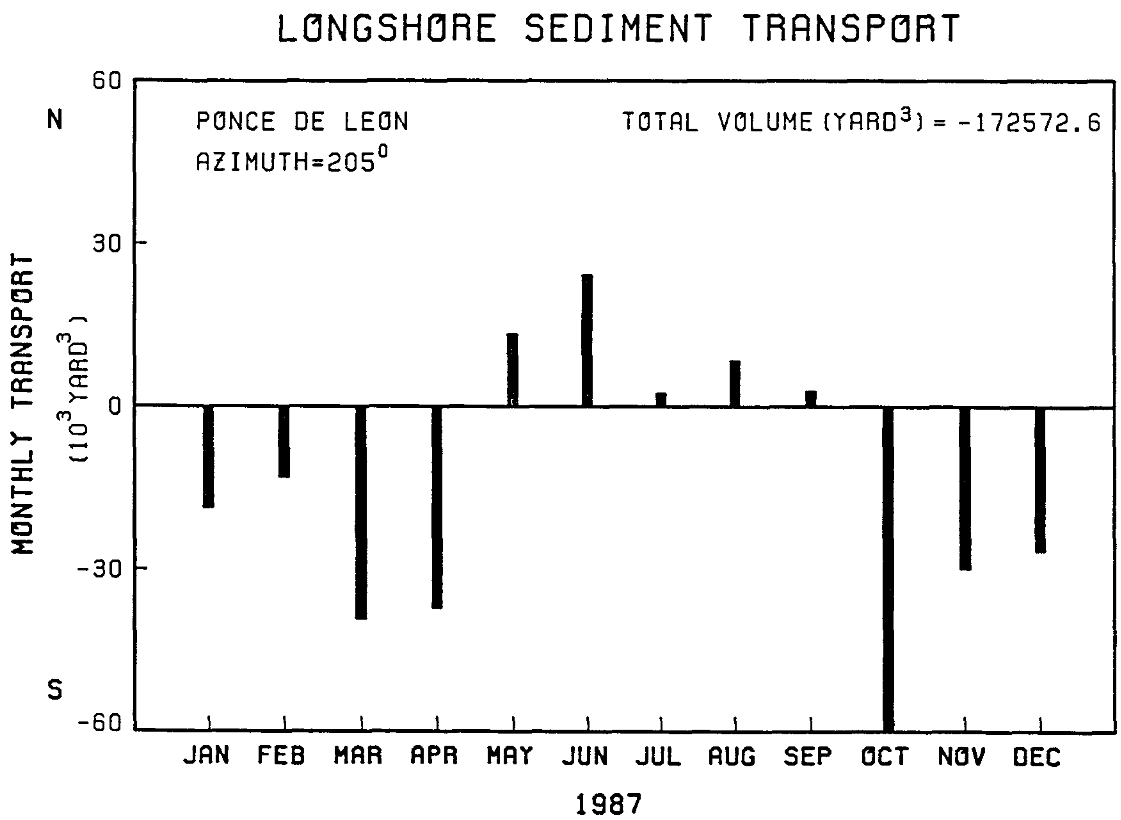

Figure 3.26. **Histogram of Longshore Sediment Transport Rate at Ponce de Leon Inlet, 1987.**

The Army Corps of Engineers Wave Information Study (WIS) contains 20 years (1956-75) of hindcast wave data for the Sebastian Inlet area at every three)hour interval. This can be used as the main data base. Since there also exists about 5 years(86-90) measured data at Vero Beach, about 15 miles south of the inlet, by the Coastal Data Network, the WIS data can be calibrated and adjusted to more accurately represents the wave conditions. There are various ways for this adjustment, one of the simplest approach is to adjust the data based on ratio of the measured and hindcasted mean values. Table 3.5, for instance, shows the monthly these ratios of H and T based upon CDN and WIS data. These values are then used to adjust the WIS hindcasted data. As can be seen, the hindcasted wave height is generally higher and the wave period is generally lower than the measured. This same trend was also found at other locations along the Florida east coast.

The wave information so generated can then be used to produce longshore transport statistics by using Eq. (3.5). Usually, two steps of computations are required; the first step is to transform H and T from deepwater to the breaking line and then the second step to compute Q by Eq.(3.5). The first step is computational intensive. However, if the offshore contours can be treated as parallels, considerable computational simplification can be achieve. Under this assumption, the transport rate can be computed by the following equation using only deepwater wave conditions:

$$Q = \frac{K H_0^{2.4} T^{0.2} \cos\alpha_0 \sin\alpha_0}{8(s-1)(1-p)2^{1.4}\pi^{0.2}\kappa^{0.4}\cos^{0.2}\alpha_b} \tag{3.17}$$

If one assumes the following values: $\cos^{0.2}\alpha_b \approx 0$,$g = 32.2$ ft/sec $s = 2.65$ for sand,$p = 0.4$, and $\kappa = 0.78$, we arrive at the following practical equation:

$$Q = 0.3374 K H_0^{2.4} T^{0.2} \cos^{1.2}\alpha \sin\alpha \quad \text{in cu.ft/sec} \tag{3.18}$$

Here the value of K depends upon the definition of H as discussed earlier.

Table 3.6 tabulates the computed longshore transport values, Q, for 20 years period between 1956 to 1975. This data can also be presented as monthly transport rate as shown in Table 3.7.

Table 3.5: CDN and WIS Wave Data Comparison

Month	Mean H_{CDN} in meters	Mean H_{WIS} in meters	Coeff.	Mean T_{CDN} in seconds	Mean T_{WIS} in second	Coeff.
Jan	0.80	0.95	0.84	8.57	6.22	1.33
Feb	0.74	0.93	0.80	8.36	6.41	1.23
Mar	0.77	0.88	0.88	8.26	6.40	1.29
Apr	0.39	0.94	0.42	9.61	7.07	1.36
May	0.56	0.72	0.77	8.51	5.36	1.59
Jun	0.44	0.60	0.74	7.85	5.51	1.42
Jul	0.37	0.47	0.78	7.73	4.90	1.58
Aug	0.42	0.51	0.82	8.31	5.05	1.65
Sep	0.62	0.93	0.67	9.42	6.29	1.50
Oct	0.83	1.25	0.66	8.38	7.16	1.17
Nov	0.83	1.11	0.74	8.14	6.66	1.22
Dec	0.82	1.05	0.78	9.17	6.79	1.35

Table 3.6: Estimated Longshore Transport Values in cubic yards per year for 20 a Year Period from 1956 to 1975 (from WIS hindcast wave data)

year	Q_{south}	Q_{north}	Q_{net}	Q_{gros}	Percentage of Drift	
					% south	% north
1956	1,285,589	292,939	992,650	1,578,528	81.4	18.6
1957	837,038	540,438	296,601	1,377,476	60.8	39.2
1958	943,635	540,438	296,601	1,484,220	63.6	36.4
1959	1,399,702	682,261	717,441	2,081,962	67.2	32.8
1960	1,174,818	551,168	623,651	1,725,986	68.1	31.9
1961	1,072,201	524,167	548,034	1,596,368	67.2	32.8
1962	1,626,030	283,857	1,342,173	1,909,888	85.1	14.9
1963	1,365,831	357,598	1,008,233	1,723,429	79.3	20.7
1964	1,138,687	523,711	614,976	1,662,398	68.5	31.5
1965	874,692	537,943	336,749	1,412,635	61.9	38.1
1966	1,088,506	678,399	410,107	1,766,904	61.6	38.4
1967	1,328,348	258,571	1,069,776	1,586,919	83.7	16.3
1968	528,106	209,537	318,569	737,643	71.6	28.4
1969	1,102,298	546,021	556,277	1,648,319	66.9	33.1
1970	866,443	619,472	246,971	1,485,915	58.3	41.7
1971	942,897	384,551	558,346	1,327,448	71.0	29.0
1972	1,118,288	482,037	636,252	1,600,325	69.9	30.1
1973	1,802,433	275,782	1,526,651	2,078,215	86.7	13.3
1974	625,441	203,190	422,251	828,631	75.5	24.5
1975	570,328	289,374	280,954	859,702	66.3	33.7
Aver.	1,084,566	439,080	645,486	1,523,646	70.7	29.3

Table 3.7: Estimated longshore transport values in cubic yards per month based upon 20 years WIS wave data.

Month	μ	σ	μ_{log}	σ_{log}
Jan (South)	9,124	14,273	7.949	1.850
(North)	14,061	6,081	7.162	1.861
Feb (South)	7,352	11,406	7.772	1.788
(North)	4,486	6.929	7.291	1.829
Mar (South)	6,810	10,196	7.806	1.677
(North)	4,788	8,048	7.329	1.732
Apr (South)	968	1,402	6.105	1.377
(North)	1,132	1,298	6.043	1.946
May (South)	3,125	6.150	6.874	1.905
(North)	3,055	4,398	6.780	2.041
Jun (South)	1,462	3,150	5.919	1.875
(North)	2,077	4,102	6.132	1.937
Jul (South)	964	1,247	5.597	1.997
(North)	1,384	2,357	6.075	1.913
Aug (South)	1,974	4,784	6.208	1.929
(North)	1,466	2,367	6.212	1.701
Sep (South)	3,870	7,428	7.057	1.626
(North)	2,642	5,201	6.704	1.811
Oct (South)	5,687	8,965	7.647	1.522
(North)	3,387	5,125	7.119	1.594
Nov (South)	7,609	10,948	7.859	1.714
(North)	3,992	5,197	7.322	1.734
Dec (South)	7,516	10,997	8.024	1.557
(North)	4,442	6,829	7.287	1.798

(a) Magnitude, μ = mean value. σ = standard deviation.

Month	% North	% South	% Zero
Jan	65.7	34.2	0.1
Feb	65.6	34.2	0.2
Mar	61.0	39.0	0.0
Apr	61.8	37.7	0.5
May	44.2	54.8	1.0
Jun	40.5	58.7	0.8
Jul	26.3	71.6	2.1
Aug	36.3	62.1	1.6
Sep	57.3	42.2	0.5
Oct	76.9	22.9	0.2
Nov	70.0	30.0	0.0
Dec	70.0	29.8	0.2

(b) Direction

These annual or monthly transport rates can be used to generate various types of statistics or used to produce simulated synthetic longshore sediment transport. For example, the long term annual statistics can be represented by fit the annual data with any number of known statistical functions such as normal–, log–normal–, or Weibull–distribution curves. The log–normal function is found to fit well both the annual and the monthly statistics (Harris, 1991). Extreme value statistics, such as extreme transport rate per day can also be constructed.

Harris also produced synthetic sediment longshore sediment transport by using Monte Carlo technique. His method consists of two steps:

1. Generate a random variable to determine the direction of transport based on the statistics of transport direction. For example, suppose the 20 years transport data yielded 0.56% southward transport, 0.34% northward and 10% calm and a random number generator 1 to 100 is used then an outcome between 1 to 56 will dictate southward transport, an outcome between 56 to 90 will dictate northward transport and between 90 to 100 will yield no transport.

2. Another random number is then generated to determine the magnitude of the transport based upon the distribution curve which has a range between 0 to 1.

Figure 3.27 shows one realization of the synthetic transport. The cumulative transport shown in 3.27b is of special interest since it provides a good indication of seasonal transport direction as well as magnitude. This information is useful for planning dredging activities as well as bypassing schedules. As can be seen, there are two calm windows suitable for dredging one from day 90 to day 170 in the late spring and the other from day 210 to 260 in the early fall. The littoral dirft is clearly predominantly southward with the exception of a rare event of about once a year that a storm from southeast would result in northward transport. It is also clear that littoral transport is dominated by storm events. The contribution to the total annual transport under normal weather is of minor quantity.

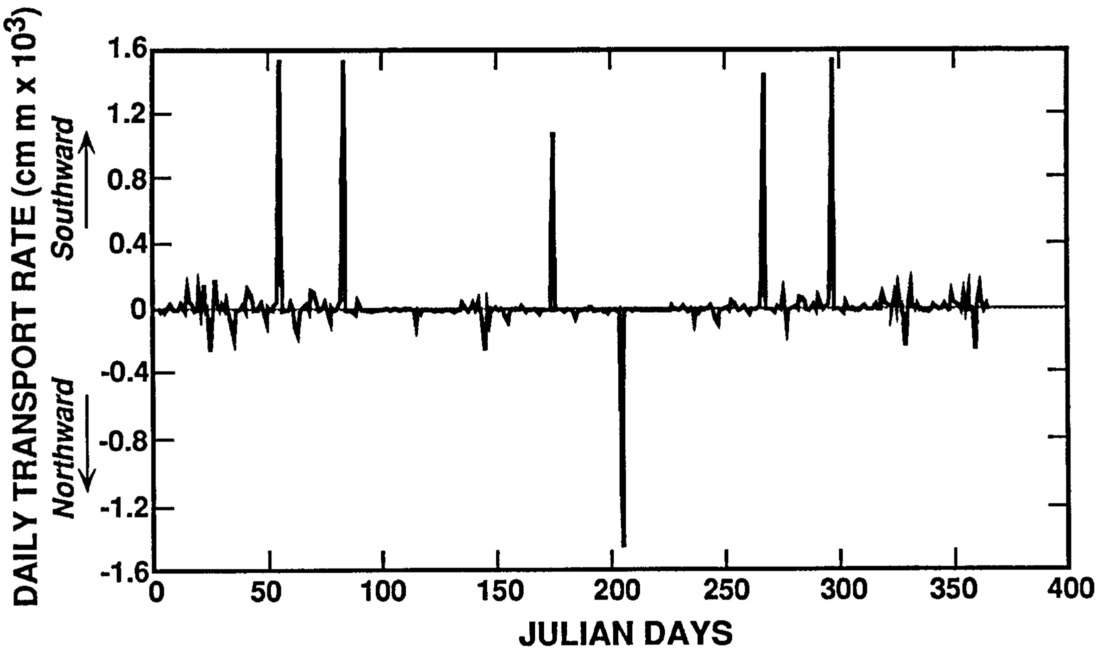

(a) Daily transport rate

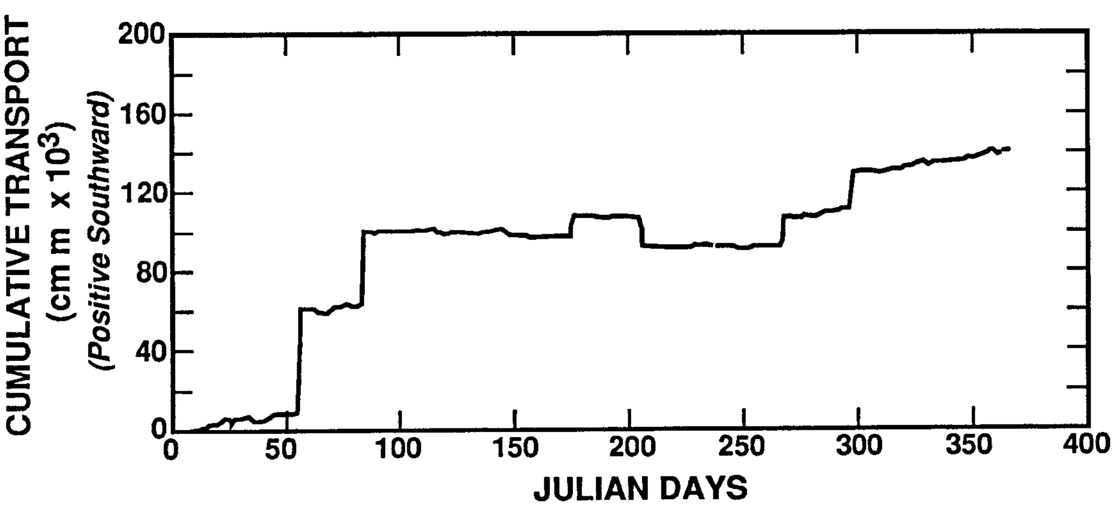

(b) Cumulative transport rate

Fig. 3.27. A realization of synthetic longshore transport at Sebastian Inlet.

SAND SOURCES

The economic feasibility of beach nourishment project depends heavily upon the availability of suitable sand sources. There are three major sand sources from offshore, (1) inlet dredging and maintenance, (2) ebb tidal shoals, and (3) offshore borrow sites. Various Federal, State and local interests have undertaken investigations in attempts to locate and quantify the sand sources.

Recently, Bodge and Rosen (1988 a. b) have attempted to summarize the offshore sand sources for beach nourishment along the Atlantic and Gulf coasts of Florida. Marino and Mehta (1986) have compiled the sediment volumes around Florida's east coastal tidal inlets. Many of the offshore sand sources can be found from the Inner Continental Shelf Sediment and Structure (ICONS) studies conducted by U.S. Army Corps of Engineers. Table 3.8a,b provides a list of sand sources along the Florida coast. The suitability and potential available volume of offshore and inlet related sources are limited by several factors, among them (Bodge and Rosen, 1988a):

1). sediment grain size,

2). population of clays, silts, and rock,

3). local water depth,

4). environmental considerations,

5). gross size of sand deposit,

6). distance to the project area, and

7). potential impacts of borrowing to local littoral process.

BIOLOGICAL CONDITIONS AND WATER QUALITY

In the United States, environmental impact study becomes an integral part on any dredging and beach fill project. Although the scope of environmental impact is expanding

Table 3.8a Sand inventory along Atlantic coast, FL.

Inlet	Ebb shoal Vol. $\times 10^{-6}$ (cu.yd)	Dredging/ by passing Vol. $\times 10^{-3}$ (cu.yd/yr)	Nearshore site Vol. $\times 10^{-6}$ (cu.yd)	Offshore site Vol. $\times 10^{-6}$ (cu.yd)	Offshore site Distance (Mi)
St. Marys	126.0	1000.0			
			43.0(2)	? (2)	11.0
Nassau Sound	53.0	- - -			
			- - -	?	14.0
Ft. George	174.0	280.0			
			22.0(3)	186.0(2)	8.0
St. Augustine	110.0	200.0			
			- - -	- - -	- - -
Matanzas	6.0	- - -			
			50.0	105.0(4)	11.0
Ponce de Leon	22.0	140.0			
			50.0	- - -	- - -
Port Canaveral	6.0	200.0			
			- - -	- - -	- - -
Sabastian	0.1	100.0			
			56.0(5)	16.0	12.0
Ft. Pierce	30.0	23.0			
			78.0(3)	- - -	- - -
St. Lucie	22.0	260.0			
			77.0	- - -	- - -
Jupiter	0.4	35.0			
			100.0	- - -	- - -
Lake Worth	3.8	70.0			
			100.0	- - -	- - -
S. Lake Worth	1.4	60.0			
			76.0	- - -	- - -
Boca Raton	0.8	60.0			
			8.0	- - -	- - -
Hillsboro	***	60.0			
			10.0	- - -	- - -
Pt. Everglades	***	40.0			
			12.0	- - -	- - -
Haulover	0.6	15.0			
			3.0	- - -	- - -
Gov'nt Cut	***	***			
			5.0	- - -	- - -
Key West	- - -	- - -			
			1.0	- - -	- - -

Number in parenthesis indicates number of sites more than one
? Quantity unknown
***Quantity negligible
- - - No estimate

Table 3.8b Sand inventory along Gulf coast, FL.

Inlet	Ebb shoal Vol. × 10^{-6} (cu.yd)	Dredging/ by passing Vol. × 10^{-3} (cu.yd/yr)	Nearshore site Vol. × 10^{-6} (cu.yd)	Offshore site Vol. × 10^{-6} (cu.yd)	Offshore site Distance (Mi)
Hurricane P.	0.2	- - -	- - -	- - -	- - -
Dunedin P.	0.2	- - -	- - -	- - -	- - -
Clearwater P.	0.2	40.0	- - -	- - -	- - -
Johns P.	0.6	60.0	0.2	- - -	- - -
Blind P.	0.2	- - -	12.0(2)	- - -	- - -
Bunces P.	- - -	- - -	30.0	- - -	- - -
Passage Key	- - -	- - -	14.0(3)	- - -	- - -
Longboat Key	8.0	47.0	1.0	- - -	- - -
New P.	4.4	74.0	- - -	- - -	- - -
Big Sarasota P.	14.0	- - -	- - -	- - -	- - -
Midnight P.	0.6	- - -	- - -	- - -	- - -
Venice I.	0.4	7.0	5.0(2)	- - -	- - -
Stump P.	- - -	4.0	- - -	- - -	- - -
Gasparilla P.	3.5	- - -	?	- - -	- - -
Boca Grande P.	160.0	290.0	- - -	- - -	- - -
Captiva P.	12.0	- - -	- - -	- - -	- - -
Redfish P.	3.0	- - -	?	- - -	- - -
San Carlos/ Ft. Myers	26.0	31.0	18.0(5)	- - -	- - -
Doctors P.	- - -	- - -	4.0(2)	- - -	- - -
Gordon P.	0.6	32.0	?		

Number in parenthesis indicates number of sites more than one
? Quantity unknown
***Quantity negligible
- - - No estimate

and varies from region to region, the primary concern is still the impact on the biological communities and water quality during the following three phases:

– dredging

– transport

– placement

Since biological communities are closely related to site and the implementation method of nourishment, a site - and method - specific analysis is usually required. In the State of Florida, the common questions addressed by the regulatory agencies include:

⋆ detailed biological sampling data from the borrow sites and nourishment sites;

⋆ detailed surveys of rock outcrops, reefs, grass beds, and any other features in the areas of the borrow and nourishment sites;

⋆ a survey of turtle nesting sites;

⋆ details on dredging, transport and placement methods and the techniques to maintain water quality standards, particularly in relation to turbidity monitoring and control.

Although there is no central data bank on biological communities along the Florida coast, a considerable amount of information is available in open literatures. Nelson (1985) gave an excellent account on the background information of biological effects of beach nourishment. He stated that there is considerable more information on the effects of dredging on benthic communities but much less is known about the specific environmental consequences of beach nourishment.

The area that a major void exists is the lack of background information on water quality and the effects of turbidity created by the nourishment operation.

Nelson also suggested biological monitoring procedures on beach nourishment project.

NATURAL AND MAN-MADE STRUCTURES

An inventory of natural and man-made structures is also important for beach nourishment design. Since a nourishment project is expected to interact with its adjacent beaches, the inventory should include zones beyond the immediate nourishment area to the boundaries of a natural littoral drive cell. In Florida, this often means between two adjacent inlets. The following types of structures are particularly significant:

- inlets (existing and old)
- seawalls and revetments
- past nourishment projects
- sand dunes and vegetations
- outcrops

REFERENCES

Bodge, K.R., and Rose, D.S. (1988) Offshore sand sources for beach nourishment in Florida; Part 1: Atlantic coast, *Proc. National Beach Preservation Technology 88*, Gainesville, FL, Florida Shore and Beach Preservation Association.

Bodge, K.R., and Rose, D.S. (1988) Offshore sand sources for beach nourishment in Florida; Part 2: Gulf coast, *Proc. National Beach Preservation Technology 88*, Gainesville, FL, Florida Shore and Beach Preservation Association.

Dean, R.G. (1983) Shoreline erosion due to extreme storms and sea level rise, *UFL/COEL-83/007*, Coastal and Ocean. Engr. Dept., Univ. of Fla., Gainesville.

Dean, R.G. (1984) Application of equilibrium beach profile concepts, *19th International Coastal Engr. Conf.*, ASCE, Houston, TX.

Dean, R.G. and Chiu, T.Y. (1981) Hurricane tide frequency analysis for Broward County, Florida, *UFL/COEL-81/001*, Coastal and Ocean. Engr. Dept., Univ. of Fla., Gainesville.

Harris, D.L. (1982) The prediction of hurricane storm surges, a state-of-the-art survey, *SGR 49*, Florida Sea Grant College, Univ. of Fla., Gainesville.

Harris, P.S. (1991) The influence of seasonal variation in longshore sediment transport with applications to the erosion of the downdrift beach at Jupiter Inlet, Florida. UFL/COEL–91/015, Coastal and Oceanographic Engineering Department, Univ. of Fla., Gainesville.

Jensen, R.E. (1983) Atlantic coast hindcast, shallow-water, significant wave information, wave information study, *Report 9*, U.s. Army Engineer Waterways Experiment Station, Vicksburg, Mississippi.

Lin, L. (1988) A coupled discrete spectral wave hindcast model, *Technical Report TR-076*, Coastal and Ocean. Engr. Dept., Univ. of Fla., Gainesville.

Lin, L., and Wang, H. (1988) Analysis of extreme wind speed and significant wave height along Florida coast, *proc. Ocean Structural Dynamics Symposium '88*, Oregon, Oregon State University Press.

Moore, B. (1982) Beach profile evolution in response to changes in water level and wave height, *M.S. thesis*, Dept. of Civil Engr., Univ. of Del., Newark.

Nelson, W.G. (1985) Guidelines for beach restoration projects, Part 1: Biological, *SGR-76*, Florida Sea Grant College, Univ. of Fla., Gainesville.

Walton, T.L. (1973) Littoral drift computations along the coast of Florida by means of ship observations, *Rept. UFL/COEL/TR-015*, Univ. of Fla., Coastal Engr. Lab., Gainesville.

Wang, W.C. and Wang, H. (1987) Data compilation of the historical shorelines and offshore bathymetry for the southeast coast of Florida, *Rept. UFL/COEL-87/015*, Coastal and Ocean. Engr. Dept., Univ. of Fla., Gainesville.

Wilson, E.E. (1975-1986) *Mariners Weather Log*, National Oceanic and Atmospheric Administration, Environmental Data and Information Service, U.S. Dept. of Commerce, Volumes 19-30.

WIS Wave Models

Corson, W.D., et al. (1981) Wave information studies of U.S. coastlines; Atlantic coast hindcast, deepwater, significant wave information, *WIS Report 2*, U.S. Army Engineer Waterways Experiment Station, CE, Vicksburg, Mississippi.

_________________ (1982) Wave information studies of U.S. coastlines; Atlantic coast hindcast, Phase II wave information, *WIS Report 6*, U.S. Army Engineer Waterways Experiment Station, CE, Vicksburg, Mississippi.

Jensen, R.E. (1988) Wave information studies of U.S. coastlines, methodology for the calculation of a shallow-water climate, *WIS Report 8*, U.S. Army Engineer Waterways Experiment Station, CE, Vicksburg, Mississippi.

_________________ (1983) Atlantic coast hindcast, shallow-water significant wave information, *WIS Report 9*, U.S. Army Engineer Waterways Experiment Station, CE, Vicksburg, Mississippi.

Chapter 4

SEDIMENT STORAGE AT TIDAL INLETS

Ashish J. Mehta, modified by Hsiang Wang
Coastal & Oceanographic Engineering Department
University of Florida, Gainesville

INTRODUCTION

Accumulation of sediment around tidal inlets has become a matter of renewed interest mainly for three reasons. The first of these is the need to estimate the shoal volumes, particularly the ebb shoal, as a potential source of sediment for beach nourishment. Portions of the ebb shoal can be transferred to the beach provided there are no measurable adverse effects on navigation, or on the stability of the shoreline near the inlet. Such an operation, for example, was carried out successfully at Redfish Pass, on the Gulf of Mexico coast of Florida (Olsen, 1979). A schematic example of a potential site for ebb shoal excavation and sand transfer to the downdrift beach is shown in Fig. 4.1.

The second reason is the need to assess the role of the inlet in influencing the rate of erosion of the downdrift shoreline, as a result of interruption or deflection of the littoral drift. For example, the effect of construction of Port Canaveral Entrance channel, Florida, on the downdrift beach is shown in Fig. 4.2 (Dean, 1987). The beach shoreline eroded at a comparatively rapid rate of a $\sim 5\ km$ stretch immediately south of the inlet, and a beach nourishment project was consequently carried out in 1974.

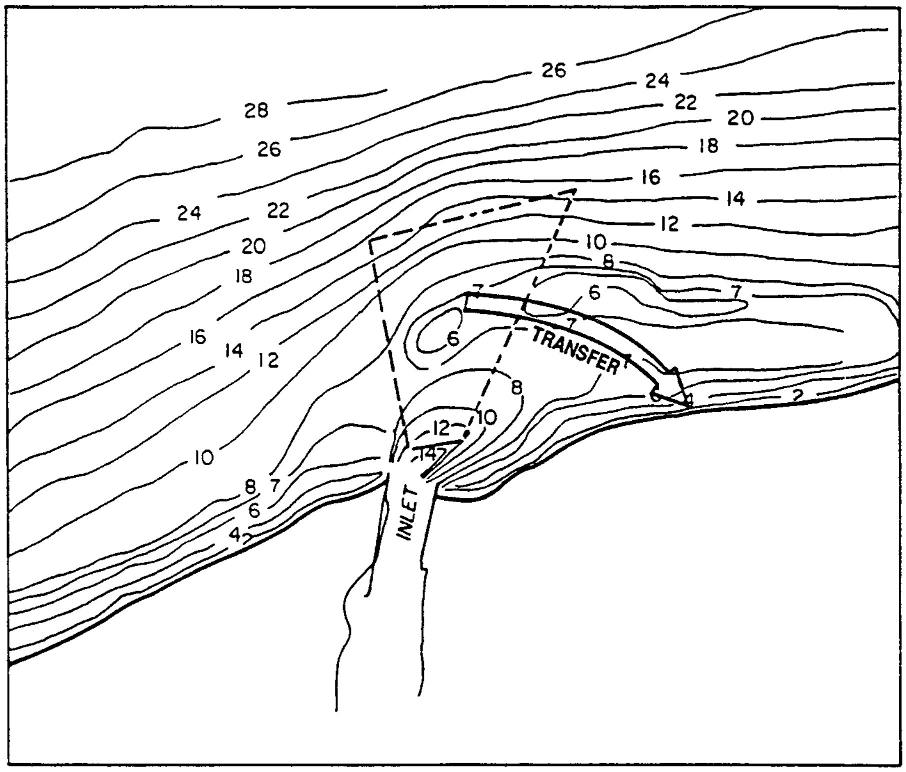

Figure 4.1. A Schematic Example of a Potential Site (Area Enclosed by Dashed Lines) for Ebb Shoal Excavation and Sand Transfer. Depth Contours are Hypothetical.

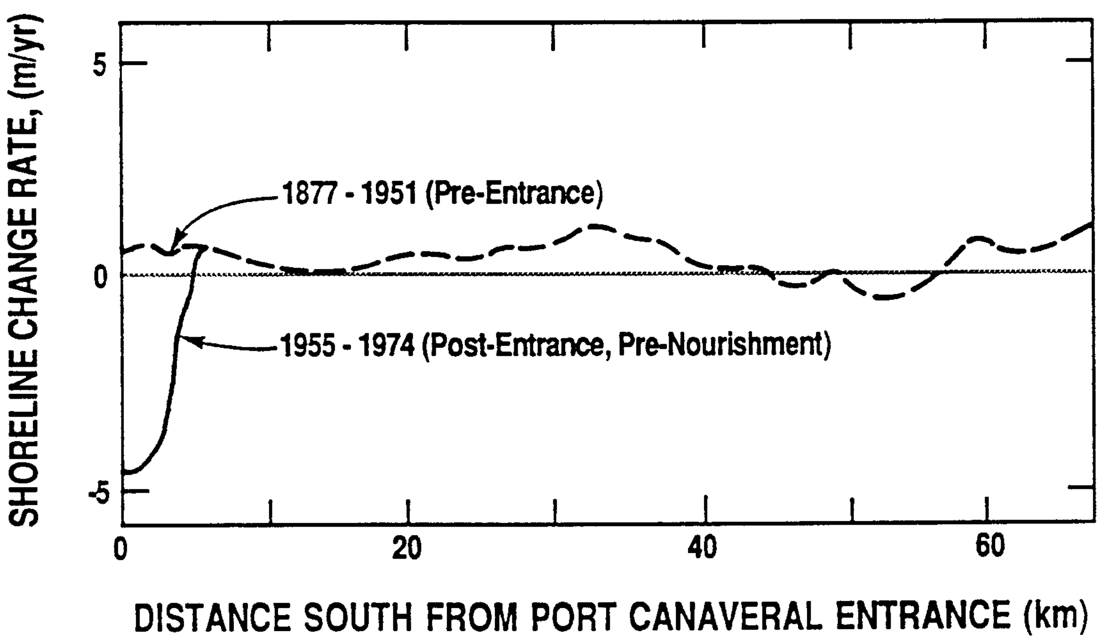

Figure 4.2. Effect of Construction of Port Canaveral Entrance, on the Atlantic Coast of Florida, on Downdrift (Southward) Shoreline (After Dean 1987).

Finally, an evaluation of inlet sediment accumulation is essential to account for the long term sedimentary budget of shorelines interrupted by inlets, as schematized in Fig. 4.3a. The budget in this case is for the "box" volume enclosed by shore-parallel and shore-normal boundaries. Q_1 through Q_8 are volumetric rates of sediment transport across these boundaries. The algebraic sum of all the Q's equals the time-rate of change of sediment volume within the box, which would be equal to zero for a stable inlet/shoreline system. For an illustrative example of the application of this method see Jones and Mehta (1978). In the same context it is also worth noting the participatory role of shoals in governing sediment pathways in the inlet region. In Fig. 4.3b such pathways are exemplified (Buckingham, 1984). The numbers may be considered as representing annual volumetric rates in 10^3 m^3. Areas enclosed by dashed lines are flood shoal traps from which material is transported to the downdrift beach by artificial means.

In reference to these issues, quantities of particular interest are the volume of sediment presently stored in the ebb shoal, and the volume of material trapped, either as a result of training works such as jetties, or as a consequence of the opening of an artificial inlet and the growth of associated shoals. There is also the related question of volumetric erosion of the downdrift shoreline. These issues will be examined with specific reference to major inlets on the east coast of Florida together with some examples from Georgia inlets, following some comments concerning natural and artificial sediment bypassing at sandy inlets.

INLET HYDRAULICS

The sediment process near inlets is intimately related to the inlet hydraulics. Two major natural forces are at work: tides and waves. The effects of tide are mainly due to tidal-induced current which transport material in and out the inlet. Wave, on the other hand, is the prime mover of nearshore sediment, both on/offshore and longshore. In the vicinity of inlet, waves, currents, beaches and training structures interact with each other to form a complicated hydrodynamic problem. Our current knowledge on inlet hydraulics is still

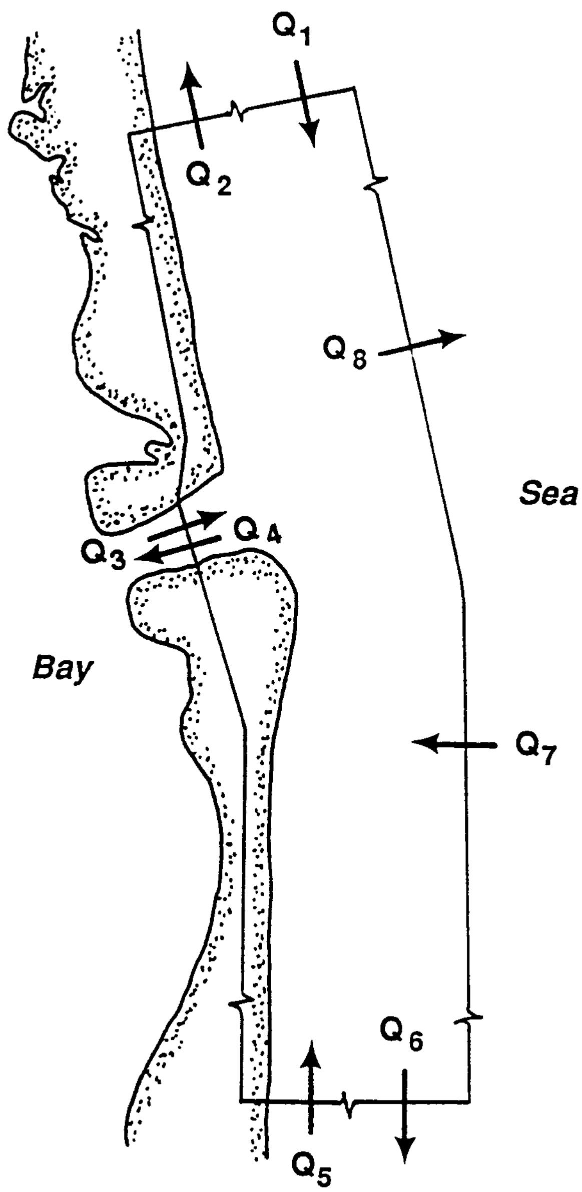

Figure 4.3a. Box Volume Approach for Sediment Budget Near a Tidal Inlet.

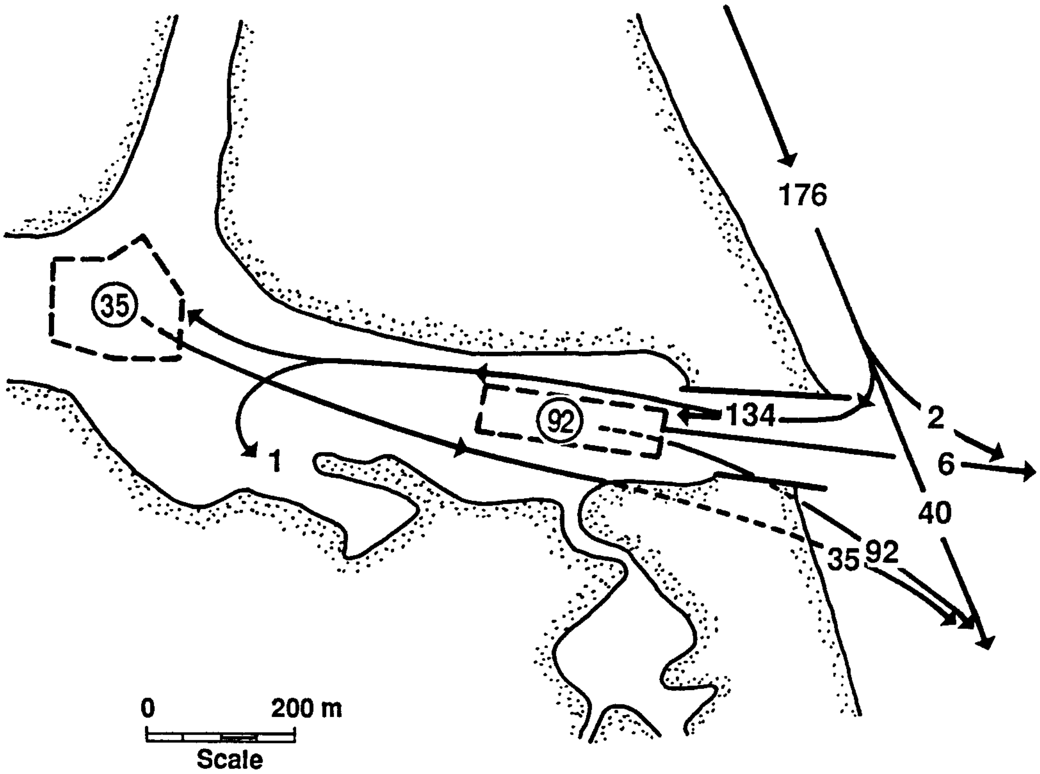

Figure 4.3b. Illustration of Sediment Pathways (Natural and Artificial) in the Inlet Area.

rather limited. However, with the recent advancement on current-wave interaction theories and the aid of computer simulations, we are certainly much better equipped than before to prescribe the hydraulics and to examine the effects.

The tidal induced current enters the inlet during flood much like water drains into a sink such that water converges from all directions. During ebb flow, on the other hand, the flow leaves the inlet like a jet expanding into the surrounding often creating trailing eddies on both sides which entrain water into the main jet. These conditions of flood and ebb flows are illustrated in Fig. 4.4.

The current strength in the inlet passage can be established by energy and continuity considerations. Keulegan (1967) showed that for a given tidal range and channel charecteristics the current strength, repesented by the peak current strength, U_m at the throat of the inlet and throat cross-sectional area, A_C has a definite relationship as shown in Fig. 4.5. It says that, initially, as the cross-sectional area increases the current will also increase due to the fact that the head loss in the inlet is inversely related to current strength. The current, however, will reach a peak value $(U_m)_p$, beyond which the it will decrease as the cross-sectional area increases further. This is because the inlet has a finite capacity of handling discharge, thus, the the larger the cross-sectional aera the smaller the velocity. This curve is useful in inlet stability analysis as will be addressed later.

If the inlet is improved with jetties, the current field will be affected. The ebb tidal current, carrying a concentrated momentum , will be deflected in accordance with the jetty contours and will form new ebb tidal channel. Flood tide is much more diffused, thus, is less affected by the jetties. However, long and curved jetties could cut down flow entrance zone and create strong current locally. These situations are illustrated in Fig. 4.6.

Waves induce oscillatory water motions in the offshore region but produce uni-directional current along the shoreline within the surf zone. This longshore current, as addressed earlier, is the main agent of transporting longshore sediment. With the presence of inlet and/or jetties, the interactions become extremely complicated. They often have to be determined

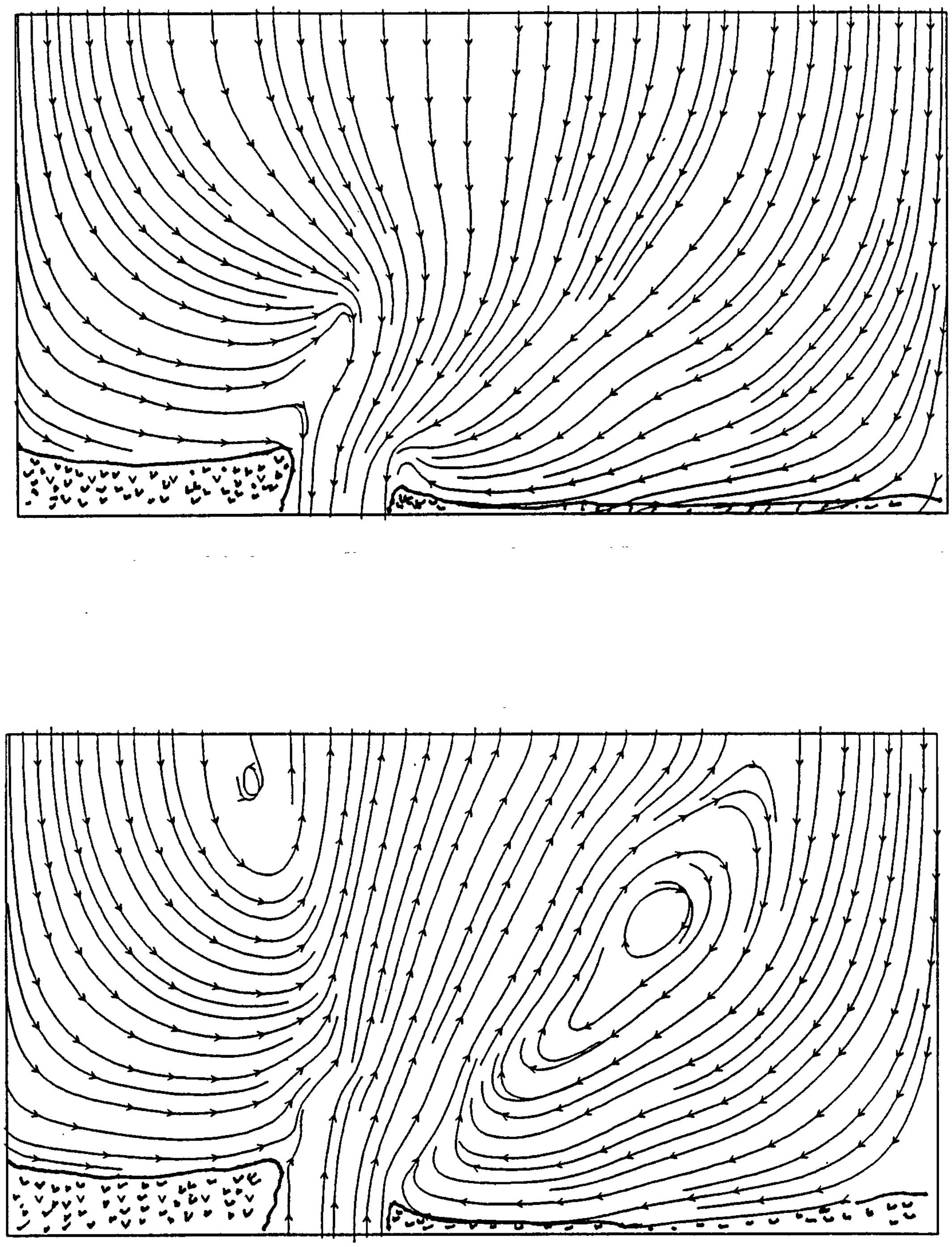

Fig. 4.4. Illustrations of flood and ebb flows near an inlet.

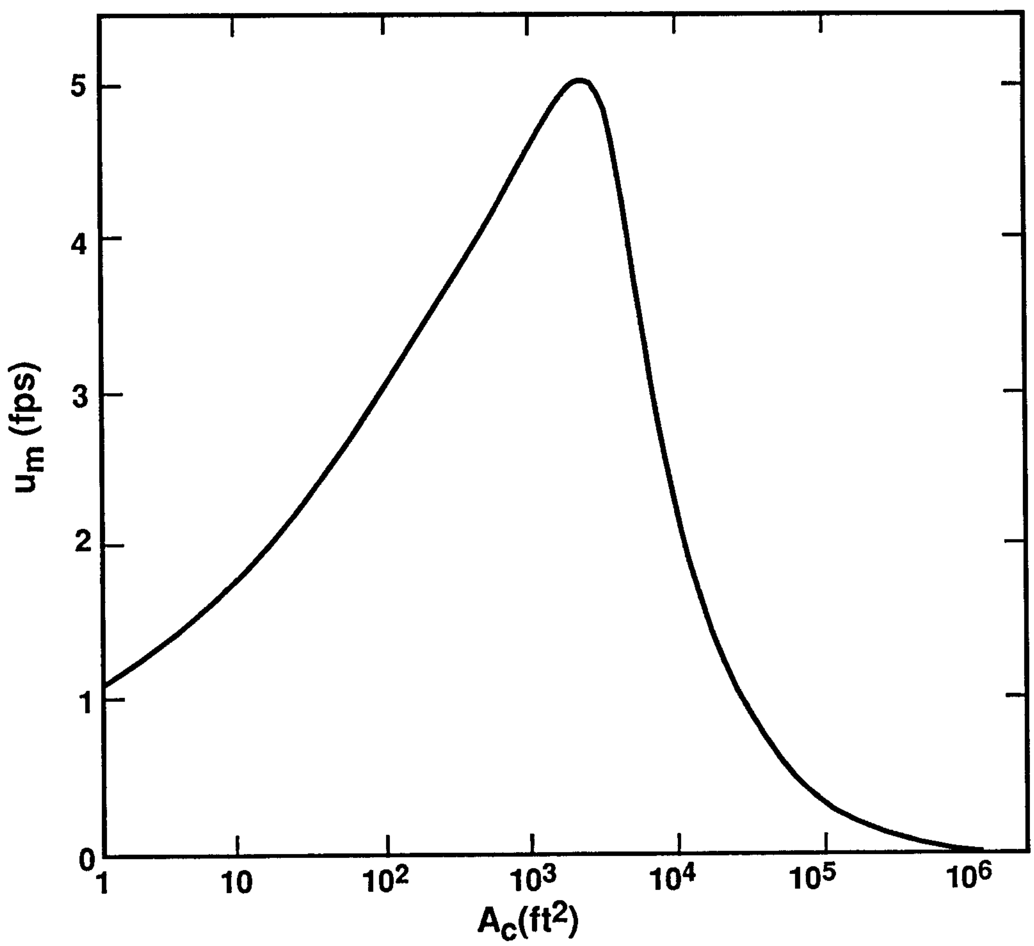

Fig. 4.5. Relationship between throat cross section, A_c, and current amplitude at the throat.

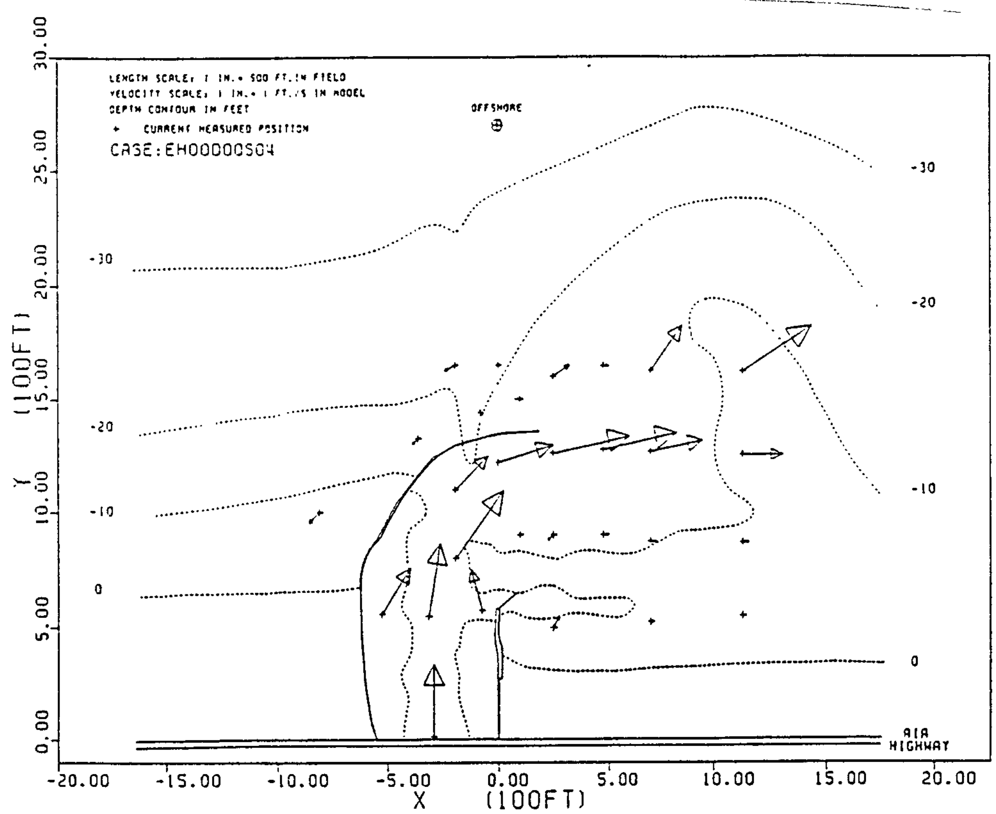

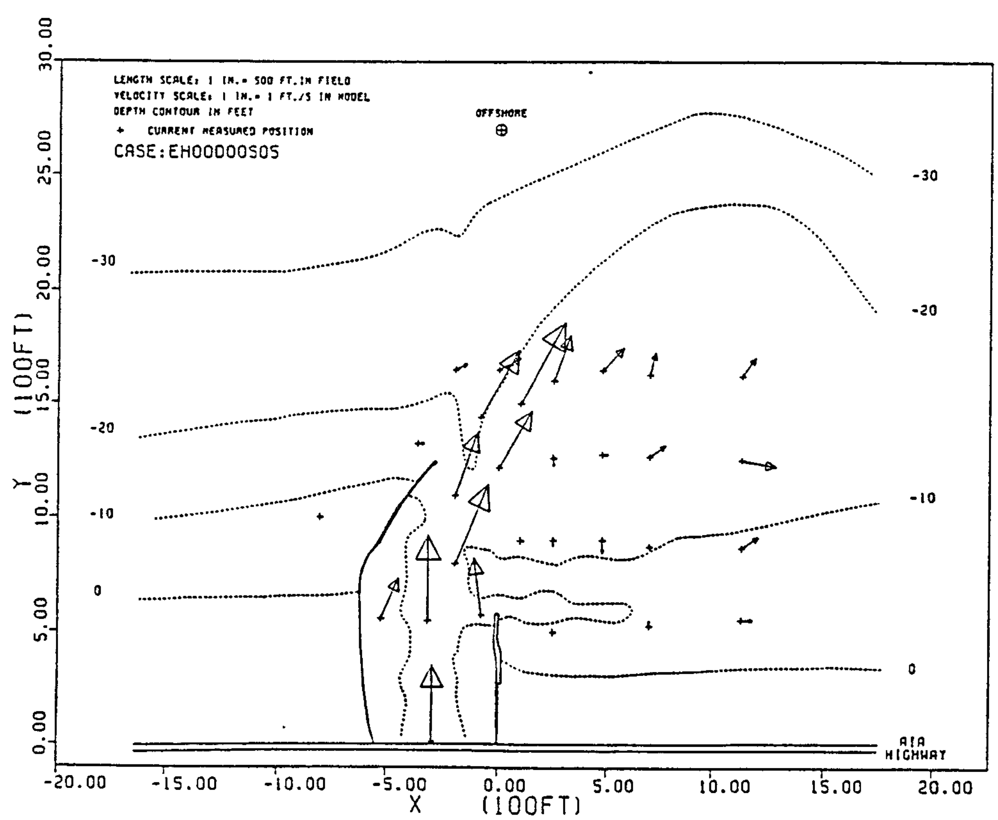

Fig. 4.6a. Effects of jetty configurations on ebb flows.

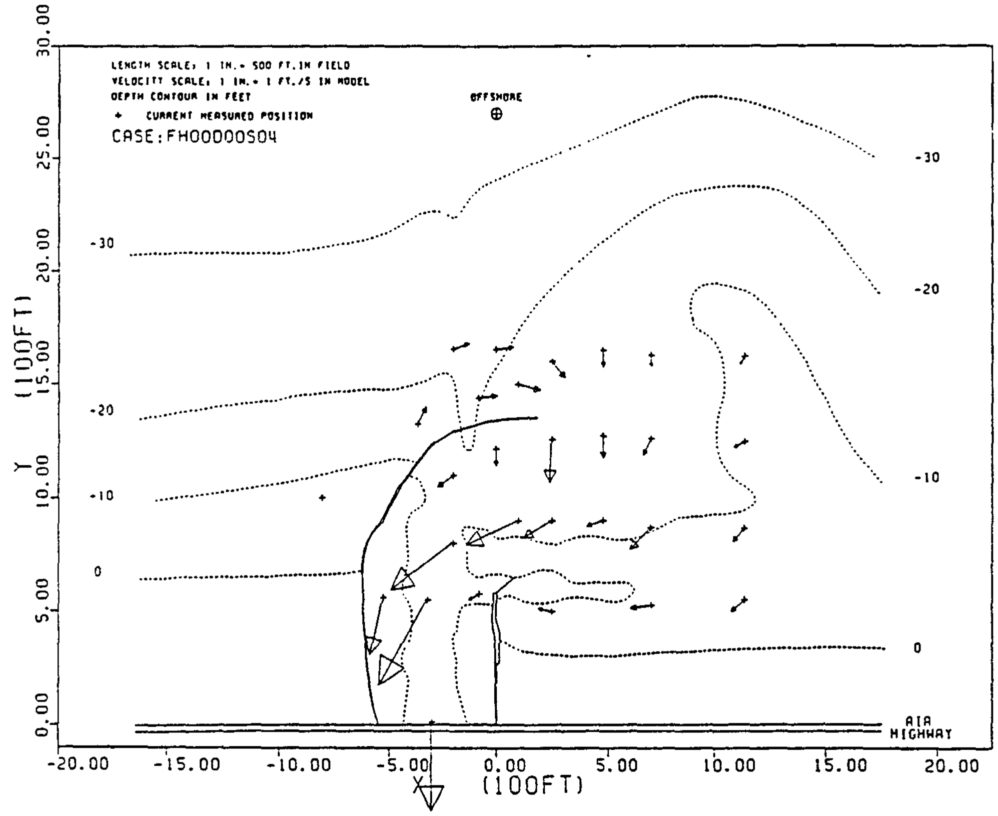

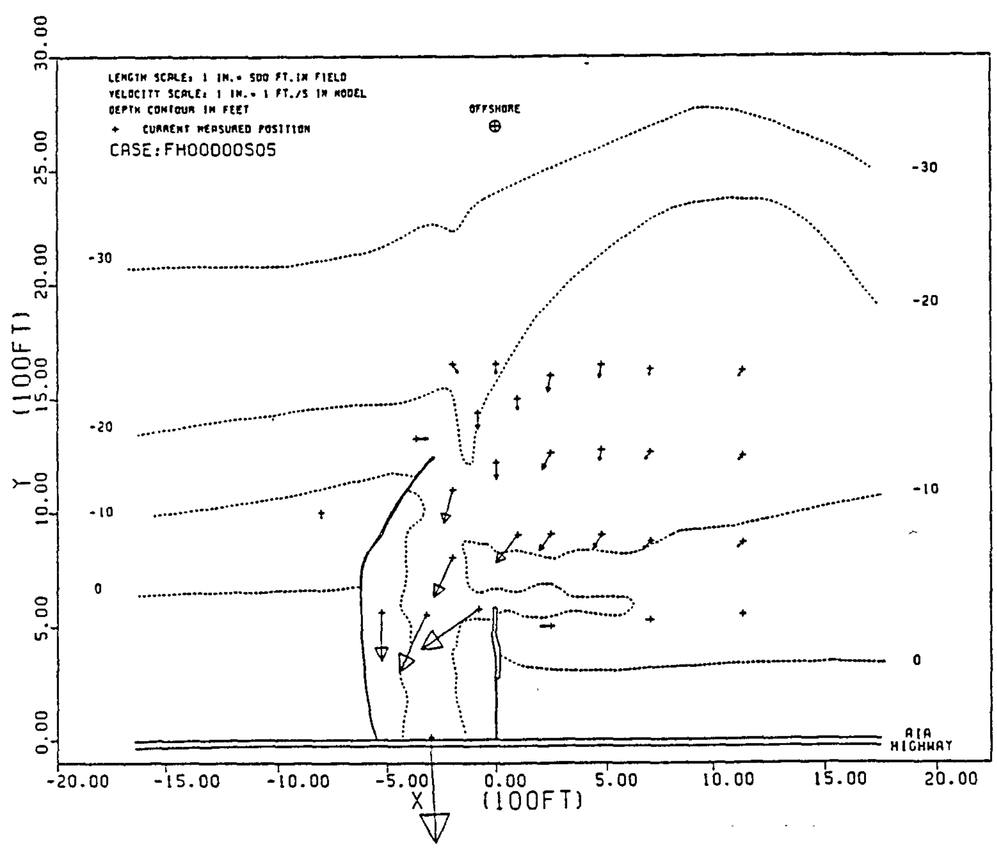

Fig. 4.6b. Effects of jetty configurations on flood flows.

by numerical and physical models augmented by field measurements. Figures 4.7 to 4.8 present some of the results from numerical and physical models of Sebastian Inlet with comparasions to field measurements. Some of the features discussed earlier are further revealed here.

Under normal condition and in the absence of waves, sediment will be transported by tidal current mainly in the form of bed load. Flood tide tends to erode the inlet banks and beaches just adjacent to the inlet entrance through current–induced shear stress. The stronger the current the higher the erosion. Ebb tide transports the material offshore to form ebb tidal shoal or delta. The stronger the current the further the ebb tidal shoal and the larger the ebb tidal shoal. Unless there is a large quantity of sediment carried into the inlet from upstream tributories, tidal current is usually a force that maintains the inlet opening.

Waves, on the other hand, transport sediment across the inlet, thus, tend to fill the inlet with sand. It is an inlet closure force. Consequently, the relative magnitude of wave energy to tidal energy is the major factor that governs the inlet stability. Bruun and Gerristsen (1960) suggested to use the ratio of tidal prism,P, to the littoral transport rate, M_T, as the parameter to grade inlet stability. Here, P is defined as the discharge per half tidal cycle:

$$P = \int_0^{\frac{T}{2}} Q dt \qquad in \;\; M^3 \tag{4.1}$$

and M_T is volumetric material transport per year in M^3/yr. For Florida inlets, Bruun et al. (1978) suggested the following grading:

$\frac{P}{M_T}$	Stability Condition
> 150	Good stability, small bar
100-150	less satisfactory, more prounced bar
50-100	Large bar, channel through bar
20 50	Large cresent bar, threatening closure
< 20	Unstable, overwash channel rather than inlet

Another approach to inlet stability is based on the Escoiffier's (1940) stablity concept. Based on field surveys, O'Brien (1966, 1969) plotted the data of throat area and the tidal

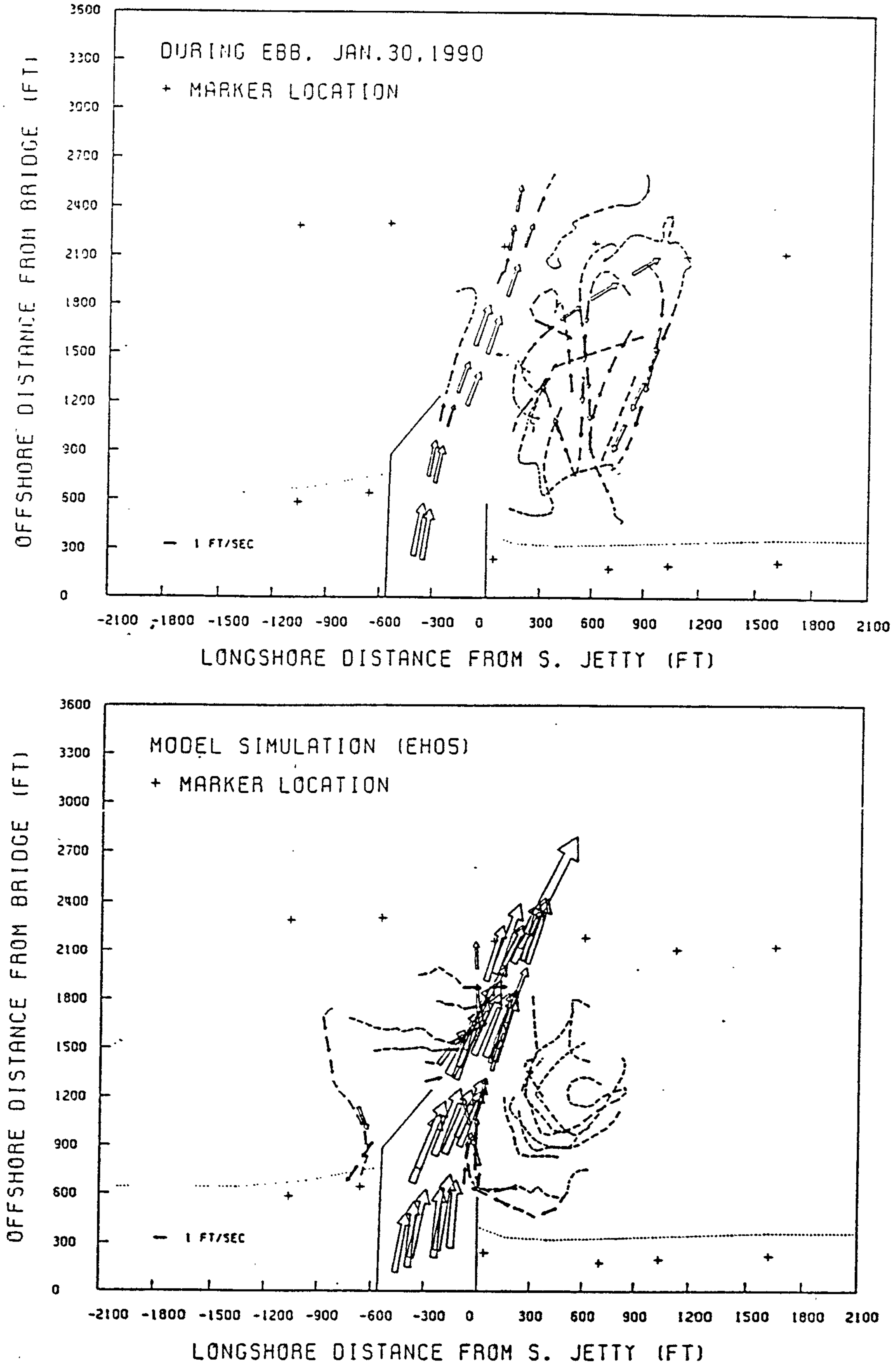

Fig. 4.7. Ebb current patterns measured in the field and laboratory.

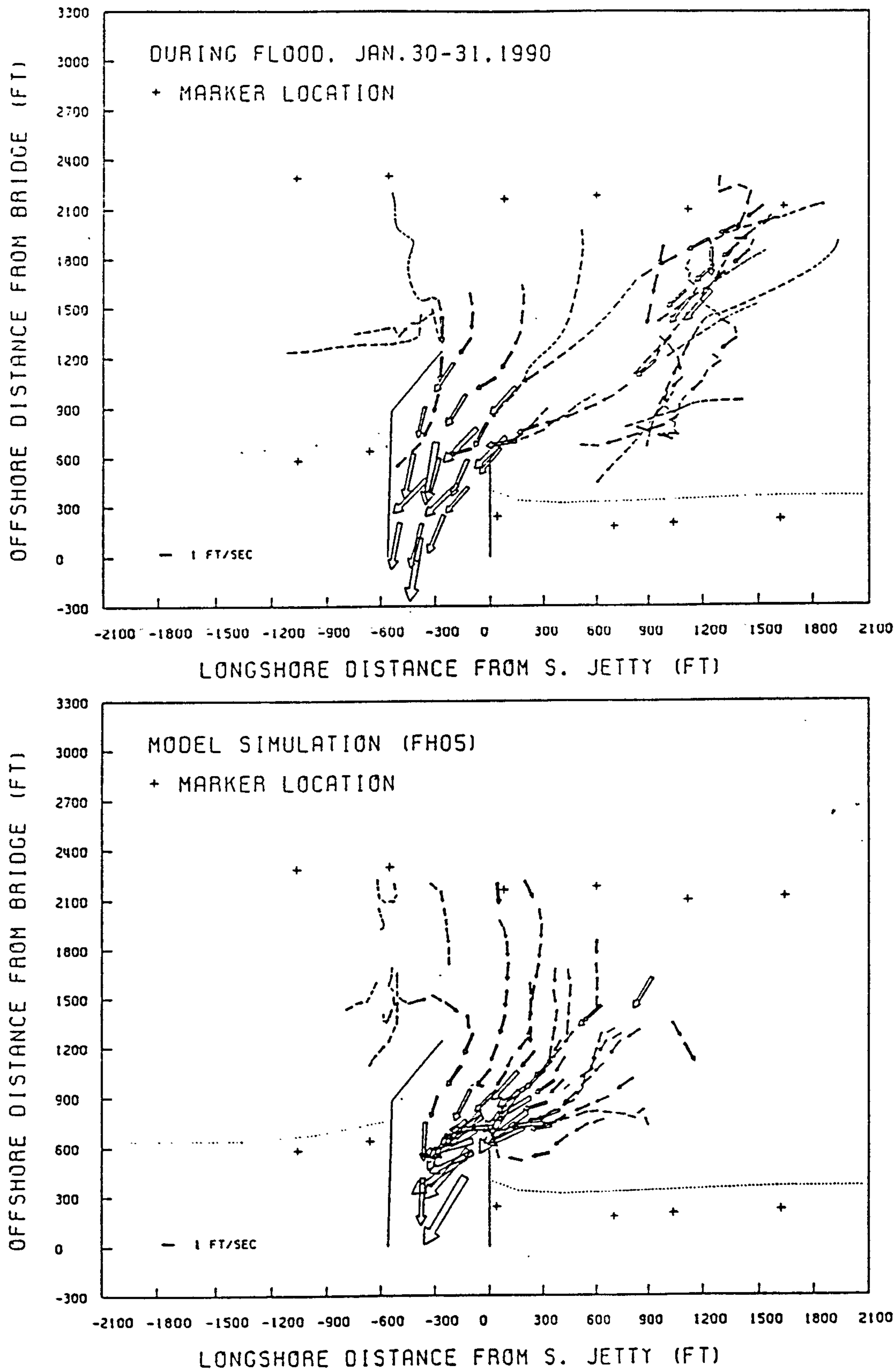

Fig. 4.8. Flood current patterns measured in the field and laboratory.

prism for stable inlets as shown in Fig. 4.9 and fitted an empirical curve:

$$A = 4.7 \cdot 10^{-4} P^{0.85} \tag{4.2}$$

This curve can be viewed as an inlet equilibrium condition and can be interpreted as follows: If the inlet condition falls on the right hand side of the curve, the cross-sectional area is too large for a given tidal prism and shoaling will occur to reduce the area bringing the condition towards the curve. On the other hand, if the inlet condition is on the left of the curve, erosion will also occur to bring the condition to the curve. This P-A_c curve, which is established by sedimentation consideration, together with the $U_m - A_c$ curve given in Fig. 4.5, which is established by hydaulic consideration, enables us to examine the inlet stability. This is illustrated in Fig. 4.10. When the U-A curve falls below the P-A curve, the inlet is unstable as the inlet is accretional but the hydraulic condition of the inlet is insufficient to bring the inlet into equilibrium. If the P-A curve intersects the U-A curve, the inlet is stable beyond point "K" but is unstable below point K. The equilibrium condition of the specific inlet is at the intersect "O".

SEDIMENT BYPASSING

Natural Bypassing

It has been well established that waves striking obliquely along the coastline cause a significant transport of sediment along the coastline in what has been called "the littoral drift system." An inlet located along such a coastline represents a discontinuity in the littoral drift system, and although the exact processes of the interaction between the inlet and the littoral drift system are not fully understood, the gross effects are; namely, accumulation of sediment in the ebb and flood shoals and a considerable degree of sediment exchange between the inlet channel and the shoal complexes (Dean and Walton, 1975, Byrne et al., 1974, and FitzGerald, et al., 1976).

A schematic representation of the sediment transport processes at an inlet has been given by Bruun et al., (1978) and is shown in Fig. 4.11 (Winton and Mehta, 1981). Sediment

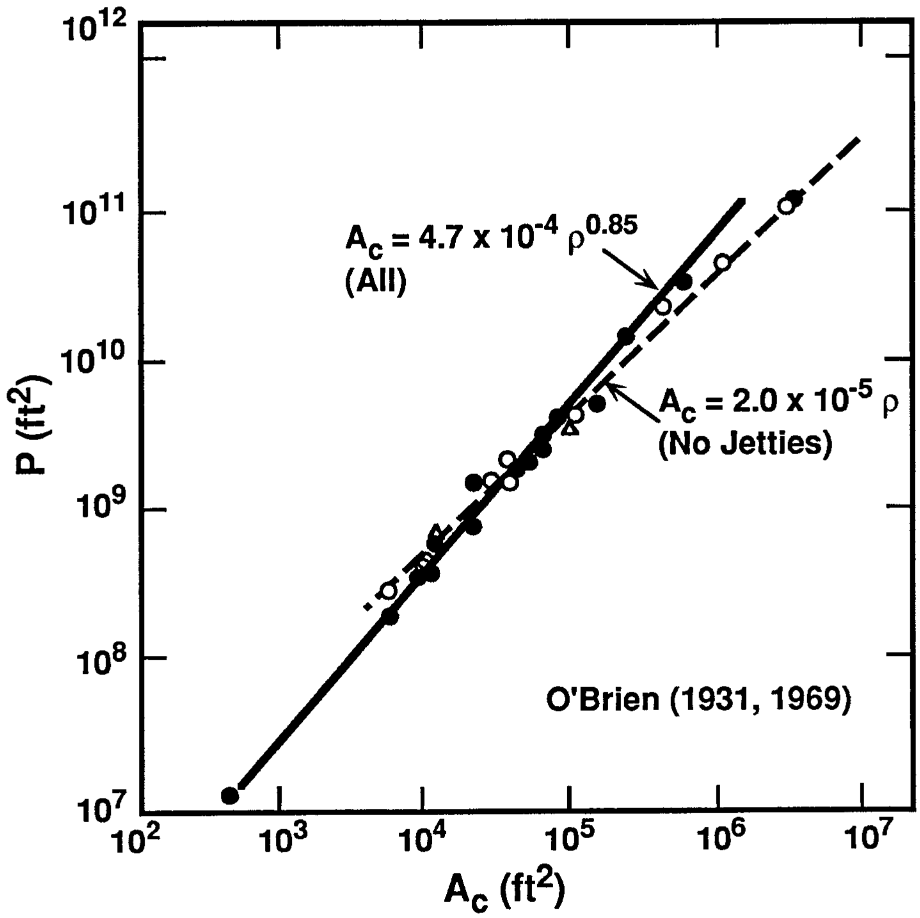

Fig. 4.9. O'Brien's relationship between tidal prism and throat area.

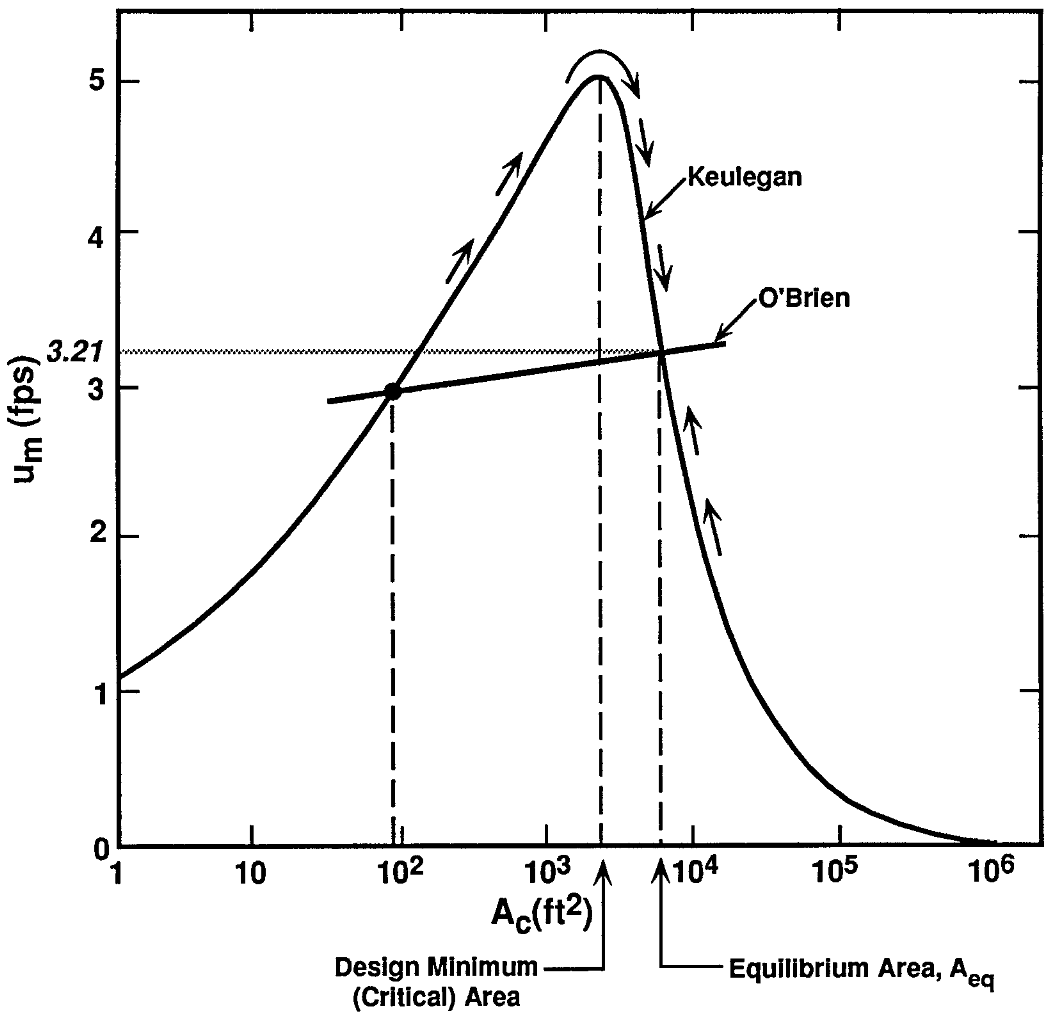

Fig. 4.10. Inlet stability criterion based on Escoiffer concept.

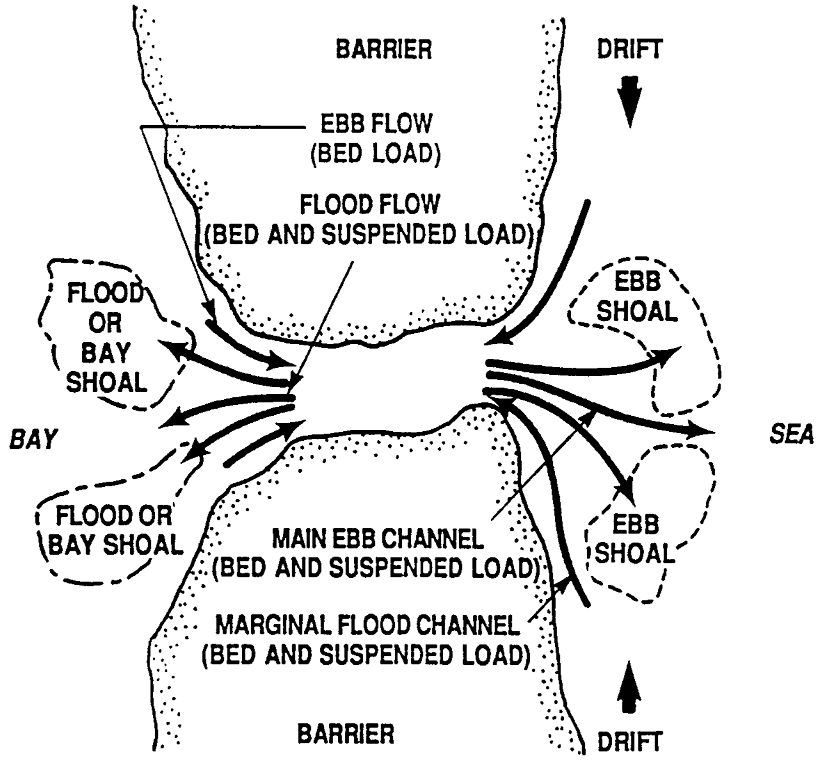

Fig. 4.11. **Schematic Diagram Showing Inlet Ebb/Flood Shoals and Sediment Transport (After Winton and Mehta, 1981).**

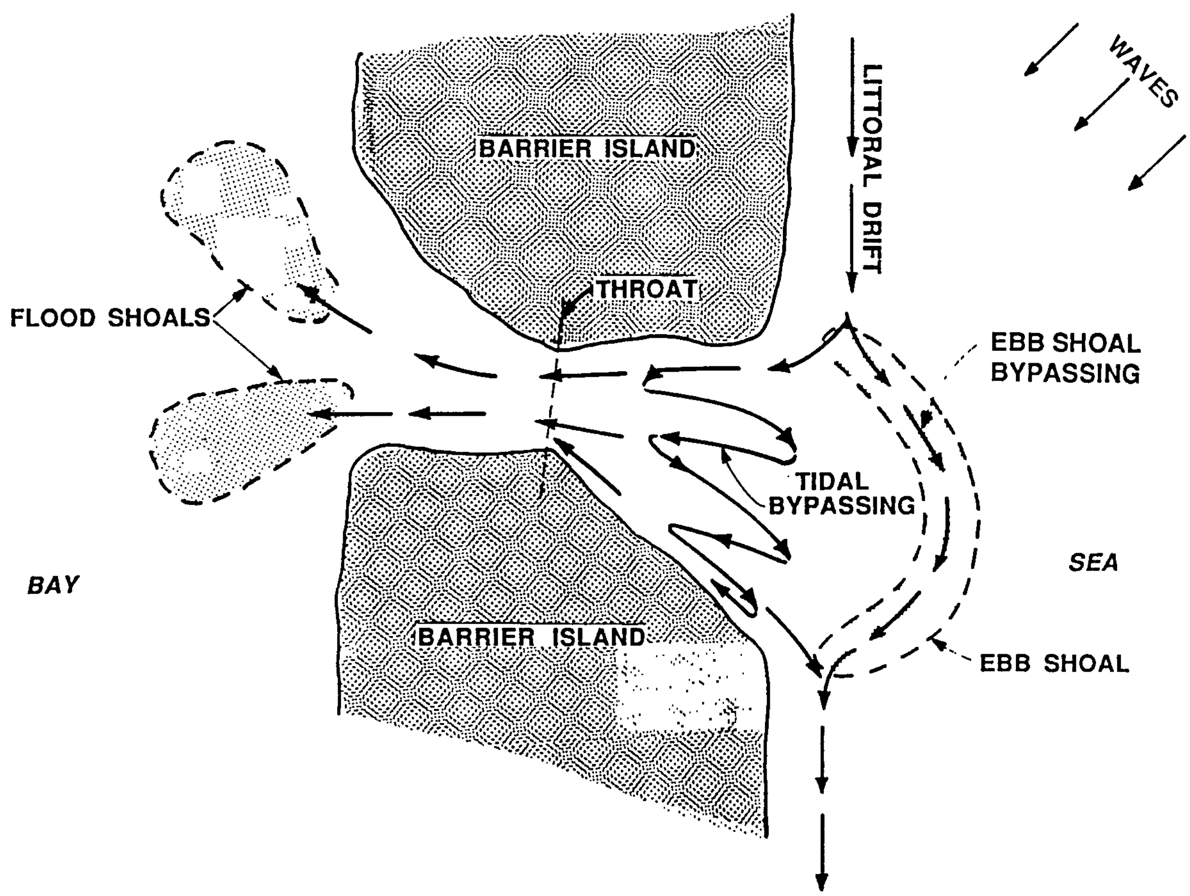

Fig. 4.12a. **Bar Bypassing and Tidal Flow Bypassing at an Inlet.**

moving along the coast in the littoral drift system enters the inlet mouth mainly through the swash or marginal flood channels, and to a lesser extent over the ebb shoals. When the flow through the inlet is in the flood stage, some of the littoral drift will be carried through the inlet to the bay or flood tidal shoals, some still in suspended form and the rest as bed load. When the flow through the channel is in the ebb stage, some of the material which was transported through the channel to the bay shoals may be transported back through the channel to the ebb shoals and beyond, and "new" material (i.e. deposited from the littoral drift) will also be transported out onto the ebb shoals and/or beyond. For inlets with certain morphologic characteristics and strong ebb flow, some littoral material would be transported as bed load in deep water past the inlet, while for inlets with relatively small ebb flows subject to strong wave action at low tide, part of the material in the littoral drift may effectively bypass the inlet and not pass back and forth through the main channel.

Thus as noted by Bruun et al. (1978), there are essential two ways by which sediment (sand) is bypassed naturally around an inlet (Fig. 4.12a). These two modes are referred to as bar or ebb shoal bypassing – in which sand is predominantly transported from updrift to downdrift beach via the ebb shoal, and tidal flow or channel bypassing – in which the material enters the channel and, under the combined action of tidal currents and cross- flow (alongshore current), is eventually transported downdrift. However, during this process of natural transfer, particularly in the case of tidal flow bypassing, a certain fraction of the sediment mass transported per unit time may end up in the interior, bayward of the throat section, thus forming flood shoals.

In Fig. 4.12c a very approximate relationship between a parameter b, referred to as the bypassing ratio, and the maximum flow discharge through the inlet channel, Q_m, has been presented in order to enable a preliminary assessment of the nature of sediment bypassing. The plot, including the data points from inlets with known bypassing characteristics which were used to differentiate between the modes of bypassing, is based on the works of Bruun (1966), Bruun et al. (1978) and Jones (1977). The ration b is equal to Q_n/Q_m^3, where Q_n

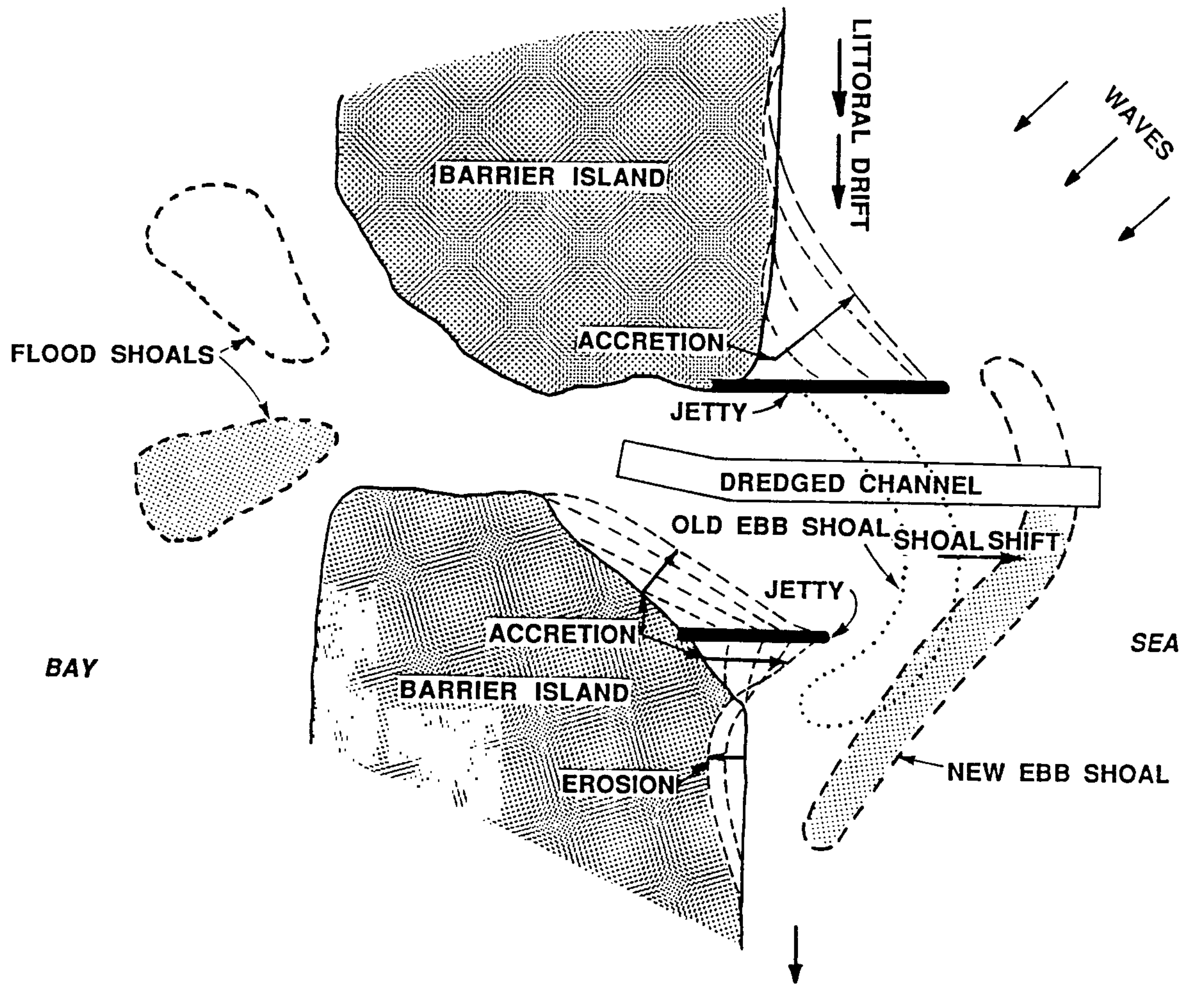

Fig. 4.12b. **Plan View Changes at an Inlet Due to Jetties and Dredged Channel: Shoreline Response to Modification.**

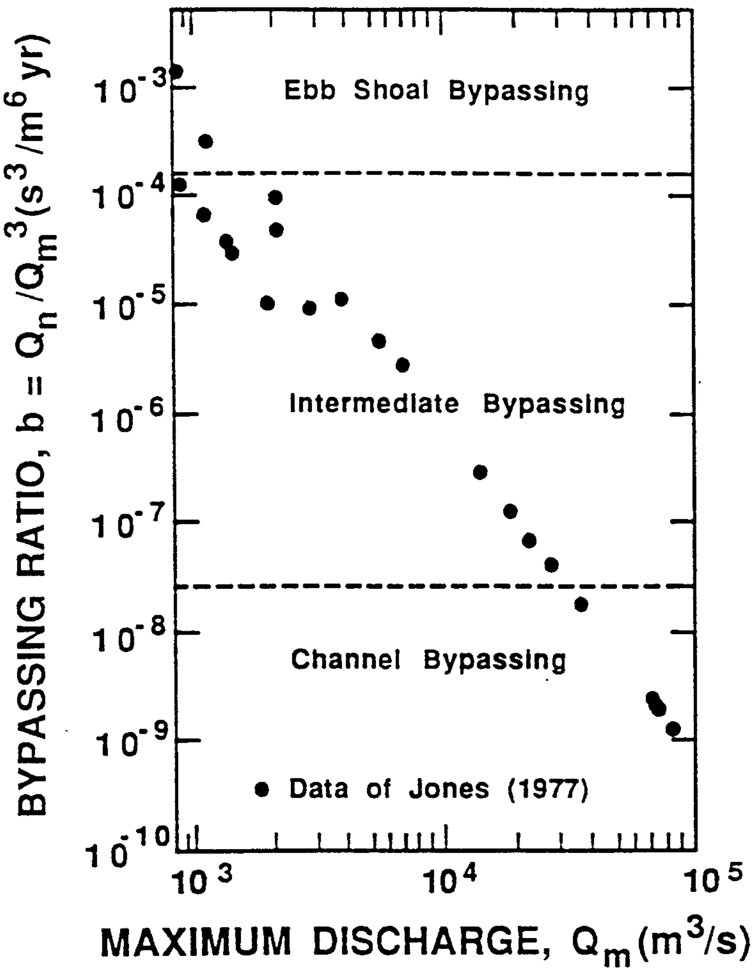

Fig. 4.12c. Plot for Assessing Natural Bypassing Mode from a Relationship between the Bypassing Parameter and the Maximum Discharge.

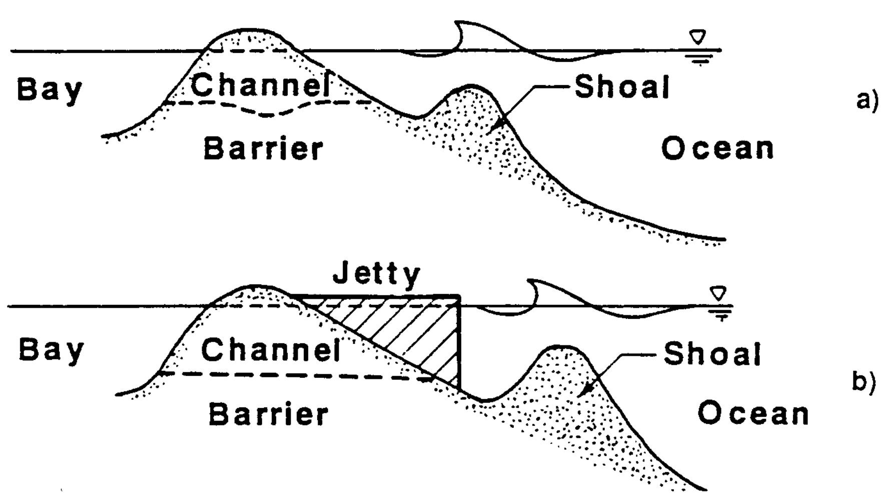

Fig. 4.13. Ebb Shoal Elevation View: a) Natural Inlet, b) Trained Inlet (After Marino and Mehta, 1988).

is the net (annual) rate of littoral drift (algebraic sum of Q_1, Q_2, Q_5 and Q_6). Notice the wide range of b values over which bypassing, defined as intermediate, essentially occurs by both modes.

Under natural conditions, inlets generally differ in character from those modified, as for example in the case of Florida's east coast inlets prior to their modification. These natural entrances and their associated shoals approached long term equilibrium with the sand transport processes under prevailing wave and tide environment. Due to the predominant northeast direction of wave approach, the net longshore transport of sand along the shoreline is from north to south. Typically, as demonstrated by Fineren (1938), the characteristics of these inlets included a broad shallow ebb shoal or ocean bay; perhaps with a channel incised through the bar. Table 4.1 demonstrates that the bar depth was typically 1 to 2 m, much too shallow for navigational purposes. Although the channels through the bar were considerably deeper, most of them were still too shallow for modern commercial purposes. Additional serious navigational disadvantages of these natural channels were their tortuous alignments and migrational tendencies.

When an inlet of natural origin is trained by jetties, the associated sedimentary volumes change until the bottom topography reaches a new configuration, which can be considered to be approximately in equilibrium with the prevalent currents and wave climate (Dean and Walton, 1975). Often, the net accretion in the updrift beach fillet is of the same order of magnitude as the corresponding erosion downdrift. The flood shoal may experience only minor change in shoal volume. The most dramatic effect occurs at the ebb shoal, which typically contains most of the stored material (Marino and Mehta, 1986).

Jetties, possibly coupled with a dredged channel, concentrate the ebb flow and cause the shoal to move seaward into deeper waters (Fig. 4.12b). Furthermore over the long term, a secular rise in relative mean sea level will cause the nearshore waters to become deeper. The contribution to shoal volume, if any, from sea level rise along Florida's east coast cannot be evaluated easily; however, at all the jettied inlets, training is likely to be the dominant factor

Table 4.1: Natural Depths in Channels and on Ebb Shoals of Florida's East Coast Inlets[a]

Inlet	Depth on Bar (m)	Channel Depth (m)
Nassau Sound	1.2	6.4 - 8.2
Fort George	1.2	3.4 - 7.9
St. Augustine	1.8	3.1 - 9.1
Matanzas	Nearly blocked	3.7 - 5.5
Mosquito	Nearly blocked	2.7 - 7.9
Canaveral Bight	1.8 to 5.5	9.1 - 12.2
Indian River	Blocked	2.1 - 2.4
St. Lucie	1.2	2.4 - 3.7
Jupiter	Blocked	0.9 - 1.5
Lake Worth	0.9	0.9 - 2.7
New River	2.4	3.1 - 4.6
Hillsboro	0.8	0.9 - 1.2
Norris Cut	Not affected by sand	Shoal
Bear Cut	1.2	2.1 - 5.2
Cape Florida Channel	Not affected by sand	Coral reefs

[a]Source: Fineren (1938)

Table 4.2: Some Sand Bypassing Systems in Florida[a]

Entrance	Bypassing System
Ponce de Leon	II (I)
Canaveral Harbor	IV
Sebastian	I
Jupiter	I
Lake Worth	III (I)
South Lake Worth	III (I)
Boca Raton	I
Hillsboro	II (I)
Mexico Beach	VI (V)
East Pass	II (I)
Perdido Pass	II (I)

[a]Source: Jones and Mehta (1977)

in causing shoal modification. Given the same tide and offshore wave conditions, the seaward shoal at a trained inlet can store a larger quantity of impounded sediment (Figs. 4.13a,b) than prior to training. Indeed, in many cases, the impounded volume associated with the ebb shoal due to training is the only significant trapped quantity of practical significance (Marino and Mehta, 1986).

Artificial Bypassing

Sediment bypassing systems are oftentimes necessary components in an inlet improvement system for two reasons. First, the ability of a tidal inlet to naturally flush material from its channel may not be adequate to meet navigation requirements. Second, the improvement of a tidal inlet may interfere with the inlet's ability to naturally bypass materials from one side to the other; hence, shoreline erosion is frequently intensified in the vicinity of the inlet, and human interference becomes essential, as for example shown in Fig. 4.3b. As indicated therein, pathways for sediment transport are required to be created, e.g. through hydraulic dredging and transport. Figure 4.14 and Table 4.2 illustrate the locations and types of several sand bypassing systems in Florida. Note that more than one system may be employed at an entrance; the principal method is listed first and the others are enclosed in parentheses. At Canaveral Harbor Entrance a moveable sand bypassing plant designed decades ago has not been built. Perdido Pass, Alabama has been included since it can be physiographically considered to be part of the Florida panhandle. The jet pump system at Mexico Beach Inlet is no longer operational.

The bypassing systems have been divided into six types as follows (Jones and Mehta, 1977):

Type I: Hydraulic dredging from the inlet, navigation channel, shoal areas or sand trap (excluding weir jetty systems).

Type II: Hydraulic dredging in the entrance vicinity from an impoundment basin adjacent to a weir jetty.

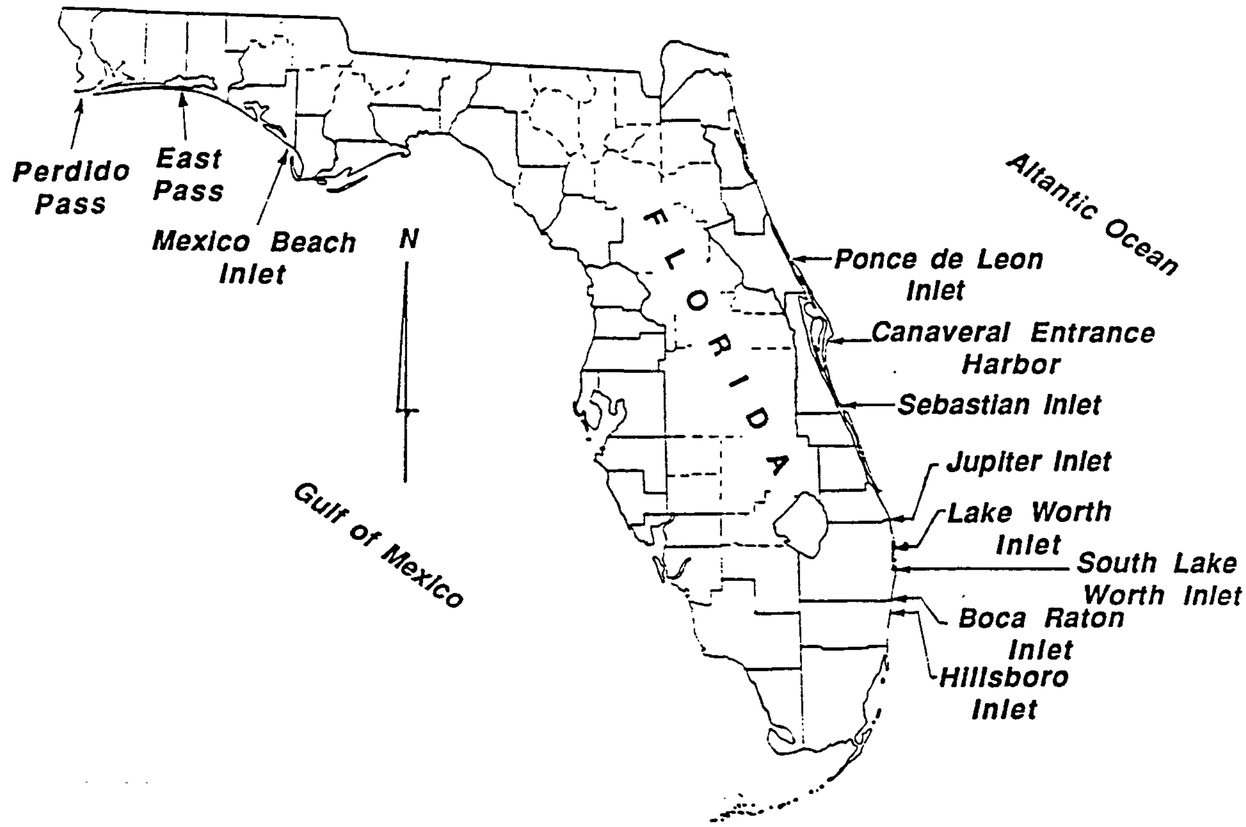

Fig. 4.14. **Locations of Several Sand Transfer Systems in Florida (After Jones and Mehta, 1977).**

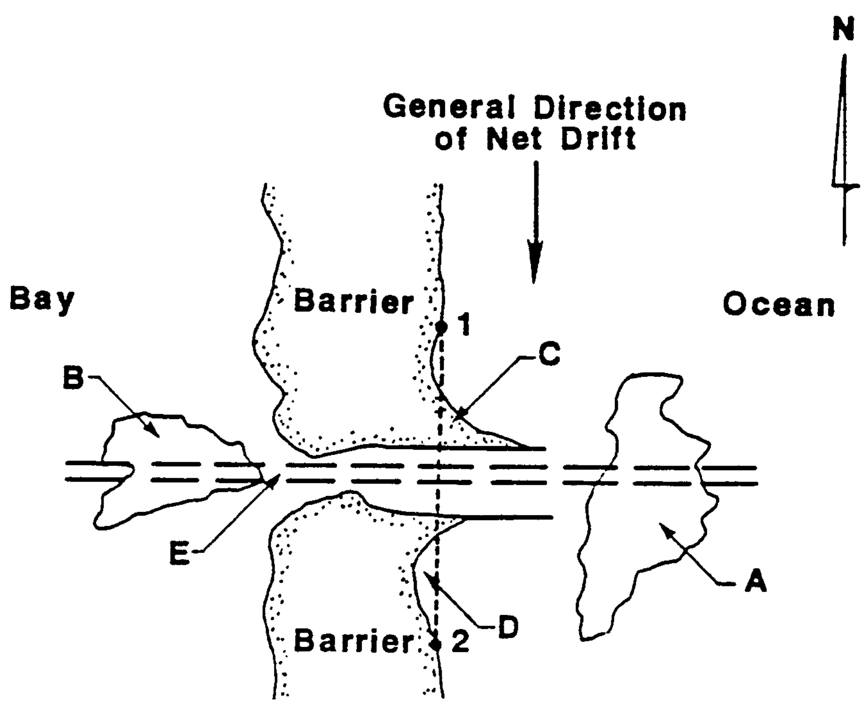

Fig. 4.15. **Sediment Volumes near an Inlet (After Marino and Mehta, 1988).**

Type III: Fixed bypassing plant.

Type IV: Moveable bypassing plant.

Type V: Land-based transfer by dragline, truck, etc.

Type VI: Jet pump system.

The stability of a tidal entrance is generally thought to depend upon the balance between the littoral movement of sediment which tends to close the entrance, and the ability of the entrance to scour the sediment that has been deposited in the channel. If an entrance cannot maintain a stable navigation channel by its own flushing capability, then this must be supplemented by artificial means. However, merely improving an entrance and undertaking an artificial sand bypassing program does not guarantee that navigable depths will always occur through the entrance. Nor is there any guarantee that beach erosion conditions on the downdrift side of the entrance will be measurably improved. These depend upon the stability of the entrance, the manner in which it naturally bypasses materials from the updrift to the downdrift side, the method of artificial transfer, and the geomorphologic characteristics of the entrance. Furthermore, the direction of wave approach during the period when sand deposition on the downdrift beach is carried out is quite important. If this direction is such as to result in an updrift sand transport along the shoreline, then a portion of the bypassed material may be transported into the channel, thus clogging it (Mehta et al., 1990).

Observed entrance stability, based primarily on historic information for tidal entrances shown in Fig. 4.14, is cited in Table 4.3. Also included in this table are descriptions of the natural bypassing tendencies (tidal flow bypassing, intermediate between tidal flow and ebb shoal, and ebb shoal bypassing) of the entrances as determined by the bypassing ratio presented in Fig. 4.12c. At entrances where the numerator predominates, the ebb shoal plays a major role in bypassing material. At entrances where the denominator predominates, tidal flow bypassing occurs. The ebb shoal in this latter case is usually limited in size and volume.

Table 4.3: Florida Inlet Stability and Bypassing Tendency[a]

Entrance	Observed Stability	Bypassing Tendency
Ponce de Leon	Fair	Intermediate
Sebastian	Good	Tidal Flow
Jupiter	Poor	Ebb Shoal
Lake Worth	Fair	Intermediate
South Lake Worth	Poor	Ebb Shoal
Boca Raton	Poor	Ebb Shoal
Hillsboro	Fair	Ebb Shoal
Mexico Beach	Poor	Ebb Shoal
East Pass	Good	Intermediate
Perdido Pass	Fair	Intermediate

[a]Source: Jones and Mehta (1977)

Table 4.4 gives an evaluation of the bypassing effectiveness of each entrance and its associated transfer system, as related to their combined ability, i.e. natural and artificial, to aid in maintaining navigable depths and in retarding downdrift erosion. These estimates are based upon shoreline changes on both sides of the entrance, dredging data, and discussions with individuals having local knowledge of the entrance behavior and shoreline history. As a result, these estimates are essentially subjective, but are believed to fairly representative of actual performance. Unacceptable bypassing effectiveness for prevention of beach erosion at several inlets in Florida has led to strong recommendations for enhancing sand bypassing capabilities at these inlets (Dean and O'Brien, 1987a,b).

SEDIMENT VOLUMES NEAR AN INLET

Figure 4.15 shows the schematic of an inlet through a land barrier. This description applies, for instance, to Florida's east coast inlet down to Government Cut except Nassau Sound and Matanzas, which have no jetties or dredged channel. Significant features are the sea or ebb shoal, A; bay or flood shoal, B; updrift and downdrift beach fillets, C and D; and navigation channel, E. For convenience in describing Florida's east coast inlets, the updrift

Table 4.4: Florida Inlet Bypassing Effectiveness[a]

Entrance	Navigation	Beach Erosion
Ponce de Leon	Fair	Fair
Sebastian	Good	Good
Jupiter	Fair	Fair
Lake Worth	Fair	Fair
South Lake Worth	Fair	Fair - Poor
Boca Raton	Fair	Fair - Poor
Hillsboro	Good	Fair - Poor
Mexico Beach	Poor	Fair
East Pass	Good	Fair
Perdido Pass	Fair	Fair

[a]Source: Jones and Mehta (1977)

Table 4.5: Florida's East Coast Inlets[a]

Inlet	Origin	Training works	Spring tidal range (m)	Wave energy parameter ($m^2 sec^2$)
St. Marys	natural	jetties	2.1	10.9
Nassau Sound	natural	none	1.9	10.9
St. Johns/Ft. George	natural	jetties	1.7	18.3
St. Augustine	opened, 1940[b]	jetties	1.6	18.7
Matanzas	natural	closure[c]	1.5	20.6
Ponce de Leon	natural	jetties	1.3	26.7
Port Canaveral	opened, 1950	jetties	1.2	24.0
Sebastian	opened, 1948	jetties	0.9	28.7
Ft. Pierce	opened, 1921	jetties	0.9	26.5
St. Lucie	opened, 1892	jetties	1.0	29.1
Jupiter	natural	jetties	0.9	27.5
Lake Worth	opened, 1917	jetties	0.8	14.6
South Lake Worth	opened, 1927	jetties	0.8	15.0
Boca Raton	opened, 1925[b]	jetties	0.8	16.0
Hillsboro	natural	jetties	0.8	5.2
Port Everglades	opened, 1926[b]	jetties	0.8	5.2
Bakers Haulover	opened, 1925	jetties	0.8	5.2
Government Cut	opened, 1902	jetties	0.8	3.8

[a]Source: Marino (1988)
[b]Replacing a natural inlet in the vicinity; two near Port Everglades
[c]Storm breakthrough closure inside the bay by a dike

beach may be considered to be north and downdrift beach south of the inlet. Among these features, the flood shoal is typically the most poorly described area at most inlets, because it occurs in confined waters where limited bathymetric information exists. Additionally, the history of dredging or spoil deposition from the internal waterways is not documented well. The beach fillets, which define alongshore distances corresponding to the updrift and downdrift influences (up to points 1 and 2, respectively), of the inlet are difficult to identify unambiguously. The dashed line between points 1 and 2 indicates shoreline position in the absence of the inlet. Point 2 is particularly difficult to locate, with consequent limitation for the accuracy of estimates of downdrift loss of sediment over the selected time interval. At some inlets the ebb shoal distribution varies widely and shoal contours are not defined clearly.

EVOLUTION OF EBB AND FLOOD SHOALS

Prior to evaluating the various volumes associated with an inlet, it is instructive to make reference to the manner in which ebb and flood shoals evolve at a newly cut entrance. Although each situation is obviously unique, the following examples are illustrative of probable trends.

To trace the evolution of an inlet ebb shoal, a time history of the inlet must be studied. St. Augustine Inlet, for example, has a unique history and helps in understanding evolutionary trends as well as difficulties which are typically encountered in precisely determining the shoal volume at any particular point in time.

St. Augustine Inlet was cut 4 km north of an existing inlet in 1941. Figure 4.16 depicts both the previous (1937) and relatively recent (1985) shoreline and shoal contours. Locations I and J represent the areas through which the old, natural inlet meandered prior to the new inlet opening at location K in 1940. The shoal contour lines delineate significant levels of sediment deposition above an "ideal" offshore profile. The ideal profile is defined as the natural offshore profile in that local area, as if the inlet were not present. It can

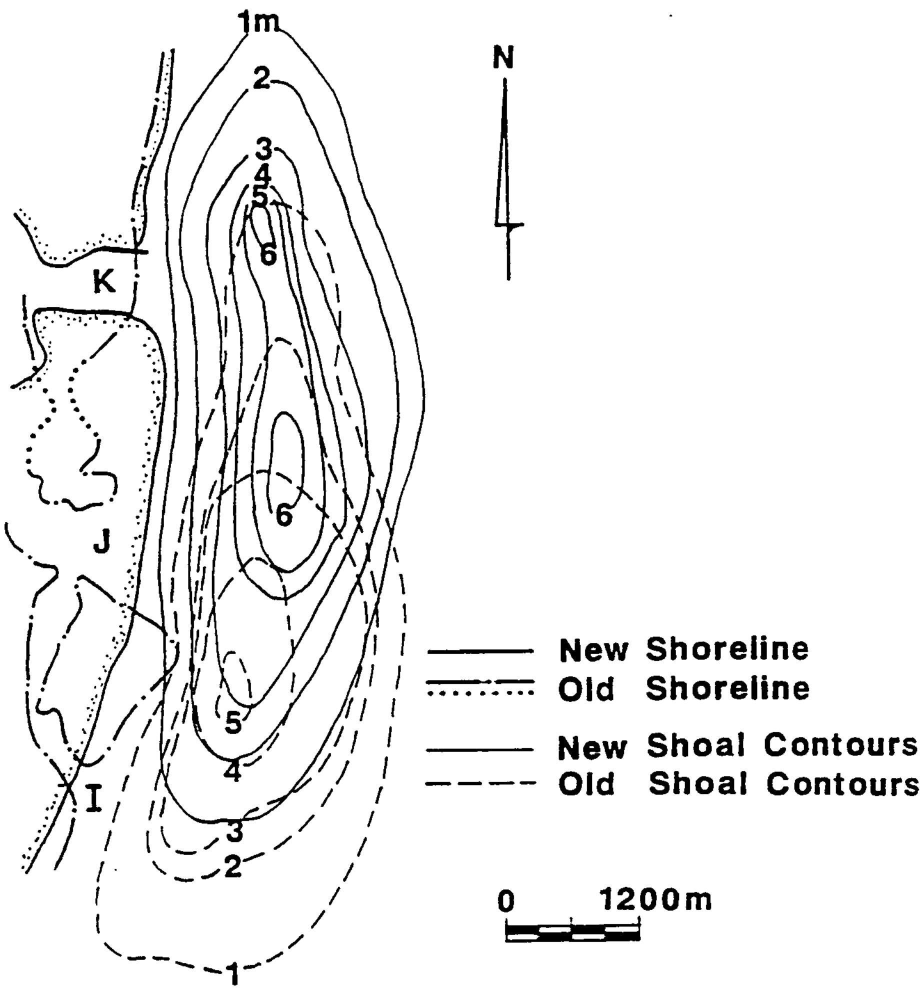

Fig. 4.16. **Ebb Shoal Changes at St. Augustine Inlet, Florida (After Marino and Mehta, 1987).**

be seen that as a result of the opening of a new inlet, the previous ebb shoal was caused to migrate. The old shoal formation moved both westward, to form what is now known as Conch Island, and northward to the new inlet. The old inlet was completely closed by sand deposition by 1957. The elongated shape of the recent shoal is believed to be due to the presence of a predominant longshore current to the south. The narrowest part of the shoal directly east of the inlet is evidence of the dredging done by sidecast dredges in the shoal area since 1940. The large bulge adjacent to the south jetty is a direct result of jetty construction in 1957. The shoreline since construction has moved eastward approximately 750 m adjacent to the jetty. This suggests jetty sand-trapping during seasonal reversals of the littoral drift.

This inlet is a mere example of the manner in which ebb shoals form and how the coastline responds to inlet formation. By constructing jetties of sufficient length to stabilize an inlet, as was done at St. Augustine, the shoals are maintained a significant distance away from the inlet. It may also be noted that dredging seems to have significantly affected the shape of the shoal. Where a channel has been dredged, the shoal is divided into two distinct lobes, rather than one large mass as is the case for example at Boca Raton Inlet, where there is no dredged channel.

Figure 4.17 presents a history of St. Lucie Inlet interior shoaling volumes (Dean and Walton, 1975). As observed this inlet shoaled rapidly in its earlier years and gradually approached a much smaller "equilibrium" shoaling rate as represented by the slope of the right-hand sides of the curves. The two curves represent shoaling over different areas considered as a "bay". The widely differing results are indicative of problems inherent in flood shoal calculations.

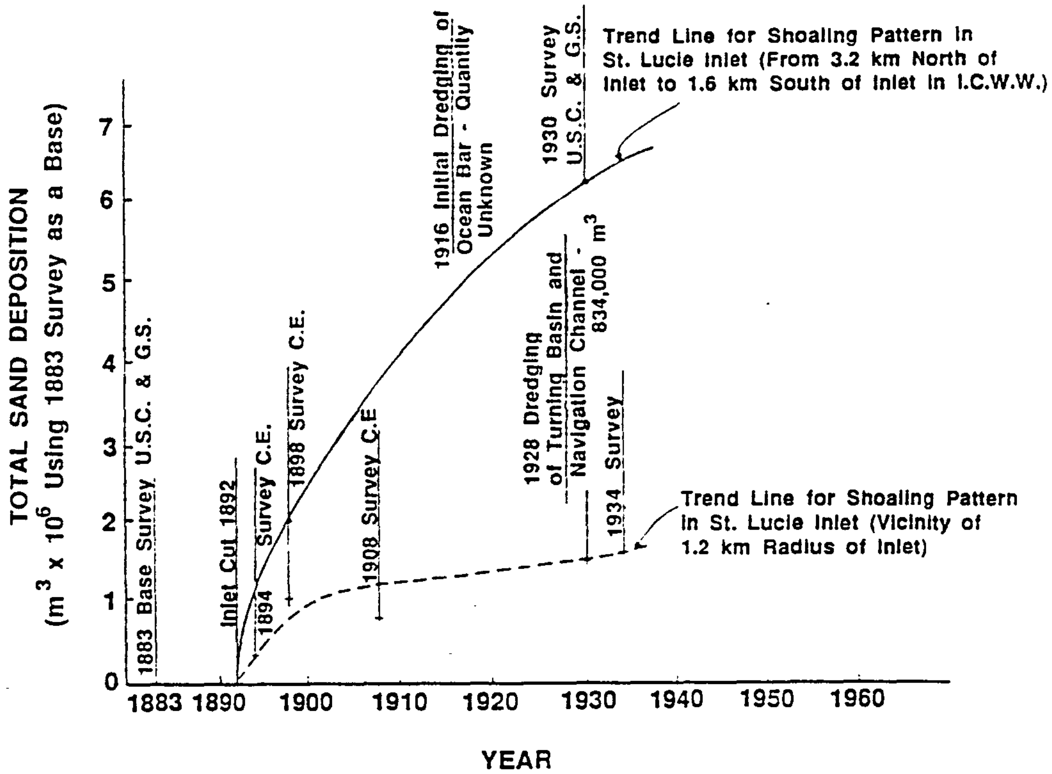

Fig. 4.17. Time-History of Sediment Deposition in the Interior of St. Lucie Inlet (After Dean and Walton, 1975).

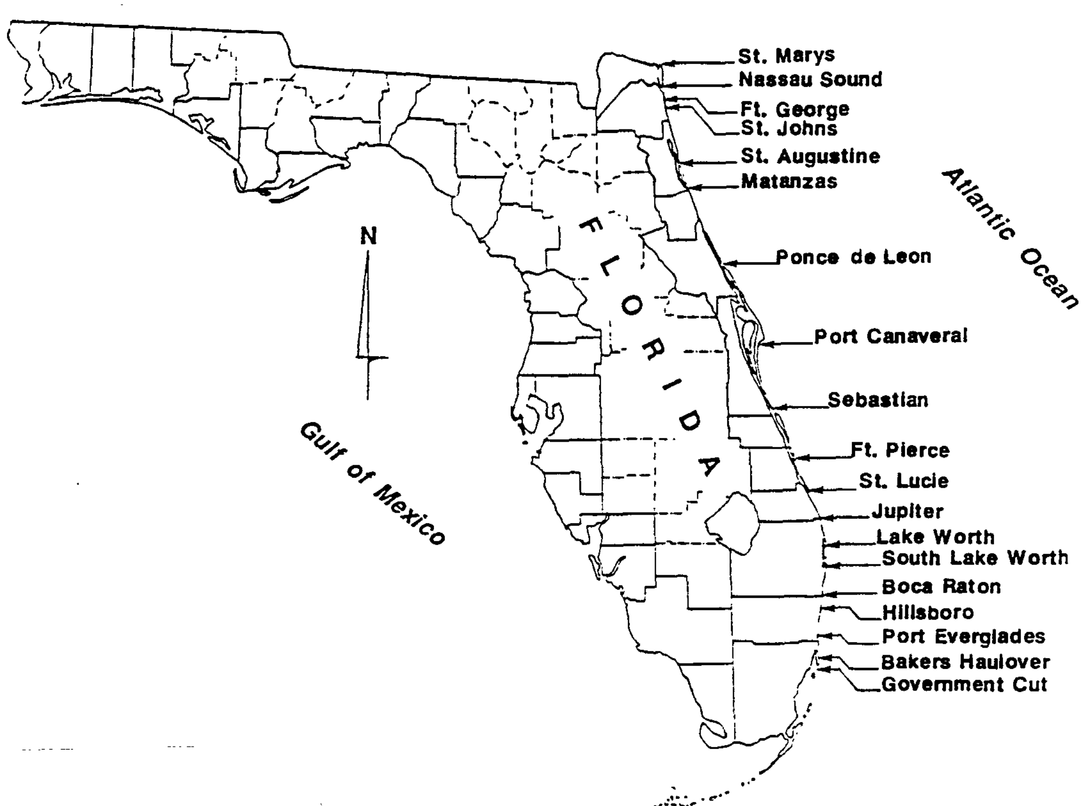

Fig. 4.18. Nineteen Inlets along Florida's East Coast.

SAND TRAPPING

Selected Inlets and Physical Environment

Nineteen inlets along the 580 km shoreline between St. Marys Entrance at the Florida/Georgia border to Government Cut, Miami, are listed in Table 4.5 (see also Fig. 4.18). St. Johns River Entrance and Ft. George Inlet are two separate inlets at proximal locations. Ft. George, a small riverine entrance, occurs immediately north of St. Johns. They are together characterized by a single large ebb shoal and are therefore treated here as a single inlet system. Eleven inlets were opened artificially, although three (St. Augustine, Boca Raton and Port Everglades) have replaced inlets of natural origin in the vicinity. The remainder are known to have existed naturally since the earliest recorded history. All presently have two jetties except Nassau Sound and Matanzas. No training works occur at Nassau Sound. during 1976-77 a portion of the bay at Matanzas was closed by a dike at a location where a storm-induced breakthrough had occurred in 1964. Inlet hydraulics and sediment distribution were influenced measurably by this closure operation (Hayter and Mehta, 1979).

The tidal range and nearshore wave energy are two common descriptors of the coastal physical environment. The semi-diurnal spring tidal range in the area of interest varies from 2.1 to 0.8 m (Table 4.5). A nearshore wave energy characterizing parameter can be defined as the square of the product of the wave height and the period, and the annual average significant wave height and modal period may be selected for this purpose (Marino, 1986). The range of wave energy parameter values are from 29.1 to 3.8 m^2sec^2. Thus both the tidal range and the wave climate exhibit some variability along the coast, although this variability is relatively minor in a global context. For the point of view of tide and waves, Florida's east coast environment has been classified as moderate (Walton and Adams, 1976; Marino, 1986).

The net littoral drift is generally from north to south, although local reversal is suggested at some inlets, due to peculiar wave conditions arising from bathymetry and structures such as jetties. At. St. Marys, the net southward drift is believed to be 420,.000 m^3/yr, while near Government Cut it is on the order of 15,000 m^3/yr (Marino, 1986). While these estimates are admittedly rough, the littoral drift rate in the stretch between St. Marys and Jupiter is considerably larger than that in the stretch between Lake Worth and Government Cut. There is thus a general correlation with wave energy, which is relatively low in southern Florida due to the intervening influence of the Bahama Banks.

Volumetric Calculation

St. Marys, St. Augustine and Lake Worth may be selected as illustrative examples. Sediment volumes have been calculated for each site by routine procedures based primarily on bathymetric information, making allowances for complicated bathymetry or lack of adequate data (Marino and Mehta, 1986). Relevant quantities listed in Table 4.6 are self-explanatory.

Summary of Results

Three noteworthy quantities are given in Table 4.7 for all nineteen inlets. These include the most recent, available (post-training) estimate of the ebb shoal volume, the total material trapped due to training during the approximate period indicated, the corresponding change of volume downdrift and the quantity of sediment disposed at sea. The trapped volume in each case represents the sum of ebb shoal volume change, flood shoal volume change (where computed), updrift beach fillet volume change, and material disposed at sea or placed upland, but not on the beach. A positive number indicates accretion and a negative number implies erosion.

At shorelines where the littoral drift is predominantly unidirectional, the total volume of sediment trapped by the updrift beach fillet, the ebb shoal and the flood shoal must equal the volume of sediment denied downdrift. However, no strong correlation between trapped volume and downdrift volume change is apparent from the data in Table 4.7, although a general (but not uniform) trend of decreasing magnitudes of both quantities from north to south can be discerned. At four inlets – St. Marys, Nassau Sound, St. Augustine and Ponce

Table 4.6: Sediment Volumes at Three Florida Inlets[a]

	St. Marys		St. Augustine		Lake Worth	
	Quantity ($\times 10^{-6} m^3$)	Period (yr)	Quantity ($\times 10^{-6} m^3$)	Period (yr)	Quantity ($\times 10^{-6} m^3$)	Period (yr)
Ebb shoal	89.2	1870	59.4[b]	1924	0.0[c]	1917
	95.1	1974	83.3	1979	2.9	1967
Updrift	-1.3	1870-1975	1.1	1937-1970	4.8	1883-1957
Downdrift	8.8	1857-1957	5.5	1924-1976	-0.7	1883-1957
Flood Shoal	–[d]	–	0.0	1940	0.0	1917
	–[d]	–	0.5	1970	–[d]	–
Deposit-sea	9.4	1903-1985	0.0	–	2.1	1929-1985
-beach	0.3	1982	1.2	1940-1976	0.5[e]	1929-1985
-inland	0.0	–	0.0	–	0.9	1970-1985

[a]Source: Marino and Mehta (1988)
[b]Old inlet
[c]Inlet opened in 1917
[d]Not calculated; believed to be small compared to ebb shoal
[e]Excluding 1.1 x $10^6 m^3$ bypassed from updrift to downdrift beach, 1968-1986

Table 4.7: Florida Inlet Sediment Volumes[a]

Inlet	Ebb Shoal ($\times 10^{-6} m^3$)	Material trapped Volume ($\times 10^{-6} m^3$)	Material trapped Period (yr)	Downdrift Vol. change ($\times 10^{-6} m^3$)	Disposed Vol. at sea ($\times 10^{-6} m^3$)
St. Marys	95.1	14.0	1857-1979	8.8	9.4
Nassau Sound	40.5	6.3	1871-1970	3.2	0.0
St. Johns/Ft. George	131.3	120.9	1874-1978	-23.4	15.7
St. Augustine	83.3	25.6	1924-1979	5.5	0.0
Matanzas	4.8	5.4	1963-1978	-0.2	0.0
Ponce de Leon	17.0	0.7	1925-1974	1.7	0.0
Port Canaveral	4.3	13.8	1953-1985	-0.8	7.5[b]
Sebastian	0.1	3.2	1924-1976	-0.2	1.4
Ft. Pierce	22.2	66.3	1882-1983	-35.9	2.0
St. Lucie	16.4	20.3	1888-1984	-34.7	0.0
Jupiter	0.3	-3.0	1883-1978	-2.4	0.0
Lake Worth	2.9	4.3	1883-1985	-0.7	2.1
South Lake Worth	1.1	1.5	1927-1979	-0.4	0.0
Boca Raton	0.8	1.3	1920-1981	$\sim$ 0.0	0.0
Hillsboro	-0.2[c]	-1.7	1883-1967	-0.5	0.5
Port Everglades	$\sim$ 0.0	6.0	1927-1981	-0.5	2.1
Bakers Haulover	0.5	0.3	1919-1969	-0.5	0.2
Government Cut	$\sim$ 0.0	3.5	1867-1978	$\sim$ 0.0	0.0

[a]Source: Marino and Mehta (1988)
[b]Excluding 15.9 x $10^6 m^3$ dredged during harbor construction and disposed at sea
[c]Negative sign is indicative of a scour hole at the site

de Leon – downdrift beach fillet volume showed an apparent increase. Notwithstanding the likelihood of the effect of local reversals in the direction of littoral drift at these sites, it must be noted that the downdrift volumetric changes calculated are very approximate. Considerably lower confidence can be placed in these values than in the estimates of material trapped.

Over the indicated 99-year period, Nassau Sound trapped 6.3 x $10^6 m^3$, despite the fact that no modifications have been made at this large entrance. An approximately 0.3 m relative mean sea level rise which has occurred during this period is a possible cause. Furthermore, modifications carried out at St. Marys are believed to have influenced sand distribution at Nassau Sound. At Jupiter and Hillsboro, there was actually a post-training loss of sediment, although in both cases the volume lost was small in comparison with the gains at inlets between St. Marys and St. Lucie, with the exceptions of Ponce de Leon and Sebastian.

At four inlets – St. Marys, St. Johns/Ft. George and Port Canaveral – sizeable quantities of sediment have been disposed at sea over decades. The type and quality of the disposed sediment have not been investigated, hence no conclusion can be drawn regarding the potential suitability of this sediment for such uses as beach replenishment. It is significant, however, that a total of 40.9 x $10^6 m^3$ have been disposed offshore. This number does not include, for example, an additional 15.9 x $10^6 m^3$ which also were deposited offshore during the construction of Port Canaveral harbor. It is not known how much of this material was derived from upland dredging.

EBB SHOALS

Florida Inlets

Ebb shoals at eight out of the nineteen inlets contain a total of 405.8 x $10^6 m^3$ of sediment (Table 4.7). These eight inlets – St. Marys, Nassau Sound, St. Johns/Ft. George, St. Augustine, Ponce de Leon, Ft. Pierce and St. Lucie – thus contain nearly 97% of the ebb shoal sediment. Out of these, the five northernmost inlets – St. Marys, Nassau Sound, St. Johns/Ft. George and St. Augustine – store 350.2 x $10^6 m^3$, or 83% of the total sediment. Clearly, most of the stored sediment is found in northern Florida, with relatively small contributions from the south. Below St. Lucie there is practically negligible storage of sediment in the ebb shoals.

The observed variability in the ebb shoal volume, ranging from as high as 131.3 x $10^6 m^3$ at St. Johns/Ft. George to almost zero at Port Everglades and Government Cut, is indicative of the influences of a wide variety of physical factors that determine ebb shoal configuration and volume. Prominent among these factors are tidal range, wave climate and littoral drift, offshore bathymetry, type of sediment, inlet and bay geometries and runoff. For the east coast of Florida, tidal range, wave climate and littoral drift, and inlet and bay geometries are more important. At least in some cases however, an overriding influential factor, one would suspect, is the holocene processes which have led to nearshore sand deposition ultimately from riverine sources (Oertel, 1988). Quite simply, sand seems to be available at shorelines where it was deposited in the first place.

Georgia Inlets

The inlets of Georgia are of particular interest since they are contiguous to those of Florida's east coast inlets, and because their ebb shoals store significant quantities of sand. In Table 4.8 nine major inlets are listed including representative spring tidal range at each inlet, the corresponding wave energy parameter, and ebb shoal volume. The tidal range places this shoreline in the mesotidal regime, as opposed to Florida's east coast which, with the exception of St. Marys area, is microtidal (Table 4.5). On the other hand, the wave energy parameter values suggest wave action similar to that along the northern part of Florida's east coast (Table 4.5), which is moderate. Overall, therefore, these nine Georgia inlets are much more tide dominated than for example Sebastian through Boca Raton.

The ebb shoal volumes, ranging from 15.1 x $10^6 m^3$ to 191.0 x $10^6 m^3$, are quite large, and with the exception of St. Catherines Sound are comparable to northern Florida inlets

Table 4.8: Georgia Inlet Ebb Shoal Volumes[a]

Inlet	Spring tidal range (m)	Wave[b] energy parameter $(m^2 sec^2)$	Ebb shoal volume (x $10^{-6} m^3$)
Nassau Sound	2.5	13.7	86.6
Ossabaw Sound	2.6	17.1	51.3
St. Catherines Sound	2.5	13.3	15.1
Sapelo Sound	2.5	15.6	165.8
Duboy Sound	2.4	14.2	33.0
Altamaha Sound	2.3	14.2	66.7
Hampton River	2.4	14.2	33.2
St. Simons Sound	2.3	12.5	185.6
St. Andrew Sound	2.3	9.5	191.0

[a]Data generated by Millard Dowd, University of Florida.
[b]Energy parameter values derived from Jensen (1983).

Table 4.9: Influence of Inlet Aspect Ratio on Ebb Shoal Volume[a]

Inlet	Spring tidal prism (m^3)	Wave energy parameter $(m^2 sec^2)$	Throat area (m^2)	Width/ depth	Ebb shoal volume (m^3)
Matanzas	1.42 x 10^7	20.6	910	123	4.8 x 10^6
Ponce de Leon	1.63 x 10^7	26.7	1,170	75	1.7 x 10^7
Ft. Pierce	1.73 x 10^7	26.5	980	64	2.2 x 10^7

[a]Source: Marino and Mehta (1987)

between St. Marys and St. Augustine. The sum of these volumes, 828.3 x $10^6 m^3$, is double that stored in Florida east coast ebb shoals. The two southernmost inlets, St. Simons Sound and St. Andrew Sound, together account for 376.5 x $10^6 m^3$ or 45% of the total.

Ebb Shoal and Nearshore Environment

Following the opening of a new inlet or the training of a natural inlet, the rate of growth of the ebb shoal is contingent mainly upon the rate of supply of sediment from the littoral drift. The larger the drift, the faster the rate at which the ebb shoal will develop to its new equilibrium size (Dean and Walton, 1975). It may therefore be argued that, for example, northern Florida inlets have nearly attained equilibrium, while the southern inlets have not, given the significantly lower drift in the south compared to the north. In other words, as mentioned previously the availability of sediment can be a factor influencing variations in the ebb shoal size as well as the volume of material trapped. It is however noteworthy that, as noted in the case of St. Lucie Inlet (Fig. 4.17), when a new inlet is dredged or a natural inlet trained, sediment trapping usually occurs rapidly initially, followed by a much slower rate of entrapment. It is believed that most of the nineteen Florida inlets considered have passed the stage of rapid entrapment, that they are approaching equilibrium sedimentary distributions at a slow rate, and that, in most cases, the quantities (ebb shoal volume and material trapped) in Table 4.7 are close to those at equilibrium.

This hypothesis, i.e. that inlet sediment distribution is in equilibrium with the governing forces due to tides and waves, would imply that variability in littoral drift may not correlate measurably with variability in ebb shoal volumes. Without evaluating this hypothesis further, however, it is worthwhile noting some observations by assuming that one is dealing with ebb shoals of equilibrium size.

The assumption of equilibrium ebb shoal size was used by Walton and Adams (1976) to empirically relate the ebb shoal volume to the spring tidal prism, considering the prism to be the characteristic parameter representing inlet hydraulics, encompassing the effects of tidal range and inlet-bay geometry. By further assuming the variability in wave energy to be relatively small, all Florida east coast inlets were treated as being influenced by a similar wave climate. The result was a power law expression indicting the ebb shoal volume, V, to be proportional to prism, P, raised to the power 1.3, approximately. In Fig. 4.19 this relationship is plotted together with a similar, but reassessed, relationship proposed by Marino (1986). As observed there is significant data scatter about the mean trend. Such a scatter suggests that the ebb shoal volume may not be related uniquely to prism, and that the influence of additional parameters must be considered. One possible candidate is the inlet width-to-depth aspect ratio. The influence of this parameter is suggested by the data presented in Table 4.9. Three Florida inlets, Matanzas, Ponce de Leon and Ft. Pierce, are characterized by similar values of the prism, the wave energy parameter and the channel throat or minimum flow area. There is only a slight increase in prism from Matanzas to Ponce de Leon, but a significant decrease in the aspect ratio. The data thus suggest a stronger correlation between increasing ebb shoal volume and decreasing aspect ratio, than with increasing prism.

Notwithstanding the fact that the Matanzas channel is untrained while both Ponce de Leon and Ft. Pierce have jetties and dredged channels, it may be inferred from Table 4.9 that given the same tidal prism, wave energy and inlet throat area, a wide and shallow inlet will have a smaller ebb shoal than a narrower and deeper inlet. Although depth at the channel throat is by no means uniquely related to the natural, shoal-free depths as might occur in the ebb shoal region, it seems possible to associate a shallow throat with shallow offshore depths and a deep throat with deeper waters offshore. In the ebb shoal region, currents are relatively weak compared with those in the channel, and the prevailing bed shear stress is predominantly due to waves. The minimum flow depth over the ebb shoal is therefore determined mainly by waves (Mehta and Joshi, 1988). Any excess material that may deposit over the shoal will be carried shoreward by wave action (Walton and Adams, 1976). Consequently, all other conditions being equal, the thickness of stored ebb shoal sediment will be greater at an inlet with a small aspect ratio than at one with a larger

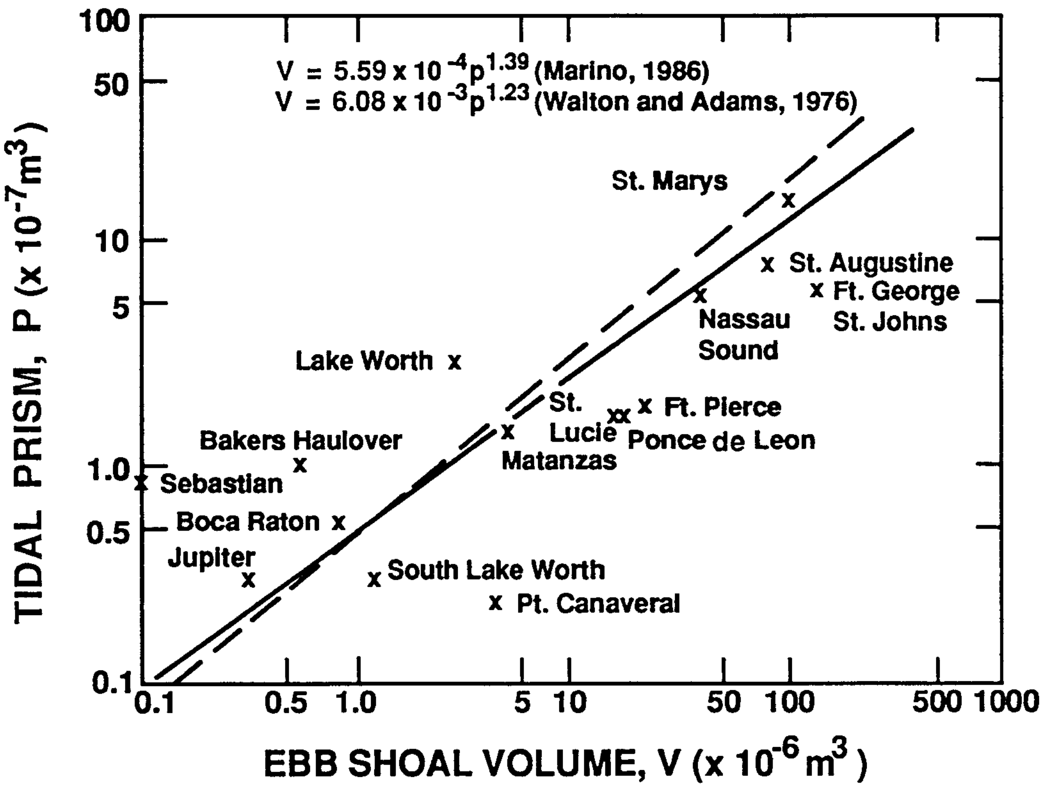

Fig. 4.19. **Tidal Prism - Ebb Shoal Volume Relationship for Florida's East Coast Inlets (After Marino, 1986)**

ratio. The inlets of Table 4.9, where the sediment size is similar ($\sim$ 0.2-0.4 mm), appear to illustrate this process, although this concept requires further consideration including the role of geomorphologic factors.

The role of bed shear stress in reference to the relationship between the inlet aspect ratio and ebb shoal volume may be formalized via an illustrative example. The critical shear stress is that value of the bed shear stress that is exerted at the point of incipient sand grain motion. When the actual bed shear stress exceeds the critical shear stress, bed material is put into motion.

Jonsson (1966) noted that the wave friction factor, f_w, is in general significantly larger than the current friction factor, f_c. The constitutive expressions representing the shear stress due current, τ_c, and waves, τ_w, respectively are

$$\tau_c = 0.5\rho f_c u_c^2 \tag{4.3}$$

and

$$\tau_w = 0.5\rho f_w u_w^2 \tag{4.4}$$

where ρ is the density of seawater, u_c is the depth-mean flow velocity due to current and u_w is the near-bed velocity amplitude due to waves.

For the issue at hand, it is sufficient to consider two inlets of the same cross section, but having different width over depth aspect ratio, W/D. Let inlet 1 be 3 m deep by 400 m wide, and inlet 2 be 6 m deep by 200 m wide. Thus both inlets have a cross-sectional area of 1,200 m^2, but the corresponding aspect ratios are 133 and 33, respectively. It can be shown that the maximum ebb velocity through both the inlets will be the same because the flow areas, and therefore the tidal prisms, are equal (O'Brien, 1969). Let us assume that the velocity, u_c over the ebb shoal is as well the same in both cases, in spite of the differences in the flow depth over the bar. Let u_c be 0.3 m/sec, a representative value. Select further, a representative wave height of 1 m and a wave period of 7 sec applicable to ebb shoals at both inlets. For current, a typical value of 4.1x10^{-3} may be selected for f_c.

The f_w values can be estimated to be 8.0x10^{-3} and 9.0x10^{-3} for inlets 1 and 2, respectively (Marino, 1986).

The current shear stress, τ_c, and wave shear stress, τ_w, for the two inlets are given in Table 4.10. It is observed that in the case of both inlets, the wave shear stress is dominant. Hence the precise selection of the magnitude of u_c for the inlets is not a matter of critical importance, so long as reasonable values are selected. Since the wave shear stress is twice as much in the shallower inlet, it follows that the critical shear stress will be exceeded there more often than in the deeper inlet. As the sand is put into motion, it is moved by the longshore current and the wave forces back towards the shore. This movement of sand, therefore, occurs more significantly in shallower inlets than in deeper inlets, allowing the shoals of deeper inlets to grow to greater volumes than those of shallow inlets. This reasoning is in agreement with the conclusion of Walton and Adams (1976), who state that more material is stored in the shoals of low wave energy coasts than high wave energy coasts. This is because there is more energy available to drive the sand back to shore in high energy environment after being deposited as a shoal.

Table 4.10: Bottom Shear Stresses for Inlets 1 and 2

Inlet	W (m)	D (m)	τ_c (N/m^2)	τ_w (N/m^2)
1	400	3	0.18	3.23
2	200	6	0.18	1.62

ROLE OF JETTY STRUCTURES

Inlets serving for navigation are often trained by jetty structures. Depending upon the main littoral drift direction jetties can be separated as updrift branches and downdrift branches. The main function of the updrift jetties is to prevent updrift sediment from entering the inlet and to shelter the navigation channel from severe weather. They are usually more substantial and, sometimes, curved to increase the sheltering effect. For a newly constructed jetty, littoral drift will start to accumulate on the updrift end of the jetty and as updrift shoreline advances the sediment will be diverted into deeper water. Since the updrift jetty extends into deeper water, the tidal current near the jetty entrance is also weakened. Shoals are often formed in the vicinity of the entrance. The combined tidal and wave energy will then reshape the shoals to form an integrated ebb tidal shoal. Ususally, the ebb tidal shoal is skewed to the downdrift direction and the longer the updrift jetty the more substantial the shoal volume. In the mean time, the downdrift shore will be deprived from the normal sand supply. As the ebb tidal shoal gradually matures sediment will eventually be bypassed to the downdrift shoreline. In theory, the sediment budget will eventually reach a steady state and an equilibrium ebb tidal shoal will be formed. However, storms will disturb the equilibrium by moving substantial quantity of sand into the entrance and on the same time significantly increases the bypassing quantity. While waves break over the ebbtidal shoal they induce strong nearshore current and higher water level in the shadow of the ebb tidal shoal. This condition is illustrated in Fig.4.20.

The down drift jetties traditionally received much less attention in engineering design. Along Florida coast many of them were designed much shorter than the updrift jetties and were configured to conform with the updrift jetties so as not to introduce adversed effects in navigation. However, from the beach nourishment point of view, the downdrift jetty plays a very important role. First of all, as discussed earlier, a nourished beach will spread sediment to both ends, i.e., both updrift and downdrift, irrespective to the littoral drift direction. Therefore, if a nourishment project is carried out on the downdrift side of a inlet, too short a downdrift jetty means greater loss. This loss is further compounded by the strong nearshore current directing towards the inlet during both flood and ebb tidal cycles. These nearshore circulation conditions together with the associated sediment transport patterns are illustrated in Fig. 4.21 for the Sebastian Inlet.

REFERENCES

Bruun, P. (1966). *Tidal Inlets and Littoral Drift*, University Book, Oslo, Norway.

Brunn, P., and Garritsen, F., 1960. Stability of Coastal Inlets. North Holland Publ.Co., (ELSEVIER), Amsterdam, 123 pp.

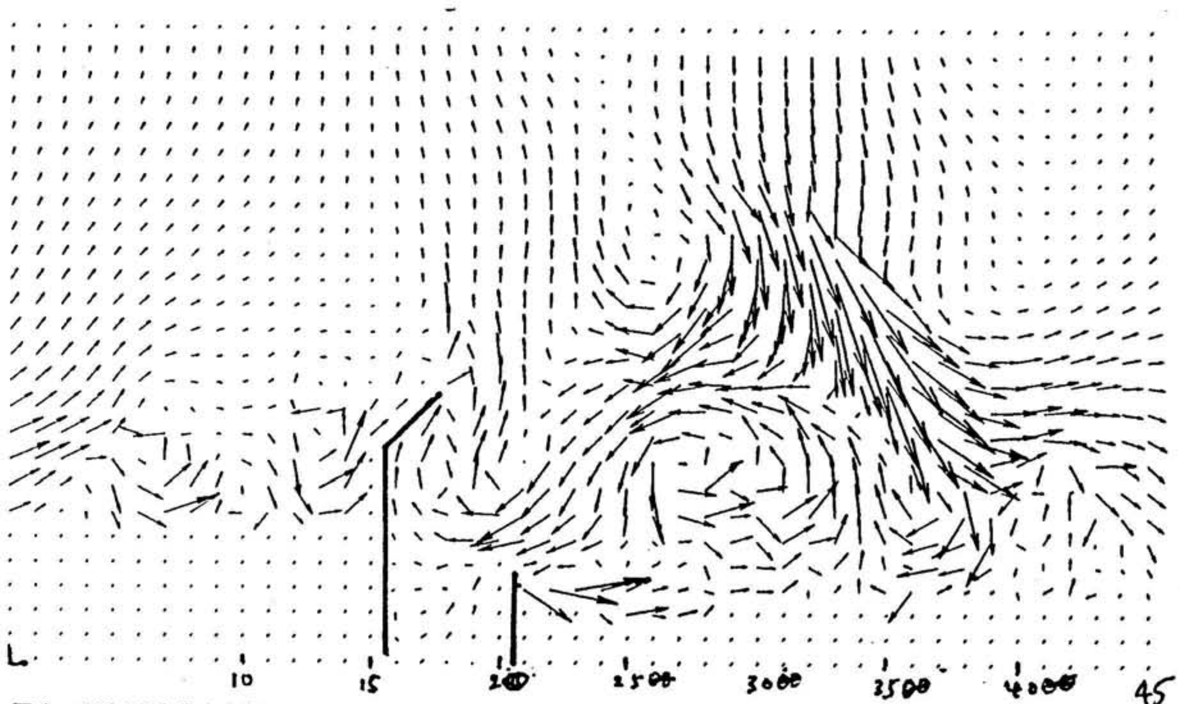

FØR PLØTTING: X,Y,U,V,ETA(BAR) DATA:

Grid size: 100ft x 100ft.

Fig. 4.20. Current vectors under storm condition at slick tide H = 2 m. $\theta = 10^{\circ}$ from North. T = 6 sec. Notice strong transport potential on ebb tidal shoal, causing by-passing and channel shoaling.

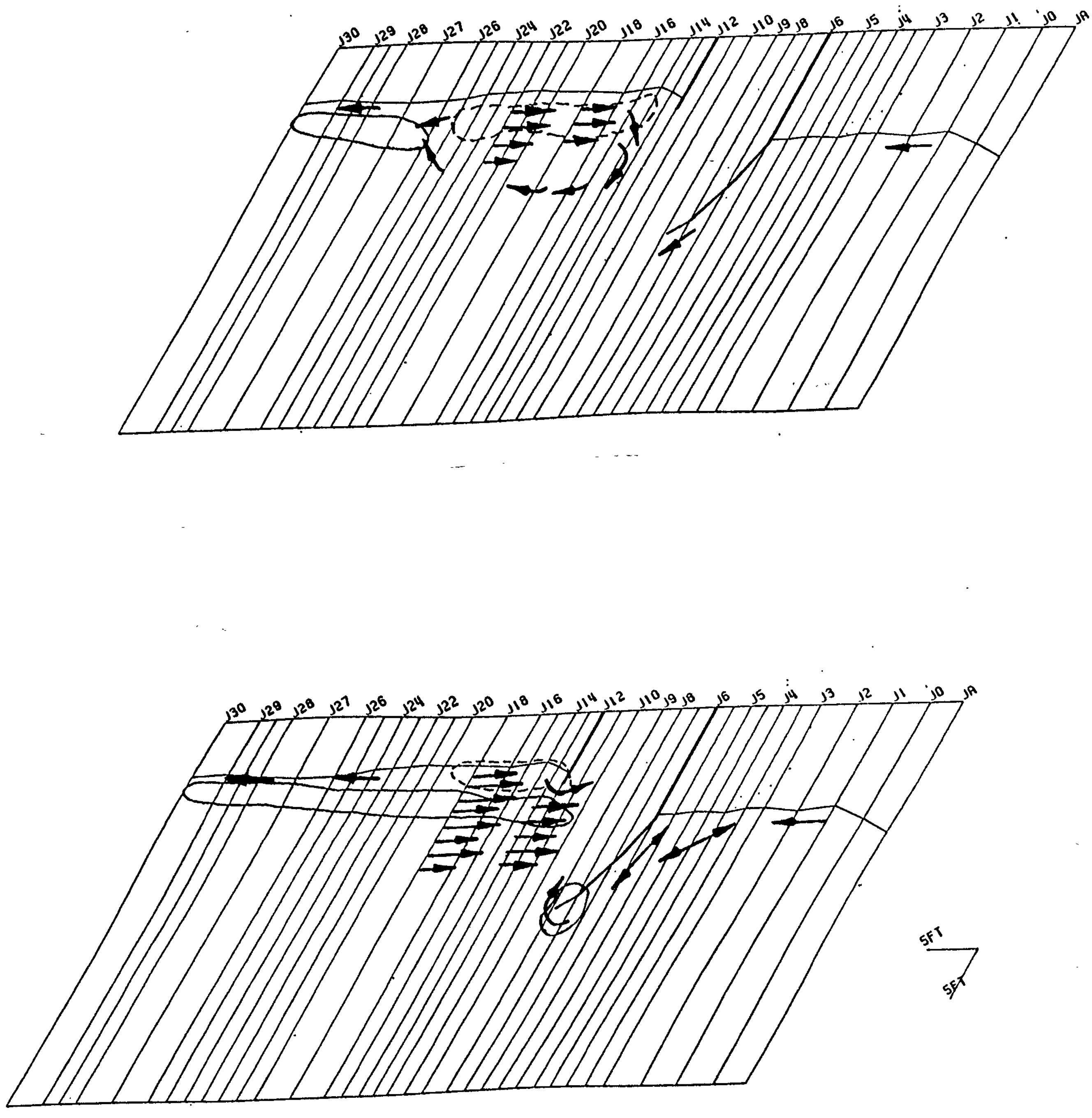

Fig. 4.21. Region of accretion and erosion with patterns of sediment motion and the effects of downdrift jetty.

Bruun, P., Mehta, A.J. and Jonsson, I.G. (1978). *Stability of Tidal Inlets: Theory and Engineering*, Elsevier, Amsterdam.

Bryne, R.J., and DeAlteris, J.T. and Bullock, P.A. (1974). Channel stability in tidal inlets: a case study. *Proc. 14th Coastal Engineering Conf.*, ASCE, Copenhagen, Denmark, 1585-1604. (1974).

Buckingham, W.T. (1984). Coastal engineering investigation at Jupiter Inlet, Florida. *UFL/COEL-84/004*, Coastal and Ocean. Eng. Dept., Univ. of Fla. Gainesville.

Dean, R.G. (1987). Additional sediment input to the nearshore region. *Shore and Beach*, 55(3-4), 76-81.

Dean, R.G. and Walton, T.L. (1975). Sediment transport processes in the vicinity of inlets with special reference to sand trapping. *Estuarine Research*, L.E. Cronin ed., Vol. II, Academic Press, New York, 129-149.

Dean, R.G. and O'Brien, M.P. (1987a). Florida's east coast inlets - shoreline effects and recommended action. *UFL/COEL- 87/017*, Coastal and Ocean. Engr. Dept., Univ. of Fla., Gainesville.

Dean, R.G. and O'Brien, M.P. (1987b). Florida's west coast inlets - shoreline effects and recommended action. *UFL/COEL- 87/018*, Coastal and Ocean. Engr. Dept., Univ. of Fla., Gainesville.

Escoffier, F.F., 1940. The Stability of Tidal Inlets, Shore and beach, Vol. 8, No.4.

Fineren, W.W. (1938). Early attempts at inlet construction on the Florida east coast. *Shore and Beach*, 6(3), 89-91.

FitzGerald, D.M., Nummedal, D. and Kana, T.W. (1976). Sand circulation pattern at Price Inlet, South Carolina. *Proc. 15th Coastal Engineering Conf.*, ASCE, Honolulu, 1868-1880.

Hayter, E.J. and Mehta, A.J. (1979). Verification of changes in flow regime due to dike breakthrough closure. *Proc. Coastal Structures, 79*, ASCE, Alexandria, Virginia, 729-746.

Jensen, R.E. (1983). Atlantic coast hindcast, shallow-water, significant wave information. *WES Wave Information Studies No. 9*, U.S. Army Engineer Waterways Experiment Station, Vicksburg, Mississippi.

Jones, C.P. (1977). An evaluation of sand bypassing systems at tidal inlets in Florida. *M.S. thesis*, Univ. of Fla., Gainesville.

Jones, C.P. and Mehta, A.J. (1977). A comparative review of sand transfer systems at Florida's tidal entrances. *Proc. Coastal Sediments '77*, ASCE, Charleston, South Carolina, 48-66.

Jones, C.P. and Mehta, A.J. (1978). Ponce de Leon inlet, Glossary of Inlets Report No. 6. *Rept. No. 23*, Florida Sea Grant Program, Gainesville.

Jonsson, I.G. (1966). Wave boundary layers and friction factors. *Proc. 10th Conf. on Coast. Engr.*, ASCE, Vol. 1, Tokyo, Japan, 127-148.

Keulegan, G,H. (1967). Tidal Flow in Entrances: Water Level Fluctuations of Basins in Communication with Seas. TB.14, Committee on Tidal hydraulics, U.S. Army Corps of Engineers.

Marino, J.N. (1986). Inlet ebb shoal volumes related to coastal physical parameters. *UFL/COEL-86-017*, Coast. and Ocean. Engr. Dept., Univ. of Fla., Gainesville.

Marino, J.N. and Mehta, A.J. (1986). Sediment volumes around Florida's east coast tidal inlets. *UFL/COEL-86-009* Coast. and Ocean. Engr. Dept., Univ. of Fla., Gainesville.

Marino, J.N. and Mehta, A.J. (1987). Inlet ebb shoals related to coastal parameters. *Proc. Coastal Sediments '87*, Vol. II, ASCE, New Orleans, Louisiana, 1608-1623.

Marino, J.N. and Mehta, A.J. (1988). Sediment trapping at Florida's east coast inlets. In: *Hydrodynamics and Sediment Dynamics of Tidal Inlets*, D.G. Aubrey and L. Weisher (eds), Springer-Verlag, New York, 284-296.

Mehta, A.J. and Joshi, P.B. (1988). Tidal Inlet Hydraulics. *Journal of Hydraulic Engineering*, 114(11), 1321-1338.

Mehta, A.J., Montague, C.L. and Parchure, T.M. (1990). Tidal inlet management at Jupiter Inlet, Florida. First Progress Report *UFL/COEL-90/005*, Coast. and Ocean. Engr. Dept., Univ. of Fla., Gainesville.

O'Brien, M.P. (1969). Equlibrium flow areas of inlets on sandy coasts. *Journal of Waterways and Harbors Division*, ASCE, 95(WW1), 43-52.

Oertel, G.F. (1988). Processes of sediment exchange between tidal inlets, ebb deltas and barrier islands. In: *Hydrodynamics and Sediment Dynamics of Tidal Inlets*, D.G. Aubrey and L. Weisher (eds), Springer-Verlag, New York, 297-318.

Olsen, E.J. (1979). Engineering report for the South Seas Plantation beach improvement project. *Contract No. 3287 Report*, Tetra Tech, Jacksonville, Florida.

Walton, T.L. and Adams, Wm.D. (1976). Capacity of inlet outer bars to store sand. *Proc. 15th Coast. Engr. Conf.*, ASCE, Vol. 2, Honolulu, Hawaii, 1919-1937.

Winton, T.C. and Mehta, A.J. (1981). Dynamic model for closure of small inlets due to storm-induced littoral drift. *Proc. XIX Congress of IAHR*, Subject B(c), paper 2, New Delhi, India, 154- 159.

Chapter 5

THE BEACH RESTORATION PROCESS IN FLORIDA

Thomas J. Campbell, P.E.
Coastal Planning & Engineering, Inc.

COURSE OUTLINE

5.1 INTRODUCTION

- Design process is an iterative process balancing design, permitting and funding constraints into a final design.
- The primary objective is to rebuild an eroded beach and to maintain the beach.
- The final design is a composite of coastal engineering findings, environmental considerations and economic and funding constraints.

DESIGN

Sand Source:

Where to look

- Directly offshore – cheapest methods, seismic, probes, vibracores
- Ebb tidal shoals – high quality
- Inland sources – Ortona
- Foreign sands – Bahama Aragonite

How to compare sands:

- Overfill ratios – formula
- Renourishment ratios – formula
- Equilibrium slopes
- Storm erosion
- Long term erosion

<u>**Silt & Clay:**</u>

- Percent of silt/clay determines how clean the project will be; 29 NTU's is the State standard.
- Less that 10% on cutterhead dredges – probably no damage offshore hard bottom.
- Over 3% – nearshore turbidity during project is extensive.
- Over 5% – residual silt/clay pockets nearshore after project – stirred up during storm.
- Over 1/2% nearshore turbidity exceeds state standards with 2' waves.

<u>**Rock in Fill:**</u>

- Suspended rock in fill can cause problems for bathers – not desirable for recreation beaches/storm protection?
- Can be detected in cores, seismic and probes – % found is usually an underestimate because rocks are pushed out of the way by vibracores.
- Can be removed before placement; hopper dredges or graders.
- Best to avoid rubbly sections if possible.
- Don't allow dredging below known material – watch dredger – monitor dredge depth.

Beach Design:

Initial Fill:

- Initial fill is composed of design fill and advanced fill.
- Advanced fill is amount of sand that is expected to erode before next nourishment.
- Design fill is amount of fill needed to optimize the beach investment.

Design Cross-section:

- For purposes of establishing the design cross-section, advanced fill does not exist except for its cost.
- Each width of added beach has associated with it a recreation benefit and a storm benefit.
- Each beach width also has a cost associated with it.
- The design beach yields the maximum net benefits; when costs are subtracted from benefits.

Storm Benefits:

- Storm benefits are derived from a reduction in storm damage over the life of the project.
- Storm damages are experienced when storm surge and waves wash out the uplands and cause structural damage.
- Wider beaches reduce storm damage.
- Storm recession can be predicted using a number of methods.
- Storm recession is computed for the 10, 20, 50 and 100 year storms for each of 50', 100', 150', and 200 feet beaches.

- The costs of those beaches is also computed.

Recreation Benefits:

- If the beach washes away no one can go to the beach.
- Each visit to the beach has an economic value, say \$2.00 (or determined by economic study).
- The more people that can go to the beach because of the project – yields the recreation of benefit.
- Beach visits are limited by beach area, parking and demand.
- Beach use is highest on holidays, weekends, and weekdays, respectively. No one goes to the beach in the rain.
- Demand is proportioned to a number of category days and limited by parking. For all beach widths – "extra" visits are computed and recreation benefit calculated.

Optimizing the Design:

- A plot is made of total benefits vs. total costs.
- The beach width with the maximum net benefit is the design beach.

Advanced Fill:

- Historical erosion rates are an indicator of how fast the nourished beach will erode.
- Restored beaches erode faster because of end losses.
- Finer grained beaches also erode faster.

Construction Profile:

- Sand usually takes a steeper slope during the construction process than the equilibrium profile.
- A construction cross-section is developed which can hold both design and advanced fill.
- The beach will adjust to the equilibrium profile relatively quickly; within the first year.
- Construction profiles and equilibrium profiles should be shown on permit drawings to avoid misunderstandings and problems.

Permits & Approvals:

There are a number of permits and approvals required for beach nourishment:

Department of Environmental Regulation Permits:

- Major concern is effect of project on the environment.
- Water quality is a major consideration.
- The public need for the project is balanced against potential environmental impacts.
- DER will look carefully at marine habitats near the project.
- The amount of silt/clay in the fill is important to the DER because it will determine how turbid the water is during the project, how much fallout and sedimentation will occur, and how much residual silt/clay there will be to be stirred up by storms.
- In addition to a DER permit, it may be advisable to apply for a nearshore mixing zone variance – you must show that nothing would be affected by temporary higher turbidity levels.

Department of Natural Resources Permit:

A coastal construction permit is required from the DNR:

- They look for proper coastal engineering design.
- impacts on adjacent beaches.
- Compatible sand

The Erosion Control Line

- Establishes boundary between private and public land.
- Set at the position of mean high water.
- Makes the entire new beach public.

Borrow Area Easements

- Permission to use State owned bottom lands.
- Dredge fee waiver also requested.
- Survey and description needed.

Florida Department of State, Division of Historical Resources Approval

- Magnetometer survey required to clear borrow area.
- Protection of artifacts is goal.
- Usually unidentified anomalies are eliminated from borrow area.

Upland Easements

- A portion of fill falls on private property.
- An easement is needed to place fill there.
- Hold outs are handled in court.

Corps of Engineers Permit

- Required in non Federal projects.
- Fish & Wildlife review.
- National marine fisheries review.
- EPA review.
- Mostly an environmental assessment and a check for conflicts with other Federal projects.

Funding

State Funding:

- Through DNR
- Funding for "public beach" within 1/4 mile of access
- Funds up to 75% of non Federal share of public beach areas.
- This year's assessments included minimum parking levels.
- Rules under consideration may include other public purposes. SA protection of public roads and facilities.
- State has not "required" access be added.
- Parking fees have been allowed.
- An agreement is required to obtain funds.

Federal:

Through the Corps of Engineers:

- Two types of projects, standard and reimbursable.
- Authorization is required from Congress to be eligible.

- Federal study must show positive b/c ratio
- General Design Memorandums updates old studies and provides details on segments of larger studies.
- Federal projects must be optimized beach.
- Federal funding is 65% for storm protection and 50% for recreation.
- Primary purpose of project must be storm protection.
- In Florida, because of ECL, Federal funds within 1/4 mile of accesses and in front of public features.

Local Funding:

- Beach nourishment is a proper use of advalorem tax.
- Tax districts can be established to address differential benefits of beach nourishment.
- Tourist tax can now be used for beach nourishment (the extra 1 cent).
- Resolve conflicts of inland vs. coastal residents early.